18 /1

NEWARK PUBLIC LIBRARY
JAN 8 1987
U.S. GOVT. PUBS
DEPOSITORY [illegible]

Earthquakes & Volcanoes

Vol. 18, No. 1, 1986

I19.65:

UNITED STATES DEPARTMENT OF THE INTERIOR
Donald Paul Hodel, Secretary

U.S. GEOLOGICAL SURVEY
Dallas, L. Peck, Director

Earthquakes and Volcanoes is published bimonthly by the U.S. Geological Survey to provide current information on earthquakes and seismology, volcanoes, and related natural hazards of interest to both general and specialized readers.

The Secretary of the Interior has determined that the publication of this periodical is necessary in the transaction of the public business required by law of this Department. Use of funds for printing this periodical has been approved by the Office of Management and Budget through June 30, 1989.

Henry Spall—Editor

Earthquakes and Volcanoes
U.S. Geological Survey
904 National Center
Reston, Virginia 22092
Telephone (703) 648-6078

Martha K. Penman—Publication Design

Subscription orders should be sent to:

Superintendent of Documents
U.S. Government Printing Office
Washington, DC 20402
Telephone (202) 783-3238

For sale by the Superintendent of Documents. Annual subscription rate—$15.00 (domestic) and $18.75 (foreign). Make check or money order payable to the Superintendent of Documents.

Single copy rate—$3.00 (domestic) and $3.75 (foreign). Single copy rate for issues prior to Volume 15, Number 1—$2.25 (domestic) and $2.85 (foreign). Can be purchased from the Book and Open-File Reports Section, U.S. Geological Survey, Federal Center, Building 41, Box 25425, Denver, CO 80225 (make check or money order payable to the Superintendent of Documents).

Cover: *Eruption of Pu'u O'o on Kilauea's east rift zone, January 31, 1984*
(Photograph by J. D. Griggs, USGS)

Back cover: *Stained glass window by Beverly Jackson at the Kilauea Military Camp Headquarters, depicting an eruption of Kilauea.*

Earthquakes and Volcanoes

(formerly *Earthquake Information Bulletin*)
Vol. 18, No. 1, 1986

Volcano Monitoring at the U.S. Geological Survey's Hawaiian Volcano Observatory

by Christina Heliker, J. D. Griggs, Taeko Jane Takahashi, and Thomas L. Wright

The first issue of the new *Earthquakes and Volcanoes* (formerly *Earthquake Information Bulletin*) summarizes the history and work of the Hawaiian Volcano Observatory (HVO) as it nears the 75th anniversary celebration in 1987. We want this issue to be of use for all our interested friends and visitors who have asked, "What exactly do you do at HVO?"

The impetus for this volume came from four sources: (1) Bob Decker, former Scientist-in-Charge at HVO, and Henry Spall, who originally suggested that a special issue be devoted to the recent volcanic activity in Hawaii; (2) a series of talks on "What HVO Does" delivered by Jennifer Nakata, Ron Hanatani, Barry Stokes, Christina Heliker, and Tom Wright at the 1985 Big Island Science Conference held at the University of Hawaii at Hilo; (3) the summary of USGS studies of Mount St. Helens at the Cascades Volcano Observatory, Washington, in an earlier Earthquake Information Bulletin (Vol. 16, No. 2, March-April 1984); (4) and finally, and perhaps most important, the numerous requests that we receive from visitors for a document that explains our work.

The text was written by Christina Heliker, HVO geologist, and Tom Wright, current Scientist-in-Charge. Photographs and figures were painstakingly assembled by J. D. Griggs, staff photographer. Jane Takahashi, HVO's librarian and photo archivist, provided invaluable editorial and photo support. Dallas Jackson provided us with the first draft and figures of the geoelectrical section.

We thank the entire staff of HVO for their comments on the content and scope of this summary and their help with the figures.

Volcano Monitoring at the U.S. Geological Survey's Hawaiian Volcano Observatory

Introduction

The island of Hawaii has one of the youngest landscapes on Earth, formed by the frequent addition of new lava to its surface. Because Hawaiian eruptions are generally nonexplosive and easily accessible, the island has long attracted geologists interested in studying the extraordinary power of volcanic eruptions. The U.S. Geological Survey's Hawaiian Volcano Observatory (HVO), now nearing its 75th anniversary, has been in the forefront of volcanology since the early 1900's. This issue of *Earthquakes and Volcanoes* is devoted to the work of the Observatory and its role in studying the most recent eruptions of Hawaii's two currently active volcanoes, Kilauea and Mauna Loa.

Hawaii's Active Volcanoes

The Hawaiian Islands are the best-known part of a 1500 km chain of volcanoes that has been active for over 70 million years. The origin of this chain can be explained by the theory of plate tectonics, which holds that the Earth's surface is divided into a number of rigid plates that move about on a semi-liquid mantle. Most of the earth's seismic and volcanic activity occurs at plate boundaries as adjoining plates collide or

Copyright material has been
deleted, not available for
Microfiche Edition.

move past one another. In contrast, the Hawaiian Islands were formed in the middle of the Pacific Plate, and the source of the volcanic activity that built these islands is a fixed hot spot in the Earth's mantle, currently located beneath the island of Hawaii. The hot spot can be visualized as a rising plume of hot mantle material. As the Pacific Plate drifts northwest, each volcano in turn is rafted away from the hot spot and dies.

The southeastern-most islands of the Hawaiian chain. The island of Hawaii is made up of five volcanoes. Loihi seamount, the youngest Hawaiian volcano, is still about one kilometer beneath the surface of the ocean. The site of Kilauea's current eruption is shown in red. (Adapted by permission from a map published by Dynamic Graphics, Berkeley, California using Interactive Surface Modeling-ISM)

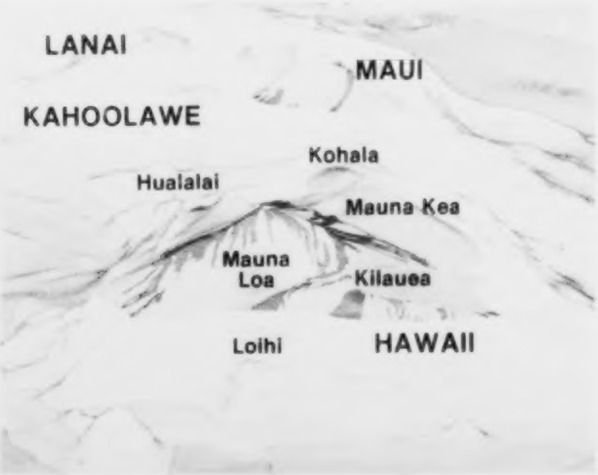
LANAI
MAUI
KAHOOLAWE
Kohala
Hualalai
Mauna Kea
Mauna Loa
Kilauea
Loihi
HAWAII

1984 eruption on Mauna Loa's northeast rift zone. During the early stages of Hawaiian eruptions, lava fountains frequently form "curtains of fire" along newly-opened fissures. The fountains in this photo are approximately one kilometer long. (Photograph by J. D. Griggs, USGS)

The island of Hawaii, the largest and southeastern-most island in the chain, is composed of five volcanoes, three of which have been active within the past 200 years. Kilauea's latest eruption continues as of this writing; Mauna Loa's latest activity was in 1984, and Hualalai's in 1800-1801. Mauna Kea last erupted near the time of the last glacial advance (3000 years before present); Kohala, the oldest volcano on the island, has been inactive about 60,000 years. In addition to the active subaerial volcanoes, a submarine volcano, Loihi seamount, lies off the south coast of Hawaii, 1000 m below sea level. Loihi probably has been active in recent years, judging from the frequent earthquake swarms and the samples of fresh basalt collected by dredging.

Eruptions of Kilauea and Mauna Loa occur both at their summit calderas and along rift zones that extend for many kilometers down their flanks to the ocean. Rift zones extend to the northeast and southwest from the summits of both volcanoes. Eruptions frequently begin along newly-opened fissures, which may be several kilometers long. During long-lived eruptions the activity generally becomes localized at a single vent. Sustained eruptions on Kilauea's rift zones have built substantial cones; Pu'u O'o, the site of the current eruption, is now over 250 m high. Following a long eruption, a deep pit crater may form due to collapse after the magma drains away from beneath the vent area. Subsequent eruptions occasionally occur in or at the edge of pit craters and create ponded lava lakes.

The historic record of Hawaii's volcanic activity begins with the oral traditions of the Hawaiians prior to the arrival of Europeans. An explosive eruption in 1790 produced a pyroclastic surge of incandescent ash that killed a band of Hawaiian warriors marching across Kilauea's summit. The ash deposit from this eruption is visible in eroded sections of the upper southwest rift zone. Part of the present Kilauea caldera was formed by subsidence following the 1790 eruption.

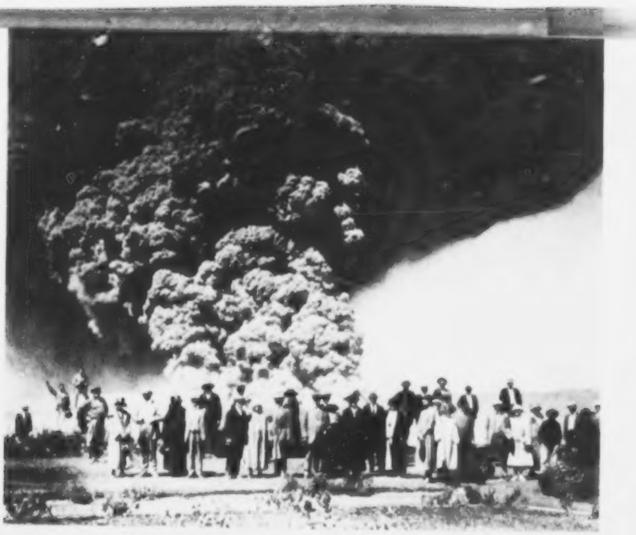

Phreatic (steam) explosions at Halemaumau in 1924. Following this eruption, Halemaumau crater was 390 m deep. Since then, repeated additions of lava have filled the crater to within one hundred meters of the rim. (Photograph by T. S. Loo, courtesy of the Bishop Museum)

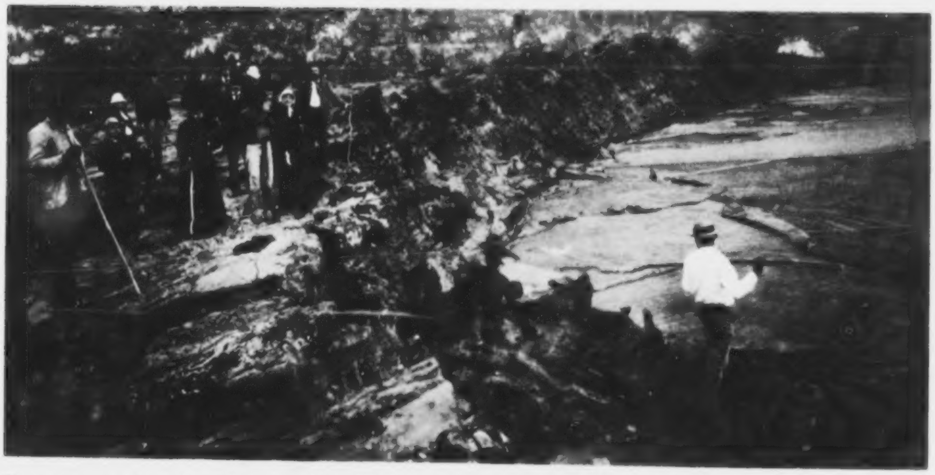

Tourists at the edge of the molten Halemaumau lava lake, around 1890. (Photographer unknown)

Throughout much of the 19th and early 20th centuries, until 1924, most of the activity at Kilauea occurred in the caldera, where an almost continuously active lava lake occupied the site of the present Halemaumau crater. In 1924 the lake drained away, ground water came in contact with the magma, and a series of explosions threw large blocks out onto the caldera floor. The sudden withdrawal of magma produced a deep collapse pit, the present Halemaumau crater. Sporadic eruptions, confined to

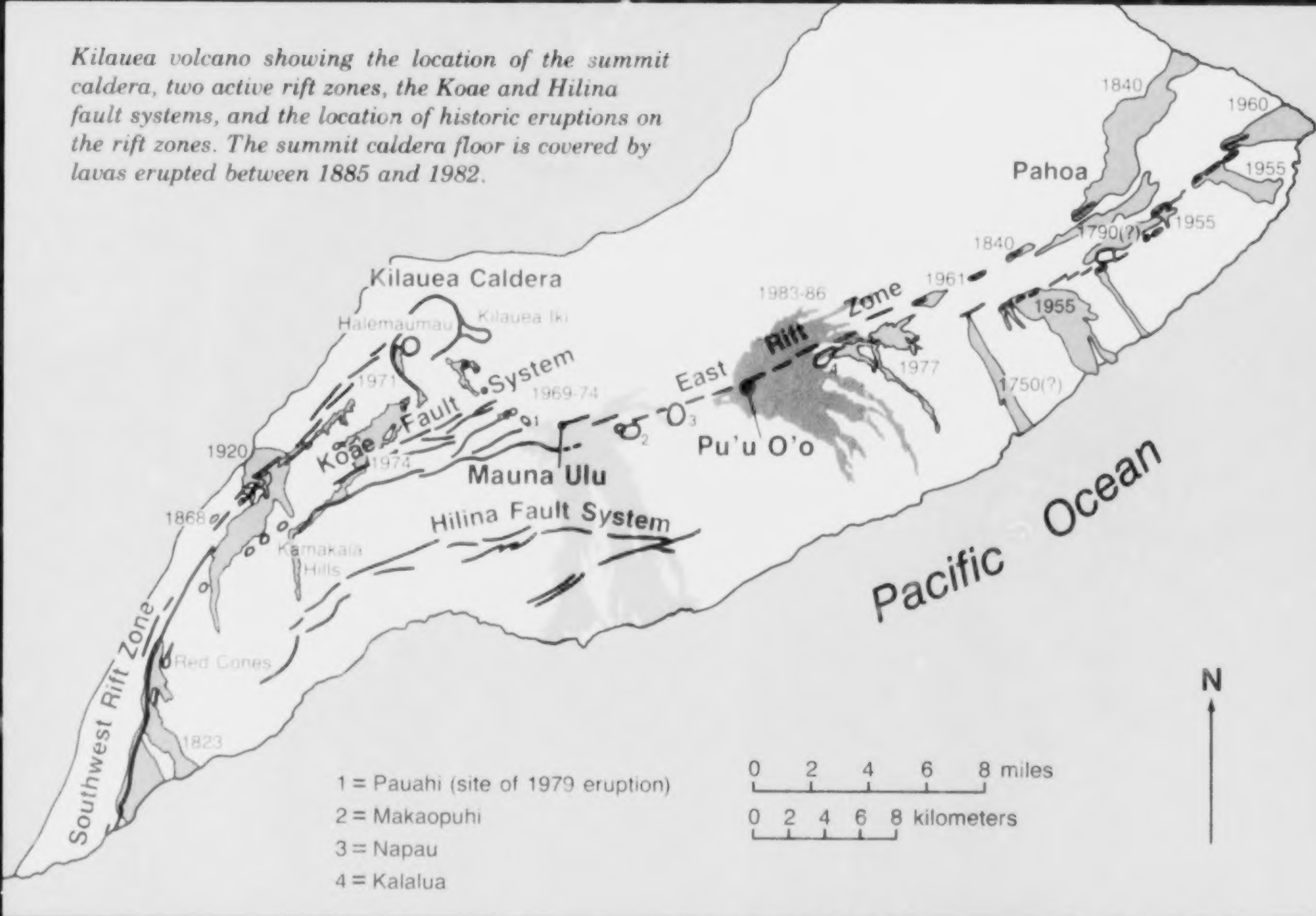
Kilauea Caldera
Halemaumau
Kilauea Iki
1971
Koae Fault System
1974
1969-74
1920
1868
Kamakaia Hills
Red Cones
1823
Southwest Rift Zone
Mauna Ulu
Hilina Fault System
East Rift Zone
1983-86
Pu'u O'o
1977
1961
1840
1955
1750(?)
1790(?)
1955
Pahoa
1840
1960
1955
Pacific Ocean
N
0 2 4 6 8 miles
0 2 4 6 8 kilometers
1 = Pauahi (site of 1979 eruption)
2 = Makaopuhi
3 = Napau
4 = Kalalua

Kilauea volcano showing the location of the summit caldera, two active rift zones, the Koae and Hilina fault systems, and the location of historic eruptions on the rift zones. The summit caldera floor is covered by lavas erupted between 1885 and 1982.

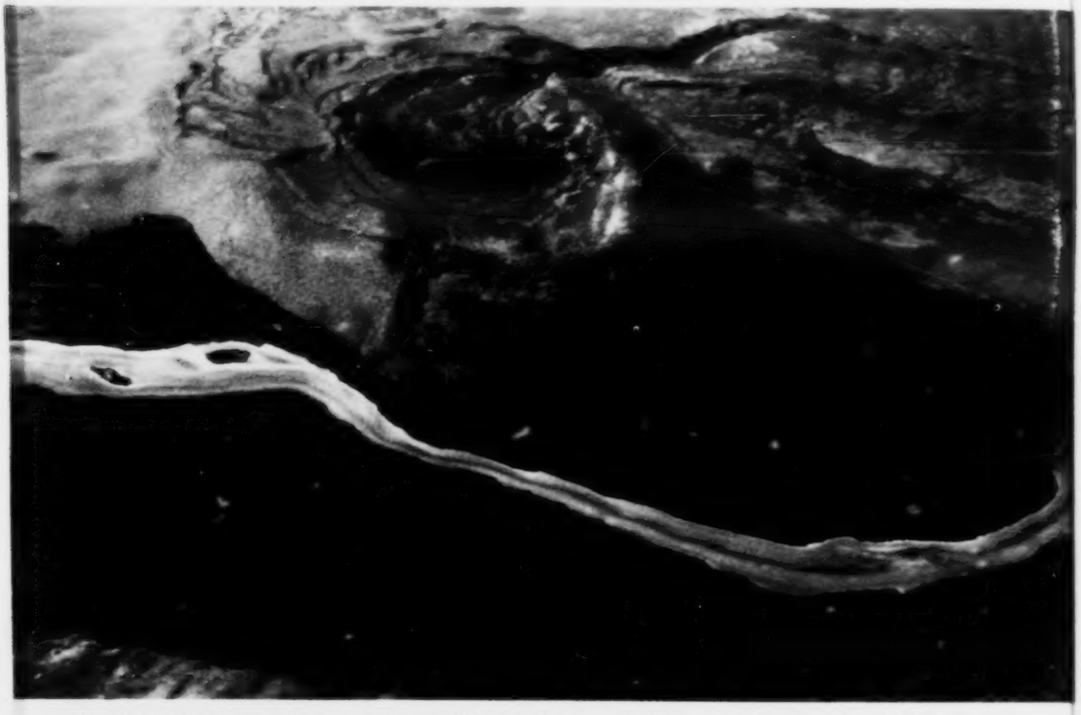

Lava channel near cinder cone on Mauna Loa's northeast rift zone, March 1984. The flow is approximately 500 m long in this view. (Photograph by J. D. Griggs, USGS)

Halemaumau, occurred until 1934, when all activity ceased for 18 years. In 1952 another eruption in Halemaumau initiated the current cycle of activity. For the past three decades, the most voluminous eruptions have occurred on the rift zones, particularly along the east rift zone.

Much less is known about Mauna Loa, which rises nearly 4,100 m above sea level, principally because of the difficulty of access. Eruptions at the summit and on both flanks occurred throughout the 19th and the first half of the 20th centuries, culminating in a large southwest rift eruption in 1950. While Kilauea became more active, Mauna Loa remained quiet until 1975, when the summit erupted briefly. Activity resumed in 1984, with a three-week-long eruption on the northeast rift zone.

Hawaiian Volcano Observatory

History, Location, and Staffing

The Hawaiian Volcano Observatory began operation in 1912, under the sponsorship of the Hawaiian Volcano Research Association, with private funding from the Whitney Fund of the Massachusetts Institute of Technology. The driving force behind its inception was Thomas A. Jaggar, a pioneering volcanologist, who took as the motto of the newly formed Observatory *Ne plus haustae aut obrutae urbis* (No longer shall the cities be destroyed).

The original Observatory was placed on the rim of Kilauea at the present site of the Volcano House Hotel. Here Jaggar set up the Whitney Laboratory of Seismology. After the Kilauea summit area was made part of Hawaii

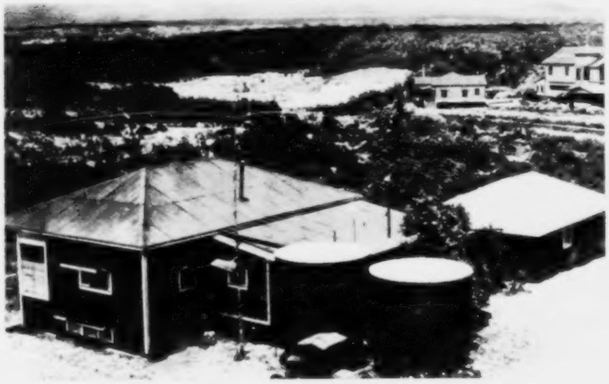

Top: Hawaiian Volcano Observatory: Original building near the site of the present Volcano House Hotel. The building in the background is the original Volcano House. Bottom: Thomas Jaggar in the Whitney Laboratory of Seismology. (Both photographs are around 1912; provided courtesy of the Bishop Museum)

Volcanoes National Park in 1916, the Observatory was moved to Uwekahuna Bluff, the highest point on the Kilauea Rim, where it shared quarters with a National Park Service museum. In the years between 1912 and 1948, when HVO came permanently under the direction of the U.S. Geological Survey, the facility was variously managed by the Hawaiian Volcano Research Association, the U.S. Weather Bureau, the U.S. Geololgical Survey, and the National Park Service.

HVO is presently administered by the Geologic Division, U. S. Geological Survey and is funded through direct congressional appropriation to the Volcano Hazards Program. In 1984 Congress approved plans for a modern building that will be finished in time for the 75th anniversary of HVO in January 1987.

The Observatory, perched on the rim of Kilauea's summit caldera, commands a breathtaking view of the caldera floor, Halemaumau crater, and Kilauea Iki crater: all are sites of recent summit eruptions. Looking to the east, beyond the caldera, several high points on Kilauea's east rift zone are visible, including Mauna Ulu, a shield-shaped cone built during nearly continuous activity in 1969-1974. Beyond Mauna Ulu lies Pu'u O'o, the site of another long-lived eruption, which began in January 1983 and continues as of this writing. Although the Pu'u O'o cone is not visible from HVO, the high lava fountains that it produces almost monthly are easily viewed from the Observatory. Behind the Observatory looms the enormous mass of Mauna Loa, a classic basaltic shield volcano and the largest volcanic edifice on earth.

HVO's staff has grown from one person (Jaggar) in 1912 to 26 in 1986. The permanent staff is augmented in the summer months by student help recruited from the Minority Program in the Earth Sciences, Alu Like (a program for young people of Hawaiian ancestry), and the National Association of Geology Teachers. Positions are divided among a permanent, locally-recruited staff and scientists from USGS mainland centers, who serve two-to-five year tours of duty. Currently, the rotating staff consists of a

Hawaiian Volcano Observatory, 1948–1985. The wing in the left foreground was begun in 1927. In 1986 this will be renovated for National Park Service use as the Thomas A. Jaggar Museum. The wing toward the rear was added in 1958 and will be renovated for continued use by the U.S. Geological Survey. (Photograph by D. W. Peterson, USGS)

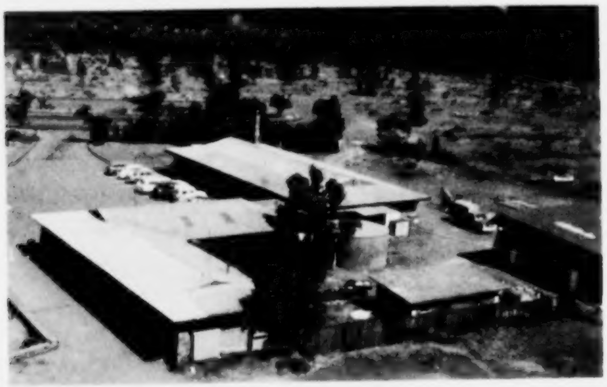

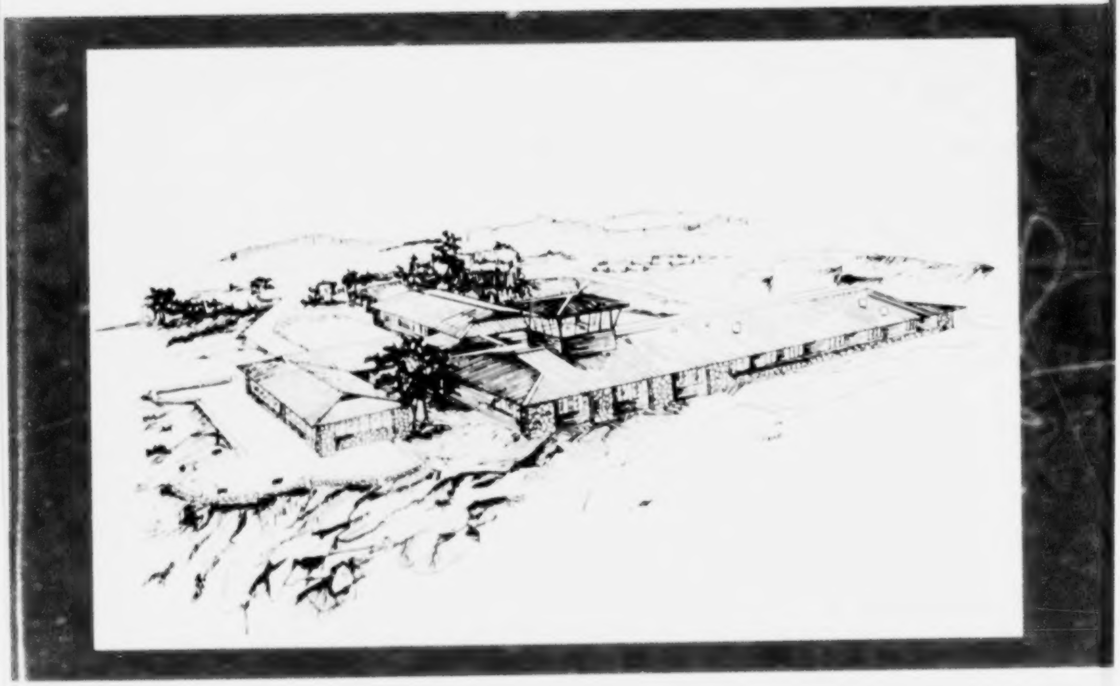

Artist's conception of the new Hawaiian Volcano Observatory under construction in 1985–86. The tower will afford a 360 degree view of volcanic activity. (Drawing by Tom Fake, National Park Service)

Hawaiian Volcano Observatory viewed from the northwest, looking across Kilauea caldera to Kilauea Iki crater and the Pu'u Pua'i cinder cone (middle background), to Pu'u O'o, site of the current eruption (far background with white plume) and Mauna Ulu (right far background). (Photograph by J. D. Griggs, USGS)

Hawaiian Volcano Observatory viewed from the southeast, with the rim of Kilauea caldera in the foreground and Mauna Loa in the background. (Photograph by J. D. Griggs, USGS)

scientist-in-charge, a seismologist, a ground deformation specialist, a geochemist, a geologist, and a geophysicist. The scientist-in-charge is assisted by a local staff headed by a chief of opertions with professional and technical personnel in seismology (three), ground deformation (three), geology (one), geochemistry (one), computer science (two), electronics (five), plus a photographer, a librarian/archivist, a purchasing clerk, and a typist.

Purpose and Objectives

Thomas Jaggar's pioneering work was impelled by the belief that loss of life and property from volcanic eruptions could be minimized only through better understanding of how volcanoes work. The detailed observations of active volcanism, initiated by Jaggar, form the basis for both hazard assessment and research on volcanic processes. These three areas of endeavor—monitoring, hazard assessment, and research—still are the principal functions of the Observatory.

In order to provide timely information on potential activity, HVO continuously monitors seismic and volcanic activity, including the changes that occur both underground and on the Earth's surface as magma rises from the mantle prior to eruption. Monitoring is HVO's principal task and generates a vast accumulation of data on seismicity, ground deformation, chemistry of volcanic gases and erupted lavas, changes in electrical and magnetic properties, and changes in gravitational attraction. Research on volcanic processes is carried out using the data bases provided by the monitoring. The ultimate aims of the research are to provide (1) models of the physical processes that govern the generation of basaltic magma and its movement from the mantle to crustal storage and eventual eruption; (2) volcano-tectonic models that relate the accumulation of strain from subsurface movement of magma to the release of seismic energy in the form of earthquakes; (3) sufficient understanding of both volcanic and tectonic processes to make accurate forecasts of volcanic and seismic activity.

Short-term hazard evaluations are made in conjunction with other government agencies. Eruptions within the boundaries of Hawaii Volcanoes National Park fall under the jurisdiction of the National Park Service, and those outside, under that of Hawaii County Civil Defense. HVO is responsible for alerting the appropriate officials about an imminent eruption or damaging earthquake. Once an eruption starts, HVO keeps officials informed as to where and how fast the lava flows are moving. The evaluation of longer-term volcanic and seismic hazards, made by studying the geologic record of past eruptions, is outside the realm of HVO activities, but is carried out by other projects funded under the Volcano Hazards Program.

Highlights of HVO Research

Over the last three decades, beginning with the pioneering geophysical work of Jerry Eaton, HVO has developed a model for the storage and eruption of magma at Kilauea. Data from the recent eruption at Mauna Loa suggest that the Kilauea model also fits the larger volcano, although far fewer studies have been made of Mauna Loa. All of the magma that reaches the surface of Kilauea first passes through a summit reservoir, which extends from about 2 to 6 km beneath the summit. The reservoir is defined by a zone of reduced seismicity and by the ground deformation that occurs at the summit as the reservoir inflates and deflates during an eruption cycle. Prior to every eruption, basaltic magma accumulates in the summit reservoir until the growing pressure forces the magma to either erupt at Kilauea's summit or to leak into one of the rift zones. Magma that is transferred into a rift zone may either erupt or remain in storage as an intrusion.

Following an intrusion, the connection with the summit reservoir may be broken, allowing the magma to cool and crystallize. The portion of the intruded magma that remains liquid may later erupt with a composition quite different from that which was originally intruded. It has been estimated that 50 percent of all magma that enters the summit reservoir remains in the ground as intrusions, indicating that the volcano grows by endogenous (internal), as well as by exogenous (lava extrusion), processes. Because of the great volume of intruded magma stored in the rift zones, magma fed from the summit reservoir to rift zone eruptions frequently mixes with stored magma to form lavas of hybrid chemical composition.

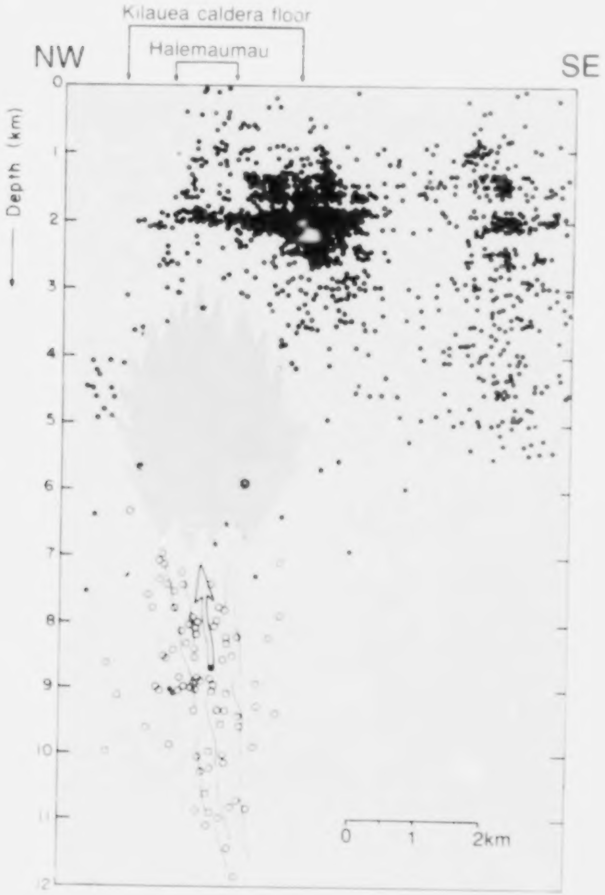

Cross section of Kilauea showing distribution of earthquake hypocenters. The low seismicity of the shaded area delineates the zone of magma storage. Shallow, high-frequency earthquakes (solid circles) occur above the magma storage region, reflecting brittle fracture of the roof rocks. Long-period earthquakes (open circles) define the conduit through which magma travels from the mantle source. (From Koyanagi and others, 1974)

Ground deformation at Kilauea's summit related to filling and emptying of the magma reservoir. (a) Inflation begins. (b) Tiltmeters on the summit record the amount of inflation. (c) Kilauea summit subsides as magma drains laterally to feed an eruption on a rift zone and the magma reservoir deflates. Vertical scale greatly exaggerated. (From Tilling, 1983)

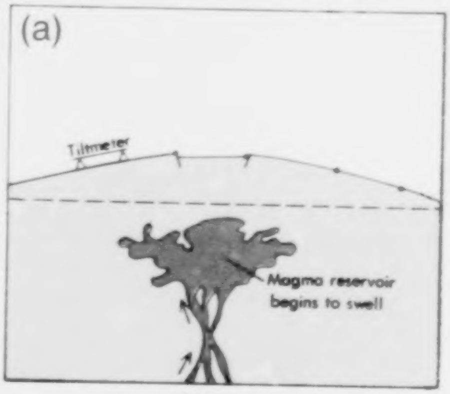
(a)
Tiltmeter
Magma reservoir begins to swell

STAGE 1
INFLATION BEGINS

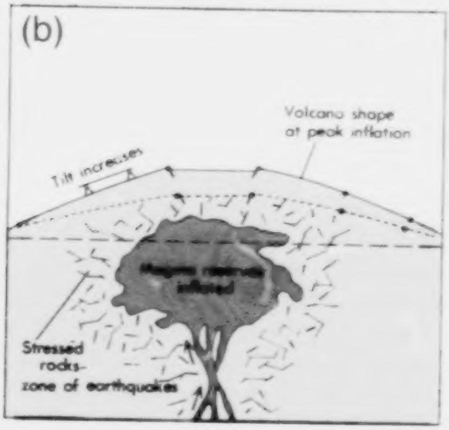
(b)
Volcano shape at peak inflation
Tilt increases
Magma reservoir inflated
Stressed rocks-zone of earthquakes

STAGE 2
INFLATION AT PEAK

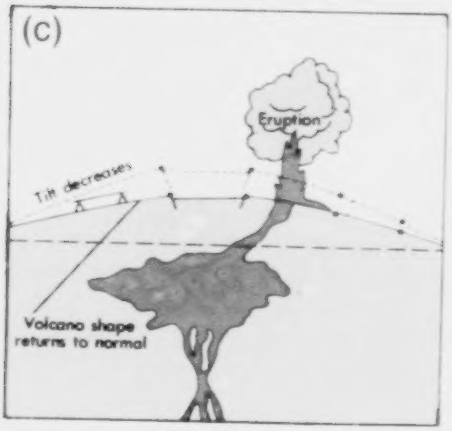
(c)
Eruption
Tilt decreases
Volcano shape returns to normal

STAGE 3
ERUPTION-DEFLATION

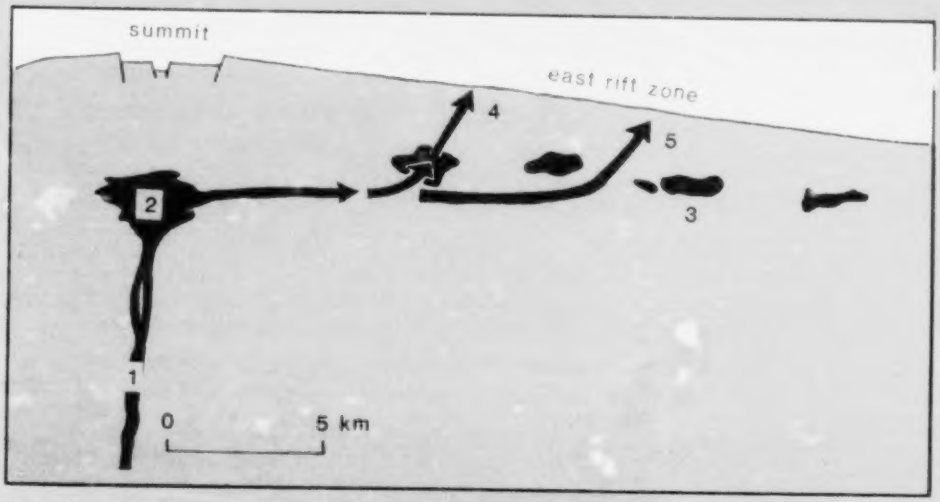

Simplified diagram of Kilauea showing magmatic plumbing system. Magma from the mantle (1) enters Kilauea's principal storage reservoir (2). Magma that leaks into either of the rift zones may be stored beneath the Earth's surface as an intrusion (3). Later batches of magma may intersect bodies of stored magma to produce a lava of hybrid composition (4). Only magma that is fed directly from the summit reservoir to an eruption site (5) may match the composition of summit eruption lavas. (From Wright and Fiske, 1971)

	Summit lavas		Rift lavas
SiO_2	47.45	50.16	51.18
Al_2O_3	9.82	13.14	13.78
'FeO'	11.70	11.33	12.53
MgO	18.75	8.83	5.39
CaO	8.08	10.88	9.35
Na_2O	1.63	2.23	2.80
K_2O	.34	.47	.80
TiO_2	1.86	2.53	3.64
P_2O_5	.19	.25	.42
MnO	.17	.17	.19

Typical major-oxide chemical composition of lava erupted from the summit reservoir, contrasted with lava erupted from a body of magma stored beneath a rift zone. The two compositions on the left are chemically related by addition or subtraction of magnesian olivine. The analysis with the higher amount of MgO is typical of the lower part of the summit reservoir where olivine accumulates, leaving the upper part of the reservoir depleted in both olivine and MgO. The chemistry of rift lava is further modified by crystallization of augite, plagioclase and iron-titanium oxide.

During summit eruptions, relatively little subsidence of the summit occurs, an indication that magma is erupted at nearly the same rate that it is supplied from the mantle. During a rift eruption, however, the summit rapidly deflates as magma is diverted from the summit reservoir into the rift zone. This condition is short-lived, and when the eruption or intrusion ends, the summit once again begins to inflate. These relations are shown graphically by the remarkable record of summit subsidence and inflation measured by tiltmeters in the Uwekahuna vault near the Observatory.

The magma that feeds the Hawaiian volcanoes originates in the earth's mantle at depths below 60 km, where the deepest earthquakes are recorded. Crustal seismicity (shallower than 15 km) outlines the feeding conduits directly beneath each of the three active volcanoes — Kilauea, Mauna Loa, and the recently discovered Loihi Seamount. Deep-seated seismicity, related to the movement of magma at depths greater than 30 km, is concentrated in a broad zone within the triangle formed by the three volcano summits. Since the seismicity suggests a common magma source for all three volcanoes, one of the challenges of current research is to explain why each volcano is erupting basalt that is chemically distinct from the others.

Much of the shallow seismicity associated with Kilauea is concentrated in the volcano's south flank, which is bounded by the two rift zones to the north and the ocean to the south.

A continuous record of ground tilt from daily readings of a water-tube tiltmeter in the Uwekahuna vault, 1956-1983, is shown on page 21. Each period of inflation shows a gradual upward trend, each deflation a sharp drop. Eruptions (E) and intrusions (I) correspond to the table of historic activity at Kilauea on page 22 and 23. (From Dzurisin and others, 1984) →

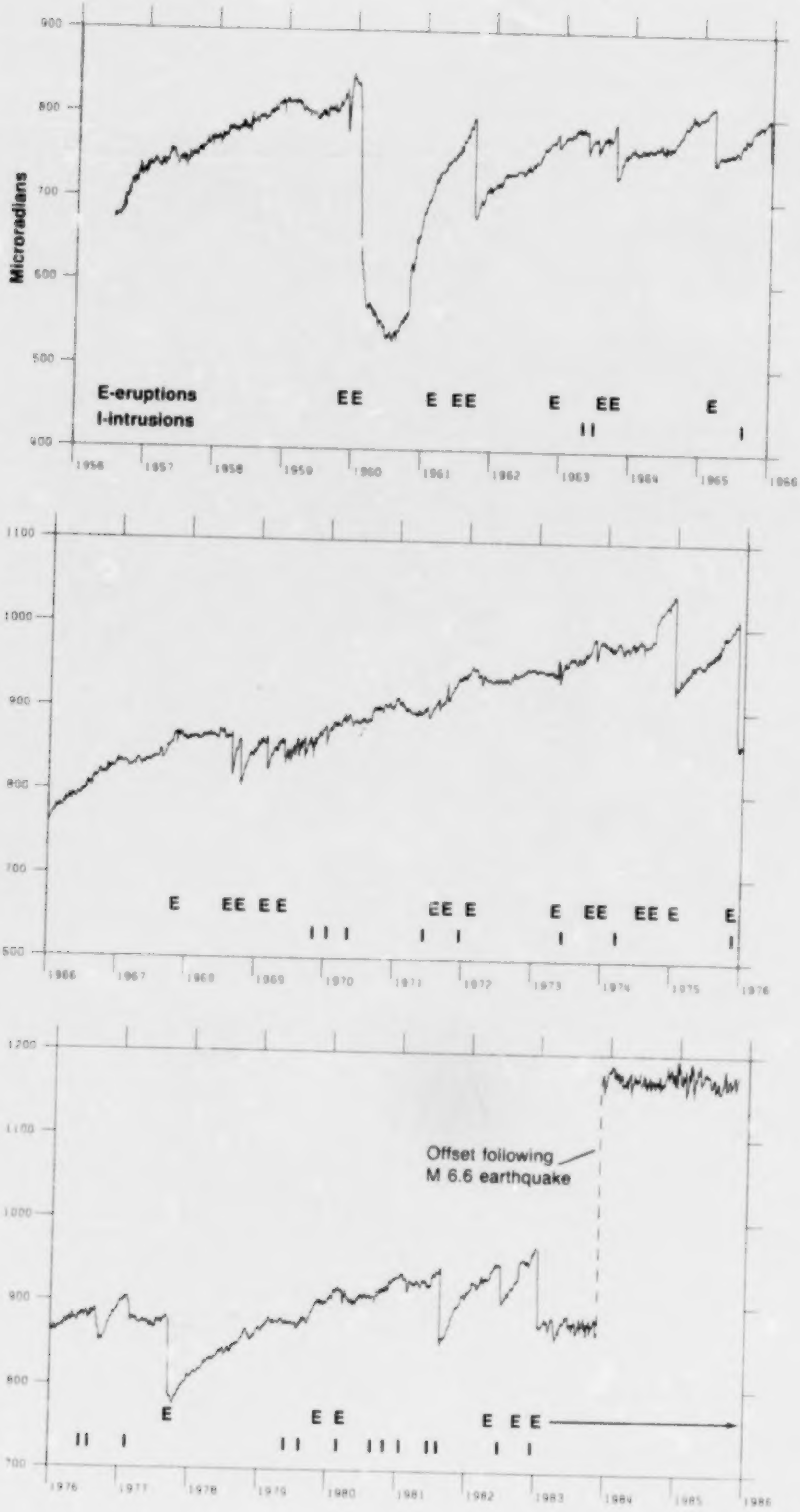

Microradians
900
800
700
600
500
400
E-eruptions
I-intrusions
EE
E EE
E EE
E
II
I
1956
1957
1958
1959
1960
1961
1962
1963
1964
1965
1966
1100
1000
900
800
700
600
E EE EE EE E E EE EE E E
I I I I I I I I
1966
1967
1968
1969
1970
1971
1972
1973
1974
1975
1976
1200
1100
1000
900
800
700
Offset following M 6.6 earthquake
E
E E
E E E
II I II I III II I I
1976
1977
1978
1979
1980
1981
1982
1983
1984
1985
1986

Kilauea eruptions and intrusions 1959–1983

Date	Duration (days)	Location and type of event*			Erupted volume (10^6 m^3)
		S	ERZ	SWRZ	
11/14/59	36	E	—	—	40
1/13/60	36	—	E	—	119
2/24/61	1	E	—	—	0.2
3/ 3/61	22	E	—	—	0.3
7/10/61	7	E	—	—	13
9/22/61	4	—	E	—	2.5
12/ 7/62	3	—	E	—	0.3
5/ 9/63	1	—	—	I	—
7/ 1/63	2	—	I	—	—
8/21/63	3	—	E	—	0.8
10/ 5/63	2	—	E	—	8
3/ 5/65	11	—	E	—	18
8/25/65	1	—	I	—	—
12/24/65	2	—	E	—	0.8
11/ 5/67	251	E	—	—	84
8/22/68	5	—	E	—	0.01
10/ 7/68	16	—	E	—	7
2/22/69	7	—	E	—	17
5/24/69	875	—	EP	—	185
11/ 3/69	1	—	I	—	—
1/22/70	1	I	—	—	—
5/15/70	2	—	I	—	—
6/11/71	3	—	—	I	—
8/14/71	1	E	—	—	10
9/24/71	5	—	—	E	8
12/24/71	6	—	—	I	—
2/ 4/72	455	—	EP	—	125
5/ 5/73	1	—	E	—	1
5/ 7/73	187	—	EP	—	2.5
6/ 9/73	1	—	I	—	—
11/10/73	30	—	E	—	3
12/12/73	222	—	EP	—	30
3/24/74	1	—	I	—	—
7/19/74	3	E	—	—	10
9/19/74	1	E	—	—	11
12/31/74	1	—	—	E	15
11/29/75	1	E	—	—	0.2
6/21/76	1	—	I	—	—
7/14/76	1	—	I	—	—
2/ 8/77	1	—	I	—	—
9/12/77	20	—	E	—	40
5/29/79	1	—	I	—	—
8/12/79	1	—	I	—	—
11/16/79	1	—	E	—	0.4
3/ 2/80	1	—	I	—	—

Date	Duration (days)	Location and type of event*			Erupted volume (10^6 m^3)
		S	ERZ	SWRZ	
3/10/80	1	—	E	—	0.000003
8/27/80	1	—	I	—	—
10/22/80	1	—	I	—	—
11/ 2/80	1	—	I	—	—
1/19/81	2	I	—	—	—
1/24/81	16	—	—	I	—
6/24/81	1	I	—	—	—
8/10/81	2	—	—	I	—
4/30/82	2	E	—	—	0.5
6/22/82	3	—	—	I	—
9/25/82	2	E	—	—	3
12/ 9/82	1	—	I	—	—
1/ 3/83	363+	—	EP	—	140+

*E = Eruption.
EP = Major eruptive period of sustained eruption, after Klein (1982).
I = Intrusion.
S = Summit.
ERZ = East rift zone.
SWRZ = Southwest rift zone.

As magma forcefully intrudes the rift zones, the volcanic edifice must yield in order to make room for the new material. To the north and west of Kilauea, the great mass of Mauna Loa acts as a buttress, allowing very little expansion in these directions. In contrast, Kilauea's south flank faces the open ocean and is able to move outward to accommodate the internal growth along the rift zones. This seaward movement accelerates during periods of intrusion and is marked by greatly increased seismicity and ground deformation. The continual deformation on Kilauea's south flank is relieved only by large earthquakes; the Kalapana earthquake of 1975 ($M=7.2$) released strain that had been accumulating for decades.

The next sections describe in more detail the monitoring program at HVO, and some of the specific volcanic and tectonic events that the Observatory has been concerned with over the last decade.

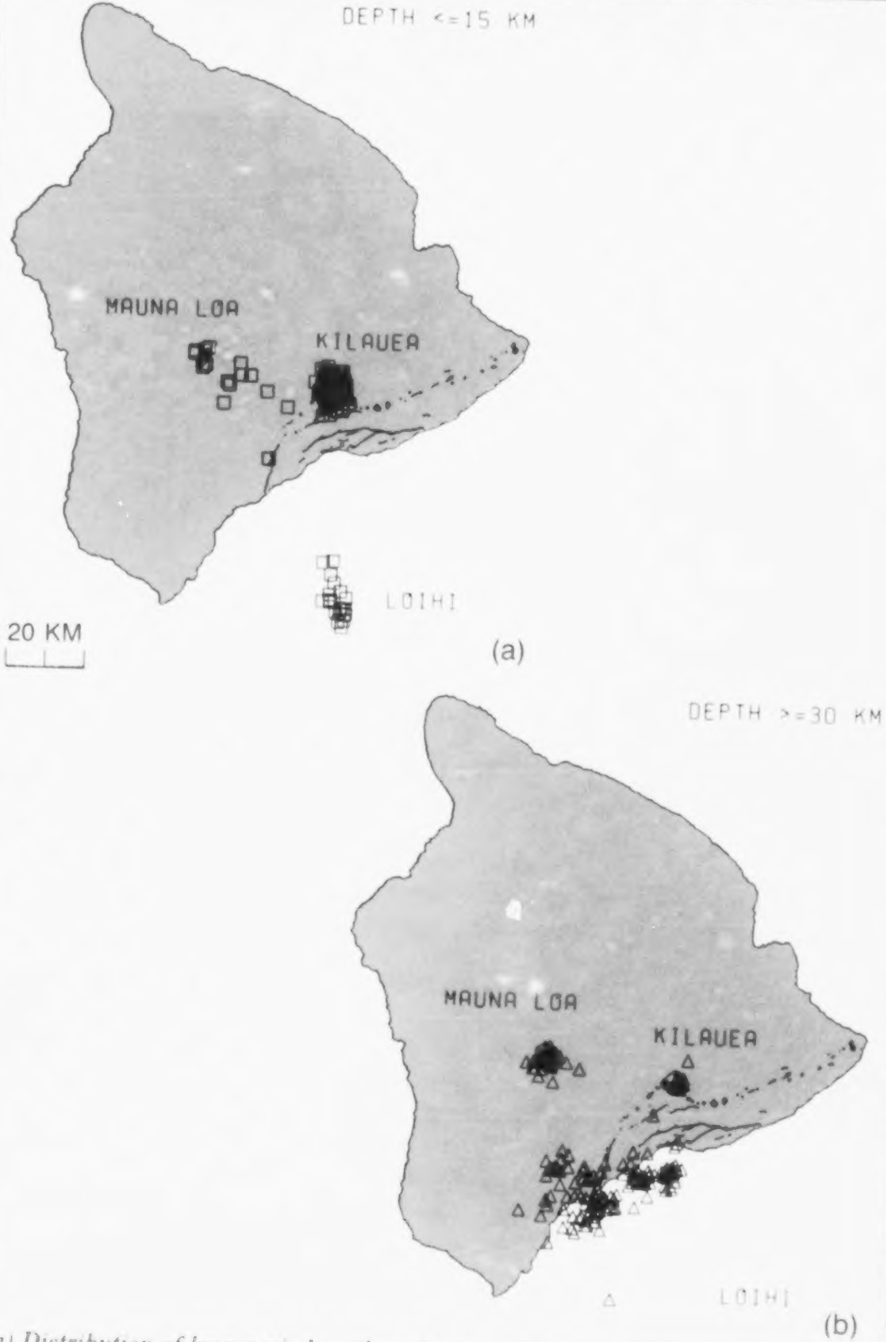
DEPTH <=15 KM
MAUNA LOA
KILAUEA
LOIHI
20 KM
(a)
DEPTH >=30 KM
MAUNA LOA
KILAUEA
LOIHI
(b)

(a) Distribution of long-period earthquakes caused by shallow magma movement within the three volcanic centers that are currently active, 1972–1984. (b) Distribution of long-period earthquakes and volcanic tremor associated with deep magma movement. Note that the seismicity is centrally located with respect to the three active volcanic centers. (From Koyanagi and others, 1986)

Seismic Program

The purpose of the seismic monitoring program is twofold: first, to define the regional seismicity of the island of Hawaii; and second, to distinguish and study tectonic and volcanic earthquakes as they relate to major fault zones and to the eruption and intrusion of magma. Several generations of instruments are in use at HVO. Fifty-one seismometers are located around the island, with a high concentration on Kilauea and Mauna Loa. Most stations send data back to the Observatory via radio telemetry, where the signals are recorded in a variety of ways. The oldest recorders are rotating drums covered with smoked glassine paper on which a stylus etches the seismic trace. These are gradually being replaced by drum recorders that use a heat-sensitive paper inscribed by a heat stylus. The six drum recorders, connected to a wide net of stations, provide an immediate overview of daily seismic events.

All the telemetered stations also send data to a Develocorder, which records the traces on 16 mm film. The film takes ten minutes to develop, after which earthquake arrival times can be read and a preliminary location, depth, and magnitude established. The telemetered data

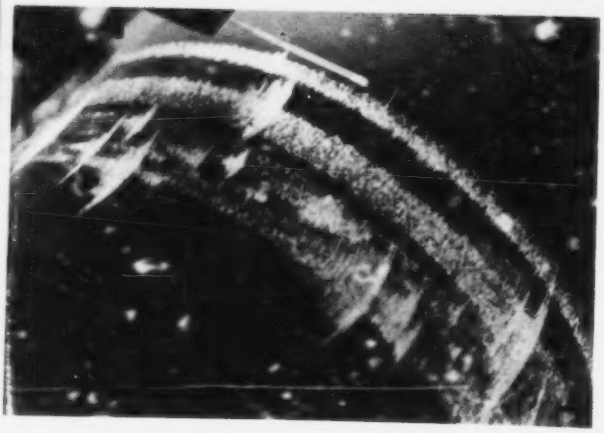

Portion of a smoked-drum seismograph record, showing a swarm of shallow, high-frequency earthquakes. (Photograph by R. W. Decker, USGS)

Seismologist reading Develocorder film record of earthquake activity.

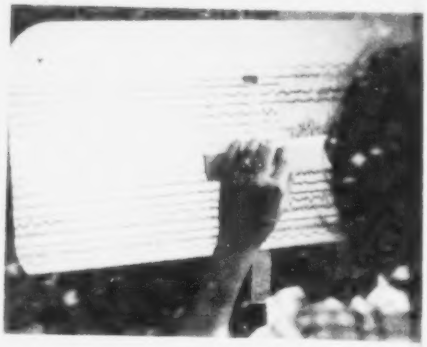

are also recorded in digital form on magnetic tape. The digitized earthquake is displayed on a computer screen, where arrival times are determined for the final location.

A newly installed real-time seismic processing system, Caltech-USGS Seismic Processing (CUSP) reduces the time spent manually processing the records. The system can identify earthquakes (to less than M=1) as they arrive and calculate a preliminary hypocenter (the initial rupture point of the earthquake) and a magnitude. Film records will soon be used only as a backup to detect earthquakes missed by the CUSP system, spurious signals misidentified as earthquakes by CUSP, and seismic signals caused by water waves. The CUSP system is capable of plotting the locations of earthquakes shortly after they occur. This will be especially useful during earthquake swarms, which are frequently precursors of volcanic activity.

Seismicity on the island of Hawaii is heavily concentrated on the most active volcano, Kilauea, with secondary concentrations beneath Mauna Loa and Loihi. Even during years with no eruptions or large earthquakes, the seismicity still defines zones associated with magma movement under each of the volcanoes.

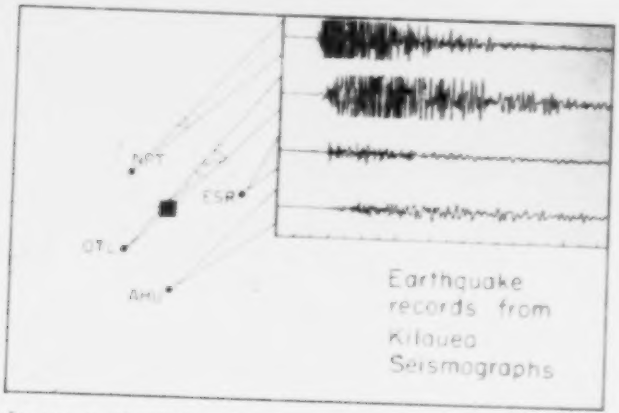

Location of earthquake epicenter from first-arrival times on digital film records. The square marks the epicenter of an earthquake near Kilauea's summit that was recorded on the four labeled seismometers. Note that the closer the station was to the epicenter, the earlier it recorded the earthquake's arrival.

Computer screen showing digitized earthquake traces taken from data that was either stored on tape or recorded directly (real time) by the CUSP system. (Photograph by J. D. Griggs, USGS)

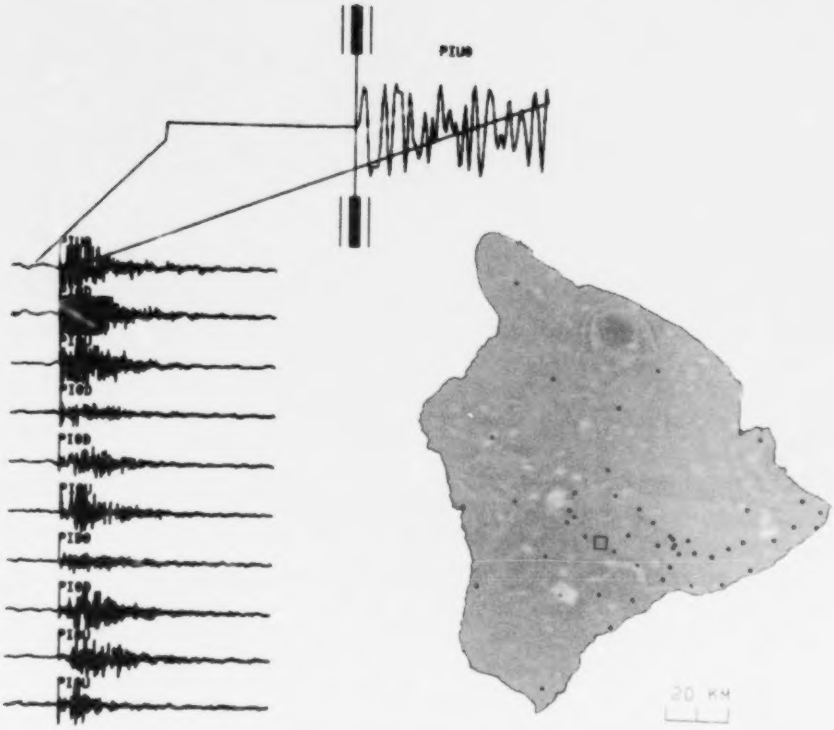

The CUSP automated procedure for picking first-arrival times and locating earthquakes. On the left are shown digitized traces from several stations in order of their distance from the calculated epicenter depicted by the square. The traces are lined up according to the first motion times picked by a computer algorithm. The first motion picked by the computer is shown above in an expanded view of one digitized trace.

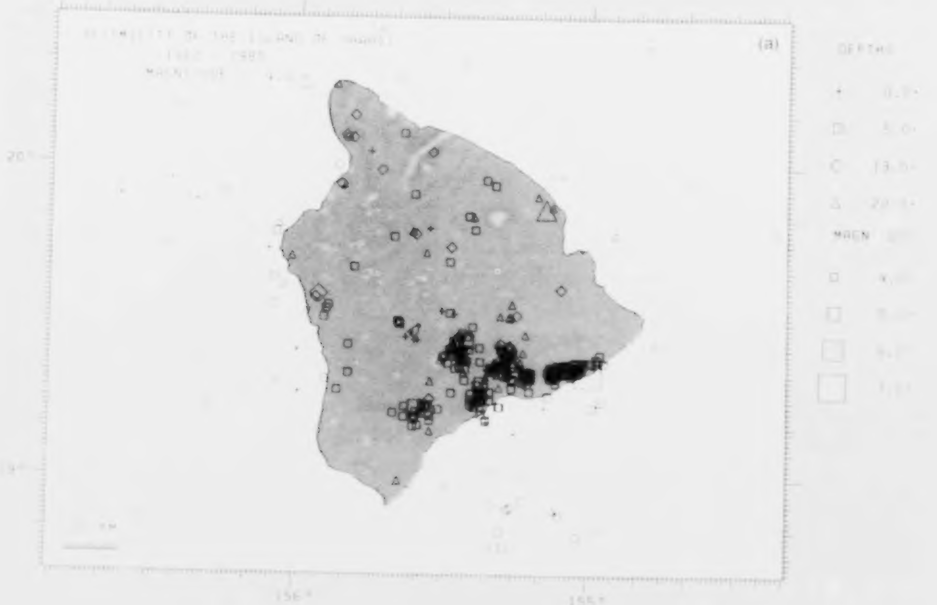
SEISMICITY OF THE ISLAND OF HAWAII
1962 - 1985
MAGNITUDE
(a)
DEPTHS
0.0+
5.0+
13.0+
20.0+
MAGN
20°
19°
156°
155°

Seismicity of the island of Hawaii, 1962-1985.
Top: Epicenters coded by depth and magnitude.
Bottom: Stereo pair showing the distribution of epicenters below Kilauea and Loihi, viewed from the north. The grid is at a depth of 13 km, and the height of the box is 50 km. The deeper events at 30 km mark Kilauea's conduit. Shallow earthquakes (6-10 km) are concentrated beneath Kilauea's mobile south flank. (Klein and others, 1987)

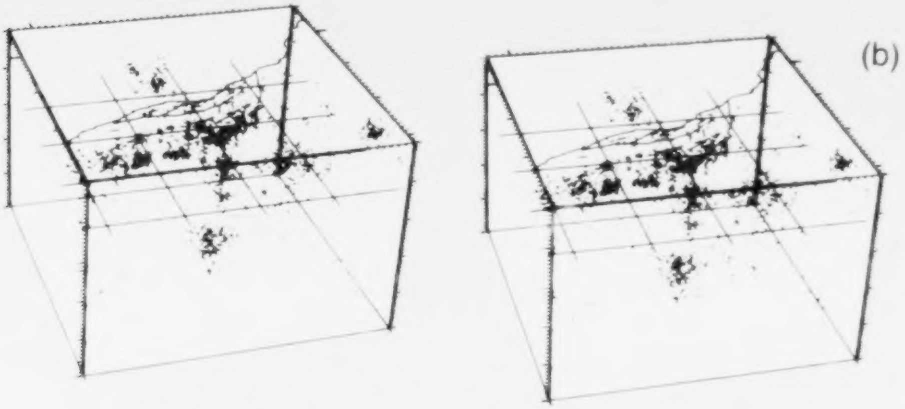

Seismic strain release in the Kaoiki region plotted against time for the 28-year period preceding the magnitude 6.6 Kaoiki earthquake of November 16, 1983. (From Koyanagi and others, 1984)

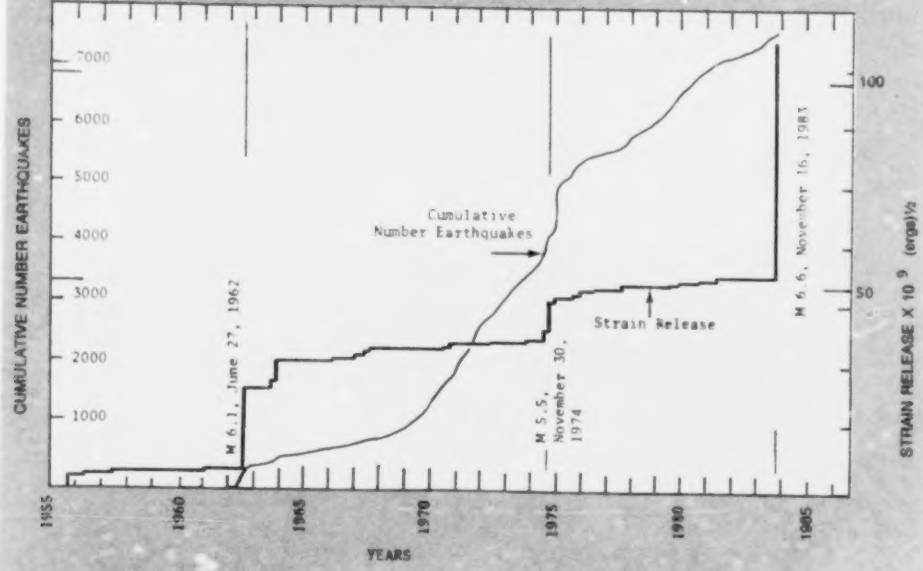

An important measure of regional seismicity is the degree of strain release, which is a function of the number of earthquakes and their magnitudes. Strain buildup in certain areas may presage large, damaging earthquakes, as it did before the M=6.6 earthquake on the Kaoiki fault zone in November 1983.

Earthquake swarms frequently precede eruptions or intrusions; commonly, epicenters migrate ahead of the intruding dike, revealing the probable location of the eruptive outbreak. The seismic swarm preceding the January 1983 eruption on the east rift zone of Kilauea allowed seismologists to trace a dike emplacement as earthquake epicenters migrated toward the point of eventual eruption. Seismic swarms also occur as aftershock sequences, which follow large earthquakes that are not directly related to the movement of magma. In this case the epicenters do not migrate with time, but instead delineate a broad zone of adjustment around the epicenter of the main shock.

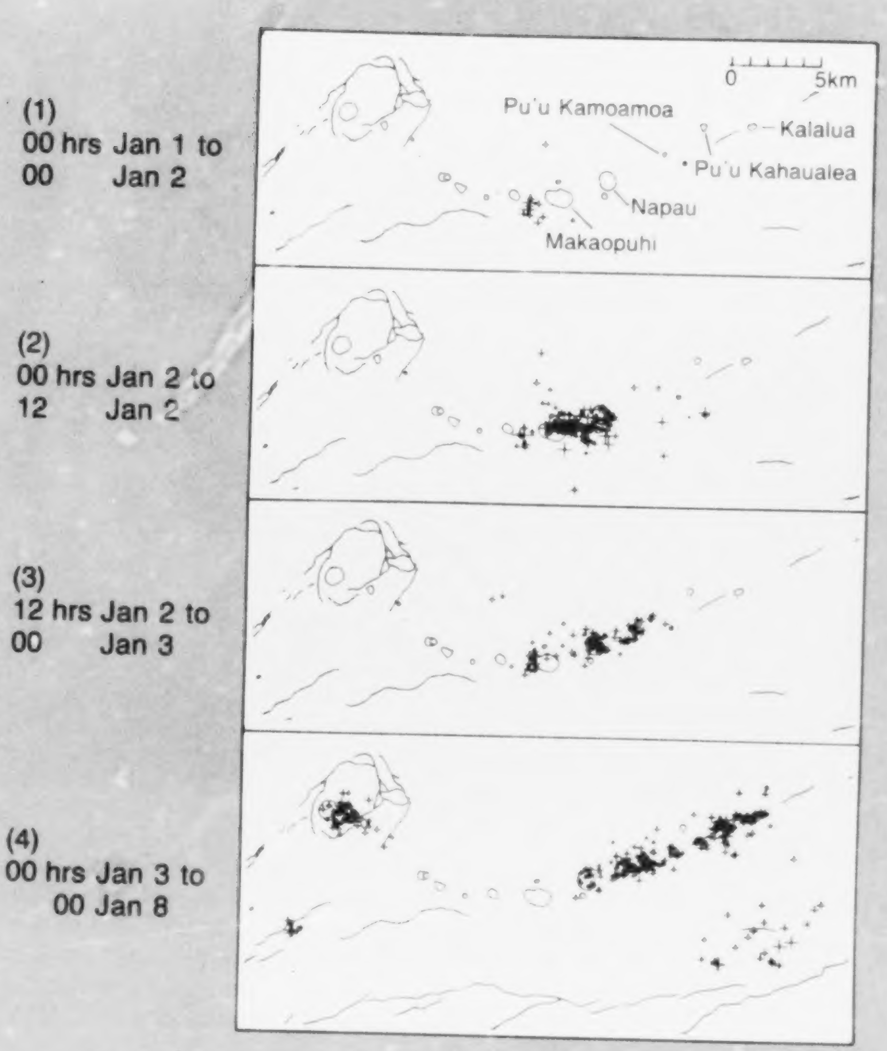
(1)
00 hrs Jan 1 to
00 Jan 2
(2)
00 hrs Jan 2 to
12 Jan 2
(3)
12 hrs Jan 2 to
00 Jan 3
(4)
00 hrs Jan 3 to
00 Jan 8
0
5km
Pu'u Kamoamoa
Kalalua
Pu'u Kahaualea
Napau
Makaopuhi

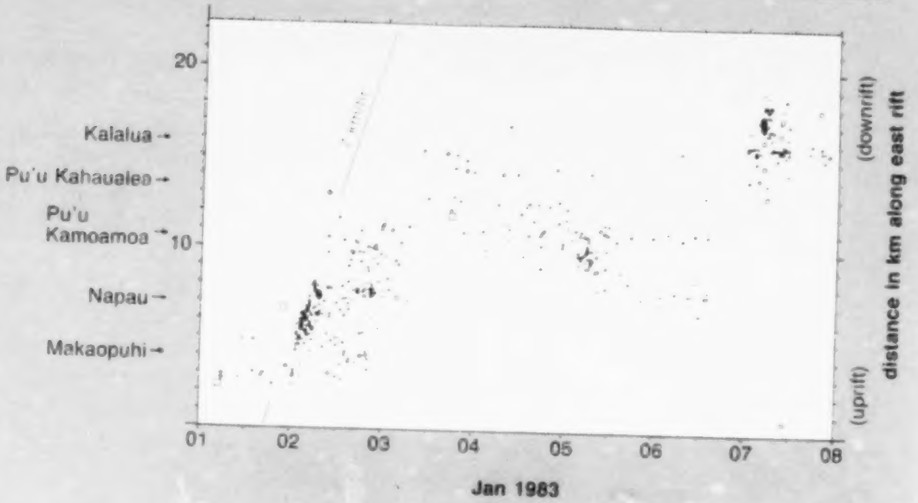
20
10
Kalalua
Pu'u Kahaualea
Pu'u Kamoamoa
Napau
Makaopuhi
01
02
03
04
05
06
07
08
Jan 1983
(uprift)
(downrift)
distance in km along east rift

Migration of earthquake epicenters preceding and accompanying dike emplacement at the onset of the January 1983 Kilauea east rift zone eruption.

***Top, page 30:** Migration of epicenters is shown for four time intervals between January 1 and January 8, 1983.*

***Bottom, page 30:** Time-distance plot showing epicenter migration of about 0.7 km/hr along a 22 km stretch of the east rift zone. This is assumed to represent the rate of lateral propagation of the dike. (From Koyanagi and others, in press)*

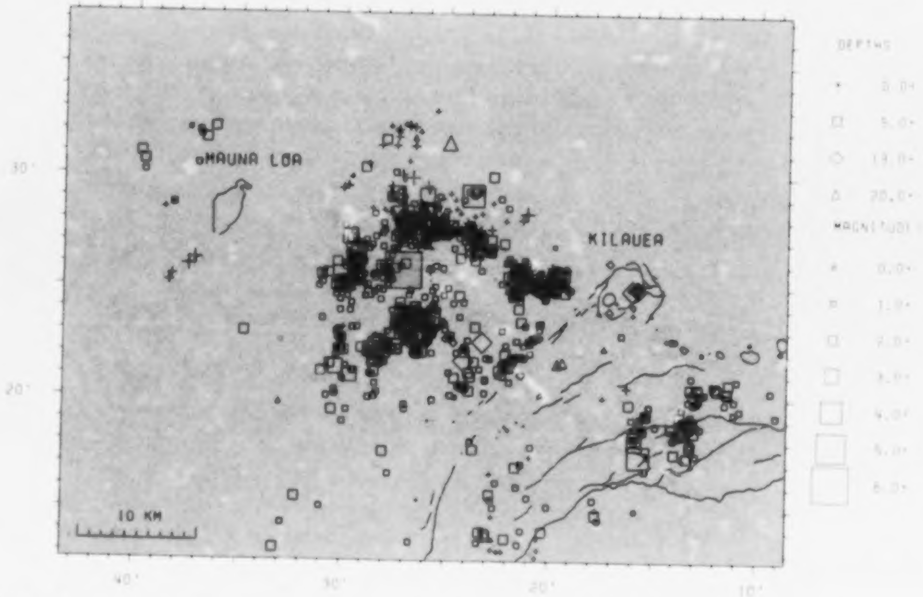

Main shock and aftershock epicenters of the magnitude 6.6 Kaoiki earthquake, November 16, 1983. The epicenter of the earthquake is at the center of the shaded square.

Seismic monitoring at HVO has helped to clarify the distinction between the two main classes of earthquakes, volcanic and tectonic. Although all earthquakes associated with active volcanoes are ultimately related to volcanic processes, volcanic earthquakes are directly associated with magma movement, while tectonic earthquakes occur in zones separated from the principal areas of magma movement. Tectonic earthquakes on Hawaii share characteristics with seismic events elsewhere that are not associated with volcanic systems, such as the earthquakes generated by the San Andreas fault zone in California.

Other topics of seismic research include first motion studies, fault plane solutions, and focal mechanisms. All of these help determine the type of earthquake motion (horizontal or vertical). The fault plane solution for the 1975 Kalapana earthquake (M = 7.2) defines a low-angle thrust fault at a depth corresponding to the base of the volcanic edifice, where Kilauea meets the sea floor. This solution contrasts with the high-angle normal faulting on the Hilina fault system and indicates that the surface faulting is a superficial gravitational response to deep, lateral seaward sliding of Kilauea's south flank. The sliding probably takes place along the zone of weakness separating the volcano from the older basalts and sediments of the sea floor.

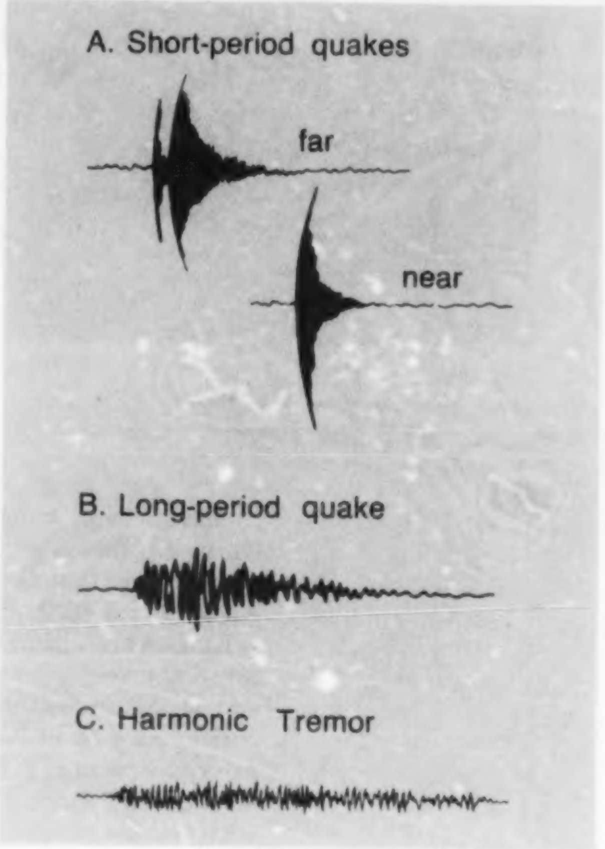

Signatures of (a) tectonic (short-period) and (b) volcanic (long-period) earthquakes and (c) harmonic tremor at Kilauea. (From Tilling and others, 1975)

Geodetic Program

Together with the seismic array, a network of geodetic stations forms the backbone of HVO monitoring. The network is designed to monitor the ground deformation that results from magma moving beneath the Earth's surface. Many of the techniques used on Hawaii were developed especially to monitor the rapid and large changes that occur during volcanic cycles and large earthquakes. These techniques have been adapted for use at many other volcanoes around the world. The following methods are used to form a complete picture of ground deformation associated with a typical eruptive cycle.

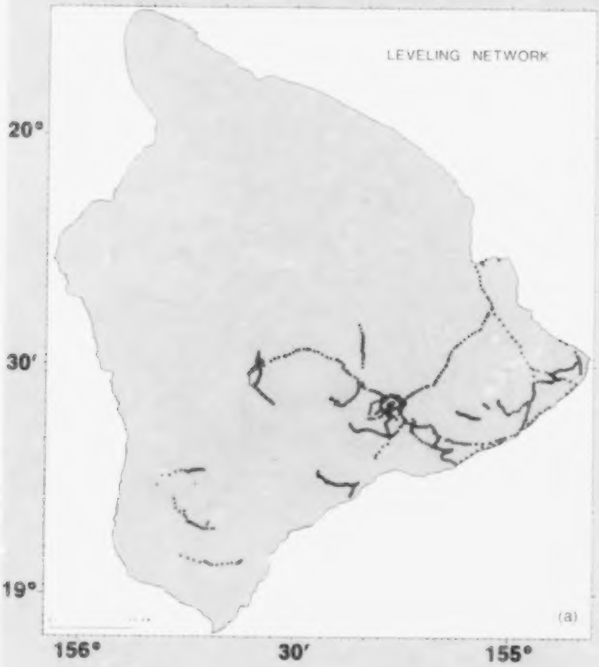

Geodetic networks on the island of Hawaii. (a) Level lines (continued).

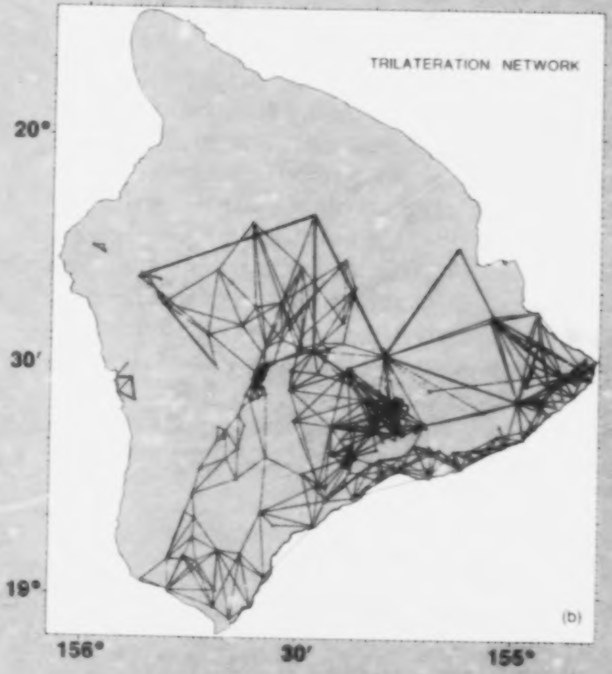
TRILATERATION NETWORK
20°
30′
19°
156°
30′
155°
(b)

Geodetic networks (b) EDM network (c) Dry tilt stations.

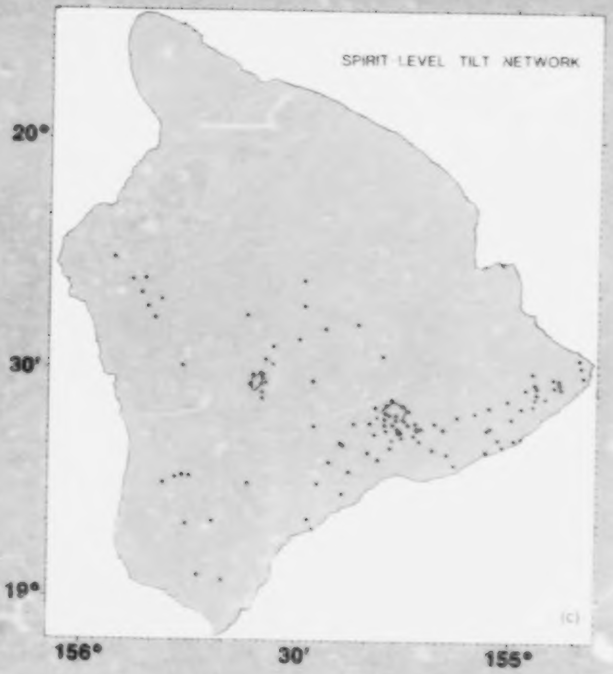
SPIRIT LEVEL TILT NETWORK
20°
30′
19°
156°
30′
155°
(c)

1. Vertical changes, relative to a reference benchmark, are measured by second-order leveling over a network of closed loops and lines. Leveling is labor and time-intensive, but it is the only way to determine absolute vertical changes. Every few years the base stations are tied to the tide gauge at Hilo, a more stable reference. Leveling data are compiled on maps of contoured elevation changes. Elevation changes can be measured to an accuracy of a few millimeters.
2. Horizontal distance changes are measured using a variety of electronic distance measurement (EDM) instruments, which employ a laser beam aimed at a reflector station. The instrument compares the waveform of the light beam going out with that of the returning reflected beam and converts this difference to a slope distance. The magnitude and direction of the distance change are calculated for each station in the network. The displacements are relative to one or more points that are assumed to be fixed. The calculated displacement vectors are plotted on maps to locate the focus of deformation. The precision of the EDM data is ±6 mm, with an additional uncertainty of ±1 mm per km of line length.

Leveling survey on Kilauea's east rift zone, with Pu'u O'o in the background. (Photograph by J. D. Griggs, USGS)

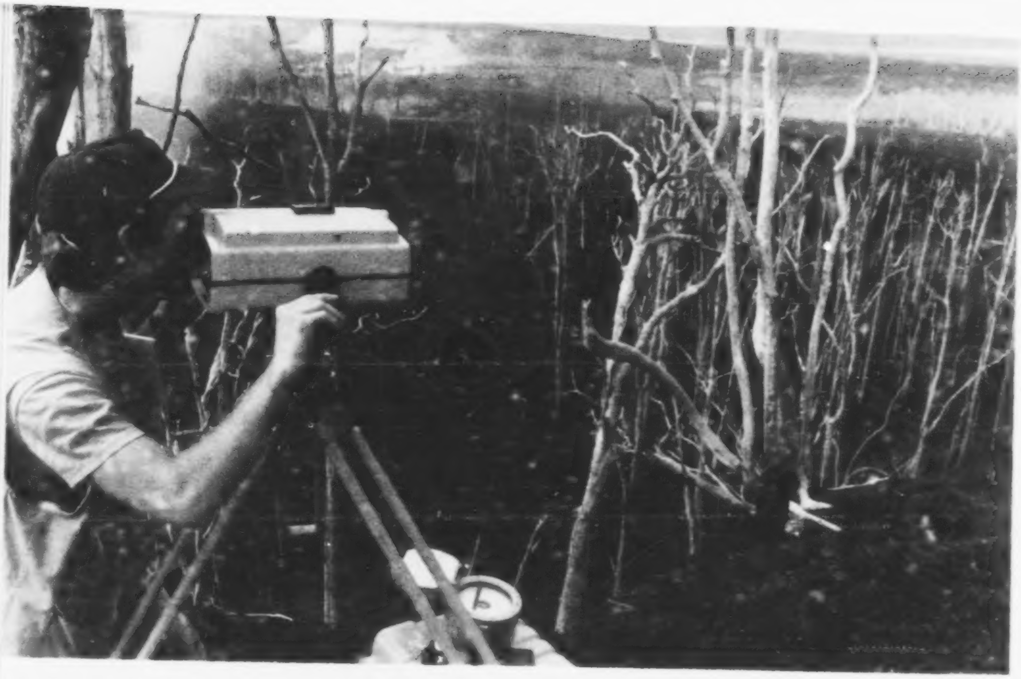

Above: EDM measurements being made near Pu'u O'o instrument station. Right: Reflector station with triad of glass prisms mounted on a tripod. The fishing pole holds a thermometer to record air temperature. (Photographs by J. D. Griggs and R. T. Holcomb, USGS)

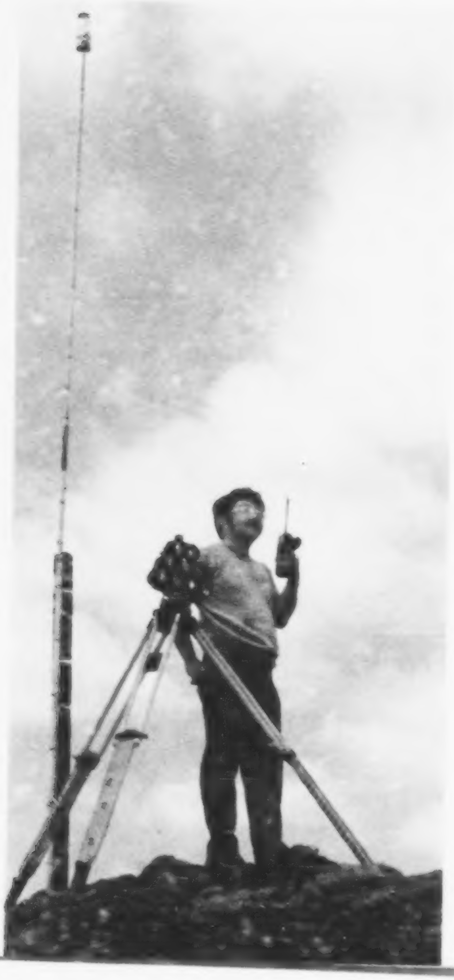

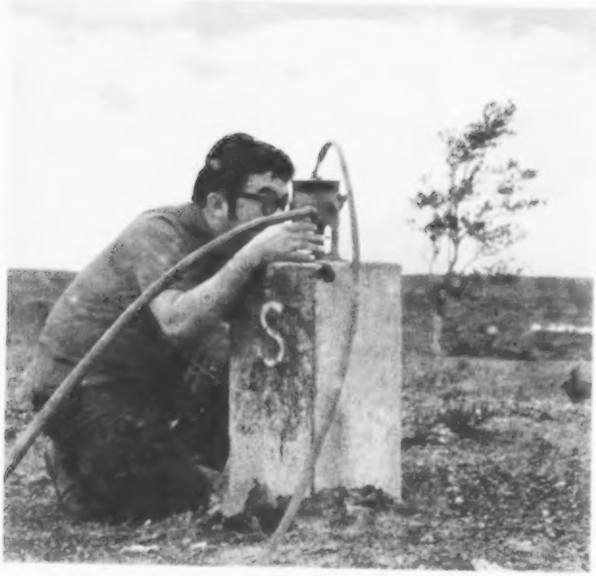

Water-tube method of measuring ground tilt ("wet tilt"). (Photograph by P. Crosland, National Park Service)

3. Ground tilt is measured by three techniques. The oldest method used at Kilauea is the water-tube tiltmeter ("wet tilt"). At present the only water-tube station in use is a short base station in the Uwekahuna vault. A water-tube tiltmeter consists of three brass water pots mounted on cement piers in a triangle. The pots are connected by water hoses to establish a common water level and by air hoses to equalize the atmospheric pressure at each pot. Readings at outdoor stations are best made at night under an overcast sky in order to equalize temperature differences. Measurements are made simultaneously by two operators, who manipulate a micrometer screw that is read at the moment it pierces the water meniscus. Water-tube tilt measurements have been curtailed at HVO because they are both too time-consuming and more precise than is necessary to measure the large changes observed.

Water-tube tiltmeters have been replaced by "dry tilt" meaurements, which are made by leveling around a 40 m triangle using a precise spirit level and invar metal rods. Dry tilt has a precision of ±2-3 microradians. (One microradian equals 0.0000573 degrees and can be visualized in terms of a board 1 km long that is elevated by 1 mm, the thickness of a dime, on one end.) This method is inexpensive and suited to all relatively flat areas where the elevation difference around the 40 m triangle does not exceed 3 m, the height of the rods. Dry tilt changes are displayed on a map as vectors that point in the downward direction and are proportional in length to the amount of change since the last occupation.

Electronic tiltmeters have been in use since 1966 and, where properly sited, are of immense value for continuous tracking of changes in ground tilt. Signals from remote field stations are telemetered into the Observatory, where they are recorded and stored on computer files. Several electronic tiltmeters have been tested in the Uwekahuna vault; a mercury capacitance instrument produces the continuous tilt record shown later (see Geology section).

Because of their short base, electronic tiltmeters require careful site selection to ensure that the tilt being measured is representative of the regional ground deformation. One disadvantage of these tiltmeters is that tilt changes associated with large earthquakes or large and rapid inflations or deflations may necessitate resetting the tiltmeter, which presents a problem at remote stations. The accuracy of the Uwekahuna tiltmeter is checked by daily reading of a water-tube tiltmeter; in the field, electronic tiltmeters are checked by locating a dry tilt station around each borehole or platform installation.

In spite of these difficulties, electronic tiltmeters have proven their worth by providing a record of instantaneous ground movements that is unobtainable by any other means. Electronic tiltmeters performed successfully at the beginning of the Mauna Loa eruption of 1984, when

Dry tilt
Above: A spirit levvel is used to read invar leveling rods. (Photograph by R. Y. Hanatani, USGS)
Below: The configuration of a dry tilt station, with leveling rods set up on three benchmarks forming an equilateral triangle.

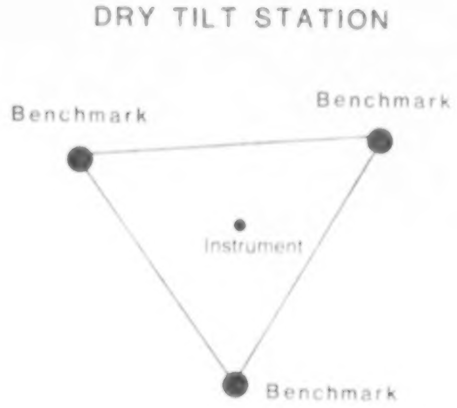

the three summit tiltmeters recorded a rapid inflation one hour before the outbreak, an observation impossible to make with normal field surveys. Electronic tiltmeters have also recorded the intrusion of magma in long, bladelike dikes, which may extend for many kilometers. An array of tiltmeters at different points along Kilauea's east rift zone recorded the passage of the leading edge of the January 1983 dike and allowed quantitative evaluation of both the depth and the rate of emplacement of the dike.

(a) Index map of electronic tiltmeter sites on Kilauea's east rift zone. (b) Tiltmeter response to the dike emplacement preceding the onset of the current east rift zone eruption in January 1983. The arrows mark the passage of the magma beneath each station. (From Okamura and others, in press)

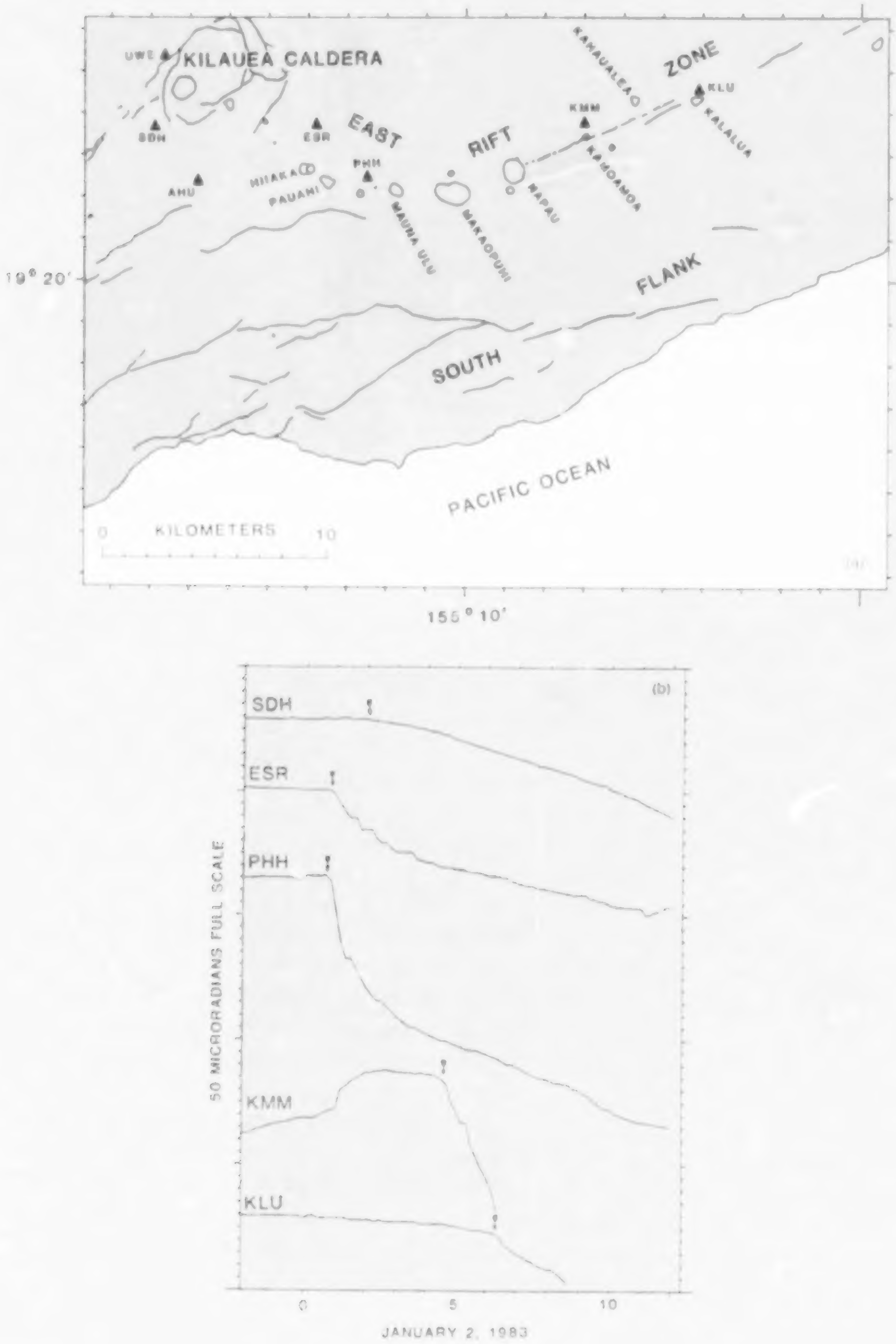

HVO is in the process of converting its electronic tiltmeter telemetry to a "polling" telemetry system. Instead of a fixed transmitting interval, a computer at HVO will poll each station in the network, at intervals of two minutes to one hour, and obtain a digital record of the current reading, which can then be plotted. The polling frequency and the array of stations being polled can be changed in response to heightened activity in a particular area.

Ground deformation data (vertical, horizontal, and tilt) during a single eruption cycle at Kilauea serve to define a center of inflation or deflation and can be used to model the depth and size of the deformation source. The combination of seismic and ground deformation data is the principal means of defining the magma reservoir beneath Kilauea's summit.

Forecasts of impending activity at Hawaii's volcanoes rely heavily on the results of geodetic monitoring. Although eruptions do not occur at exactly predictable values of summit inflation, the relative likelihood of eruption may be estimated from the tilt data. The buildup of strain in Kilauea's south flank is also monitored by deformation measurements,which led to a successful forecast in early 1975 of the large earthquake that occurred later that year. Geodetic measurements are also used to evaluate the nature of the magma plumbing system at Kilauea. Studies have documented a great increase in open space in the plumbing system as a result of the $M = 7.2$ 1975 Kalapana earthquake and have traced the subsequent filling of the system by intrusions.

Another technique used to monitor the deformation of the volcano is measurement of the force of gravity at a given point on the Earth's surface. The Earth's gravitational attraction changes in response to elevation changes (gravity is stronger the closer one is to the center of the Earth) and to subsurface mass changes (for example, gravity increases when intruding magma fills void space in the volcanic edifice). Data from a network of gravity stations on the island of Hawaii show higher gravitational attraction over the summits and rift zones of the

---

Kilauea deformation June-August 1981. Data records summit deflation associated with emplacement of a dike within the southwest rift zone on August 10, 1981. Top: Level contours and tilt vectors. The tilt data are actually the derivative (slope) of the level map, but cannot be used alone to calculate the maximum elevation changes. Bottom: Horizontal displacements measured by EDM.

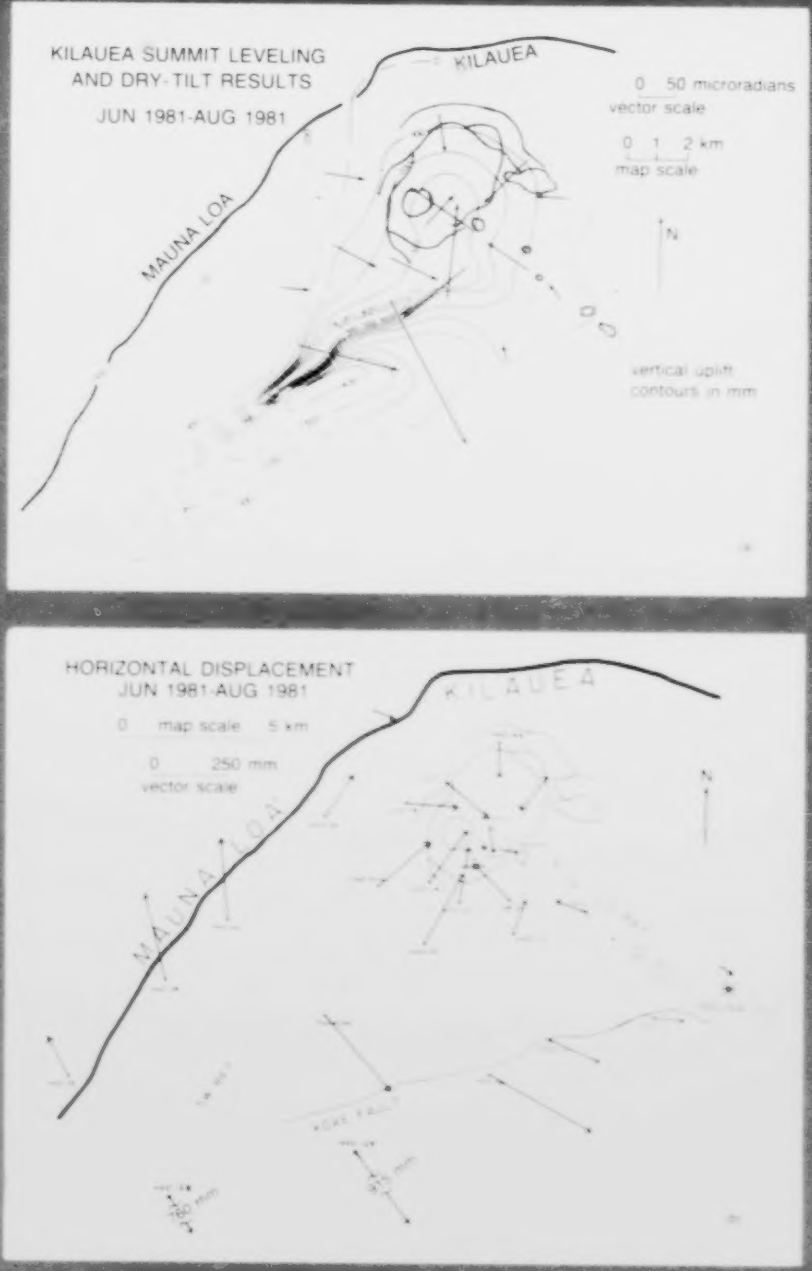
KILAUEA SUMMIT LEVELING
AND DRY-TILT RESULTS
JUN 1981-AUG 1981
KILAUEA
MAUNA LOA
0 50 microradians
vector scale
0 1 2 km
map scale
N
vertical uplift
contours in mm
HORIZONTAL DISPLACEMENT
JUN 1981-AUG 1981
0 map scale 5 km
0 250 mm
vector scale
KILAUEA
MAUNA LOA
N

active volcanoes. These anomalies are caused by the subsurface concentration of dense dikes and bodies of olivine, one of the first minerals to crystallize from basaltic magma.

In addition to monitoring gravity over a large area, more precise gravity measurements are made at the summits of Kilauea and Mauna Loa to record the gravitational response of the volcanoes to eruptive activity. Two gravity meters are used to make periodic readings at a stable base station and at a station near the center of inflation/deflation. Leveling or con-

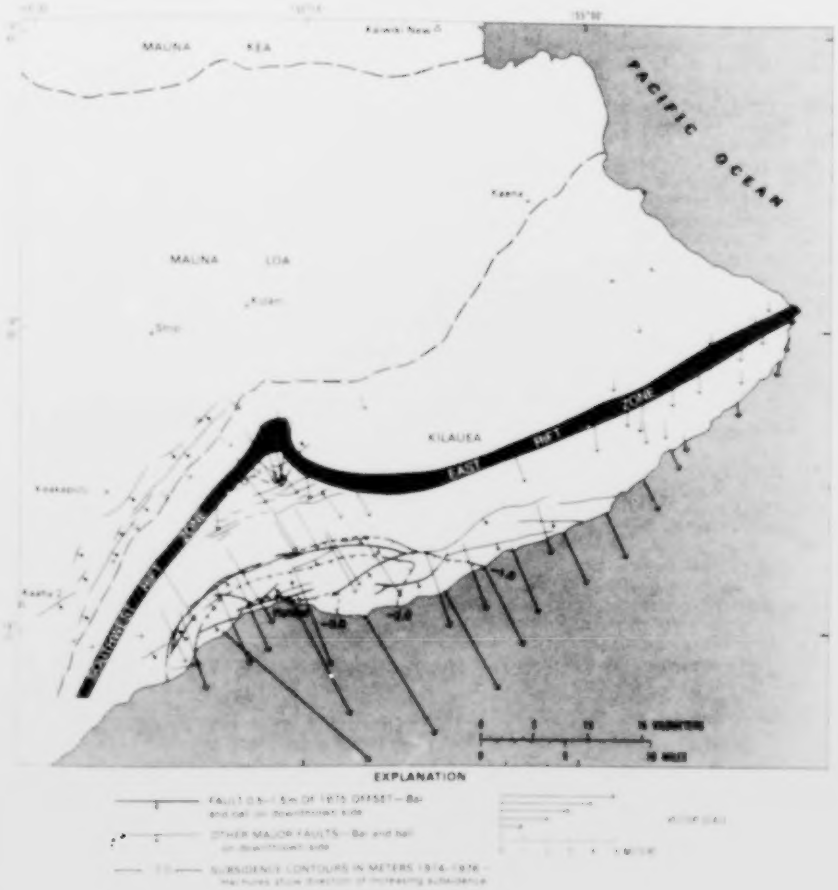
MAUNA KEA
PACIFIC OCEAN
MAUNA LOA
KILAUEA
EAST RIFT ZONE
SOUTHWEST RIFT ZONE
0 5 10 15 KILOMETERS
0 5 10 MILES
EXPLANATION
FAULT 0.5–1.5 m OF 1975 OFFSET—Bar and ball on downthrown side
OTHER MAJOR FAULTS—Bar and ball on downthrown side
SUBSIDENCE CONTOURS IN METERS 1974-1976—Hachures show direction of increasing subsidence
0 1 2 3 4 5 METERS

Horizontal displacements associated with the 1975 M = 7.2 Kalapana earthquake. Vectors represent seaward movement of Kilauea's south flank in response to slippage on a low-angle thrust plane. (Lipman and others, 1985)

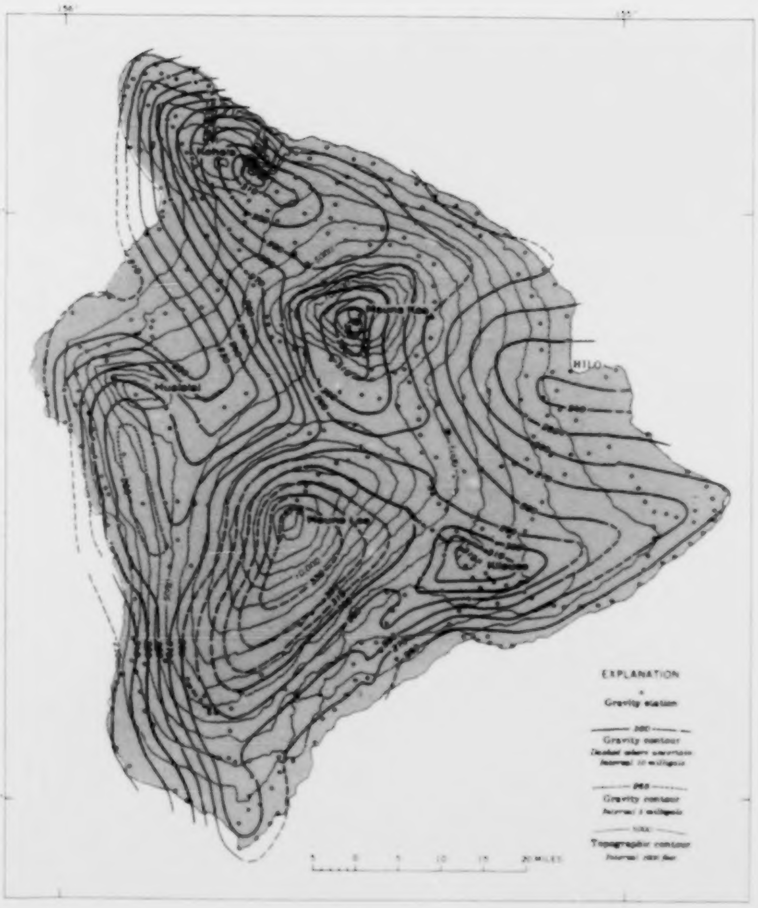
HILO
EXPLANATION
Gravity station
Gravity contour
Dashed where uncertain
Gravity contour
Topographic contour
20 MILES

Regional gravity map, island of Hawaii. Large positive anomalies mark the summit and rift zones of the active volcanoes. (From W. T. Kinoshita and others, 1963)

tinuous tilt measurements are used to establish the station elevations at the time of gravity measurements. The gravity data, after they are corrected for elevation change, reveal the addition or loss of mass (magma) from the volcanic system.

The Kilauea summit measurements show that during deflation, mass changes in the magma reservoir more than offset the gravity increase expected from elevation loss, resulting in a net gravity decrease. During periods of inflation, a net gravity increase occurs, reflecting the addition of mass to the reservoir. Over the longer term, the summit data show a slight increase in residual gravity, possibly reflecting the addition of mass to the summit from both repeated intrusions and the accumulation of settled olivine in the growing reservoir.

HVO scientist reading gravity meter. Readings are made periodically during Kilauea summit inflation/deflation cycles (Photograph by T. J. Takahashi, USGS)

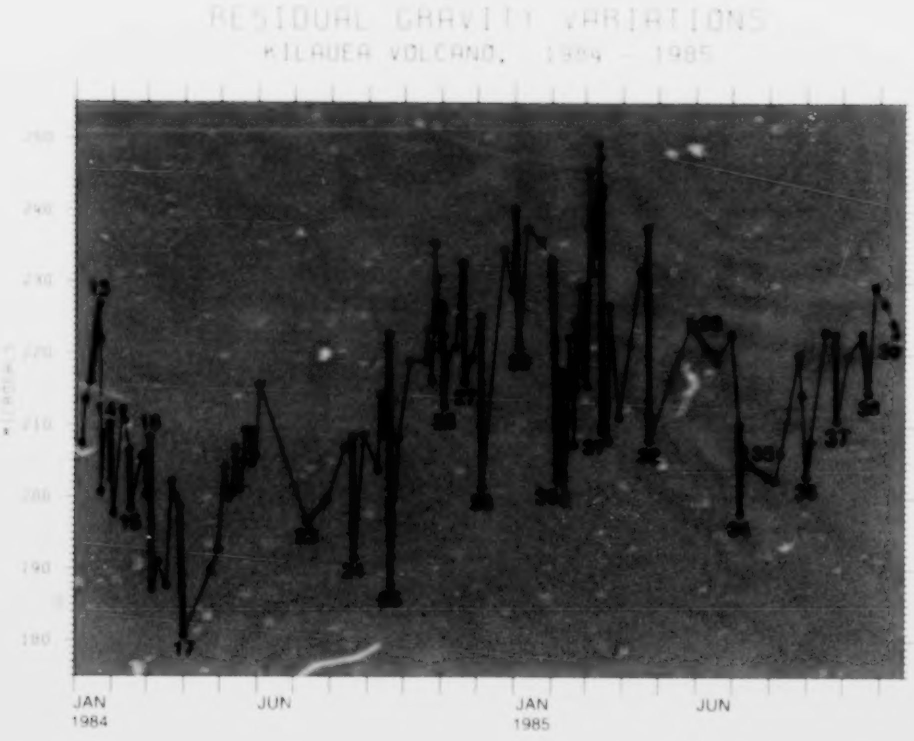

Gravity measured at Kilauea summit during 1984 and 1985 (corrected for elevation changes). The gravity variations reflect mass changes produced by the flow of magma into and out of the storage reservoir. Measurements spanning eruptive episodes at Pu'u O'o are marked by bold lines. Eruptive episodes are numbered.

Geology

The role of the geologic program at HVO is both to assess the potential hazards to life and property during eruptions and to conduct research that will help define the physical and chemical processes that take place during magma storage and transport. In the process of studying active volcanoes, geologists learn to apply their observations to features seen at extinct volcanoes elsewhere in the world. Thus the body of knowledge acquired at HVO becomes a valuable resource for anyone studying older eruptions of basalt—even millions of years older—where there was no opportunity to observe the actual activity itself.

The geologic monitoring program is currently focused on an eruption of Kilauea that began in January 1983 in a relatively inaccessible part of the east rift zone. The ongoing eruption has

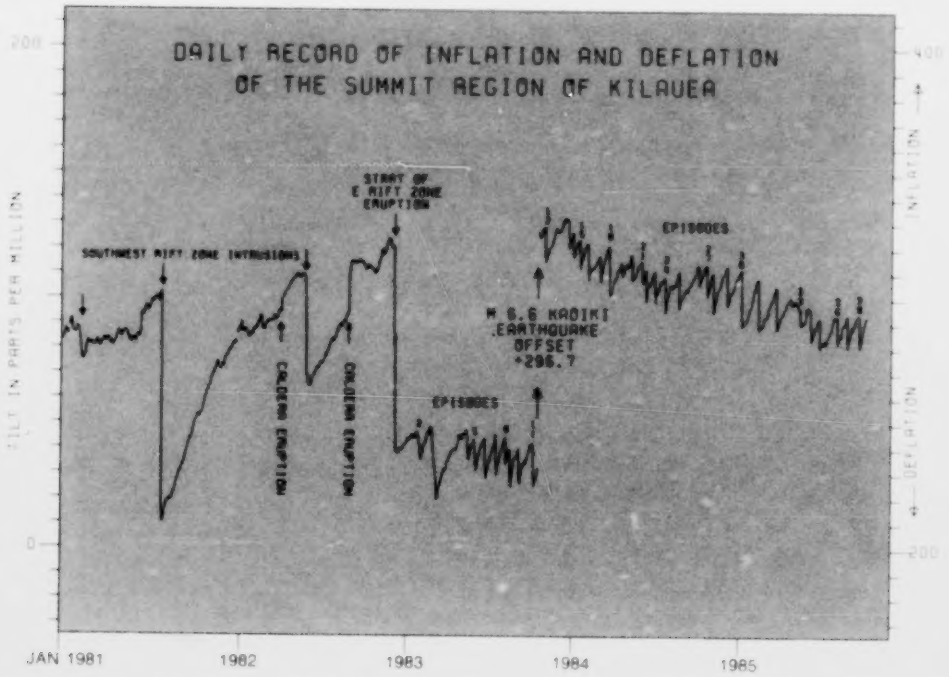

E-W component of ground tilt at Kilauea summit, 1981–1985. Data show the large subsidence that accompanied the beginning of the east rift zone eruption in January 1983, and the episodic inflation/deflation cycles that characterize the continuing eruption at Pu'u O'o

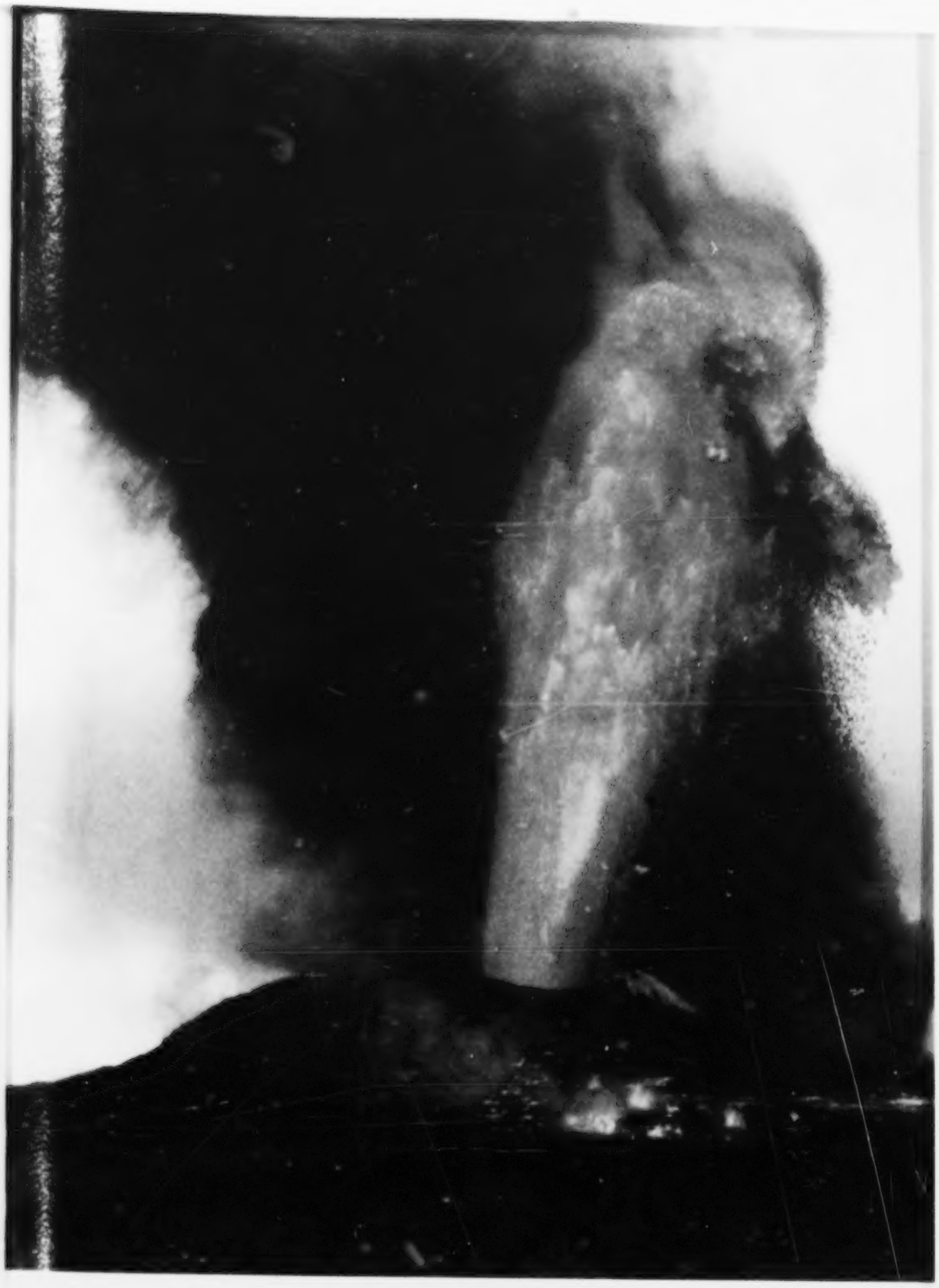

Lava fountain at Pu'u O'o, September 1984. The fountain is about 450 m high. (Photograph by C.C. Heliker, USGS) shown episodic behavior, with discrete periods of eruptive activity that are defined by cycles of inflation and deflation at Kilauea's summit. Most episodes last from 5 to 60 hours, separated by periods of repose lasting from 8 to 60 days, with an average of 25 days. Since June 1983, the activity has been localized at the Pu'u O'o vent.

Although eruptive vents on both Kilauea and Mauna Loa are generally located well away from populated areas, lava flows moving inexorably seaward do pose a threat. Flows from the eruption at Pu'u O'o have repeatedly entered a subdivision that was built on land classified as having a high volcanic risk because of its proximity to Kilauea's east rift zone.

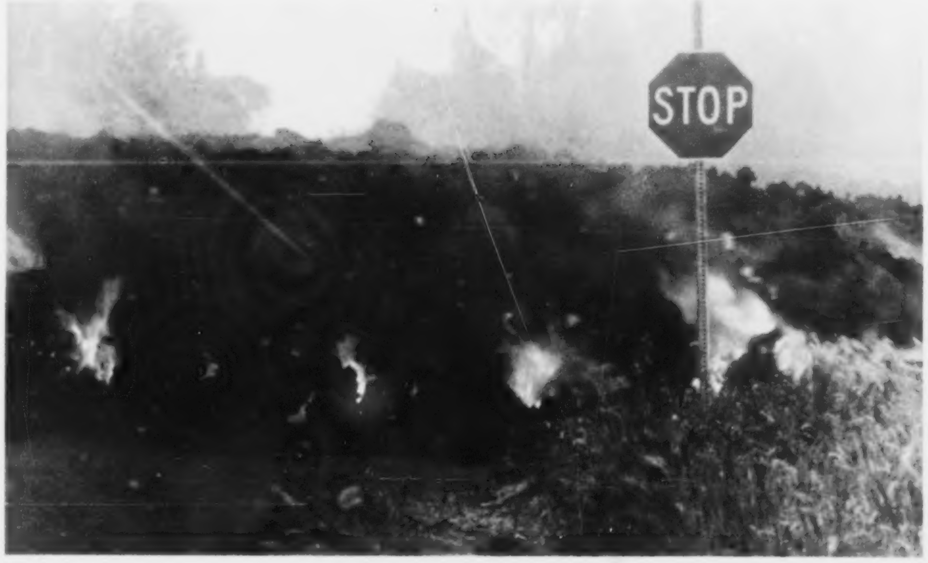

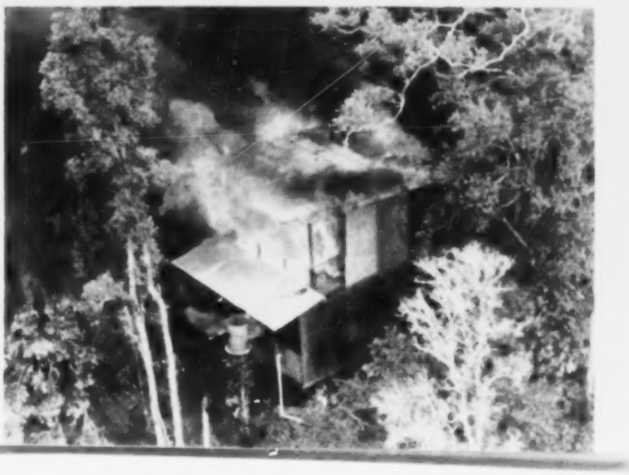

The Royal Gardens subdivision, located downslope of Pu'u O'o, has become a costly lesson in land-use planning. Above: Road blocked by a'a flow. Right: Residence consumed by advancing a'a flow. (Photographs by J. D. Griggs and J. J. Dvorak, USGS)

Left: HVO camp established in 1984 on a spatter cone 1.5 km east of Pu'u O'o. Time-lapse cameras to the left of the shed provide a continuous record of activity. (Photograph by J. D. Griggs, USGS)

Right: Measuring the temperature of a pahoehoe *flow. One person holds a heat shield, while others manipulate a chromel-alumel thermocouple. (Photograph by J. D. Griggs, USGS)*

Geologists at HVO are responsible for keeping local officials informed about the location and rate of lava flow motion so that evacuation plans can be made, if necessary. To facilitate both hazard evaluations and routine fieldwork, a makeshift camp was established on Pu'u Halulu, a spatter cone built during early episodes of the Pu'u O'o eruption. Accessible by helicopter, the site is used as a base for observing eruptions during the night.

During eruptive episodes, lava and tephra (airfall) samples are collected at intervals, and lava temperatures are obtained when possible. Special studies, generally made in collaboration with other groups, concentrate on fountain characteristics such as the velocity and acceleration of tephra; on the velocity structure of lava rivers, which can define physical parameters such as viscosity and yield strength; and on other topics that require field observation of the eruption. Visual observations are supplemented by photography of various kinds. Time-lapse cameras, which expose one frame every three minutes, are particularly useful for continuous documentation of activity, even when observers are not present.

Following eruptive episodes, aerial photographs are taken, and maps are made of the new lava flows. The thickness of the flows is measured at selected points, and, using the area obtained from the map, eruptive volumes are calculated. Periods of repose also provide an opportunity to carry out geodetic and seismic studies near the vent. These short-term investigations supply information on the local magma conduit and storage system at Pu'u O'o and supplement the data gained by the permanent monitoring network.

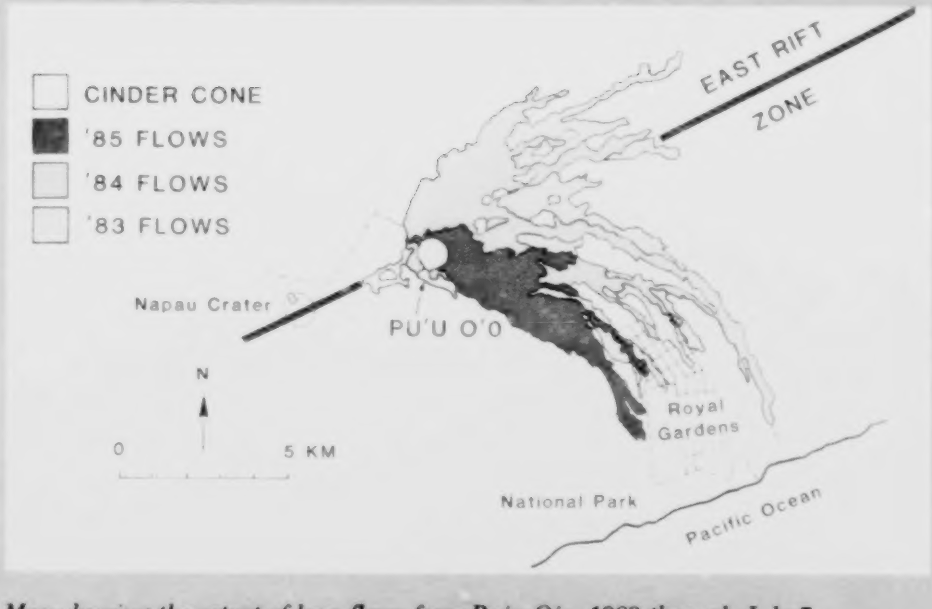

Map showing the extent of lava flows from Pu'u O'o, 1983 through July 7, 1985. The Royal Gardens subdivision is shown at the lower right, directly downslope from the axis of the east rift zone.

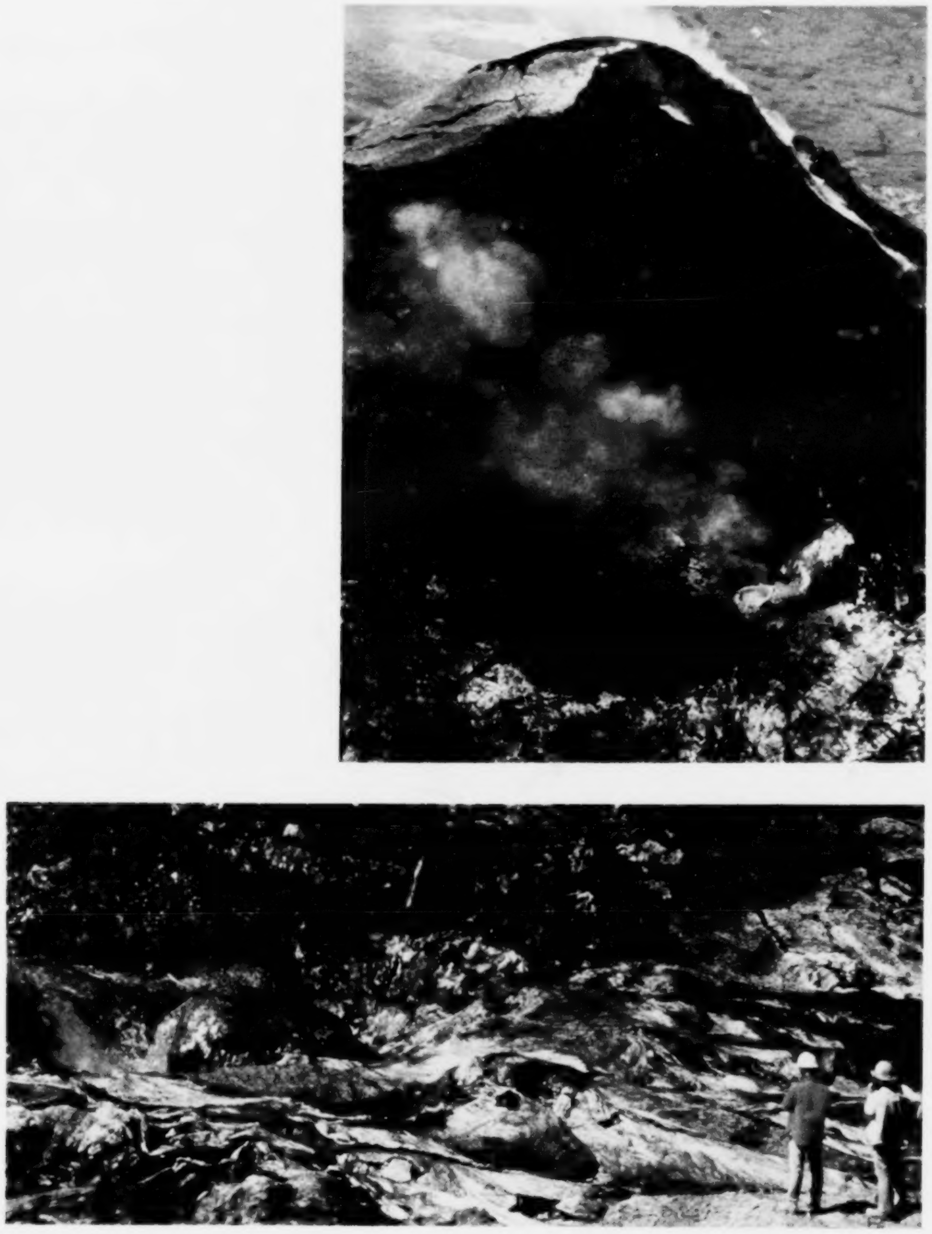

Interphase activity inside the crater of Pu'u O'o. Top: Aerial view to the southwest showing the Pu'u O'o vent, which is approximately 110 m lower than the top of the cone. This photograph was taken one day before episode 39 in November 1985, when the magma was three meters below the conduit rim. Bottom: Spatter is rising from the conduit, which is about 20 m in diameter. The HVO geologists are standing on fresh pahoehoe *overflows. (Photographs by J. D. Griggs and C. C. Heliker, USGS)*

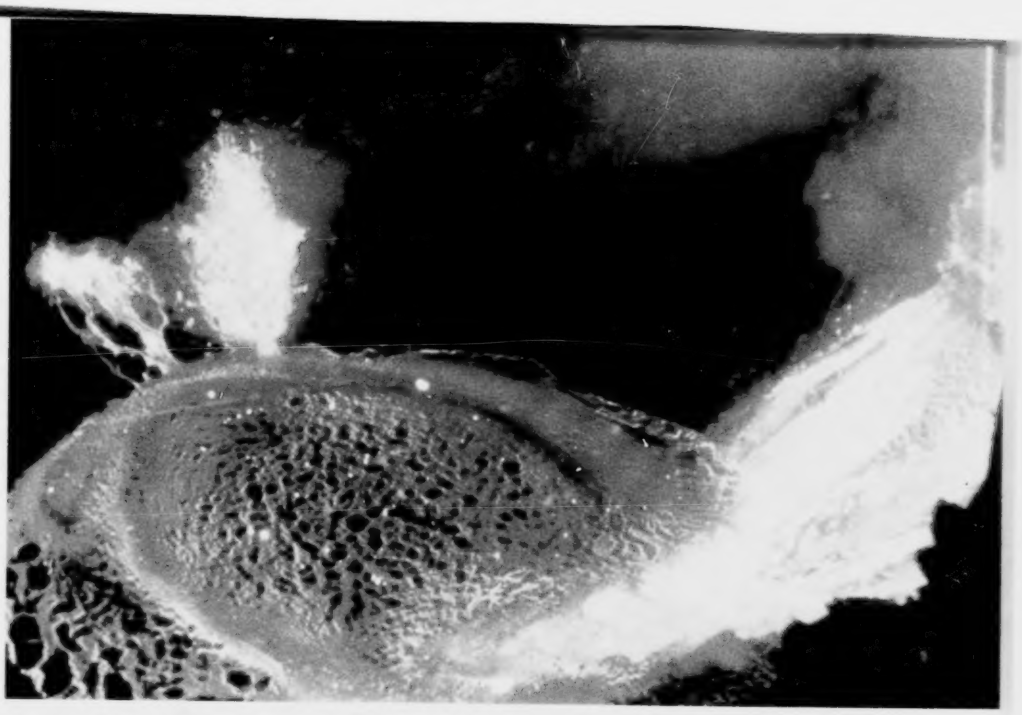

The eruption of Pauahi crater, November 11, 1973, formed a lava lake. (Photograph by R. I. Tilling, USGS)

During repose periods, the magma slowly rises in the vent and may produce low fountains and small overflows in the crater, hours to days before high fountaining begins. These conditions allow crews to sample lava and gases directly from the vent. Samples collected during either repose periods or eruptive episodes contain a record of the changing conditions within the magma reservoir. The bulk chemistry of most samples is determined, and thin sections of the lava are prepared to identify under a microscope the minerals present at the time of extrusion. Samples collected at intervals during the eruption are particularly valuable, as the earliest products of most eruptions are covered by later activity at the same vent, or ultimately, by other eruptions.

Interpretations of the mineralogy and petrology of the current eruption of Kilauea are aided by a unique body of data obtained from lava lake studies conducted in the 1960's and 1970's. During this period, three eruptions occurred within or at the edge of pit craters and created ponded lava lakes that were investigated by core drilling after the lake surface had cooled.

The drill core was examined to determine its chemical composition, density, and vesicularity. Open drill holes were used to measure temperature profiles and the composition of gases escaping from the crystallizing basalt. Occasionally, it was possible to emplace casings into the melt through the bottom of the drill hole; a rotational viscometer could then be lowered into the melt to measure its viscosity.

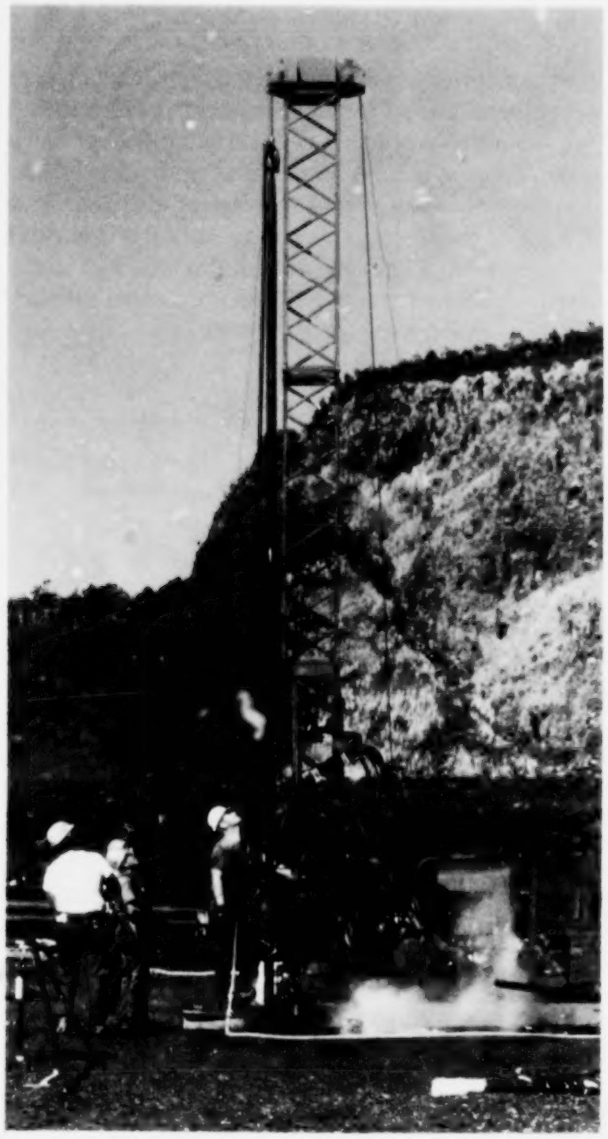

Drill rig in Kilauea Iki crater rests on the surface of the lava lake, which has been drilled six times since it formed in 1959.

From the lava lake studies we have direct knowledge of what happens when Kilauea magma cools and crystallizes, including the temperature at which different mineral phases appear, the processes by which crystals are separated from the liquid magma, and the rates of crystal growth. This knowledge, combined with the chemical and petrographic (study of rocks using a microscope) data collected during every eruption since 1952, has yielded insights into the differentiation processes that occur during storage and transport of the magma. Magmas of subtly different chemistry are supplied from the Earth's mantle to Kilauea's summit reservoir at intervals from months to years. These are the magmas available for eruption or further storage anywhere in the volcano, and their chemistry can be used as a fingerprint to track their progress through the summit and rift plumbing system.

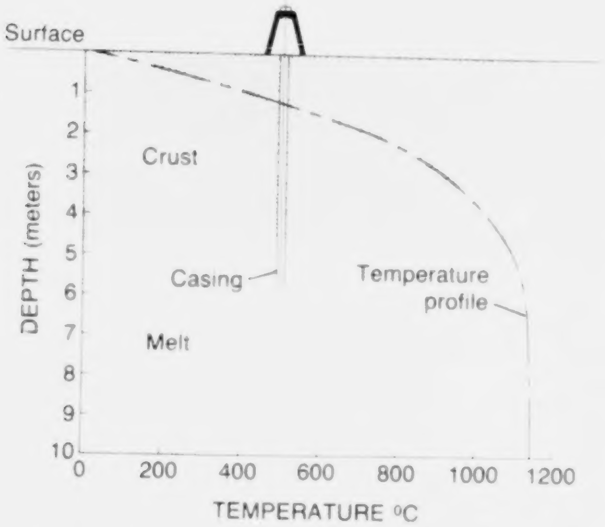

Sketch showing results of drilling into a Kilauea lava lake. Drilling took place five months after the eruption was over when the crust was 4.5 m. thick. Drilling establishes the rate of growth of the upper crust. The boundary between the crust (shaded), which behaves as a solid, and the melt, which behaves as a liquid, is at a temperature of 1070°C, with about equal amounts of melt and crystals. (From Shaw and others, 1968)

It is common for magma from the summit to encounter magma previously stored in the rift zone whose liquid composition has already changed due to cooling and crystallization. A hybrid lava results, and the evidence of mixing is demonstrable, both from chemical and petrographic analyses. Thus, lava chemistry and petrography can reveal the source of the magma, the length of time in storage, and whether or not mixing has taken place.

Using a combination of geologic, geochemical, and geodetic data, the magma balance of Kilauea can be determined by comparing the volume of magma entering the summit reservoir to the volume of erupted lava. The surprising conclusion is that over the past three decades nearly 50 percent of all magma arriving from the mantle remains below ground to cool and crystallize as intrusive dikes and sills. Thus a large part of the volcano's growth results from internal accretion, as well as from the addition of new lava to the surface.

Geoelectrical Studies

The movement of magma beneath the earth's surface changes the local electrical properties of the earth. These effects can be measured by a variety of surface instruments. Two techniques that are used for monitoring the geoelectrical properties of active volcanoes are self-potential (SP) surveys and controlled-source electromagnetic (CSEM) measurements.

Self-potential refers to the spontaneous electrical potentials generated in the ground by electrochemical reactions between hot volcanic water and the surrounding rocks. Two types of SP measurements are made on Kilauea: profiling for mapping or monitoring and fixed-array monitoring. Profiling measurements are made by advancing a measuring electrode to successive positions along a single traverse line and reading the naturally-occurring electrical potentials, relative to a stationary reference

Location of self-potential (SP) profiles on Kilauea.

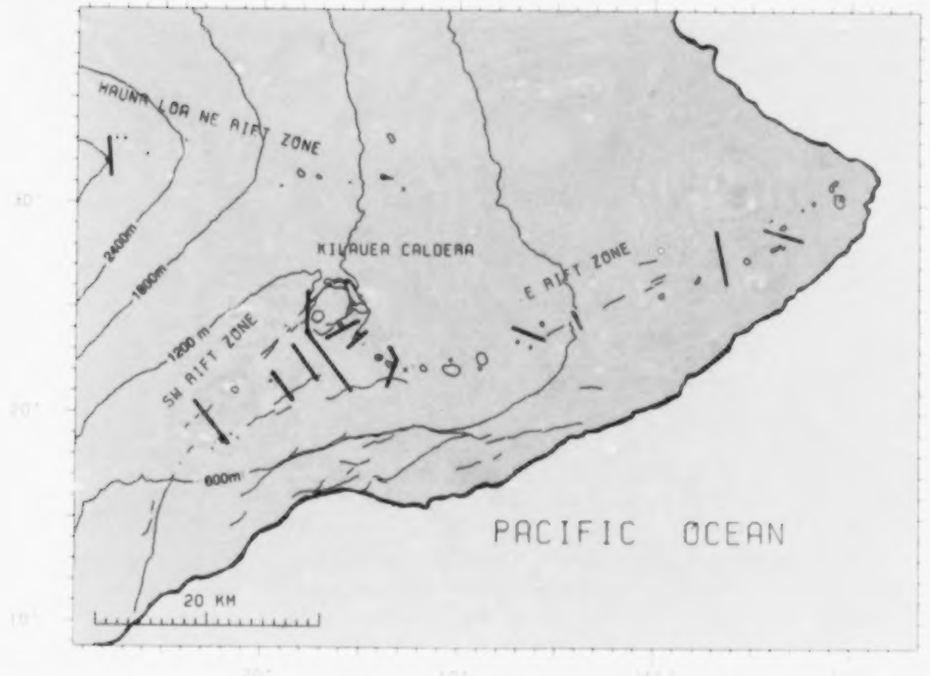
MAUNA LOA NE RIFT ZONE
KILAUEA CALDERA
E RIFT ZONE
SW RIFT ZONE
2400m
1800m
1200 m
600m
PACIFIC OCEAN
20 KM
30'
20'
10'
20'
10'

electrode. Fixed-array SP monitors use electrodes permanently sited along a traverse, and electrical potentials are read relative to a permanently-sited reference electrode.

Large SP anomalies (in some cases greater than one volt) are caused by electrokinetic and/or thermoelectric effects, both of which are ultimately related to a source of subsurface heat. Electrokinetic potentials are generated by the flow of fluid through porous rocks in response to differential pressures, such as those developed by convection in a geothermal cell, and perhaps by ascending steam or magma in fractures. Thermoelectric potentials are generated by temperature gradients across a section of rock, such as at the boundary between an intrusion and the adjacent wall rock. Either thermoelectric or electrokinetic mechanisms can produce the positive monopolar anomalies typically measured over intrusions and across eruptive fissures at Kilauea. The SP method is particularly useful for locating and mapping the extent of shallow bodies of intruded magma that may not have a visible surface expression, such as steam emission or ground displacement.

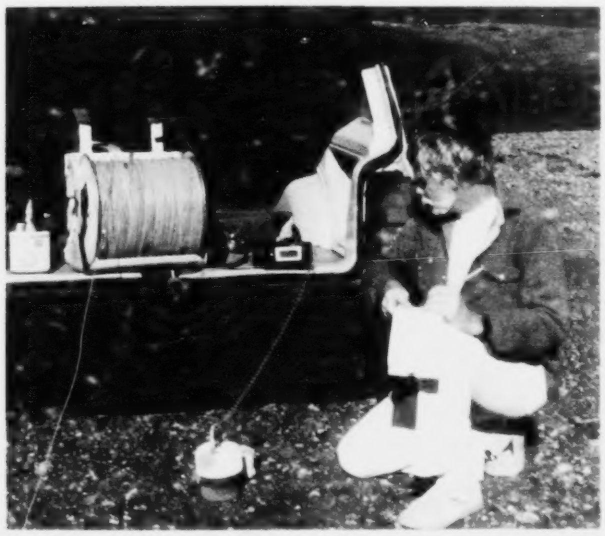

HVO geophysicist reading SP meter at base station on Kilauea's summit. (Photograph by J. D. Griggs, USGS)

Self-potential profile across the southwest rift zone of Kilauea. Positive SP peaks, in some cases greater than 800 millivolts in amplitude, are associated with both the noneruptive fissures of the 1963 intrusion and the eruptive vents of 1971 and 1974. Some prehistoric eruptive vents show moderately large SP anomalies, suggesting that they still have continuity to heat sources at depth. Depth and configuration of the heat sources are hypothetical.

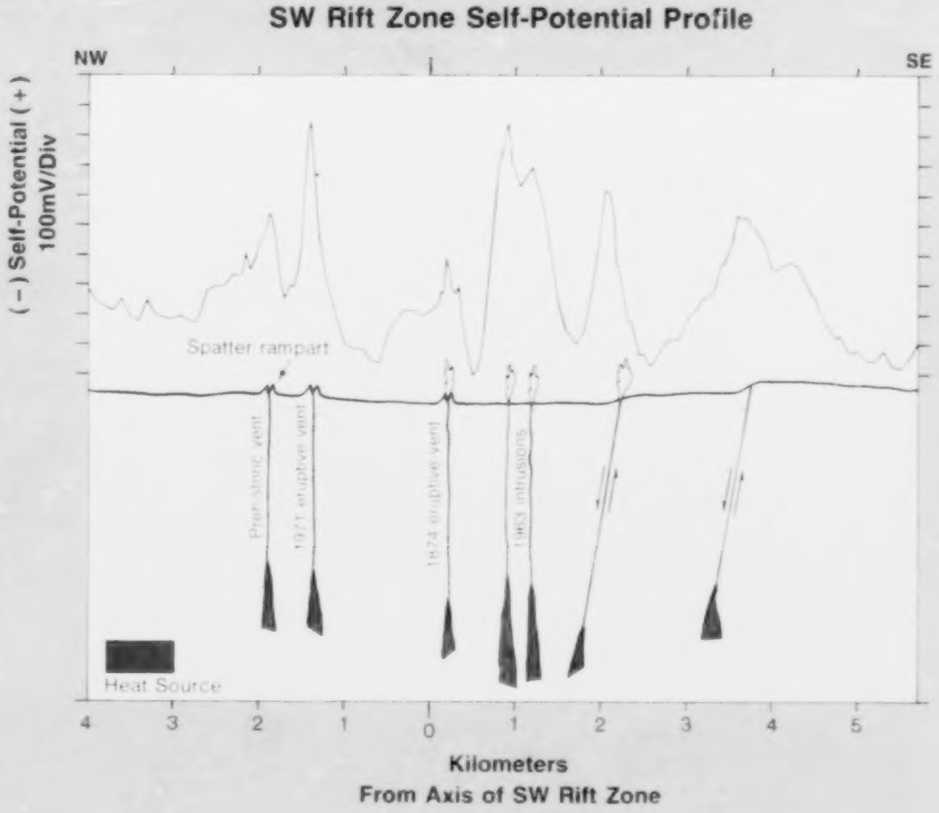

Top right: CSEM array on Kilauea's summit. Crosses mark epicenters of earthquakes accompanying the January 20, 1981, south summit and southwest rift zone intrusion. →

Bottom right: CSEM amplitude and phase response at the OTL receiver loop to a nearly aseismic intrusion during the period from January 10 to 19 that preceded the highly seismic intrusion of January 20. Minimal ground displacement, shown by the trace of the Sand Hill tiltmeter, suggests that the intrusion may have been largely filling preexisting voids until January 25. (From Jackson and others 1986)

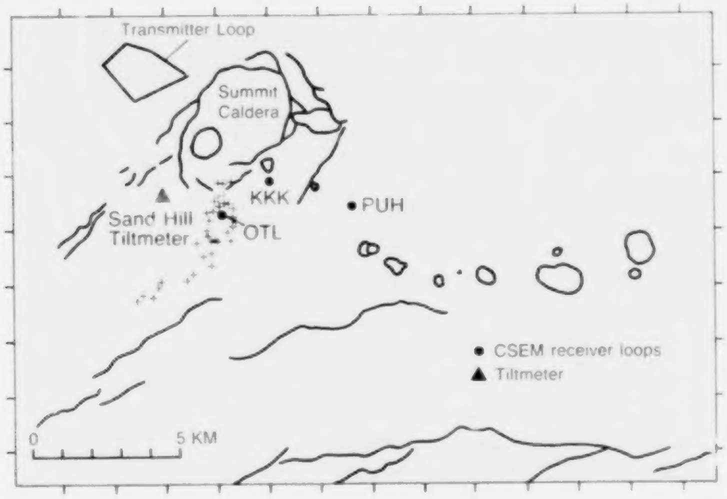
Transmitter Loop
Summit Caldera
KKK
PUH
Sand Hill Tiltmeter
OTL
● CSEM receiver loops
▲ Tiltmeter
0
5 KM

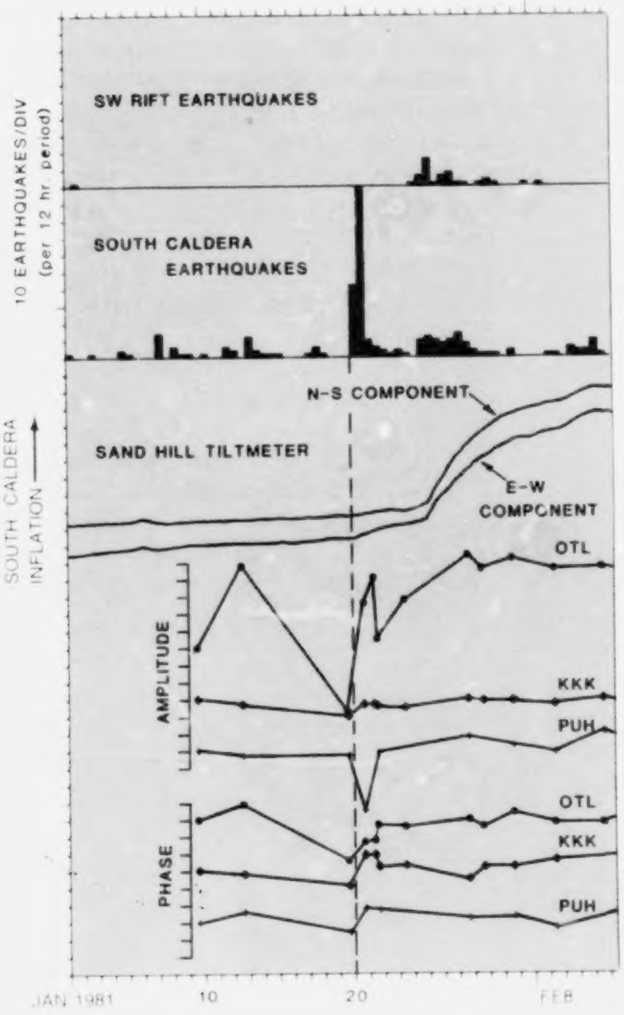
10 EARTHQUAKES/DIV (per 12 hr. period)
SW RIFT EARTHQUAKES
SOUTH CALDERA EARTHQUAKES
SOUTH CALDERA INFLATION ⟶
SAND HILL TILTMETER
N-S COMPONENT
E-W COMPONENT
AMPLITUDE
OTL
KKK
PUH
PHASE
OTL
KKK
PUH
JAN 1981
10
20
FEB

SP anomalies over intrusions generally decay with time as the magma body cools, unless continuity with a heat source at depth is maintained. In the latter case, self-potentials may vary with time in response to a changing heat flux. These changes can be recorded on a fixed array monitor and may indicate the passage of new magma beneath the recording site.

A CSEM experiment has been run at Kilauea since 1979. The phase and amplitude of the electromagnetic field produced by a transmitter loop, about 1 km northwest of HVO, is monitored in the summit and upper rift zone areas on three receiver loops. Since June of 1985, all data have been collected using a computer-controlled telemetry system.

The maximum depth to which an intrusion of molten magma may be identified is primarily a function of the frequency used and the resistivity of the earth surrounding the intrusion. As the frequency of the transmitted electromagnetic field decreases and/or the resistivity of the earth increases, the depth of investigation increases. Because the CSEM system uses extremely low frequencies, its depth of investigation is several kilometers, complementing the relatively shallow response of SP networks.

Thus far the significant CSEM changes observed at Kilauea are interpreted to represent shallow dike emplacement near the receiver loops. Because the electromagnetic monitor senses a low-resistivity target directly, it can identify passive intrusions or magma transport, through open areas of the volcanic edifice, that may cause little seismicity or ground displacement.

Gas Geochemistry

Much of the early scientific interest in Kilauea was directed at collecting gases emitted from the circulating lava lake in Halemaumau crater, which provided ideal sampling conditions prior to 1920. These samples resulted in some of the best data ever obtained on the chemistry of volcanic gases. In the last decade, gas geochemistry has come into its own once again, with HVO obtaining accurate analyses of Kilauea gases both from permanent fumaroles and from vents associated with recent eruptions. Gas collections are made using evacuated and "flow-through" sampling tubes and are analyzed for several chemical components.

Above: HVO geochemist collecting gases near an active vent on Kilauea's east rift zone, using a flow-through sampling bottle.
Right: Sampling gases at the Pu'u O'o vent.
(Photographs by J. D. Griggs and E. W. Wolfe, USGS)

Composition of Kilauea gases (weight per cent)

	Water Vapor (H_20)	Carbon Dioxide (CO_2)	Sulfur Dioxide (SO_2)
Magma arriving in summit reservoir	.32	.32	.09
Magma stored in rift zone	.28	.03	.08
Erupted lava	.05	<.01	.02

Volatile content of typical Kilauea gases, showing distinction between gases collected during summit eruptions, rift eruptions, and the residual gas content of erupted lavas. (From Greenland and others, 1985)

Measurement of sulfur dioxide in the Pu'u O'o plume using the ground-based Correlation Spectrometer (COSPEC). (Photograph by J. B. Stokes, USGS)

The composition of Kilauea summit gas is inferred to be in equilibrium with magma which has recently arrived from the mantle and is stored in the summit reservoir. Gases collected from rift eruptions are depleted in carbon dioxide (CO_2), which is above saturation levels in the magma reservoir and therefore escapes during summit or rift storage. These data, in combination with estimates of the magma supply rate, provide the basis for estimates of the amount of sulfur, carbon, and hydrogen that are added to the atmosphere each year from volcanic eruptions.

In addition to direct gas sampling, the bulk sulfur dioxide (SO_2) emissions both at Kilauea's summit and at Pu'u O'o are measured by the correlation spectrometer (COSPEC) in metric tons per day. COSPEC compares the spectra of the incoming light with the known spectra of sulfur dioxide to determine the amount of the gas in the volcanic plume. The COSPEC is

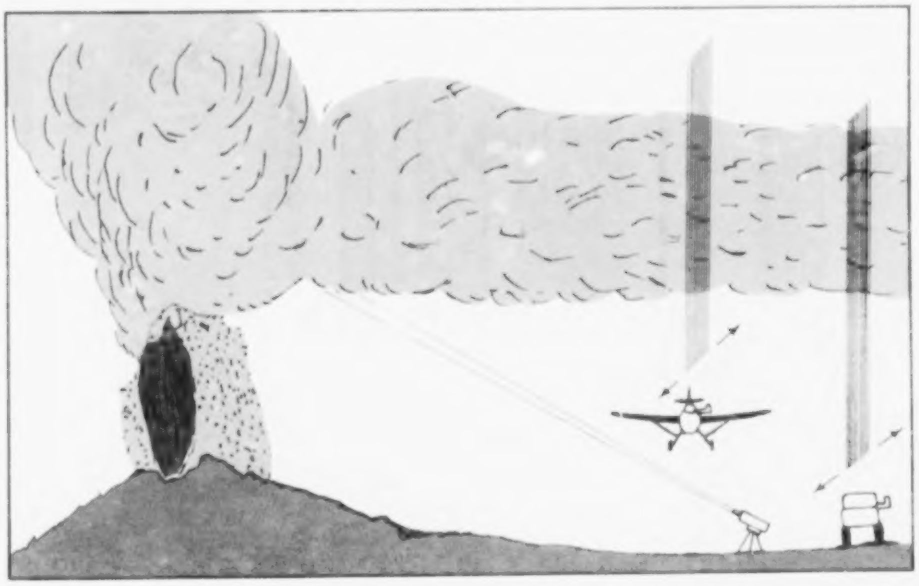

Diagram showing operation of airborne, truck-mounted, or ground-based COSPEC. In each case the instrument is placed so it can look at right angles to the volcanic plume. Measurement of wind-speed is necessary to convert the raw measurements of sulfur dioxide to a final figure of metric tons per day. (Sketch by Maurice Sako, USGS) aimed directly at a volcanic plume, either from the ground or from an airplane. Large numbers of measurements yield results that are statistically significant. COSPEC results have confirmed the calculated amount of sulfur dioxide released to the atmosphere determined from direct gas sampling.

At the beginning of the 1983 eruption of Kilauea, COSPEC measurements showed a distinct change in the total sulfur dioxide emission. Since the composition of the volatiles has been determined to be constant, the change in sulfur dioxide emission was inferred to mark an increase in the rate of magma supply, a result consistent with later analysis of ground deformation measurements and volumes of lava erupted at Pu'u O'o.

Sulfur dioxide concentrations at Kilauea summit showing the increase at the beginning of the 1983-present Pu'u O'o eruption.

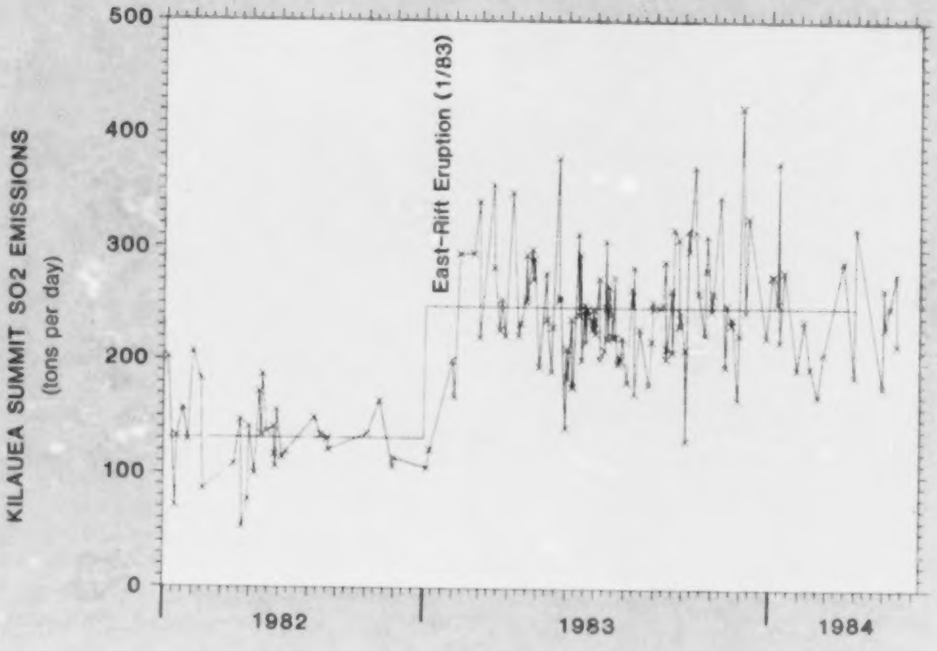

Eruptive gases collected during the 1984 eruption of Mauna Loa were the first ever obtained for that volcano. The analyses show less chlorine and fluorine than Kilauea gases, an observation in agreement with bulk rock chemistry. The Mauna Loa ratios of carbon dioxide to sulfur dioxide were more similar to gases from Kilauea rift eruptions than from summit eruptions, which implies that the magma erupted in 1984 had been stored long enough for it to degas. This is consistent with the slightly differentiated chemistry of the 1984 lavas and suggests a connection with the shallow magma intrusion in the northeast rift zone that followed the 1975 summit eruption.

The study of the physical processes by which gases are released from magma is important for understanding the mechanisms of lava fountains; further it contributes to the interpretation of harmonic tremor and other seismic phenomena associated with shallow magma movement. Gas studies have helped to explain the episodic behavior of the present Kilauea eruptions. Prior to each eruption, pressure must reach a critical level in the local Pu'u O'o reservoir before the rising magma column can push out the plug of degassed magma that is left in the upper part of the Pu'u O'o conduit at the end of each high-fountaining episode. Once this plug is extruded, the gases in the new volatile-rich magma rapidly escape, providing the energy for high lava fountains. The high extrusion rate acts to underpressurize the system, ending the eruption and setting the stage for the next episode.

Summary

In the preceding sections we have summarized the work of the Hawaiian Volcano Observatory in monitoring the active volcanoes of Hawaii. However, the impact of HVO extends far beyond this island. The Observatory regularly exports trained volcanologists, as well as the monitoring equipment and techniques developed at HVO, to volcanically-active areas all over the world.

Nearly all the USGS scientists who are trained in volcano monitoring served their apprenticeships at HVO. When Mount St. Helens became active in 1980, the Survey was able to respond rapidly because of the large number of mainland volcanologists who had been trained in Hawaii. Even now, the Cascades Volcano Observatory, established to monitor Mount St. Helens, has many HVO alumni on its permanent staff.

Current and former HVO personnel have provided the primary staff support during the Survey's recent cooperative effort with the Volcanological Survey of Indonesia to upgrade Indonesia's volcano observatories.

Hawaiian Volcano Observatory personnel are also available when foreign governments request assistance during volcanic crises. Most recently, HVO scientists traveled to Colombia to lend their expertise during the 1985 eruption of Nevado del Ruiz. In addition, HVO hosts many foreign scientists who work alongside HVO staff to learn about monitoring techniques and instrumentation.

The Hawaiian Volcano Observatory has had the unique advantage of being located on one of the world's most active and most easily-observed volcanoes. For this reason, the Observatory quickly achieved prominence in the field of volcanology, and HVO research in volcanic processes has received worldwide attention for many decades. The knowledge gained in Hawaii has been broadly applicable to research conducted elsewhere, such as studies of the physical properties of basaltic magmas, processes of basaltic differentiation, and earthquake focal mechanisms.

Once HVO's new building is complete in 1986, the Observatory will finally be able to make full use of the benefits of current scientific technology. As HVO nears its 75th anniversary, Thomas Jaggar would surely be pleased to see that much of his vision for the Observatory has been realized and that HVO continues to strive toward excellence in volcanologic and seismic studies.

HVO's new building in progress. (Photograph by J. D. Griggs)

References cited

Dzurisin, D., Koyanagi, R.Y., and English, T. T., 1984, Magma Supply and Storage at Kilauea Volcano, Hawaii, 1956–1983: J. Volcanol. Geotherm. Res., v. 21, p. 177–206.

Greenland, P., Rose, W. I., and Stokes, J. B., 1985, An Estimate of Gas Emissions and Magmatic Gas Content from Kilauea Volcano: Geochemica et Cosmochimica Acta, v. 49, p. 125-129.

Jackson, D. B., and Kauahikaua, J., 1986, Regional Self Potential Anomalies at Kilauea Volcano, Hawaii, *in* Decker, R. W., Wright, T. L., and Stauffer, P. H., U.S. Geological Survey Professional Paper 1350 (in press).

Kinoshita, W. T., Krivoy, H. L., Mabey, D. R., and MacDonald, R. R., 1963, Gravity Survey of the Island of Hawaii: U.S. Geological Survey Professional Paper 475-C, p. C114–C116.

Klein, F. W., Koyanagi, R. Y. Nakata, J. S., and Tanigawa, W. R., 1986, The Seismicity of Kilauea's Magma System, Hawaii, *in* Decker, R. W., Wright, T. L., and Stauffer, P. H., eds., Hawaiian Volcanism: U.S. Geological Survey Profissional Paper 1350 (in press).

Koyanagi, R. Y., Chouet, B., and Aki, K., 1986, Origin of Volcanic Tremor in Hawaii, Data from the Hawaiian Volcano Observatory, 1969–1985, *in* Decker, R. W., Wright, T. L., and Stauffer, P. H., eds., Hawaiian Volcanism: U.S. Geological Survey Professional Paper 1350 (in press).

Koyanagi, R. Y., Endo, E. T., Tanigawa, W. R., Nakata, J. S., Tomori, A. H., and Tamura, P. N., 1984, Kaoiki, Hawaii Earthquake of November 16, 1983. A Preliminary Compilation of Seismographic Data at the Hawaiian Volcano Observatory: U.S. Geological Survey Open-File Report 84–798, 35 p.

Koyanagi, R. Y., Tanigawa, W. R., and Nakata, J. S., Seismicity Associated with the Eruption of Kilauea Volcano from January 1983 to July 1984: U.S. Geological Survey Professional Paper (in press).

Koyanagi, R. Y., Unger, J. D., Endo, E. T., and Okamura, A. T., 1974, Shallow Earthquakes Associated with Inflation Episodes at the Summit of Kilauea Volcano, Hawaii, *in* Ferran, G., ed., Symposium on Andean and Antarctic Volcanology Problems, Santiago, Chile, September 1974, Proceedings: International Association of Volcanololgy and Chemistry of the Earth's Interior Special Series, p. 621-631.

Lipman, P. W., Lockwood, J. P., Okamura, R. T., Swanson, D. A., and Yamashita, K. M., 1985, Ground Deformation Associated with the 1975 Magnitude 7.2 Earthquake and Resulting Changes in Activity of Kilauea Volcano, Hawaii: U.S. Geological Survey Professional Paper 1276, 45 p.

Okamura, A. T., Dvorak, J. J., Koyanagi, R. Y., and Tanigawa, W. R., Surface Deformation Associated with the 1983 Kilauea Eruption: U.S. Geological Survey Professional Paper (in press).

Shaw, H. R., Wright, T. L., Peck, D. L., and Okamura, R., 1968, The Viscosity of Basaltic Magma: An Analysis of Field Measurements in Makaopuhi Lava Lake, Hawaii: American Jour. of Science, v. 266, p. 255–264.

Tilling, R. I., 1983, Monitoring Active Volcanoes: Washington, U.S. Government Printing Office, 14 p.

Tilling, R. I., Koyanagi, R. Y., and Holcomb, R. T., 1975, Rockfall Seismicity—Correlation with Field Observations, Makaopuhi Crater, Kilauea Volcano, Hawaii: Jour. Research U.S. Geological Survey, v. 3, no. 3, p. 345–381.

Wright, T. L., and Fiske,, R. S., 1971, Origin of the Differentiated and Hybrid Lavas of Kilauea Volcano, Hawaii: Journal of Petrology, v. 12, p. 1-65

EDM site at Pu'u Kamoamoa.
(Photograph by J. D. Griggs, USGS)

SUBSCRIPTION ORDER FORM

Enter my subscription to "Earthquakes and Volcanoes" at $15.00 (domestic) or $18.75 (foreign). Domestic remittance should be made by money order or check or charged to VISA or MASTERCARD. Foreign remittance should be made by international money order, draft on an American bank, or UNESCO coupons.

NAME—FIRST, LAST

COMPANY NAME OR ADDITIONAL ADDRESS LINE

STREET ADDRESS

CITY

STATE

ZIP CODE

PLEASE PRINT OR TYPE

(or) COUNTRY

☐ MasterCard ☐ VISA

MAIL ORDER FORM TO:
Superintendent of Documents
Government Printing Office
Washington, D.C. 20402

Credit Card No.

Expiration Date Month/Year

Bank No.

Signature ______________________

HVO staff photo.

Back row (L to R): *Maurice Sako, Alvin Tomori, Allen Largo, Ken Honma, Tom Wright, Gary Puniwai, Gary Honzaki, Lu Setnicka*

Middle row: *Will Tanigawa, Akira Yamamoto, Craig Crissinger, Barry Stokes, Arnold Okamura, Christina Heliker, Jane Takahashi, George Ulrich, Tom English, Zoe Jacobi, Ron Hanatani*

Front row: *Jim Griggs, John Forbes, George Kojima, Marian Kagimoto, Dallas Jackson, Paul Greenland, Jennifer Nakata, Reggie Okamura, Dorothy Footer, Bob Koyanagi*

U.S. GOVERNMENT PRINTING OFFICE
PUBLIC DOCUMENTS DEPARTMENT
WASHINGTON, D.C. 20402

OFFICIAL BUSINESS
PENALTY FOR PRIVATE USE $300

BULK RATE MAIL
POSTAGE & FEES PAID
USGS
PERMIT No. G23

Department of the Interior
U.S. Geological Survey

Earthquakes & Volcanoes

Volume 18, Number 2, 1986

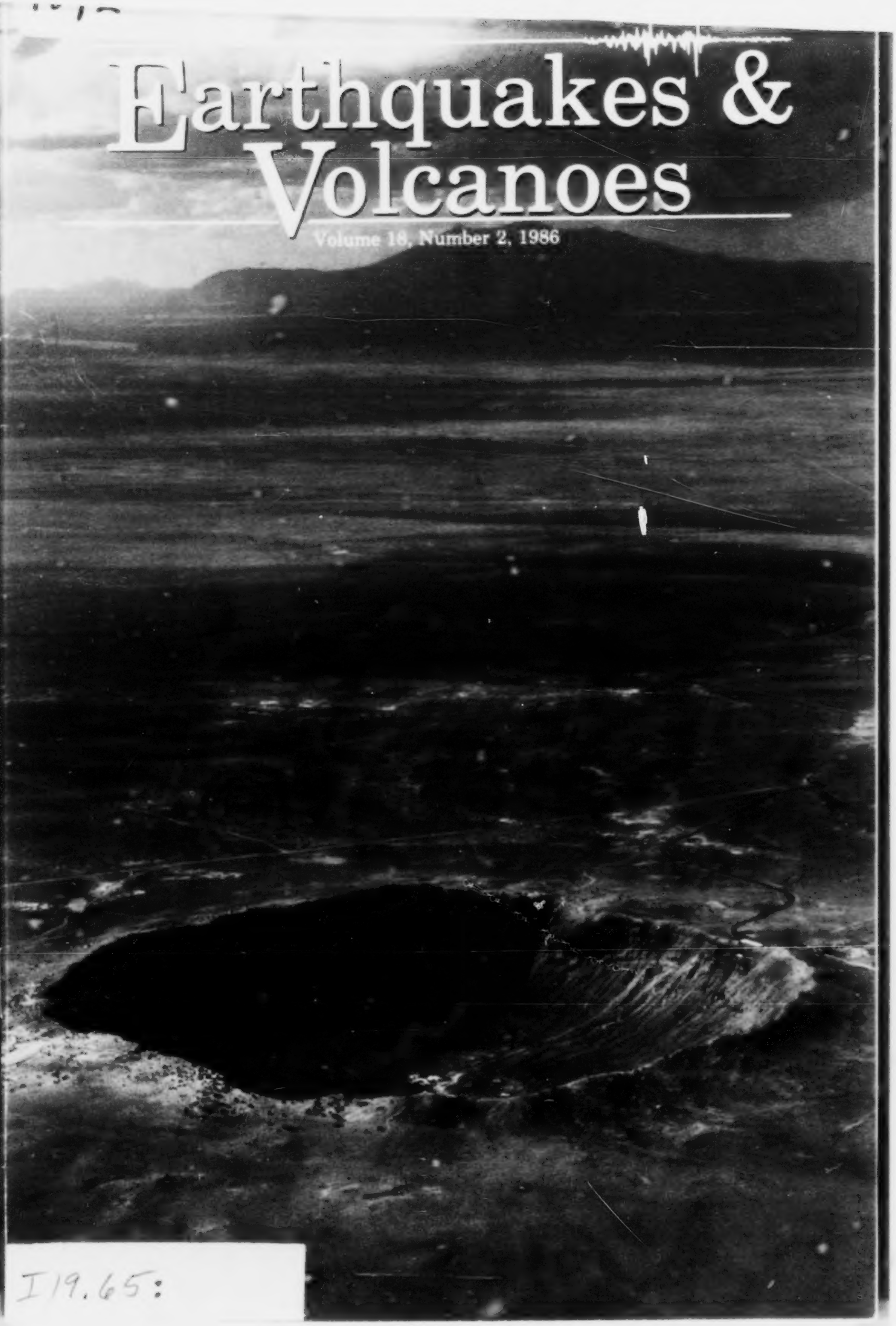

I19.65:

UNITED STATES DEPARTMENT OF THE INTERIOR
Donald Paul Hodel, Secretary

U.S. GEOLOGICAL SURVEY
Dallas, L. Peck, Director

Earthquakes and Volcanoes is published bimonthly by the U.S. Geological Survey to provide current information on earthquakes and seismology, volcanoes, and related natural hazards of interest to both general and specialized readers.

The Secretary of the Interior has determined that the publication of this periodical is necessary in the transaction of the public business required by law of this Department. Use of funds for printing this periodical has been approved by the Office of Management and Budget through June 30, 1989.

Henry Spall—Editor

Earthquakes and Volcanoes
U.S. Geological Survey
904 National Center
Reston, Virginia 22092
Telephone (703) 648-6078

Patricia Hickman—Graphics Design

Subscription orders should be sent to:

Superintendent of Documents
U.S. Government Printing Office
Washington, DC 20402
Telephone (202) 783-3238

For sale by the Superintendent of Documents. Annual subscription rate—$15.00 (domestic) and $18.75 (foreign). Make check or money order payable to the Superintendent of Documents.

Single copy rate—$3.00 (domestic) and $3.75 (foreign). Single copy rate for issues prior to Volume 15, Number 1—$2.25 (domestic) and $2.85 (foreign). Can be purchased from the Book and Open-File Reports Section, U.S. Geological Survey, Federal Center, Building 41, Box 25425, Denver, CO 80225 (make check or money order payable to the Superintendent of Documents).

Cover

Meteor Crater, Arizona—the most spectacular crater on Earth, about three quarters of a mile across and 600 feet deep. It was formed 50,000 years ago by a meteorite 150 feet across and weighing 300,000 tons. In the background are the San Francisco Peaks and their associated volcanic field. Canyon Diablo is the sinuous trace behind the crater. Photograph by David Roddy and K. Zeller.

Earthquakes & Volcanoes

(formerly *Earthquake Information Bulletin*)

Volume 18, Number 2, 1986

FEB

U. S. GOVT. PUBS.
DEPOSITORY 376

76 **Volcanoes and Atmospheres: Catastrophic Influences on the Planets**
by Susan Werner Kieffer

84 **Meteroids and Impact Craters**

90 **New Theories about Ancient Extinctions**

93 **The Tunguska Comet or the Great Siberian Mystery Explosion of 1908**

98 **Halley's Comet - A Benevolent Visitor to Earth**

106 **About the Authors**

Volcanoes and Atmospheres:

Catastrophic Influences on the Planets

Susan Werner Kieffer
U.S. Geological Survey
Flagstaff, Arizona

For a rare and brief instant in geologic time, we can imagine that the sulfurous, chromatic surface of Io (one of the satellites of Jupiter) lies quiet. Perhaps stars glisten brilliantly through the tenuous night sky. Here and there, thick icy fogs enshroud fumaroles where sulfur dioxide leaks from the underworld. Suddenly, a fissure splits the surface and billowing clouds of sulfurous gases and ice hurl orange and black ash into the atmosphere. Minute by minute, the intensity of the eruption builds; stars begin disappearing from the night sky. The rising plume inhales the nearby atmosphere, mixing it with the exhalations from the volcano. Particles of sulfur, sulfur dioxide snow and ash rise to 300 kilometers, later raining down across the planet a thousand kilometers away.

An area the size of Alaska is rapidly engulfed by the products of the erupting volcano. Under the veil of plume ejecta, dense clouds of gas and ash roll across the land, their particles mixing with ash falling from the sky; lava flows rush in torrents down the slopes. Pele, the Hawaiian goddess, is playing with Loki, Marduk and other gods and goddesses of volcanism on Io. Time and time again, they repaint the land with different sulfurous colors. Their paint brushes are lava flows, ash hurricanes and ash falls; their paint pots are reservoirs of molten sulfur, sulfur dioxide and silicate that exist in the ground and atmosphere of Io.

The mythical figures of volcanism play and paint until the excess heat in the planet is gone. Then, almost suddenly, they retire into the underworld, having sculpted anew the surface, refreshed the atmosphere, and cooled the tempers of the fiery interior. All is quiet . . . briefly.

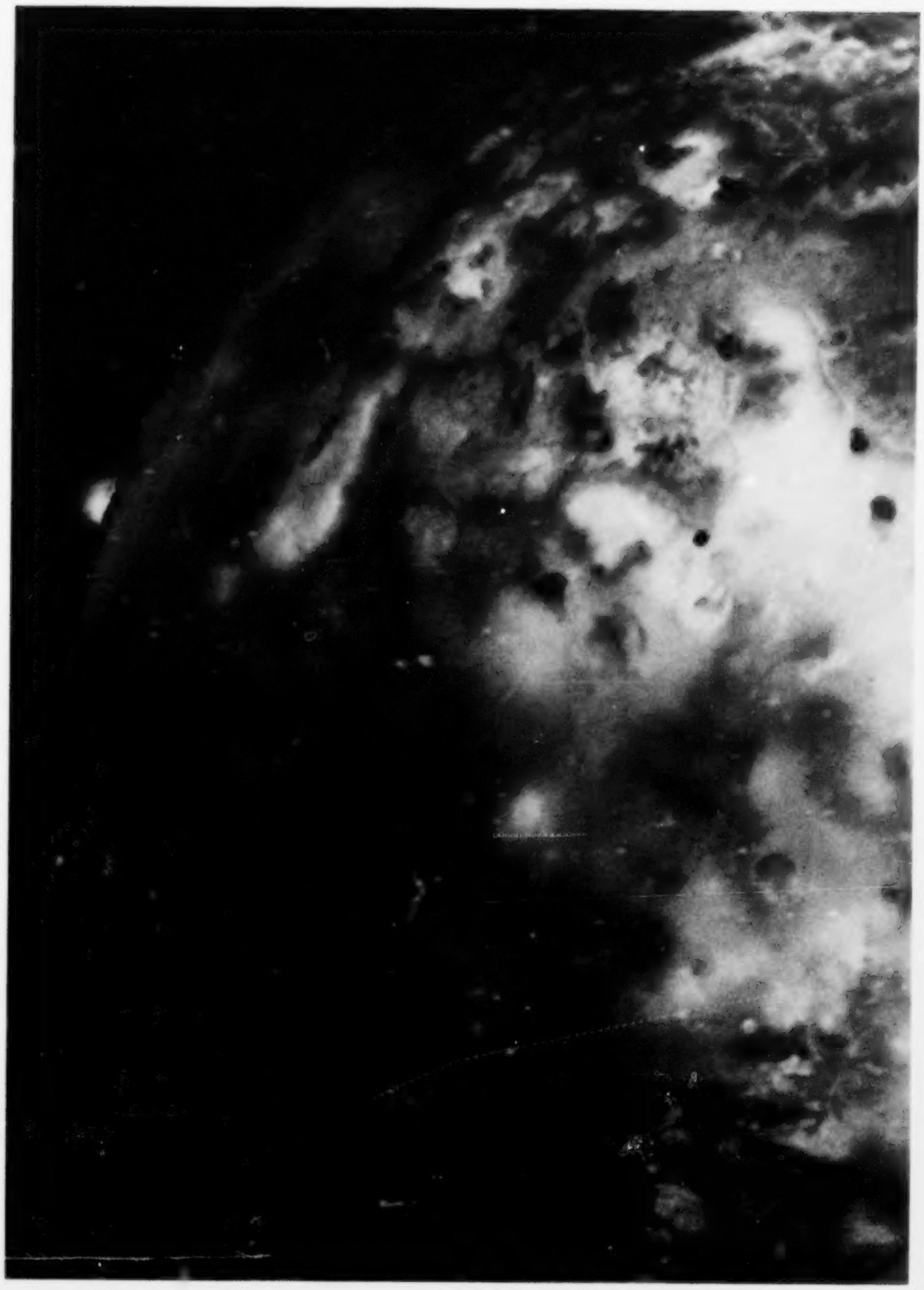

Computer-generated mosaic of Io, one of the four satellites of Jupiter—the others being Europa, Ganymede and Callisto. This photograph of Io was teken during NASA's Voyager I encounter with Jupiter from January to April, 1979. The numerous dark spots and surrounding rings were not caused by impact craters, but rather by violent volcanic action, with plumes of sulphur and sulphur dioxide extending 150 miles above the surface and eruption velocities up to 1 mile per second. On the left edge of the satellite can be seen the plume of Loki volcano. The volcanoes of Io are named after the gods and goddesses of volcanism on Earth. (Photograph courtesy of Al McEwen, USGS, and NASA).

Volcanoes and Atmospheres

Large volcanic eruptions are so common on Io that they hardly can be called catastrophes. But on Earth, even much smaller events so perturb the delicate balances of life, land and weather that we do call them catastrophes. For example, El Chichón, a small, remote volcano in Mexico, awakened in 1982. Ash flows rolled down its flanks and gullies, destroying villages and annihilating a tropical forest and its life. Ash and sulfurous droplets, propelled into the stratosphere by the towering column of gas emitted from El Chichón, circulated around Earth, reducing ever so slightly the warming effect of the Sun and causing a mildly cooler winter. El Chichón was giving us a gentle reminder that Io is not the only planet on which volcanic activity affects the atmosphere.

The historic record suggests that sometimes this reminder has been more severe. Often the most visible catastrophe from an eruption is the blanket of ash deposited from the volcanic plume, but ash is only part of the problem. In 1783, a 25-kilometer-long fissure split the ground in Iceland. For eight months lava oozed out over the Earth's surface at Laki; there were few of the fireworks and towering ash clouds that El Chichón displayed. Yet the continuous injection of sulfurous droplets from that eruption into the lower atmosphere dramatically altered the weather for several years: Red sunsets, atmospheric hazes and fogs, and cold winters were observed worldwide. Most of the livestock, and one-fourth of the people of Iceland, died from famine and starvation as a result of the weather change caused by the volcanic eruption.

Do volcanic eruptions influence long-term climatic patterns as well as day-to-day weather? Benjamin Franklin first suggested that the answer to this question was "yes." Scientists now realize that if the eruption of the 12 cubic kilometers of basalt at Laki over eight months could alter the climate for several winters, other much larger eruptions might have had even greater effects. The whole of northern and western India surrounding Bombay, an area of over 250,000 square kilometers, is covered by basalt flows, some reaching over three kilometers in thickness. About twenty million years ago over 130,000 square kilometers of Washington and Oregon were buried by thousands of cubic kilometers of basalt.

We will never know for certain the magnitude of the effects of these eruptions on the atmosphere, on life on the planet, and on glaciers and oceans. But after a century of controversy, we are beginning to believe that the effect of volcanoes on the Earth's atmosphere can indeed be catastrophic.

The eruption of El Chichón Volcano, southeastern Mexico, on April 22, 1982. The steam and ash plume is 12,000 feet high. Such clouds from the eruptions of El Chichón were the most extensive observed worldwide for many decades. (Photograph by United Press International.)

Atmospheres and Volcanoes

We are also learning that planetary atmospheres affect the type of devastation wrought by volcanoes because the atmospheres provide the "back-pressure" against which volcanic gases work when they enter the atmosphere. Volcanic gases originate in regions of a planet where pressures are a few hundred to a few thousand times greater than the atmospheric pressure at the surface of Earth. If high-pressure volcanic gases were suddenly exposed to the atmosphere, violent eruptions would blast hot gases and rock up, down and sideways—much as a water balloon exploding on a sidewalk has little directionality in selection of its victims.

But terrestrial volcanoes commonly vent their gases unidirectionally—most often vertically into the towering eruption columns that we call *plinian*, after Pliny the Younger's classic description of the eruption column from the 79 AD eruption of Vesuvius. That extremely violent eruption destroyed much of the ancient volcano and buried the Roman cities of Pompeii and Herculaneum under millions of tons of ash.

Why do many of the gases released from terrestrial volcanoes rush into these towering vertical columns instead of spreading out around the volcano? As magma (a mixture of melted rock and hot gases) rises from depth through a volcanic system toward Earth's surface, the pressure, density and temperature of the gases all decrease in response to the ascent. Energy that was stored in compression is used to overcome friction and gravity as the material rises, and to accelerate the material into the lower-pressure environment. Quantitative models of these processes indicate that the pressure on a magma can drop hundreds or thousands of times as the magma accelerates from its reservoir through the conduit to the vent where it enters the atmosphere. If there is any excess pressure left in the gas when it reaches the vent, lateral expansion in a small crater (less than 50 meters deep) relieves this pressure.

In a typical eruption then, volcanic gases are at about atmospheric pressure when they enter the atmosphere, and they simply flow from the volcano under the impetus of their own momentum—upward into a plume or, sometimes, laterally into a flow. Thus, although the scale is vastly different, the flow of gases in a plinian eruption is much like the flow of water from a fire hose, gas from an automobile exhaust pipe, or air through an orchestral flute.

Catastrophic Eruptions

Plumes *do* sometimes emerge into our atmosphere with a pressure higher than atmospheric. When this happens, the effects can be truly catastrophic. On May 18, 1980, gas and rock stored at more than 100 times atmospheric pressure in the north flank of Mount St. Helens were suddenly exposed to the atmosphere when the overlying rocks fractured and slid into the drainage of the North Fork of the Toutle River. Because the magma was stored so high in the volcano, pressure on the buried gases and hot rock could not be reduced by the normal processes that occur during ascent of magma through the crust. Instead, the depressurization happened as the flow accelerated across the land. (A similar decompression, although from lower pressure, occurs at the end of a rifle barrel, a geothermal bore or a rocket engine. The effect of varying atmospheric back-pressure can be seen as rockets ascend through the atmosphere. Their trailing plumes become more and more flared because the atmosphere becomes more tenuous and less able to confine the high-pressure gases.)

The climatic eruption of Mount St. Helens on May 18, 1980 was a typical Plinian eruption. The maximum height of the ash and gas column was about 12 miles. (Photograph by Austin Post)

Aftermath of the May 18 eruption of Mount St. Helens: tree blowdown on Smith Creek. Some of these trees were 3 feet in diameter and over 100 feet tall; note the people at the lower right. (Photograph by Lyn Topinka).

When the opening through which high pressure gases are released is large, the distance required for decompression of the gases is also large: The gases in the Mount St. Helens lateral blast remained at pressures greater than atmospheric for several kilometers, and over this distance obtained supersonic velocities over 100 meters per second. In this region, the forest was blown from the land, soil was stripped down to bedrock, and no life survived.

Because the vent through which the material within Mount St. Helens had to escape opened to the north, the blast was initially directed northward. However, because the gases in this material were at higher pressure than atmospheric, they expanded to both the east and west (as well as upward), and material was spread over the whole sector north of the volcano rather than being restricted to a narrow zone directly in line with the actual vent. The back-pressure of the terrestrial atmosphere, however, kept the blast confined to the northern sector of the volcano, and much of the southern flank was spared the direct effect of the blast (although it was devastated by later ash flows).

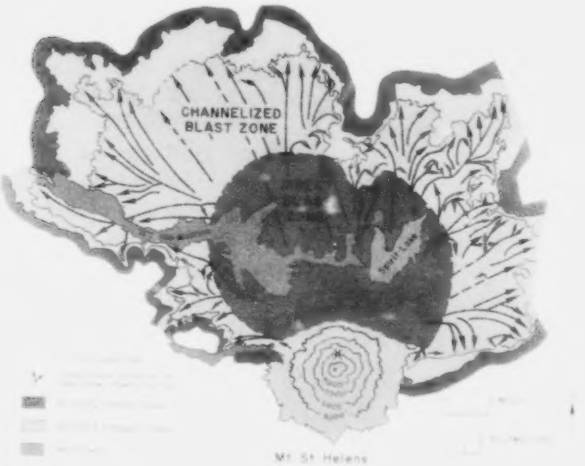

Map of the devastation caused by the lateral blast at Mount St. Helens on May 18, 1980. The arrows indicate the direction of flow as shown by the directions of fallen trees. Notice how the fallen trees show that the flow, initially directed north of the vent, diverged to the east and west.

Dramatic Io

If different ratios of magmatic and atmospheric gas pressures on Earth produce plumes of such different shapes, we might expect quite dramatic effects on Io, where atmospheric pressure is ten million times less than on Earth. If the volcanic conduits on Io were narrow and constricted, when the volcanic gases emerged they would be at much higher pressures than Io's atmosphere. The plumes on Io would look like giant rocket engines or geothermal wells, they would flare outward near the ground, and be diffuse and irregular in structure because of internal shock waves. Loki may, at times, have had such a configuration.

However, such flaring near the vent of a constricted volcanic conduit would rapidly erode the ground, and a crater would form over the conduit. The high-pressure gases would expand laterally from the conduit into the crater, reducing the plume pressure by many orders of magnitude. Gas could enter the crater at a pressure of tens to hundreds of bars and be decompressed to a millionth of a bar before leaving the crater, if the crater were a kilometer deep. (One bar equals Earth's atmospheric pressure at sea level.)

The trajectories of the volcanic gases and particles are altered by divergence into the crater, and thus, when the gases and particles reach the surface, they are launched obliquely into the atmosphere and follow trajectories that produce the characteristic umbrella shapes of the ionian plumes, rather than the vertical columns of terrestrial plinian eruptions. The plume of Prometheus is a good example of such a structure.

What would have happened if Mount St. Helens had erupted on another planet? On Io, Mars or the Moon, atmospheric pressure could not have prevented devastation around the whole mountain. In contrast, on Venus, where atmospheric pressure is nearly 100 times that of Earth, the spread of the blast would have been much less than here on Earth. In fact, we can hypothesize that eruptions on Venus would resemble terrestrial eruptions deep in the ocean, where the pressure of the overlying water suppresses the expansion of volatiles and produces nonexplosive effusions instead of high-velocity plinian eruptions or violent lateral blasts. This comparison illustrates the dramatic effect that planetary atmospheric pressure has on the nature of the catastrophes wrought by volcanoes.

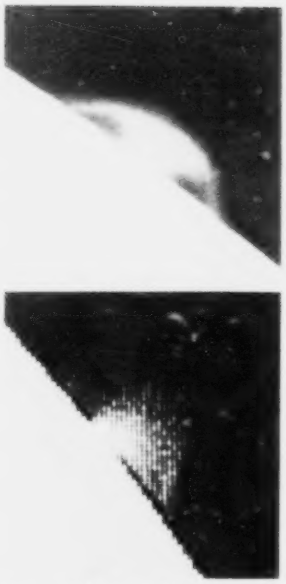

Voyager I photographed eruptions of the Ionian volcanoes Prometheus (top) and Loki (below). Compare the symmetric, umbrella shape of Prometheus with the more irregular shape of Loki. (Photographs by NASA/JPL.)

Mono Craters, California—a crescent-shaped line of volcanic craters that have erupted explosively more than 20 times during the last 2,000 years. Nearby Long Valley is a volcanic caldera, currently inactive, but evidence suggest that subterranean magma presently exists close to the surface.

Planetary Lessons

We of the 1980's are the privileged first generation of volcanologists who have been able to study active volcanoes on two planets. On Earth, truly large, catastrophic volcanic eruptions are infrequent. However, because of the finite probability that an eruption of the size that created Long Valley in California, or the calderas in Yellowstone National Park, will occur within the span of human existence, it is important that we try to understand the behavior of such volcanoes—particularly that we try to learn what activity might precede such a catastrophic event.

Perhaps some answers will come to us through studies of the large-scale events on Io. The lessons already learned from planetary volcanology have been numerous: Volcanoes are a major safety valve by which planets dissipate their excess heat; atmospheric pressure plays an important role in shaping volcanic plumes; volcanoes, in turn, play a major role in determining the composition of the atmosphere, climate and weather. The future holds promise of many more lessons as we await the portrait that Pele is creating for us on Io.

Reproduced by permission from "The Planetary Report", Volume 5, Number 1, 1985, p. 4-6.

Meteoroids and Impact Craters

Henry Spall

> "And meteors fright the fixed stars of heaven."
>
> *Richard II.* William Shakespeare

On a clear night scores of meteoroids streak across the sky. They leave light paths we call meteors or shooting stars as the Earth is showered with debris from distant parts of the solar system. When these meteoroids hit the Earth (as meteorites) they range in size from pebbles to the 34 ton Ahnighito meteorite that the American explorer Admiral Robert Peary discovered in Greenland. The unique importance of meteorites is that they have an extra-terrestrial origin and can provide us with direct evidence on the make-up of the solar system. They also give us clues to the origin of the solar system because they formed about 4.6 billion years ago at about the time the planets formed.

Many meteoroids are associated with comets; as a comet travels around the sun it leaves a trail of debris behind it and it is this debris which produces meteor showers. Other meteoroids come from the asteroid belt, a zone between Mars and Jupiter filled with thousands of dwarf worlds that failed to coalesce into planets.

Three Types of Meteorites

Iron meteorites are the most easily recognized meteorite although they represent only a small proportion of those that fall to the Earth. Iron meteorites are not pure iron but also contain nickel, sulfur, carbon and traces of cobalt, and chromium. Although such meteorites are themselves not from Earth, they provide evidence about the composition of the Earth's metallic core.

Stony meteorites are the most common type of meteorite, comprising more than 90% of all falls. They are made up of small spheres of silicate minerals in a fine-grained matrix, rather like raisins in a cake. The spheres are known as chondrules and the meteorites themselves are called chondrites. The chemical composition of most chondrites is similar to that of peridotite, the main rock type in the Earth's mantle. One of the most important and intriguing varieties of chondrite is the carbonaceous chondrite; this type

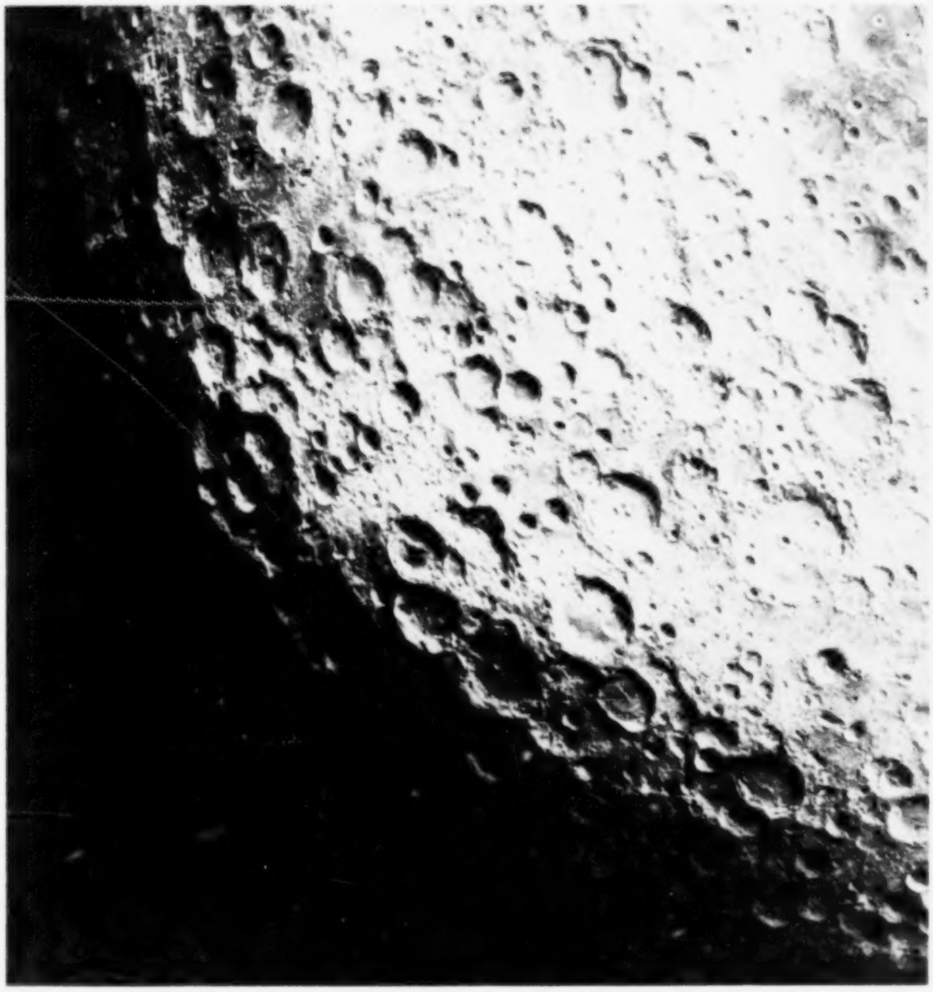

View of the heavily-cratered lunar highlands area; this is the most ancient area of the Moon and preserves a record of intense bombardment 4.5 billion years ago.

Asteroids

-are minor planets with diameters of half a mile on up to a few hundred miles. They are thought to be either remnants of a planet that disintegrated early in the life of the solar system or celestial material that never quite coalesced into a planet. About 1700 of these asteroids have been named or numbered. The majority are in elliptical orbits around the sun in a belt between the planets Mars and Jupiter. Occasionally the orbit of an asteroid is changed, perhaps by the gravitational effect of nearby Jupiter, so that the asteroid is sent closer to the sun and the inner planets, including Earth.

Some sixty asteroids have been observed to be out of this main belt and are in Earth-crossing orbits; the likelihood of a collision, however, is remote. It is believed that meteorites may be small fragments of asteroids which were broken up by collisions in space.

---

contains significant amounts of carbon compounds of the type believed to have been precursors to life on Earth.

The third kind of meteorites are the *stony irons*, which are mixtures of iron and silicate minerals; they are quite rare.

Meteorite Falls

Much of this meteoritic material arrives unnoticed on the Earth. There are probably about 500 major falls each year, and most of these accumulate on the ocean floors. By far the best hunting ground is in Antarctica where meteorites falling onto the ice surface over the centuries have been carried along by the great Antarctic ice sheet and are concentrated in areas where the glaciers ablate. Weathering processes in the Antarctic take very much longer than in other parts of the world; meteorites that fall in the deep snow are therefore protected and preserved for great lengths of time. They are easy to spot for there are no other rocks in the upper part of the ice sheet.

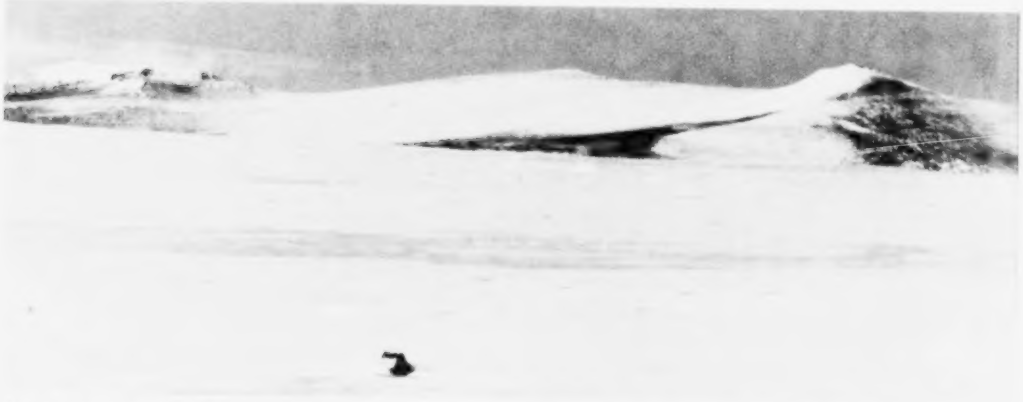

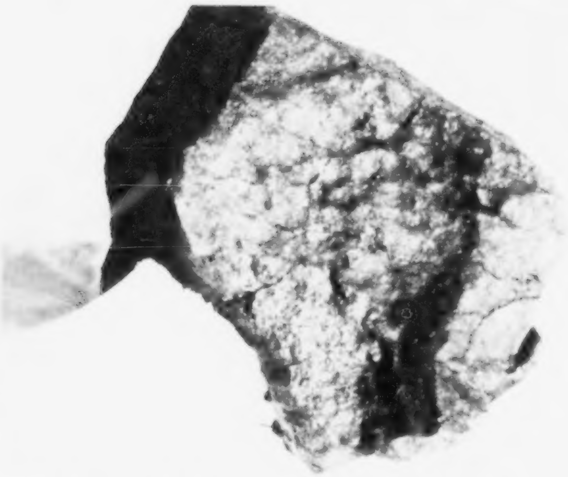

A meteorite on the ice surface at Allan Hills (background), Victoria Land, Antarctica. Photos by Keizo Yanai.

Meteoroids enter the Earth's atmosphere with very high speeds. The smaller meteoroids are slowed by drag with the atmosphere and the resulting frictional heating means that many of them burn up completely. For those that do reach the Earth's surface, the atmospheric braking effect slows down the meteorites so effectively that they rarely do much more than bury themselves a few inches deep into the surface.

Not so with the larger meteorites. Really large bodies are hardly slowed at all, and the end result is an impact on the Earth's surface at near cosmic velocities that produce a deep impact crater.

Impact Craters

The most spectacular of these surface impacts is Meteor Crater in Arizona, which is 600 feet deep and 3/4 mile across. It was formed some 50,000 years ago by impact of an iron meteorite considered to be about 150 feet across, weighing about 300,000 tons and traveling in excess of 10 miles per second. The impact occurred on flat-lying sedimentary rocks. David J. Roddy of the U.S. Geological Survey in Flagstaff, Arizona has calculated that approximately 190 million tons of rock were ejected during the event to form a blanket around the crater that is as thick as 75 feet. The cratering mechanism and the effect of the impact on rocks of the nearby desert have been worked out in careful detail by Gene Shoemaker and Susan Kieffer of the U.S. Geological Survey in Flagstaff, Arizona. The sequence of events for the formation of Meteor Crater is shown diagrammatically on page 89. While meteoritic material can still be found at Meteor Crater, most of the meteorite was probably melted during the impact. The chances of such an encounter with the Earth are about once every 25,000 to 100,000 years.

The number of impact craters that we can find now on the Earth's surface is surprisingly small—especially when compared with the Moon where impact cratering is the principal geological process. One of the reasons that impact craters are a curiosity on Earth is that they are constantly being erased by the Earth's very active agents of erosion—water and wind. Impact cratering is, however, a key geologic agent on the other terrestrial planets—Mercury, Mars and Venus; during the early evolution of these planetary surfaces, impact cratering rivalled volcanism as the most important geologic process.

Further reading

Francis, Peter, 1982, The Planets. Penguin Books. 411 p.

Gene Shoemaker:

"Picture yourself standing about 20 miles from here about 50,000 years ago. Out of the southeast, a nickel-iron asteroid about 150 feet across is hurtling towards the Earth. As it plunges into the atmosphere it forms a brilliant meteor which grows brighter and brighter, and finally, becomes much brighter than the sun. In fact, it grows so bright that you will be on the verge of being scorched.

At that point, the meteorite strikes the ground and its sends a shock wave with pressures of millions of atmospheres down into the rock and back up into the meteorite. The meteorite burrows into the ground like a hydraulic jet forcing the rock aside, flattening, and then being deflected and thrown back out again.

From the moment that the meteorite strikes, a spray of shock-melted meteorite and vaporized meteorite, and melted and vaporized rock, squirts out at high velocity, a velocity of several miles per second. The spray continues to rise and forms a plume that grows bigger and bigger. Finally, the plume becomes about 4,000 feet across at the base and by that time, the top of the plume of material ejected is extending miles up into the atmosphere. Most of the atmosphere has been blown away by the shock wave made by the meteorite.

The first thing that will happen to you after being nearly scorched is that you will hear the shock wave in the atmosphere itself and it will come like a horrendous clap of thunder. In fact, it will be strong enough to bowl you over even at 20 miles.

The plume, meanwhile, continues to grow. Finally it turns into an enormous black cloud of dust which will punch up through the atmosphere like the mushroom cloud from a nuclear explosion."

From the NOVA television program *The Asteroid and the Dinosaur*, produced by WGBH Educational Foundation, and reproduced by permission.

Close up view of Meteor Crater. Photograph by David Roddy and K. Zeller.

Sequence of events worked out by Gene Shoemaker for the formation of Meteor Crater, Arizona

1. Meteorite approaches the ground at 10 miles per second.

2. Meteorite enters the ground, compressing and fusing the rocks ahead of it. Shock effects in the meteorite reach its back side.

3. A rarefaction wave is reflected back through the meteorite, and the meteorite is decompressed, but still moves ahead at about 3 miles per second into the ground. Most of energy has been transferred to a shell of compressed, fused rock ahead of the meteorite.

4. Compressed slug of fused rock and trailing meteorite are deflected laterally along the path of penetration. The meteorite itself becomes the liner of a temporary cavity.

5. The shock wave propagates away from the cavity, the cavity expands, and fused and strongly-shocked rock and meteoritic material are shot out in the moving mass behind the shock front.

6. A shell of breccia (mixed fragments) and dispersed fused rock and meteoritic material is formed around the cavity. The shock is reflected as a rarefaction wave from the surface of the ground, and momentum is trapped in material above cavity.

7. The shock and reflected rarefaction waves reach a limit at which the sedimentary beds of the Earth's surface will be overturned. Material behind the rarefaction wave is thrown out along ballistic trajectories.

8. Fragments thrown out of the crater maintain approximate relative positions except for material thrown to a great height. The shell of breccia with mixed meteoritic material and fused rock is sheared out along walls of crater; the upper part of the mixed breccia is ejected.

9. Fragments thrown out along low trajectories land and become stacked in an order ***inverted*** *from the order in which they were ejected. Mixed breccia fragments along the walls of the crater slump back toward the center of the crater. Fragments thrown to a great height shower down to form a layer of mixed debris.*

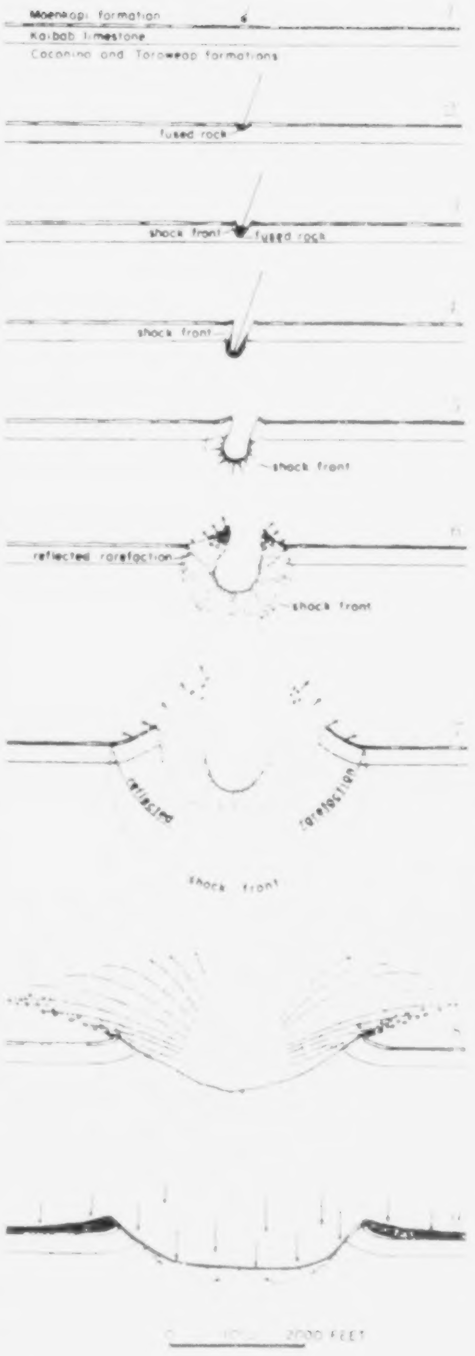
Moenkopi formation
Kaibab limestone
Coconino and Toroweap formations
1
2
fused rock
3
shock front
fused rock
4
shock front
5
shock front
6
reflected rarefaction
shock front
7
reflected
rarefaction
shock front
8
9
0 1000 2000 FEET

New theories about ancient extinctions

Henry Spall

The abrupt disappearance of all the dinosaurs about 65 million years ago, along with perhaps half the plant species and other animals, has been one of the great geological mysteries. Clues to the cause of these extinctions have been scarce and open to many interpretations.

But all this may be changing. Mass extinctions have been very much in the news in the last few years, triggered in large part by the proposal that the extinction of the dinosaurs and marine animals was caused by a catastrophic collision between the Earth and an extra-terrestrial body (bolide). Recently an equally contentious suggestion has been made that mass extinctions have swept the Earth every 26 to 31 million years for at least the last 250 million years—caused by encounters with some kind of extra-terrestrial object such as one of the asteroids or the comets.

The chronicle begins in 1980 when investigators at the University of California at Berkeley proposed an extraterrestrial origin for iridium metals found in ocean-floor clays separating the boundary between the Cretaceous and Tertiary periods of geologic time—long defined on the basis of the extinction of various life forms across the boundary. Since 1980, anomalous concentrations of iridium and other related metals have been found at this boundary in over 80 locations around the world in places as far apart as Europe, New Zealand, the North Pacific and the western U.S. With so many supporting clues, scientists knew that any explanation for the extinctions must also account for this geochemical evidence.

Iridium is rare in earthly rocks but 10,000 times more abundant in extraterrestrial bodies such as meteorites. The Berkeley group proposed that the iridium had resulted from the Earth's encounter with a bolide that had vaporized on impact, scattering its iridium into the atmosphere. Iridium dust from the impact would have circulated around the atmosphere for many years, eventually settling over much of the globe, especially in oceanic sediments.

The atmospheric dust, as well as soot and smoke from firestorms caused by incandescent rock scattered for hundreds of miles by the impact, would have blocked sunlight from the Earth's surface for a considerable period of time. (Sulphuric acid from the cataclysmic explosion of Krakatoa in 1883 circulated around the Earth for three years.) Plants may have died first, since they are dependent on photosynthesis from sunlight, followed by near-surface marine organisms, and then by land animals such as dinosaurs. To produce such profound global effects would require a large celestial body. The Berkeley group argued that this must have been an asteroid, and they calculated that it may have been six miles in diameter. Just recently, an unusually high density of soot particles has been found at the Cretaceous-Tertiary boundary layer at several sites throughout the world—suggesting that fires may have burned much of the Earth's vegetation. In addition tiny spherules discovered at the boundary might be fused extra-terrestrial and earth material that was spattered out by the impact.

The bolide impact hypothesis is compelling, although naturally there have been many counterproposals. One of these involves a gradual process of sedimentation that concentrated the metal iridium over a very long period of time. Some paleontologists maintain that at some sites the iridium layers and the bones of the last surviving dinosaur are just too far apart to have any meaningful connection. Moreover why were the extinctions so selective for certain species and not others? Indeed some would argue that the term "mass extinction" is in effect a *gradual* increase in the rate of extinctions followed by a gradual decline.

Most recently, Dartmouth geologists have proposed that iridium and other associated elements such as arsenic and antimony were not deposited instantaneously on the ocean floors. Rather there was a variable but intense influx of these metals over about 10,000 to 100,000 years, still very short in terms of geologic time. The Dartmouth group argues for a period of intense global volcanic events caused by increased activity in the Earth's mantle. Such volcanic activity would lead to increased carbon dioxide and acid-rain, global temperature rises, depletion of the ozone layer and changes in ocean circulation, all of which would have a catastrophic impact on life forms. Although shock structures found in quartz grains near the Cretaceous-Tertiary boundary could be explained as the effects of sudden impact, such structures have also been found as the products of explosive volcanism.

In the case of the impact hypothesis there remains of course the problem of finding some evidence for the impact crater itself, even though it was formed 65 million years ago. Most frustrating for the impact-theory faithful is that no evidence has been found for a land-based crater similar to Meteor Crater, Arizona, that is large enough to account for a catastrophic encounter. One alternative is that the impact occurred in the oceans where no record has been preserved, since more than half of the Cretaceous and older ocean crust has been consumed into the mantle by way of subduction zones in the plate tectonics scheme of things. Nevertheless a possible site in the northwestern Indian Ocean has recently been suggested, although there was no apparent accompanying evidence for giant tsunamis and submarine landslides.

Other mass extinctions have occurred at other times in the geologic record. Paleontologists from the University of Chicago have analysed the rate of extinctions of families of organisms over the last 250 million years and found evidence for a 26-million-year cycle. Later studies by Gene Shoemaker suggest a best-fit periodicity of 31 million years for both mass-extinctions and the formation of large impact craters on the Earth. Iridium anomalies have also been found in sediments that span other mass extinctions in geologic time. One of the early explanations offered for a periodicity in mass extinction was the proposal for Nemesis, a hypothetical companion star to the sun, whose orbit brings it close enough to our solar system every 26 to 31 million years; the resulting gravitational disruption that the star causes would trigger a rain of comets which might impact the earth. Such a proposal has been vigorously debated, as well as various other speculations that involve novel astronomical explanations.

Overall the evidence is persuasive that such catastrophic events have occurred in the geologic past and that we can expect them again in the future. Indeed Shoemaker thinks that even now the Earth may be experiencing a very weak comet shower that was stimulated by close encounter of a star with the sun. This would have two consequences for the Earth: first, we can expect an increased flux into the Earth's orbit of long-period comets from the comet cloud; second, there is a slightly greater likelihood of our encountering earth-crossing asteroids. And this fuels our efforts to plan for any kind of natural hazard whether it be earthquakes, volcanic eruptions, landslides, floods—or even an encounter with some elusive celestial body.

Silver, L.T., and Schultz, P.H., Eds. Geological Implications of Impacts of Large Asteroids and Comets on the Earth. Special Paper 190, Geological Society of America, 1982, 528 p.

An interview with Eugene Shoemaker, 1985, the Planetary Report Vol. 5, No. 1, p. 7-10.

Officer, Charles B., and Grieve, Richard A.F., The Impact of Impacts and the Nature of Nature. EOS, American Geophysical Union, Vol. 67, No. 33, 1986, p. 633.

nguska Comet or the Great an Mystery Explosion of 1908

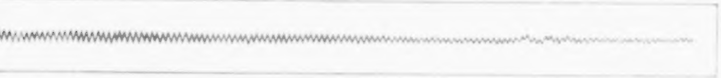

lagnetic and Meteorological Observatory, about 500 miles south of the explo
smograph recorded these earthquake waves beginning less than two minutes
In 45 minutes the explosion's air wave arrived, causing the three oscilla
sed on the record at right. Diagram from the U.S.S.R. Academy of Sciences

It is dawn on a June morning in Siberia in 1908. The sky is cloudless, but even in summer in this part of Russia the cold at dawn takes your breath away. Fur-clad nomads are beginning to herd their sheep and goats towards lush grazing on the banks of the river—one of the thousands that drift sluggishly across Siberia's vast featureless wilderness towards the Arctic Ocean. Swans glide in the dark shallows of the river. A phalanx of ducks spears into a nearby swamp and sends up a black cloud of ferocious mosquitoes; they settle again around a herd of reindeer browsing on the river bank. Here where the tiaga, the forbidding Siberia forest, obscures the sun, the cold is as sharp as the flint in the river bed. It cuts the farmer who has just emerged from his log cabin. He halts on the steps to decide whether his first task of the day will be to mend the plough that was broken yesterday when he dug too deep and reached permanently frozen ground, or whether he will hunt for rabbit for the evening meal; instead he lights his pipe. Two families of nomads are still asleep in their tents, the air strong with the scent of wet dog as the ice melts on their furs. At a trading post, trappers squabble over the price of ermine and sable pelts. On the edge of the settlement a tramp with pots and pans jingling on his back sets off on his day's journey to the nearest village, twenty miles away. At the edge of the village, a boatman pushes off from the river bank for his first crossing of the day, the crescent-shaped hull of his boat overloaded with squawking chickens, snarling dogs and silent peasants.

Without warning there is a blinding blue flash in the sky, followed by a roar and a searing blast of heat; there is a thunderous clap, the ground shudders, and the air is filled with fire, black smoke and debris.

The boat disintegrates, hurling men and animals into the freezing river. The farmer's shirt is scorched off his back; the tramp is blown off his feet, his ports and pans scattering like schrapnel. One of the trappers standing in the doorway of the trading post is knocked unconscious, overcome by the searing heat; the tents of the nomads are torn loose, the men and dogs inside being rolled over the ground like leaves in a gale. All that remain of the reindeer are charred carcasses. The forest has been turned into a crackling inferno, and a black fireball rises into the air.

Is this the stuff of science fiction? Did these events really occur? What could possibly have caused them? Why don't we read about this sort of thing more often?

The answer is that scenes like these did occur. In all probability they were caused by the first recorded impact of a comet with the earth. The reason so little is known about the Tunguska event is that it occurred in a remote part of the earth that was, and still is, sparsely inhabited; the site was not visited by Soviet scientists until 1921, thirteen years after the event. The reason so little is known about other such events in history is that the chance of such a cometary impact is about once in 50,000 years.

The historic event of June 30, 1908, was a tremendous explosion in a highly inaccessible area of the Soviet Union, but nevertheless witnessed by nomads that inhabit the region. Over an area 20 miles in radius, every tree was blown down and the trunks alined from the center of the explosion like the spokes of a wheel. Over the years various Soviet expeditions have searched for meteoritic debris, hampered by the fact that no crater was formed by the explosion. There is no clear evidence for meteorites near the epicenter of the explosion; however there was a concentration of iron oxide and glassy spherules of fused rock in a tongue stretching about 150 miles northwest of the epicenter. Such a dispersal could be expected from ablation products caused by the disintegration of an extra-terrestrial body.

Soviet expeditions led in the 1920's and 30's by Leonid Kulik and E.L. Krinov and much later in the late 50's and early 60's by Kirill Florensky have shown that the bolide came in from the southeast (so that the fallout of debris was in a northwest direc-

An uprooted tree with defoliated trees in the background.

tion). While it is curious that no worldwide astronomical sightings of such a body were made in the days before the impact, the small (125 feet diameter) size calculated for the comet would decrease this likelihood. The explosion must have occurred several miles

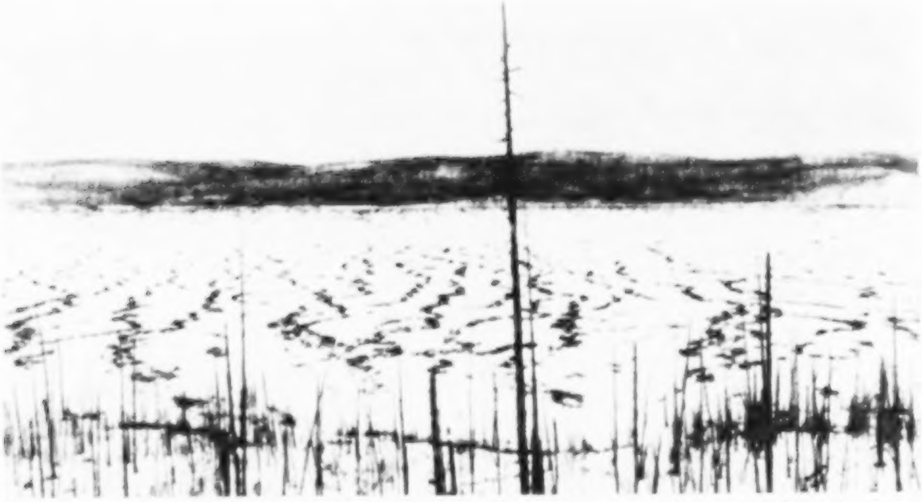

This view of the "southern swamp," in the region where the great Siberian bolide explosion occurred in 1908, was obtained by E.L. Krinov in 1929. (All photographs are from Giant Meteorites by E.L. Krinov, copyright, 1966, and reproduced by permission of Pergamon Books Ltd.)

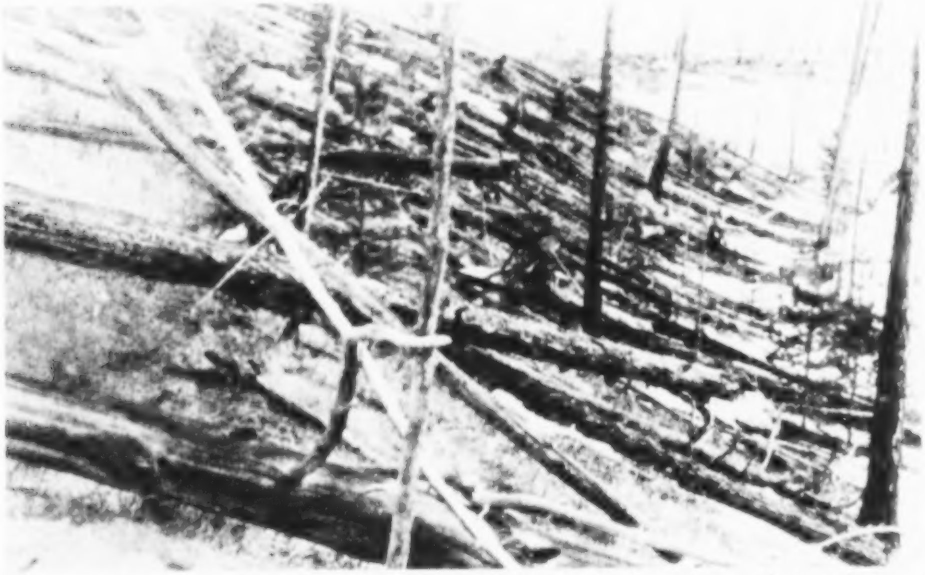

A 1929 photograph by E.L. Krinov that shows how completely the forest was destroyed, even five miles from explosion center.

above the Earth's surface, because no impact crater was found; this favors the cometary theory because a comet being mostly dirty ice, dust and frozen gas, might be more likely than a large meteorite to disintegrate well before it reached the Earth's surface. Temperatures of about 70°C were generated near the epicenter judging from scorching of the vegetation at the site. Radioactivity that was reported in trees in the blast area was established by the 1962 Soviet expedition as being fallout from modern nuclear bomb tests and not a relic of the 1908 event. Unusual sunsets and other atmospheric effects over Europe after the event were probably caused either by dust in the comet's tail ejected back into the atmosphere after the impact or by the Earth's subsequent passage through the comet's tail.

It has been estimated that the explosion was as great as the volcanic eruption that destroyed the island of Krakatoa in 1883, or about 10,000 times the energy of atomic bombs used in the Second World War. Seismic disturbances from the explosion were recorded in Russia. Barometric disturbances were recorded over most of the globe and it has been shown that the explosion's air wave circled the Earth twice. A very detailed analysis of seismograms of the Tunguska event has shown that the seismic record was triggered by the air explosion at the source. The time delay between the arrival of the body wave (in which the displacements are horizontal and perpendicular to the direction of propagation of the seismic

An early Soviet expedition to the Tunguska dragging boats across shoals in one of the rivers. The heads of the men are covered with mesh to protect them from mosquitoes.

wave) and the Rayleigh wave (a forward rolling motion of the Earth's surface) indicates that the explosion occurred about 5 miles above the ground. This study also showed that the pattern of tree blow-down was due to the superimposition of two waves—a spherical shockwave (due to the explosion) and a conical ballistic wave (due to the bolide moving at 40 miles per second).

The theory of a cometary impact for the Tunguska explosion seems to be currently favored despite the limited amount of scientific evidence that exists for the event and the proposal by Z. Sekanina that the bolide was a carbonaceous chondrite. Other more exotic proposals have been made, including a nuclear-energy source such as antimatter; the passage through the Earth of a primordial black hole with the mass of a large asteroid and negligible radius; and an extraterrestrial mass of fissionable material. When there is no firm base of quantitative scientific data then imaginative speculation is always inevitable. And so the great Siberian mystery explosion of 1908 will undoubtedly continue to provide food for conjecture well into the future.

—Henry Spall

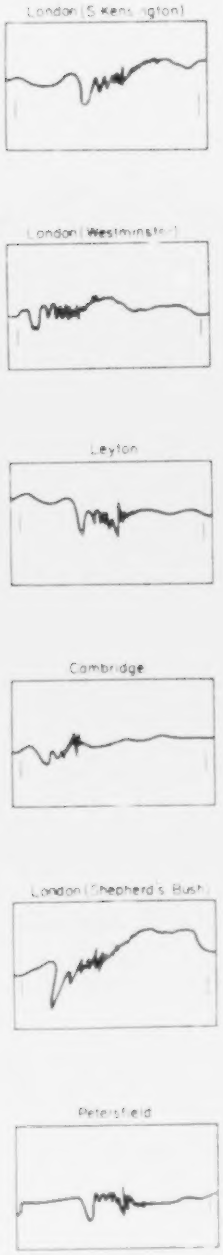

Microbarograms of six meteorological stations in England on which are recorded the air waves from the Tunguska impact.

References

Krinov, E.L., 1966, Giant Meteorites. Pergamon Press, Oxford. 397 p. (Includes a 140 page chapter on the Tunguska event.)

Florensky, Kirill P., 1963, Did a comet collide with the Earth in 1908? Sky and Telescope, Vol. 26, No. 4, p. 268-269.

Hughes, David W., 1976, Tunguska revisited. Nature, Vol. 259, p. 626-627.

Wilkerson, M. Susan and Worden, Simon P., 1978, On egregious theories—the Tunguska event. Quart. Journal Royal Astronomical Society, Vol. 19, p. 282-289.

Ben-Menahem, Ari, 1975, Source parameters of the Siberian explosion of June 30, 1908, from analysis and synthesis of seismic signals at four stations. Physics of Earth and Planetary Interiors, Vol. 11, p. 1-35.

Ridpath, Ian, 1977, Tunguska: the final answer. New Scientist, 11 August, p. 346-347.

Sekanina, Z., 1977, Astronomy, 5, p. 62.

Halley's Comet—
a benevolent visitor to Earth

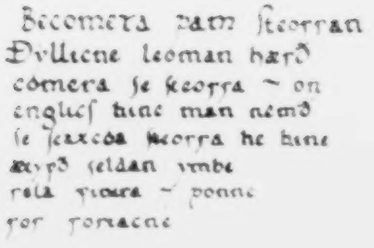

Becometa þam ſteorran
Ðyllicne leoman hæfð
cometa ſe ſteorra 7 on
englisc hine man nemð
ſe ſeaxeda ſteorra he bine
ætyƿð ſeldan ymbe
fela ƿintra 7 þonne
for foretacne

The Comet (appears) amongst the stars
The comet has thus rays of light
In english man calls this the Saxon Star
It appears seldom every many winters
Then (it is) a great wonder

(Translation by Joan Hampshire)

The Anglo-Saxon text in the Canterbury Psalter of 1145 records the first return of the comet after 1066.

In late 1985 and early 1986 a comet was visible to the Earth that has been observed for over 2000 years. One of the most famous of celestial visitors, Comet Halley appeared last in 1910 and will not be seen again until the year 2061. The comet has been the focus of intense studies during the International Halley Watch. A fleet of Soviet, Japanese and European spacecraft was launched specifically for a direct encounter with the comet in March of this year; numerous ground-based astronomical observations are being made, while other investigations are being made from Earth-, Venus- and interplantary-orbits. In short, Comet Halley will have been one of the most significant scientific occasions of the decade.

In 1705 Edmund Halley, Professor of Geometry at Oxford University, collected and organized a mass of information on comets observed in 1531, 1607, and 1682, a task for which he had an uncommon genius. He was able to show that the comets had very similar orbits, and correctly drew the conclusion that they were the same object and more importantly that comets could therefore be periodic. He predicted that this comet would again be visible from the Earth in 1759. Since then it has been known as Halley's comet and it has played a significant role in the development of astronomy.

Edmund Halley. Photograph courtesy of U.S. Naval Observatory.

Comet Halley in history

The comet has also played a significant role in history for when it appeared it was natural for people to record its passage and associate it variously with good tidings, wars, superstitions, and all manner of

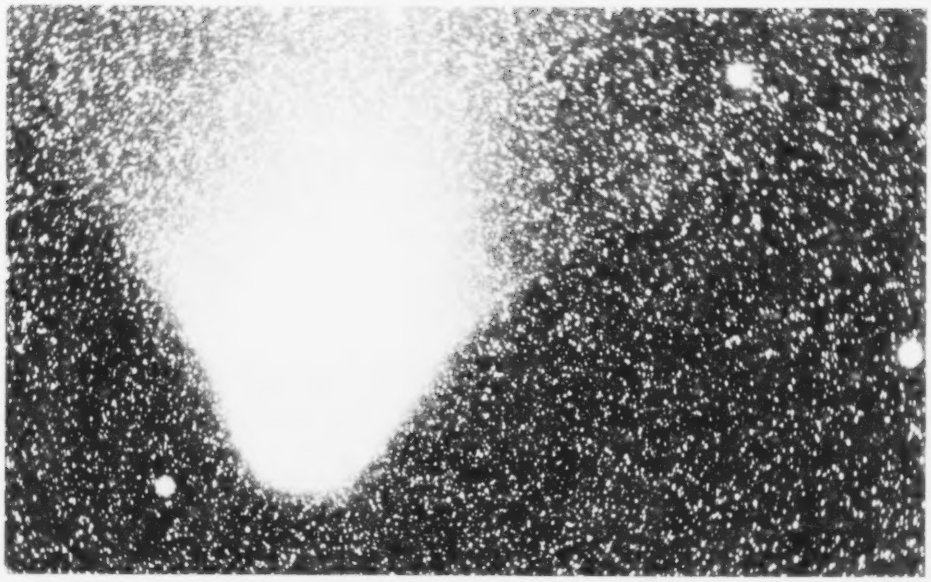

Comet Halley from Earth. This is how Halley appeared on 13 April from Costa Rica, several weeks after the armada of spacecraft passed the comet. The fine structure of the comet's tail of dust and gas changes of minutes and hours, most likely due to the changing output of the nucleus buried in the head of the comet and to the varying solar wind. When this image was taken, the plasma tail could be seen for a length of over four degrees, while the dust tail faded into the Milky Way at three degrees from the nucleus. Photograph by R. Schmidt/R. Clarke U.S. Naval Observatory.

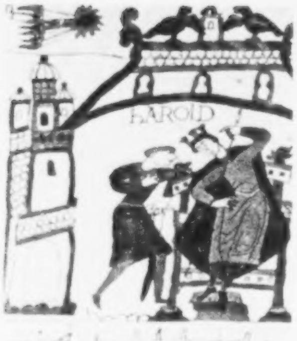

The Bayeux Tapestry chronicles the events of 1066, and here depicts news of the appearance of Halley's Comet (the "long-haired star") being given to the English King.

calamities. The first recorded siting of the comet was probably in 467 BC in China, but it was the sighting (or *apparition* in astronomical parlance) in 87 BC that was the first in a long unbroken record that has continued to the present day. Interest in the return of 12 BC stems from efforts that have been made to identify it with the Star of Bethlehem, although among other things the date discrepancy is too large.

The return of 1066 is noteworthy because of its link with the Battle of Hastings, one of the significant events in British history. The comet's sighting in April of that year caused considerable forboding among the English; Harold, last of the Saxon kings, was faced with a claim to his crown and the threat of invasion from Normandy (to be the last one on English soil). The Saxon English regarded the comet as an unfavorable omen that was confirmed by the death of the king at Hastings and the demise of the Anglo-Saxon dynasty. The comet is prominent in the Bayeux Tapestry commissioned after the battle.

The return of 1145 is well documented in China and in England (in the Canterbury Psalter). So was the return of 1301 when it was seen in China, Iceland and Italy. One man who certainly saw it then was the Florentine painter Giotto di Bondone, and his name is now remembered as the European spaceprobe to Comet Halley. The 1682 return was seen by Halley himself and led him to show that the comet was a regular visitor to the Earth.

Studies of the comet's long-term orbital behavior and brightness show that no perceptable changes have taken place over the last 2000 years. The only close encounter it has had with any of the planets was Jupiter over 16,000 years ago, although the planet obviously failed to capture the comet at that time. It is likely that the comet has been around for at least 50 orbits.

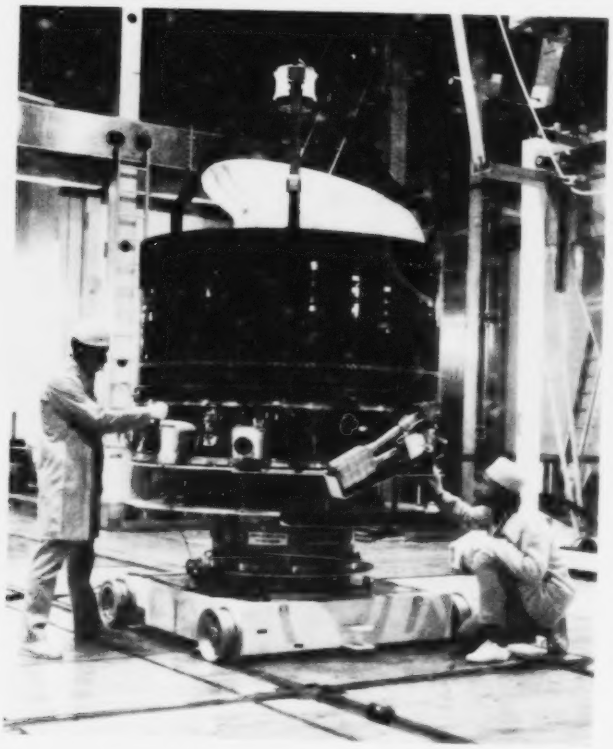

GIOTTO—the European Space Agency's spacecraft that intercepted Halley's Comet in March 1986. Photograph by British Aerospace.

Structure of Comets

It has been estimated that there are 1000 billion comets, of which about 1000 have been recorded. Most of these are in a spherical cloud (the Oort Cloud) of randomly-oriented elliptical orbits that are bound to the sun; smaller sets of comets are in orbits associated with the giant planets, primarily Jupiter. Halley's comet is unique in that it has a short-return period and shows the full range of cometary activity—halos, dust and ion tails, atmospheric jets and so forth. For these reasons the March 1986 encounters with the five spacecraft have been so significant.

The central portion of a comet is its solid nucleus from which all cometary material, both gas and dust,

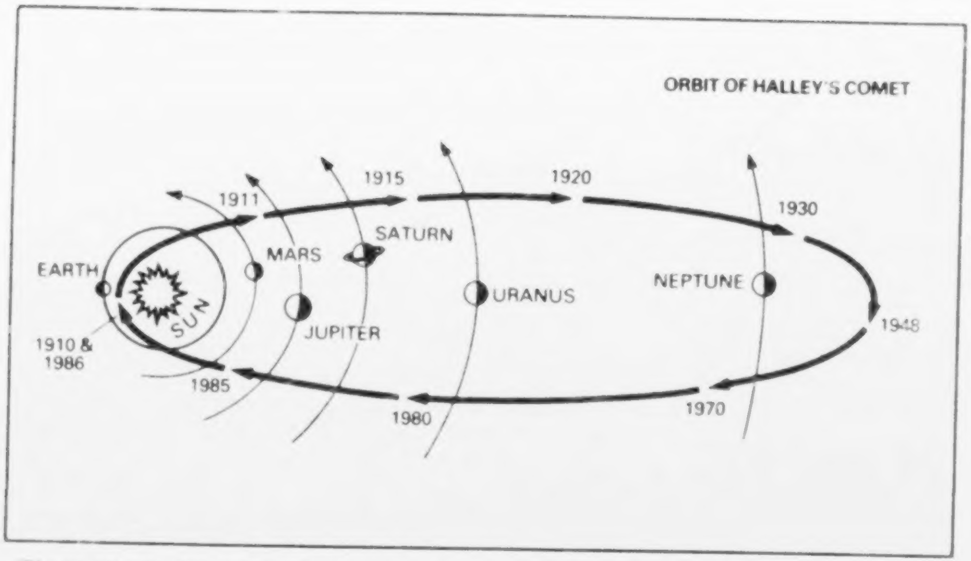
ORBIT OF HALLEY'S COMET
1911
1915
1920
1930
SATURN
MARS
EARTH
NEPTUNE
URANUS
SUN
JUPITER
1948
1910 &
1986
1985
1980
1970

The highly elliptical orbit of Halley's Comet. Note that the tail of the comet always appears to point directly away from the Sun. The fact that the comet is moving in a direction opposite to that of the planets meant that the earth-launched space-probes had time enough for only a 4 hour encounter with Comet Halley.

originates. The photographs of Comet Halley taken by GIOTTO, the European probe, from its closest approach 375 miles away show that the coal-black nucleus is irregularly shaped, like a potato, and is about 10 miles long. The nucleus consists of a roughly equal mixture of water-ice, other ices and dust (confirming the "dirty snowball" hypothesis of comet-astronomer Fred Whipple).

As the cometary nucleus approaches the sun it is warmed sufficiently that the gases and water-ice in the nucleus sublimate (the process of converting a solid directly to a vapor without the usual intervening liquid stage). This is shown as a glowing parabolic cloud of gas and dust known as the coma that surrounds the nucleus. The March 1986 encounters with the five space-probes showed that the gases in the coma of Halley's comet include carbon dioxide,

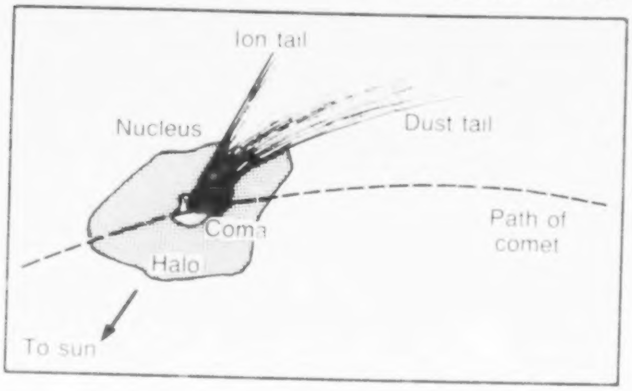
Ion tail
Nucleus
Dust tail
Coma
Path of comet
Halo
To sun

The structure of a comet.

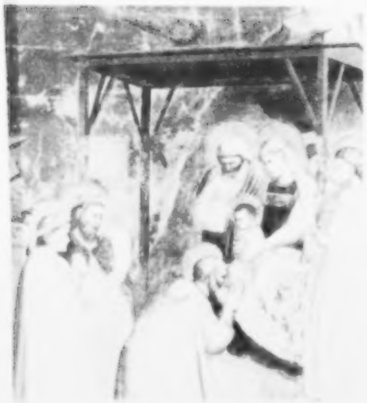

Halley's Comet was included in the Adoration of the Magi painted by the Italian painter Giotto in 1301; he depicted the comet as the Star of Bethlehem.

water vapor, ammonia and methane, as well as a number of other ions such as sodium, sulphur and iron. These substances are streaming away from the nucleus at initial speeds of several hundred feet per second; they form a number of dust, gas and plasma (ionized gas) tails ranging in length from 10 million to 100 million miles. Eventually the gases accelerate until they reach the speed of the solar wind, 250 miles per second.

There is one very important consequence of the processes described above. The gases escaping on the sun side of the nucleus cause thrusts (similar to retro-rockets on a spacecraft) which alter the orbit of the comet. It is these non-gravitational forces that, combined with the property of all astronomical bodies to rotate, cause irregularities in a comet's orbit and therefore its return frequency; for example, Comet Halley's return periodicity ranges from 74 to 80 years.

The Future

When Halley's comet was seen in 1910 it would have been inconceivable for people then to think that the next return would be observed close-up by five spacecraft. Such is the reality of the space age in which we live today. Likewise it is impossible for us to consider where this space age will have taken us over the next 76 years before the comet's return in 2061. But doubtless there will again be the keen scientific interest to view this benevolent cosmic visitor to the Earth.

—Henry Spall

References

Belton, Michael J.S., 1985, P/Halley: The Quintessential Comet: Science, Vol. 230, No. 4731, p. 1229-1236.

Calder, Nigel, 1980, The Comet is Coming: Viking Press, New York, 160 p.

Mendis, D. Asoka and Tsurutani, Bruce T., 1986, The spacecraft encounters of Comet Halley: EOS, American Geophysical Union, May 20, p. 478-481.

Moore, Patrick and Mason, John, 1984, The Return of Halley's Comet: W.W. Norton and Company, New York, 121 p.

Yeomans, D.K., 1981, The Comet Halley Handbook: An observer's guide created for the International Halley Watch: Jet Propulsion Laboratory, Pasadena, CA, 111 p.

Results from the five space probes to Comet Halley in March 1986 are described in issues of *Nature*, beginning with Volume 231, May 1986.

Bruce T. Tsurutani (Jet Propulsion Laboratory) is acknowledged for his help in preparing this article.

Another Tale of Halley

The news services seem disappointed by Comet Halley's modest performance this time around, but my enthusiasm for the spectacle is undiminished. For me, the comet's 76-yr orbital period highlights a compressed history reckoned by generations. Shifting into cometary overdrive, merely 30 orbits give a stroboscopic view of events since 240 B.C., when the earliest known visit was recorded. Just four backward ticks on the clock take us to Edmund Halley's realization that the bright comet of 1682 was the same one reported many times earlier. By its visible presence this year, the comet offers only its fourth confirmation of Halley's prediction, and with such close perspective, we become fascinated observers in a cosmic physics experiment.

Professional astronomers who keep track of many comets probably think that the excitement over Halley is rather excessive. Jaded watchers of the heavens may suggest that Comet Encke, with its 3.3-yr period, is a more worthy object, capable of providing many data sets during a scientist's career. Yet who remembers the last appearance of Encke, or West, or even the ballyhooed visit of Comet Kohoutek in 1973? Comet Halley, on the other hand, is remembered because grandparents tell grandchildren about it; the symbolic torch of responsibility is passed, and youngsters are admonished not to miss their opportunity when it comes. Halley's three-generation bridge, long enough to span a life-time, sets the present comet apart from all the others.

In the late 1950's, the world of science was punctuated by two remarkable events: the International Geophysical Year (IGY), and close on its heel, the launch of the Soviet satellite Sputnik. In those heady days moon landings and planetary exploration were confined to the nightly realm of Flash Gordon. Halley's Comet, forgotten by the press, was barely past aphelion and far out of sight near the orbit of Neptune.

Yet in those years, I was reminded of the comet, in spite of its remoteness and its low profile in the daily news. The Russian satellite became a meteor a few months before I began high school in a small town in Maine, and our science class buzzed with talk of centrifugal force and gravity. The leader and perpetrator of much of the excitement was a woman with unbounded enthusiasm for science and many years as an observer of nature. The IGY and Sputnik received their due share of attention, but Lucy H. Kilby also saw to it that her students heard how Halley's Comet lit up the sky in 1910.

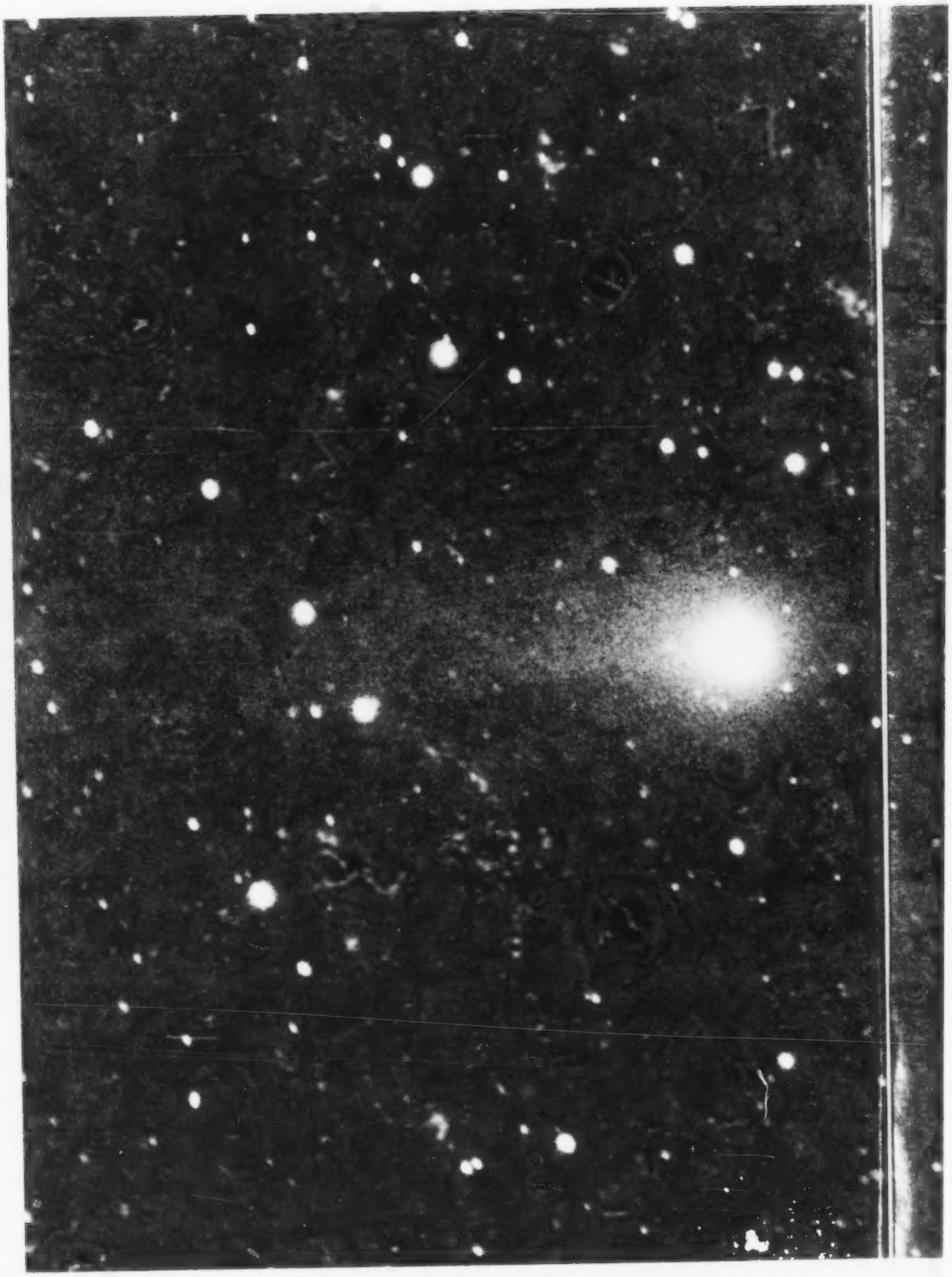

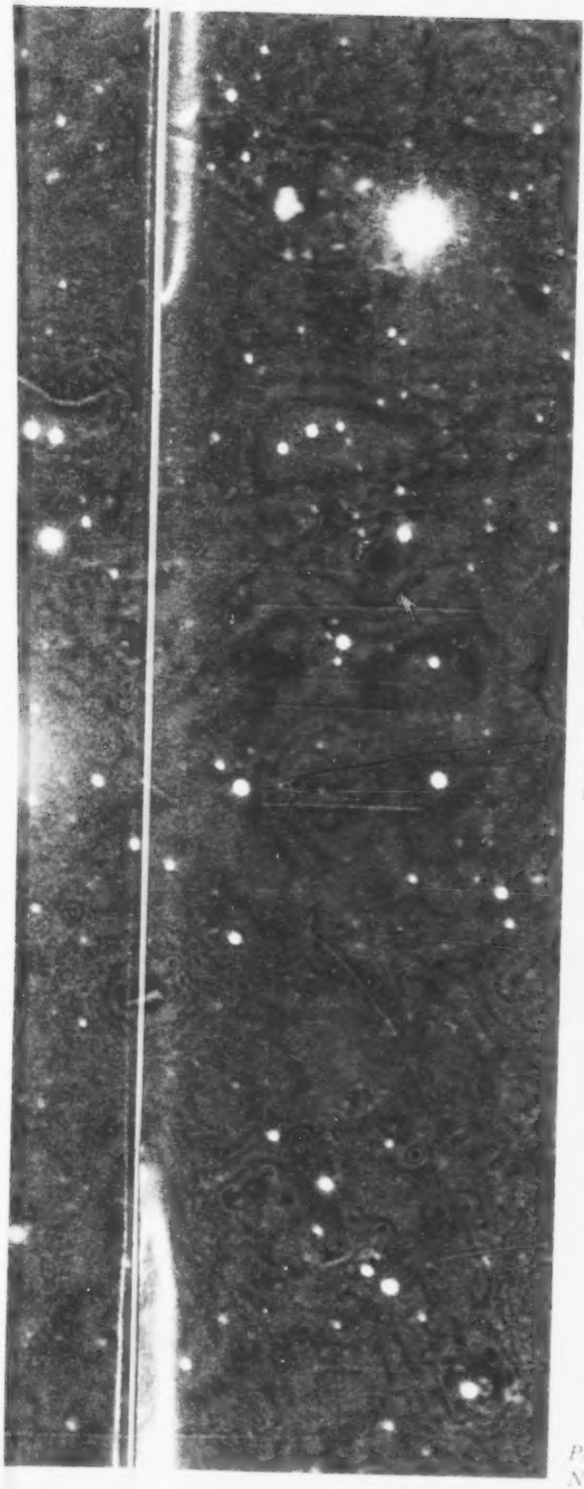

Photo of Comet Halley on 3 May 1986 by R. Schmidt, U.S. Naval Observatory.

She told us that, as a young woman, she had seen the comet's extensive tail, a luminous arc that was visible even on bright moonlit nights. She explained why the tail pointed away from the sun, and how the comet's elliptical orbit extended far out into the solar system, across the planetary orbits. We laughed about "Halley's Comet Pills," intended to ward off the perils of the earth's passage through the tail, and she produced posters and magazines from that era for inspection. When the discussion was over, the brief tutorial complete, she solemnly instructed us to write down the date 1986 and to remember her should we be so fortunate as to witness Comet Halley's return.

My 11-year-old daughter and I began looking for the comet last November, and we first found it near the Pleiades with 7x50 binoculars. Our momentary elation was worthy of the Palomar telescope. Through the binoculars, the comet appeared to be a fuzzy speck, hardly discernable, but there it was, right on schedule and in the predictable spot. In the following weeks, we tracked the comet westward past Aries and Pisces and Pegasus, until late in January it dropped into the sunset south of Aquarius, trailing a nebulous tail. Presently, while awaiting Comet Halley's reappearance in the predawn sky, I am encouraging a young astronomer and remembering Miss H[illegible]y.

—David A. Brooks
Texas A&M University
College Station, Tex.

Reprinted from EOS, February 25, 1986, by permission of the American Geophysical Union

About the Authors

Susan Kieffer received her Bachelor's Degree in Physics and Mathematics at Allegheny College, and her Ph.D. in planetary sciences at the California Institute of Technology. After post-doctoral work and teaching at UCLA, she joined the USGS in Flagstaff in 1978. Her principal research interests have been in the fluid dynamics of erupting geysers and volcanoes, the hydraulics of the Colorado River, and mineral thermodynamics. In 1986 she was elected to the National Academy of Sciences. She most enjoys spending her spare time with her husband (also a USGS geophysicist) and her 6'6" son. Each summer evening she can be found in her garden in Flagstaff trying to figure out how to grow plants to the same size.

Eugene M. Shoemaker has been a geologist with the U.S. Geological Survey since 1948 and was also, until 1985, Professor of Geology at the California Institute of Technology. As well as having a Ph.D. from Princeton University, he has received three honorary doctorate degrees and eleven major scientific awards and medals; in 1980 he was elected to the National Academy of Sciences. Gene Shoemaker was principal geological investigator for the Apollo lunar landings and has been principal investigator for the television experiments on the Ranger, Surveyor and Voyager projects. His current research is on impact processes in the solar system and the effects of large body impacts on the evolution of life.

SUBSCRIPTION ORDER FORM

Enter my subscription to "Earthquakes and Volcanoes" at $15.00 (domestic) or $18.75 (foreign). Domestic remittance should be made by money order or check or charged to VISA or MASTERCARD. Foreign remittance should be made by international money order, draft on an American bank, or UNESCO coupons.

NAME—FIRST, LAST

COMPANY NAME OR ADDITIONAL ADDRESS LINE

STREET ADDRESS

CITY **STATE** **ZIP CODE**

PLEASE PRINT OR TYPE **(or) COUNTRY**

☐ MasterCard ☐ VISA

MAIL ORDER FORM TO:
Superintendent of Documents
Government Printing Office
Washington, D.C. 20402

Credit Card No.

Expiration Date Month Year

Bank No.

Signature ____________________

Back cover

False color image of the nucleus of Halley's Comet taken from a distance of 12,000 miles by the European spacecraft GIOTTO. The cometary nucleus itself is seen as the darker potato-shaped object at the upper left against the brighter gas and dust jets streaming away from the sun. While celestial objects like Comet Halley are benevolent visitors to the Earth, other extra-terrestrial bodies have caused catastrophic impacts in the geologic past. Photograph copyright Max-Planck-Institut für Aeronomie, Lindau, Federal Republic of Germany.

U.S. GOVERNMENT PRINTING OFFICE
PUBLIC DOCUMENTS DEPARTMENT
WASHINGTON, D.C. 20402

OFFICIAL BUSINESS
PENALTY FOR PRIVATE USE $300

BULK RATE MAIL
POSTAGE & FEES PAID
USGS
PERMIT No. G23

Copyright material has been
deleted, not available for
Microfiche Edition.

Department of the Interior
U.S. Geological Survey

18/3

Earthquakes & Volcanoes

Volume 18, Number 3, 1986

I 19.65:

UNITED STATES DEPARTMENT OF THE INTERIOR
Donald Paul Hodel, Secretary

U.S. GEOLOGICAL SURVEY
Dallas, L. Peck, Director

Earthquakes and Volcanoes is published bimonthly by the U.S. Geological Survey to provide current information on earthquakes and seismology, volcanoes, and related natural hazards of interest to both general and specialized readers.

The Secretary of the Interior has determined that the publication of this periodical is necessary in the transaction of the public business required by law of this Department. Use of funds for printing this periodical has been approved by the Office of Management and Budget through June 30, 1989.

Henry Spall—Editor

Earthquakes and Volcanoes
U.S. Geological Survey
904 National Center
Reston, Virginia 22092
Telephone (703) 648-6078

Jill K. Moebus—Graphics Design

Subscription orders should be sent to:

Superintendent of Documents
U.S. Government Printing Office
Washington, DC 20402
Telephone (202) 783-3238

For sale by the Superintendent of Documents. Annual subscription rate—$15.00 (domestic) and $18.75 (foreign). Make check or money order payable to the Superintendent of Documents.

Single copy rate—$3.00 (domestic) and $3.75 (foreign). Single copy rate for issues prior to Volume 15, Number 1—$2.25 (domestic) and $2.85 (foreign). Can be purchased from the Book and Open-File Reports Section, U.S. Geological Survey, Federal Center, Building 41, Box 25425, Denver, CO 80225 (make check or money order payable to the Superintendent of Documents).

Earthquakes & Volcanoes

(formerly *Earthquake Information Bulletin*)
Volume 18, Number 3, 1986

113 **Living with the Earthquake Risk**
by Albert M. Rogers

122 **The Pacific Tsunami Warning System**
by George Pararas-Carayannis

131 **Land Subsidence**
by Thomas L. Holzer

138 **Cooperative Earthquake Research between the United States and the People's Republic of China**
by David P. Russ and Leonard E. Johnson

141 **About the Authors**

[illegible] LIBRARY
U. S. [illegible]
DEPOSITORY [illegible]

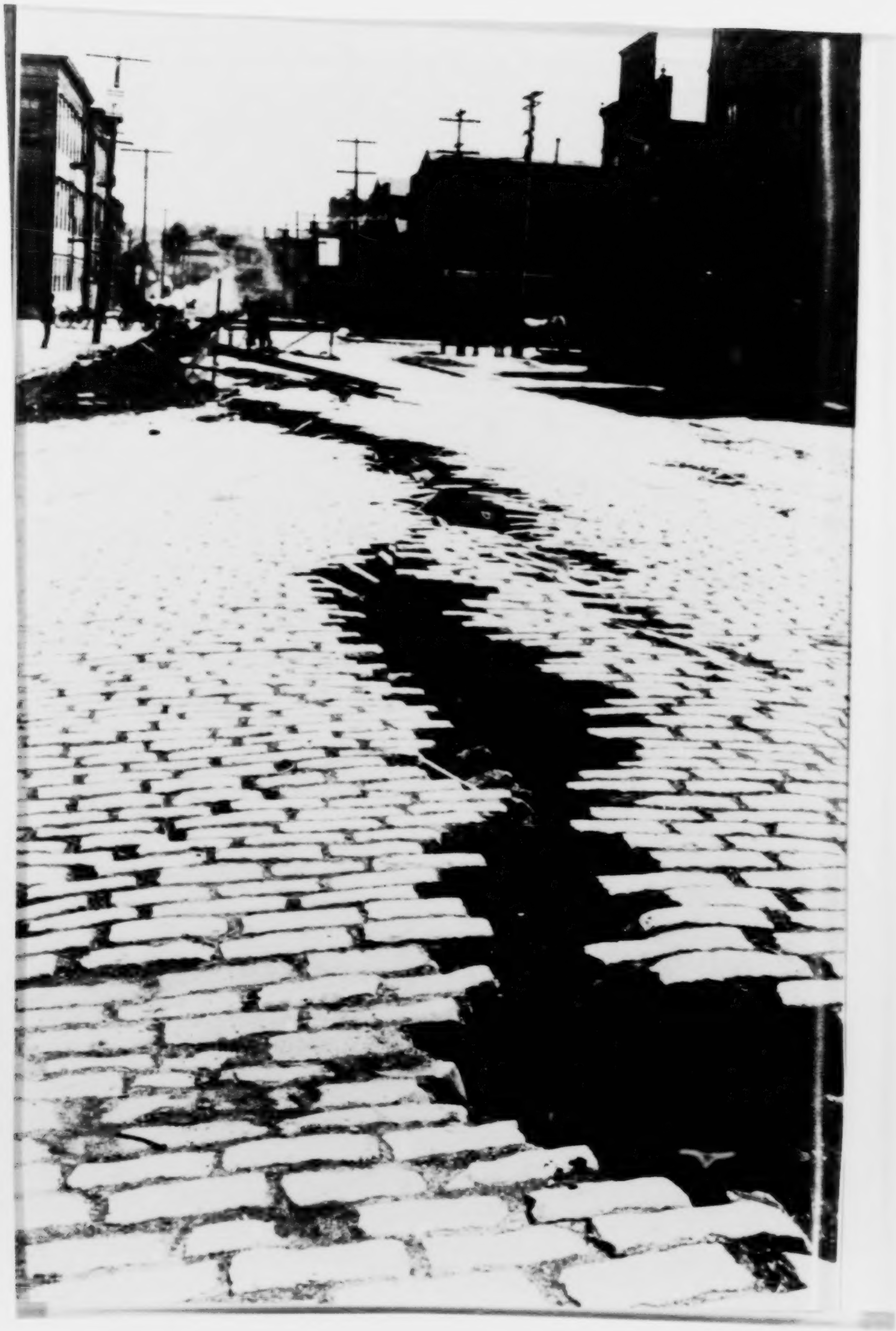

LIVING WITH THE EARTHQUAKE RISK

Albert M. Rogers
U.S. Geological Survey
Denver, Colorado

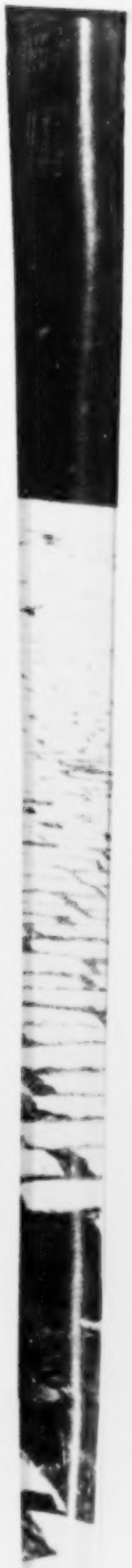

Damage to the Mission District of San Francisco after the 1906 earthquake was caused by soil failure, not faulting.

The principal hazards from earthquakes are surface faulting, ground failure, and ground shaking. In coastal areas tsunamis, or seismic sea waves, also are a potential hazard. We will consider each of these hazards briefly to assess their possible effects on the structures of man.

Surface faulting accompanies many large earthquakes, particularly in the western United States, and occurs when rock on either side of a fault is displaced at the earth's surface. The slip may be vertical, horizontal, or a combination of both. In major earthquakes, the movement along a fault can be as much as 35 feet and the length of the surface rupture as great as 250 miles. Even small amounts of slip can disrupt buried power, water supply, and communication lines. Vertical slip greater than a few inches can completely disrupt roadways where the fault crosses them. And, of course, faults that pass under structures are likely to cause severe structural damage if slippage occurs.

Ground failure, which includes landsliding, liquefaction, and settlement, is induced by earthquake shaking in some geologic materials having unfavorable physical properties. Landslides, for instance, can be caused by ground shaking, which starts the movement of loose soil and rock down a slope. The slope need not be steep. For example, the Turnagain Heights landslide in the Anchorage, Alaska, earthquake of 1964 resulted in the movement of 135 acres of material in an area having a slope of less than one-half degree. This slide destroyed about 75 homes, some of them moving 450-500 feet laterally.

Landslide in the Turnagain Heights section of Anchorage, caused by the 1964 Alaska earthquake.

Apartment buildings that tilted due to liquefaction at their base during the magnitude 7.5 1964 earthquake at Niigata, Japan.

One of the most spectacular examples of liquefaction occurred in Niigata, Japan, in 1964. In the simplest terms, liquefaction occurs when ground shaking produces high water pressure under the earth's surface and causes sand layers to act as a liquid. A number of high-rise buildings in Niigata sank more than 3 feet and some were tilted 80 degrees; the tilt was great enough to allow some residents to escape by walking down the face of the building.

Settlement is simply compaction of loose soils. This phenomenon can be damaging to roadways, particularly near bridge abutments where the roadbed may settle while the bridge remains fixed. In coastal areas, settlement of several inches can affect the coastline.

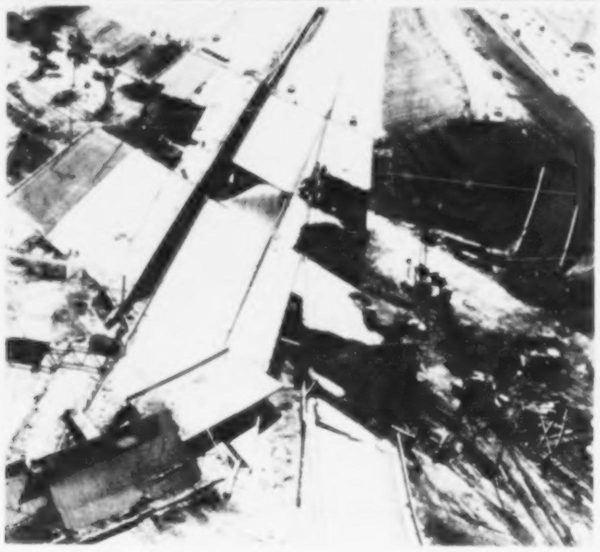

Two views of the highway overpass that collapsed during the 1971 San Fernando earthquake.

Tsunamis are fast-moving water-waves generated by certain types of earthquakes. These waves can travel hundreds or even thousands of miles from their source and may surge to damaging heights in coastal areas. Hawaii and Alaska have been repeatedly struck by severe tsunamis. California has also experienced several minor tsunamis, all of which have been under about 3 feet and have not been damaging.

Although all of these earthquake-induced phenomena can play an important role in causing damage, it is possible to experience an earthquake in which the damage is caused solely by ground shaking. In fact, in most earthquakes, ground shaking is the greatest hazard, causing the largest percentage of damage. Ground shaking is caused by earth waves that travel away from the earthquake source and may cause damage at distances of as much as 50-75 miles.

Estimation of probable ground shaking is a complicated but important technique that can serve as useful input for land-use planning, earthquake-resistant building design, and the estimation of losses from future earthquakes. Three major elements affect the severity of the ground shaking that may occur at any given location: the size of the earthquake, the distance to the earthquake source, and the geologic conditions.

Damage in Charleston, South Carolina after the 1886 earthquake.

In a general way, the larger magnitude earthquakes produce stronger ground shaking that occurs over broader areas than for a smaller event. However, regional differences in the earth's crust may modify this. In the central and eastern U.S., earthquake shaking attenuates less rapidly than in the west. For instance, the New Madrid, Missouri, earthquakes of 1811 and 1812, and the Charleston, South Carolina, earthquake of 1886, were felt over much larger areas than the 1906 San Francisco earthquake, even though the magnitude of the latter event was greater.

Site conditions are a major element affecting the likely intensity of ground shaking. Thick soils overlying solid rock tend to increase the level of ground shaking and prolong the duration of shaking. The degree to which this effect takes place is dependent on certain physical properties of the soil, especially its velocity, density, and thickness relative to the underlying rock.

Evaluation and mapping of potential earthquake hazards in major metropolitan areas will ultimately provide a useful data base for city planners, engineers, architects, and disaster relief planners. Such studies are currently under way in San Francisco.

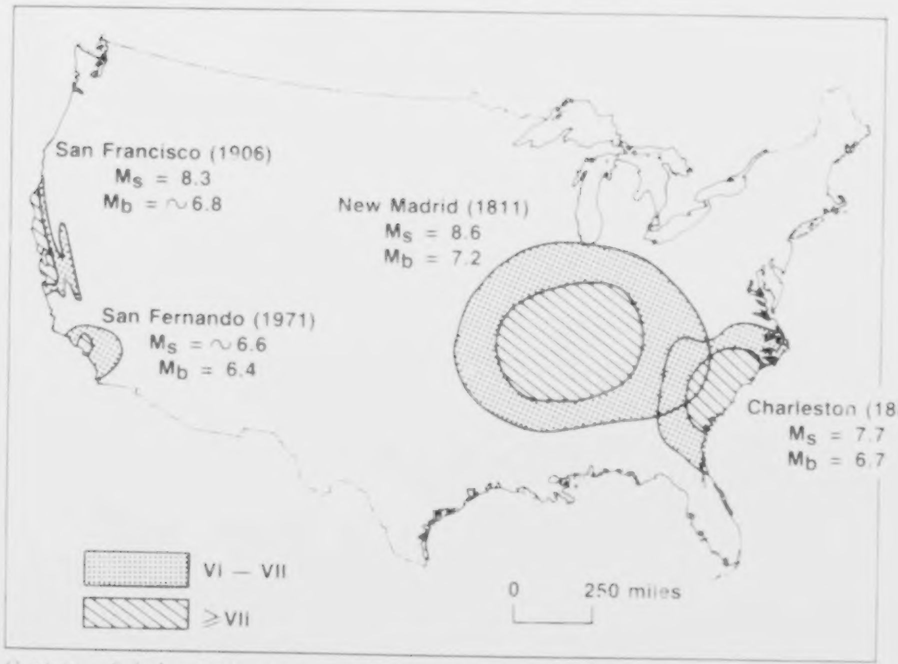

Contours of shaking intensity in four U.S. earthquakes. Differences at the site of the shaken areas reflect differences in attentuation between the eastern, central and western United States.

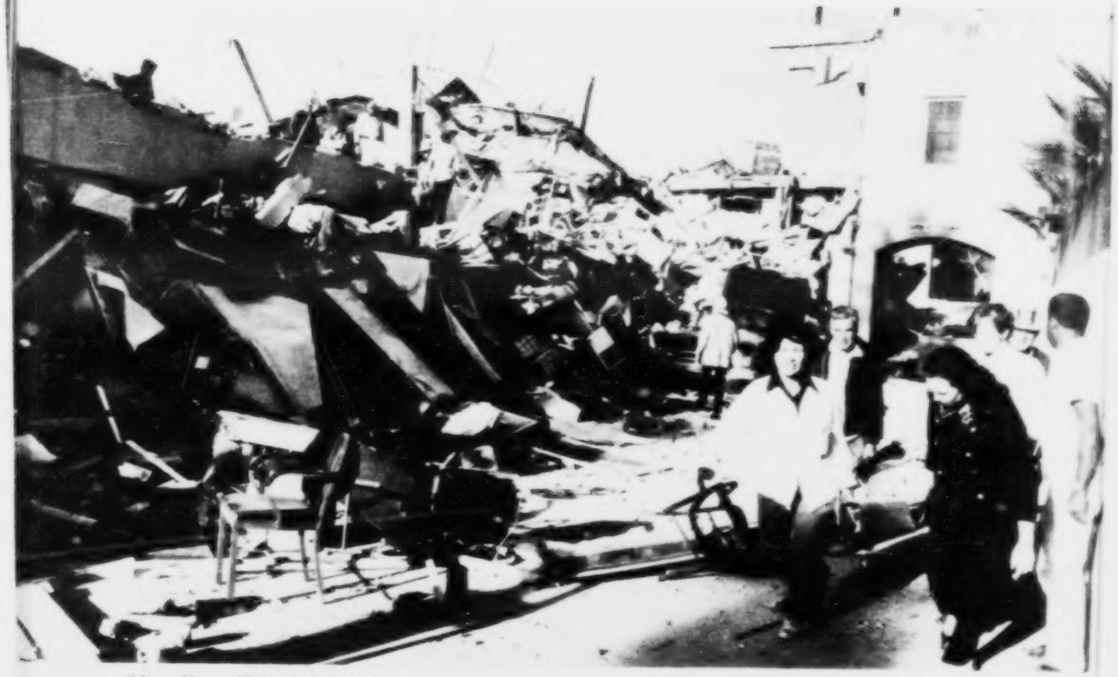

Olive View Hospital was 6 miles from the epicenter of the 1971 San Fernando earthquake (magnitude $M_s=6.5$). The hospital was new and complied with the building code but the actual ground motion greatly exceeded the code. Note the collapsed stair tower. The first floor collasped, leaving the second story at ground level.

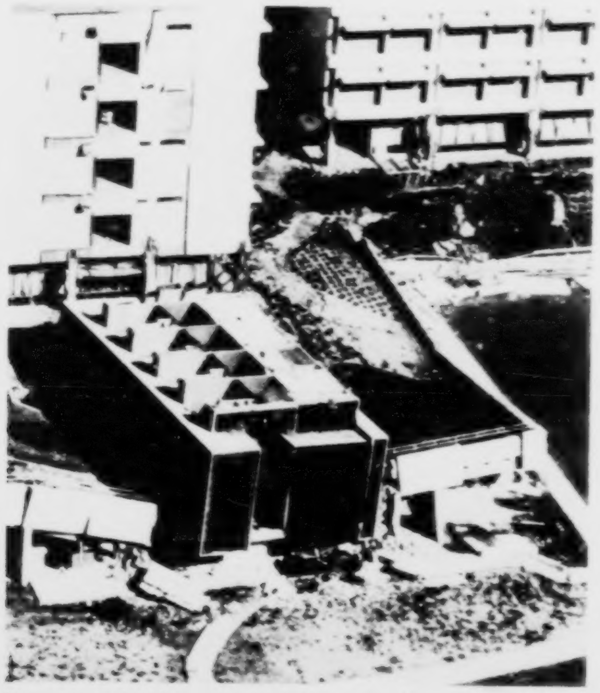

Damage to the Veteran's Administration Hospital at Sylmar, California after the 1971 earthquake.

"Buildings constructed to meet seismic codes generally fare better in earthquakes."

Los Angeles, Salt Lake City, and in Boston. In the near future, similar efforts may begin in other earthquake-prone areas.

The study of earthquake damage enables one to estimate how buildings will respond during future earthquakes, suggesting possible design improvements or estimates of future earthquake losses. A great deal can be learned in this manner, but several points are important.

The damage at the Veteran's Administration Hospital in the San Fernando Valley during the 1971 earthquake was caused by severe ground shaking, the buildings being nearly immediately above the buried earthquake source. The buildings constructed before 1933 were not designed to resist earthquake forces and 4 out of 26 buildings suffered total collapse. Of the 21 buildings built subsequent to 1933, only 4 suffered heavy damage, and these buildings, in general, suffered less damage than pre-1933 buildings. In other words, buildings constructed to meet seismic building code requirements generally fare better in earthquakes than structures that do not meet the code.

"The building codes are minimum standards."

However, the Olive View Hospital, a structure that was built to meet the building code requirements in effect during the mid-1960's, suffered massive damage in the 1971 earthquake. Larger and longer ground motions could have caused total collapse. As it was, three lives were lost and the building had to be razed. The performance of this structure illustrates several important points. First of all, the building codes are *minimum* standards. Building codes are intended to safeguard occupants of a structure, not to *prevent* substantial damage in larger earthquakes that may render a structure useless. Facilities as critical as hospitals deserve extra planning and engineering attention because they have high occupancy rates, the patients are frequently incapacitated and unable to take even simple precautions to protect themselves, and these facilities are urgently needed following the earthquake. Hospitals should be sited to avoid possible surface faulting or ground failure, and they should be designed to remain functional after the greatest earthquake intensity that might be expected during the planned life of the structures. In fact, damage to hospitals experienced in the 1971 earthquake prompted new regulations at the state and federal level to insure that hospitals remain functional after an earthquake. Similar arguments can be made for other critical facilities such as power plants and police stations.

"In the San Fernando quake 75-80 percent of the unreinforced masonry buildings were damaged."

Damage to unreinforced masonry is of particular concern because many older buildings in urban renewal projects are of this type. Unreinforced masonry structures have responded extremely poorly in earthquakes all over the world. In the San Fernando earthquake, for example, 75-80 percent of the unreinforced masonry buildings in the San Fernando Valley were damaged; and most of these subsequently were either demolished or underwent major structural alteration or repair. This type of building can be a life threat to occupants and the public, and also a financial risk to the owner. Some of these kinds of buildings can be strengthened to meet the earthquake code.

It is possible that local building codes and plans to rehabilitate structures can be devised so that structures that represent high risk to life are dealt with before low-risk structures, and owners are given reasonable periods of time to make corrections. With regard to new buildings, it is important that construction practices meet the engineer's design requirements for earthquake resistance and that engineers and architects collaborate to produce designs that not only meet the codes but combine all the elements of the building in a fashion to minimize damage. Buildings may be designed or rehabilitated to withstand ground motions that will probably not be exceeded in the lifetime of the structure. The difficulty, of course, is deciding what level of probability is acceptable.

It is in this context that a restricted definition of hazard and the concept of risk can be helpful. *Earthquake hazard* can be defined as the probability of occurrence of a specified level of ground shaking in a specified period of time. *Earthquake risk*, on the other hand, is defined as the expected (or probable) life loss, injury, or building damage, given the probabilities that specified levels of ground shaking occur. The U.S. Geological Survey has recently prepared a preliminary earthquake-shaking hazard map of the United States. The map shows the peak horizontal accelerations on rock that have a 90 percent chance of not being exceeded in a 50 year period. Another way of stating this is that the map shows accelerations that have a 10 percent probability of being exceeded in any 50 years. The accelerations are contoured at levels ranging from 0.04-0.6 g. The lower value is the acceleration below which wind loading generally is expected to dominate the design of structures. Values as large as 0.8 are postulated within the 0.6 g contour close in to the Owens Valley and San Andreas faults in California.

Damage to unreinforced brick buildings during the 1983 magnitude 6.6 earthquake at Coalinga, California.

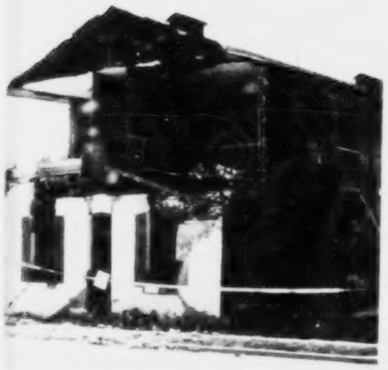

"The difficulty. . . is deciding what level of probability is acceptable."

This map is based on the historic seismic record and on reasonable suppositions about how ground motion attenuates with distance from the fault in different regions and what the largest possible earthquake is in each region. For intance, we know that very large earthquakes are possible in certain parts of the United States and that the rate of occurrence of earthquakes in many parts of the west is higher than in the midwest and east. We have already pointed out the difference in attenuation of ground shaking between the eastern and western U.S., and these factors have been incorporated in a quantitative way in the hazard map.

For ordinary structures, the hazard map probably represents the most useful estimate of the short-term shaking hazard that is available. This information, coupled with the probability of building damage due to ground shaking and the value of the building, enables us to calculate expected losses from earthquakes.

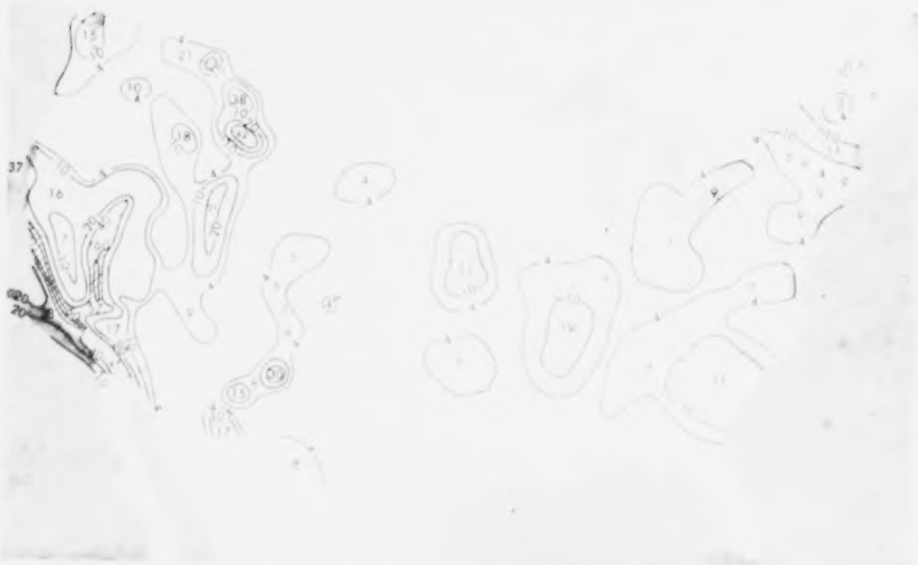

Map of earthquake hazard to be expected from ground shaking in the contiguous 48 States. The numbered contours are the horizontal acceleration in hard rock expressed as a percentage of g—the Earth's gravity. The seismic hazard is depicted at a constant-probability level: There is a 90-percent probability that it will not be exceeded in 50 years. The numbers within each contour are the maximum expected accelerations. The maximum acceleration within the 60-percent contour along the San Andreas and Garlock faults in California is 80 percent of g.

(From Algermissen, S. T. and Perkins, D. M., 1976, A probabilistic estimate of maximum acceleration in rock in the contiguous United States. U.S. Geol. Survey Open-File Rept. 76-416.)

THE PACIFIC TSUNAMI WARNING SYSTEM

George Pararas-Carayannis
International Tsunami Information Center
P.O. Box 50027
Honolulu, Hawaii 96850

Historical Background

Of all natural disasters, tsunamis are among the most terrifying and complex phenomena, responsible for great loss of lives and vast destruction of property. Enormous destruction of coastal communities has taken place throughout the world by such great waves since the beginning of recorded history.

The impact of tsunamis on human societies can be traced back in written history to 1480 BC, when the Minoan civilization in the Eastern Mediterranean was wiped out by great tsunami waves generated by the volcanic explosion of the island of Santorin. In the Pacific Ocean where the majority of these waves have been generated, the historical record, although brief, shows tremendous destruction. In Japan which has one of the most populated coastal regions in the world and a long history of earthquake activity, tsunamis have destroyed entire coastal communities. There is also history of tsunami destruction in Alaska, in Hawaiian Islands, and in South America.

A small tsunami was associated with the November 29, 1975 earthquake on the island of Hawaii. The photo shows surf surging through palm trees at a camping site at Halape (Photograph by H. Clark, Honolulu Advertiser).

The Need for a Warning System

While most of the destructive tsunamis have occurred in the Pacific Ocean, devastating tsunamis have also occurred in the Atlantic, the Indian Ocean, and in the Mediterranean Sea. In the last 30-40 years there has been tremendous growth and development of the coastal areas in most of the developing or developed Pacific nations. This is the result of population growth and of technological and economic developments that have made the use of the coastal zone more necessary than before. Many of the countries of the Pacific, for example, have populations with natural maritime orientation. For many of these countries foreign trade is a necessity so they maintain major port facilities. Others have extensive ship building facilities, electric plants, refineries, and other important coastal structures. A number of countries throughout the Pacific have now begun important aquaculture industries and canneries. This combination of social and economic factors makes a number of developed and developing countries of the Pacific vulnerable to the threat of tsunamis.

To protect life and property in the Pacific an International Pacific Tsunami Warning System has been organized using an extensive network of seismic and tidal stations, as well as communications, to ensure that the warning information is prompt and accurate. This Pacific Tsunami Warning System is an offspring of a basic U.S. warning system that was initially designed to protect the Hawaiian Islands. The following is a review of the history and evolution of this System.

Tsunami of May 24, 1960, caused enormous damage at Hilo, Hawaii. (Photograph by Honolulu Advertiser)

The U.S. and Other Tsunami Warning Systems

After the Aleutian tsunami of April 1, 1946 caused major damage and many casualties in the Hawaiian Islands, it was obvious that a means of providing warnings to the population of Hawaii was necessary. This early U.S. Tsunami Warning System was confronted with a number of problems that had to be solved. The Warning System had to detect and rapidly locate earthquakes in the Pacific region, and if one occurred in an area where tsunami generation was possible, to determine quickly whether indeed a tsunami had been generated. Also it was necessary to develop a method for accurate arrival times of the tsunami at various places. Initially a tsunami travel time chart for Honolulu was prepared. Later, travel time charts were also prepared for other stations in the System. For the prototype system a detector was actuated by unusual wave motion of the tsunami to ring an alarm.

In 1946 photographic methods were still used to record earthquakes because they were simple, practical and precise. Visual recording equipment was needed to be used in conjunction with existing seismographs. In 1947 and 1948 these new instruments were built and installed at three seismic observatories. Later these installations were modified by adding a new electronic amplifier. It included an alarm circuit so that whenever a major earthquake was recorded, an audible and/or visible alarm was tripped, thus insuring prompt observation of every major earthquake. Also a tentative communication plan was prepared utilizing existing communication of the Armed Forces and of the Civil Aeronautics Administration. The original Tsunami Warning System consisted of three seismological observatories of the Coast and Geodetic Survey at Sitka, College, Tucson, and Honolulu, and tide stations at Attu, Adak, Dutch Harbor, Sitka, Palmyra Island, Midway Island, Johnston Atoll, Hilo, and Honolulu. Honolulu Observatory was made the headquarters of this initial Tsunami Warning System. Its function was to supply tsunami watch and warning information to the civil authorities and various military headquarters in the Hawaiian Islands for dissemination to military bases throughout the Pacific and to the islands in the United States Trust Territories of the Pacific. Later, in 1953 warning information was also given to the civil defense agencies of California, Oregon, and Washington.

Other countries in the Pacific, such as Japan and USSR had also established rudimentary national warning systems, with the responsibility of warning primarily their own civil defense authorities and protecting their own national interests. These systems had limited data collection capabilities, limited communications within their own national jurisdictions, and limited warning dissemination capability.

International Cooperation

The great destruction caused by the May 1960 Chilean tsunami prompted a large number of countries and territories to join the Pacific TWS at least by contributing data and information. The great Alaskan earthquake of 1964 generated a devastating tsunami that affected a good part of the Pacific. This tsunami focused additional attention to the need for an International Tsunami Warning System.

In 1965, the United Nations Educational, Scientific, and Cultural Organization's (UNESCO) Intergovernmental Oceanographic Commission (IOC) accepted an offer made by the United States to expand its existing Tsunami Warning Center in Honolulu to become the headquarters of an International Pacific Tsunami Warning System and at the same time accepted the offer of other IOC member countries to integrate their existing facilities and communications into this System. A meeting was held in Honolulu, Hawaii in 1965 establishing the International Tsunami Information Center (ITIC) and an International Coordination Group for the Tsunami Warning System (ICG/ITSU).

ITIC was given the general mandate of mitigating the effects of tsunamis throughout the Pacific by supporting member states of ICG/ITSU in developing and improving preparedness for tsunamis; by monitoring and seeking to improve the Tsunami Warning System for the Pacific; by gathering and disseminating knowledge on tsunamis, by fostering tsunami research; and by bringing to non-member states a knowledge of the Tsunami Warning System and ITIC, and information on how to become participants through IOC/ITSU.

The International Coordination Group, established as a subsidiary body of IOC, meets every two years in a member state to coordinate and review the activities of the International Tsunami Warning System (ITWS).

The International Tsunami Warning System

The existing U.S. Warning System was integrated with the Systems of Japan, USSR, Chile, and of other regional centers, and became a truly International Tsunami Warning System. Twenty-three nations are now members of ITSU in the Pacific: Australia, Canada, Chile, China, Colombia, Cook Islands, Ecuador, Fiji, France, Guatemala, Hong Kong, Indonesia, Mexico, Japan, Republic of Korea, New Zealand, Peru, Philippines, Singapore, Thailand, USA, USSR, and Western Samoa. Several nonmember states and territories maintain stations for the ITWS. The System makes use of 69 seismic stations, 65 tide stations, and 101 dissemination points scattered throughout the Pacific Basin under the varying control of the member states of ITSU. The Pacific Tsunami Warning Center at Ewa Beach near Honolulu is operated by the U.S. National Weather Service, Pacific Region.

Also, a program of preparedness has been developed alerting coastal populations, industries, and Civil Defense agencies to respond to tsunami warnings. The International Tsunami Information Center (ITIC) has the responsibility of coordinating public educational programs for each participating country. ITIC works closely with government agencies, private institutions, and Civil Defense authorities, developing sound coastal management policies which include zoning and planning for coastal areas, as well as standard operating procedures in case of an actual event.

The objectives of the Pacific Tsunami Warning System are to detect and locate major earthquakes in the Pacific region as soon as possible, to determine whether they have generated tsunamis, and to provide timely and effective information and warnings to the population of the Pacific in order to minimize the hazards to life and property.

Seismologist at the Pacific Tsunami Warning Center checking seismic recorders

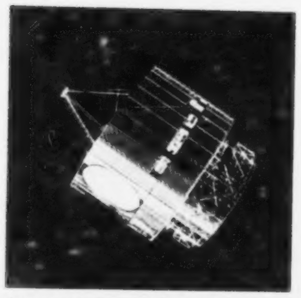

Geostationary Operational Environmental Satellite (GOES) used for transmitting seismic and tidal data among the Pacific tsunami warning stations.

How the System Works

Functioning of the system begins with the detection of an earthquake which has a magnitude and location that make it potentially tsunamigenic. The earthquake has to be of sufficient magnitude to trigger the alarm attached to the seismograph at the station where it is being recorded. The alarm thresholds are set so that ground vibrations of the amplitude and duration associated with an earthquake of approximate magnitude 6.5 or greater on the Richter scale anywhere in the Pacific region will cause them to sound. This magnitude is below the threshold for issuing watch and warning messages. Personnel at the station immediately interpret their seismograms and send their readings to the Pacific Tsunami Warning Center. Upon receipt of a report from one of the participating seismic observatories or as a consequence of the triggering of their own seismic alarm, PTWC personnel send messages requesting data from the observatories in the system.

When sufficient data have been received so that the earthquake can be located and the magnitude computed, a decision is made as to further action. If the earthquake is strong enough to cause a tsunami and is located in an area where this is possible, participating tide stations near the epicenter are requested to monitor their tide gauges. Watch bulletins are issued to the dissemination agencies for all earthquakes of magnitude 7 or greater occurring in the Aleutian Islands and all earthquakes of magnitude 7.5 or greater occurring elsewhere in the Pacific. A watch may also be disseminated by the PTWC upon the issuance of warnings by regional warning centers. Since the regional systems use different criteria for their disseminations, a watch may at times be issued for earthquakes with magnitude less than 7.5.

When reports from tide stations show that a tsunami poses a threat to the population in part or all of the Pacific, a warning is transmitted to the dissemination agencies for relay to the public. These agencies then implement plans to evacuate people from endangered areas. If the tide station reports indicate that either a negligible tsunami or no tsunami has been generated, PTWC issues a cancellation.

Capabilities and Limitations of the System

A tsunami originates in or near the epicentral area of the earthquake that creates it. It propagates outward in all directions at a speed that depends on ocean depths. In the deep ocean, the speed may exceed 600 km/s; thus, the need for rapid data handling

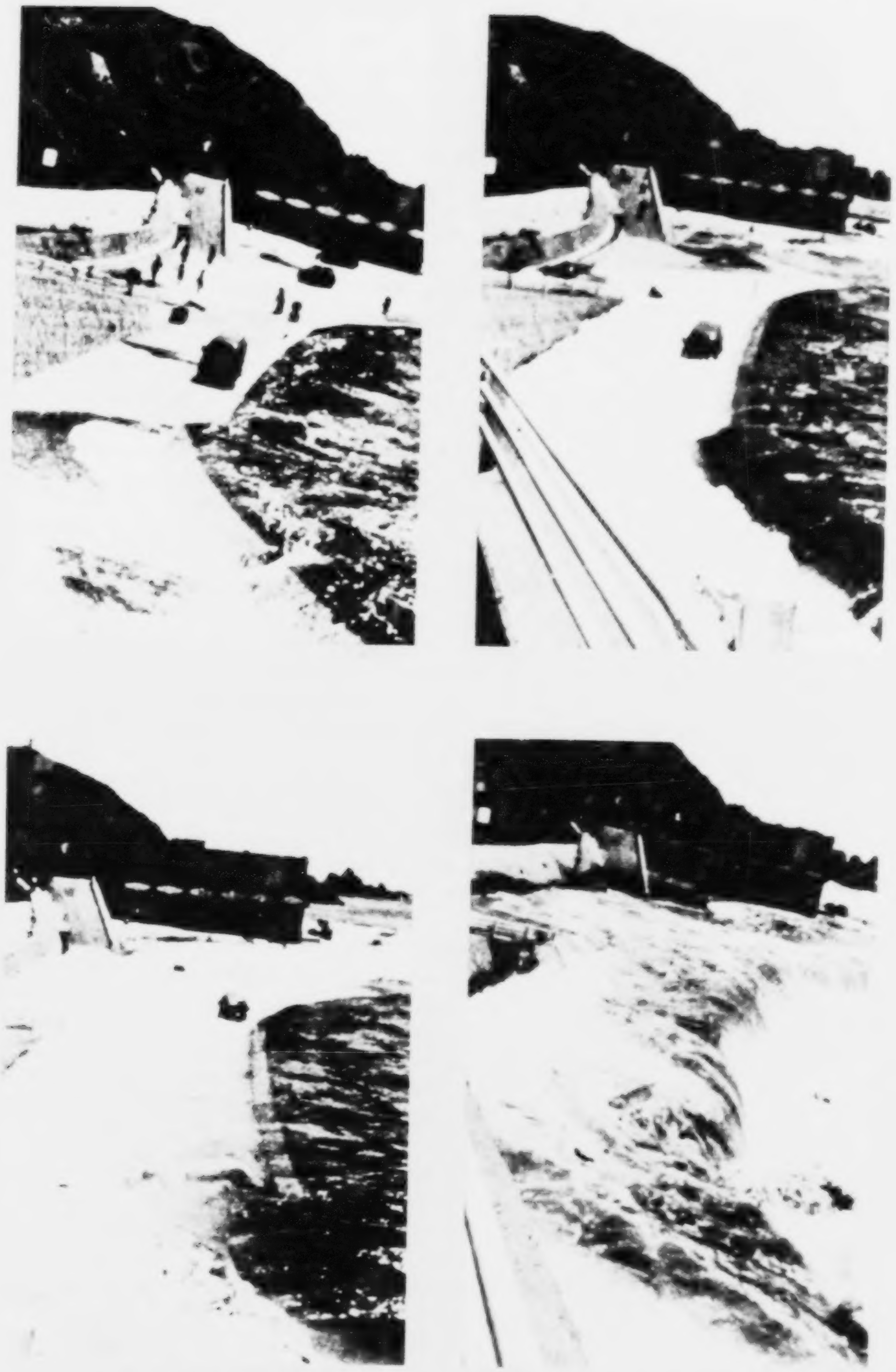

Remarkable sequence of photos of the tsunami generated by the Nihonkai Chuba (Japan) earthquake of May 26, 1983. The van was swept out to sea by the tsunami.

and communication becomes obvious. Because of the time spent in collecting seismic and tidal data, the warnings issued by PTWC cannot protect areas against local tsunamis in the first hour after generation; for this purpose, regional warning systems have been established in some areas.

The regional systems generally have data from a number of seismic and tide stations telemetered to a central headquarters. Nearby earthquakes are located, usually in 15 minutes or less, and a warning based on seismological evidence is released to the population of the area. Since the warning is issued on the basis of seismic data alone, watches or even warnings will occasionally be issued when tsunamis have not been generated. Since they are issued only to a restricted area and confirmation of the existence or nonexistence of a tsunami is rapidly obtained, dislocations of populations are minimized. To limit the number of agencies to be contacted, warnings are generally issued to only one agency in each country, territory, or administrative area.

Dissemination agencies have the continuing responsibility for educating the public concerning the dangers of tsunamis and for developing safety measures that must be taken to avoid loss of life and to reduce property damage. The agencies are encouraged to develop emergency plans for all threatened localities, clearly delineating areas of possible inundation. Evacuation routes should be designated, safe areas marked, and the amount of advance warning to insure evacuation from danger areas determined.

Planned Improvements

A general operational concept is presently being developed for the International Tsunami Warning System using updated technology and instrumentation. The objective is to reduce the time needed to evaluate the tsunami hazard, make decisions, and disseminate the warnings, on a Pacific-wide or a regional basis. The new system is using a large network of shore-based seismic and tsunami sensors transmitting real-time data to the International Tsunami Warning Center (ITWC) in Honolulu, making use of synchronous meteorological satellites for communication relay.

Future refinements may include offshore tsunami bottom sensors using crystal pressure-transducers, acoustic or wire links with existing buoy systems, data microprocessors, and data links via geostationary satellities between shore installations and the ITWC. Both the offshore and the coastal tsunami sensors will be continuously-recording, event-activated, or activated on demand. The prototypes for coastal installation are complete, tested, and working. Additional work is needed in the adaptation of microcomputers, power supplies, acoustic links with buoys, and the housing of the offshore tsunami sensors. A unique data-processing interphase system has been developed for the ITWC in Honolulu using a multitask computer system to handle increased data loads available through the synchronous satellites and other data networks. The new technology is resulting in a more efficient International Tsunami Warning System.

Finally, the International Tsunami Warning System is one of the most successful international programs ever undertaken involving a multitude of nations with the direct responsibility of mitigating the effects of tsunamis, the saving of lives, and the preservation of property. It is an effective operational program with a direct humanitarian objective—the protection of human lives in the Pacific Ocean coastal areas. The system has been made possible by the generous contributions and participation of the Community of Nations of the Pacific, by IOC's involvement, and by the active and effective coordination of ITIC and of the International Coordination Group.

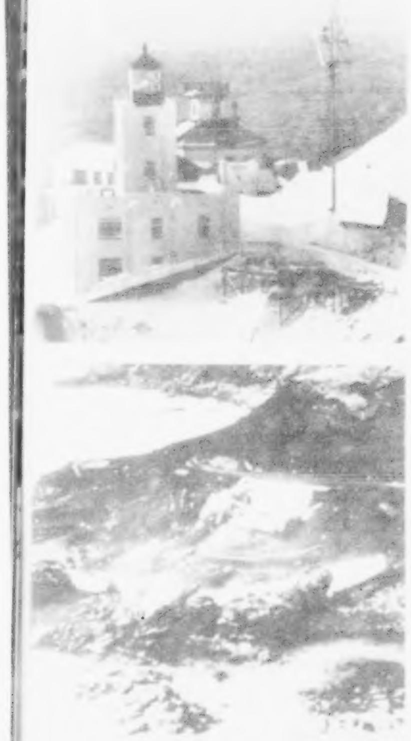

Damage to the Scotch Cap lighthouse from the Aleutian tsunami of April, 1946, Unimah Island, Alaska; before and after.

Tsunami damage at Anchorage, Alaska, after the 1964 earthquake.

A storm in 1966 caused extensive flooding in the San Marco, Venice, Italy.

Land Subsidence

Thomas L. Holzer
U.S. Geological Survey
Menlo Park, California

In November 1966, sixty percent of Venice, Italy, is inundated by a storm surge that causes waters in the Venetian lagoon to rise more than 6 feet. On December 28, 1971, a janitor at the Washington Elementary School in Johnston City, Illinois, discovers severe cracking of the school. In January 1972, the school is abandoned and subsequently razed. In the 1970's, five homes in New Orleans, Louisiana, are destroyed by gas explosions. In May 1981, a 350 feet diameter sink-hole forms in a business area in Winter Park, Florida, and swallows a home and parts of several businesses. In August 1983, Hurricane Alicia slams into the Texas Gulf Coast near Houston, Texas, and devastates the 500-home Brownwood subdivision on the north end of Galveston Bay. Homes are torn from their foundations and reduced to rubble.

What do these events have in common? Each is directly or indirectly linked to land subsidence caused by man's activities. Compaction caused by ground-water withdrawal worsened the two flooding episodes, collapse into an old underground coal mine cracked the school, differential settlements caused by drainage of organic soils severed gaslines and caused the explosions, and ground-water withdrawal from the Floridian aquifer induced formation of the sink-hole.

Earth scientists and engineers use the term "land subsidence" to describe all of these events because

House in Houston that has now subsided below sea level.

they can be attributed to predominantly vertical displacement of the land surface caused by removal of subsurface support. But as shown in the examples, the character of the displacement varies broadly, including both catastrophic collapse of the land surface, as in Johnston and Winter Park, and regional lowerings of the land surface that may take decades to become problematic as in Venice, New Orleans, and Houston. This variation is related to the different mechanisms of man-induced land subsidence. Although basically all of the processes involve removal of subsurface support, the loss of support varies from changes of stress to physical removal of subsurface material.

The most important of man's activities that cause land subsidence in the United States include (1) subsurface mining of both metals and nonmetals, but mostly coal, (2) withdrawal of both ground water and petroleum from unconsolidated sediment, (3) drainage of peat and muck soils, (4) ground-water withdrawal from limestone, (5) solution mining, and (6) surface application of water to undercompacted sediment. The diversity of technical specialists, industries, and parties affected by and involved with land subsidence has tended to discourage comprehensive overviews of the subsidence problem confronting the Nation. No single institution or government agency compiles information on its impact. The problem, however, is significant. Man-induced subsidence occurs in at least 38 states. In terms of broad regions, only New England, Alaska, and Hawaii have been spared. The total area affected is more than 16,000 square miles. Conservative estimates of annual cost exceed $100 million. Some individual communities have incurred costs of more than $30 million annually during the height of their problem. Other communities are jeopardized by subsidence that may take decades to extract its ultimate cost.

Coal-mine subsidence—A legacy from the past and for the future

Underground mining, which began around 1700 near Richmond, Virginia, has been conducted in 22 states. Approximately 12,500 square miles of land is undermined, and it has been estimated that the area will eventually grow to 62,500 squares miles. Approximately 3100 square miles of the currently undermined area already has experienced subsidence. The U.S. Bureau of Mines estimates that subsidence threatens 620 square miles of land in urban areas. Annual damage costs may be as high as $30 million. Many of the costs are associated with unmapped old abandoned mines over which urban development has expanded. Subsidence may begin a decade to as much as a century after mining has stopped. Even after subsidence has taken place at a site and periods of quiescence have been observed, the possibility of future subsidence remains. Future subsidence can be prevented only by backfilling the remaining void. The U.S. Bureau of Mines estimated in 1978 that the costs to stabilize undermined urbanized areas would be almost $12 billion.

Unregulated underground fluid withdrawal—A costly problem for some coastal areas

Withdrawal of underground fluids from unconsolidated sediment has caused some of the most costly individual subsidence problems in the United States. The subsidence is caused by sediment compaction. From the early 1940's to the mid-1960's, the port city of Long Beach, California, sank up to 29 feet during development of the Wilmington Oil Field, the most prolific field in California. Costs from this subsidence exceeded $120 million. Control of subsidence by repressuring the field required the threat of state legislation to unitize the field. In Houston, Texas, decades of ground-water withdrawal for municipal, industrial, and agricultural purposes caused portions of the coastal area to subside more than 6 feet. In the early 1970's, subsidence was costing more than $30 million annually. Aggregate costs are not known. Subsidence in the Houston area not only threatens outright inundation of low-lying land but increases susceptibility

Flooding and home devastation in the Brownwood subdivision, Houston area, Texas, caused by Hurricane Alicia in August 1983. The subdivision has subsided about 8 feet since 1915 because of fluid withdrawal. Storm surges, tides caused by the low barometric pressures of hurricanes, have been observed as high as 22 feet in the greater Houston area. More than 300,000 people live below this elevation. (Photograph by the Harris-Galveston Coastal Subsidence District)

House in Houston, Texas, that subsided as a result of withdrawal of ground water under the area. (Photograph by C.W. Kreitler)

of adjacent areas to flooding from storm surges generated by hurricanes. The worst natural disaster in American history occurred from such a storm when 6,000 people died in Galveston in 1900. To reduce future coastal subsidence, the Texas legislature authorized formation of the Harris-Galveston Coastal Subsidence District in 1975 and empowered it to regulate ground-water withdrawal.

More recently, concern has been expressed that proposed development of the potentially vast energy resources of the geopressured zone in the Gulf Coast may cause additional subsidence. Subsidence has been observed at geothermal fields worldwide including The Geysers in California. Geopressured reservoirs may be even more susceptible to compaction than geothermal reservoirs if they are extensively developed because they are incompletely compacted. The combination of permeability and rates of burial have not permitted fluid pressures in these geopressured reservoirs to reach equilibrium.

Inland rural areas in the United States also have suffered from subsidence caused by fluid withdrawal. The principal impact has been on the operation of preexisting canals and the design of new ones. A lesser impact has been localized deformation that causes large tension cracks and reactivation of faults. In Houston, one of the areas most severely affected by ground failure, more than 86 faults with an aggregate scarp length of 150 miles have damaged many structures, including hundreds of homes.

Organic soils—Drainage leads inevitably to subsidence

Subsidence associated with drainage of organic soils may be the most costly type of subsidence affecting the United States. Drainage of these soils, which

Land area that collapsed catastrophically on August 11, 1983, east of Boling, Texas. Diameter is 250 feet. Collapse occurred over a salt dome and may have been caused by natural processes. Similar man-induced collapses over soluable deposits have been reported elsewhere in the United States. (Photograph by Boyd V. Dreyer)

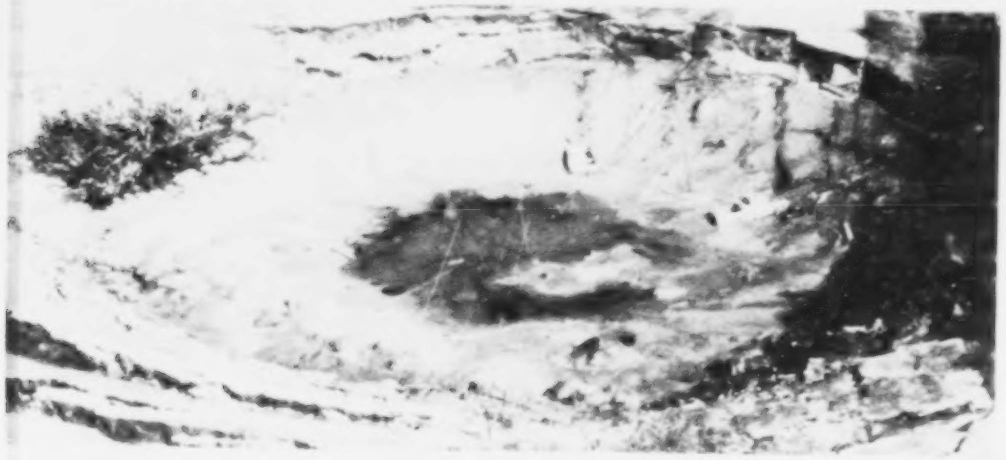

is necessary for development on them, inevitably results in subsidence. The processes causing the compaction are complex and involve both physical and biological phenomena. Rates of subsidence vary, depending on climate, type of peat, and depth to water table, but locally exceed 3 in/year. Subsidence has affected both urban and rural areas. A study in 1977 by the Department of Housing and Urban Development found that more than 10,000 square miles of organic wetlands are located within existing Standard Metropolitan Statistical Areas. About 2.5 million people live in reclaimed areas on these soils. Annual costs to repair damage to structures and for the special construction required to avoid damage may run as high as $58 million.

In agricultural areas subsidence has an additional aspect. The soil is actually being consumed and future cultivation is threatened. This is an important consideration in the Florida Everglades and the California Sacramento-San Joaquin Delta. In the Delta the problem is compounded because approximately 300 square miles of land has subsided below sea level, some as much as 25 feet, and must be protected by extensive levees. Levee failure leads to additional costs of expensive repairs, pumping, and loss of cultivation.

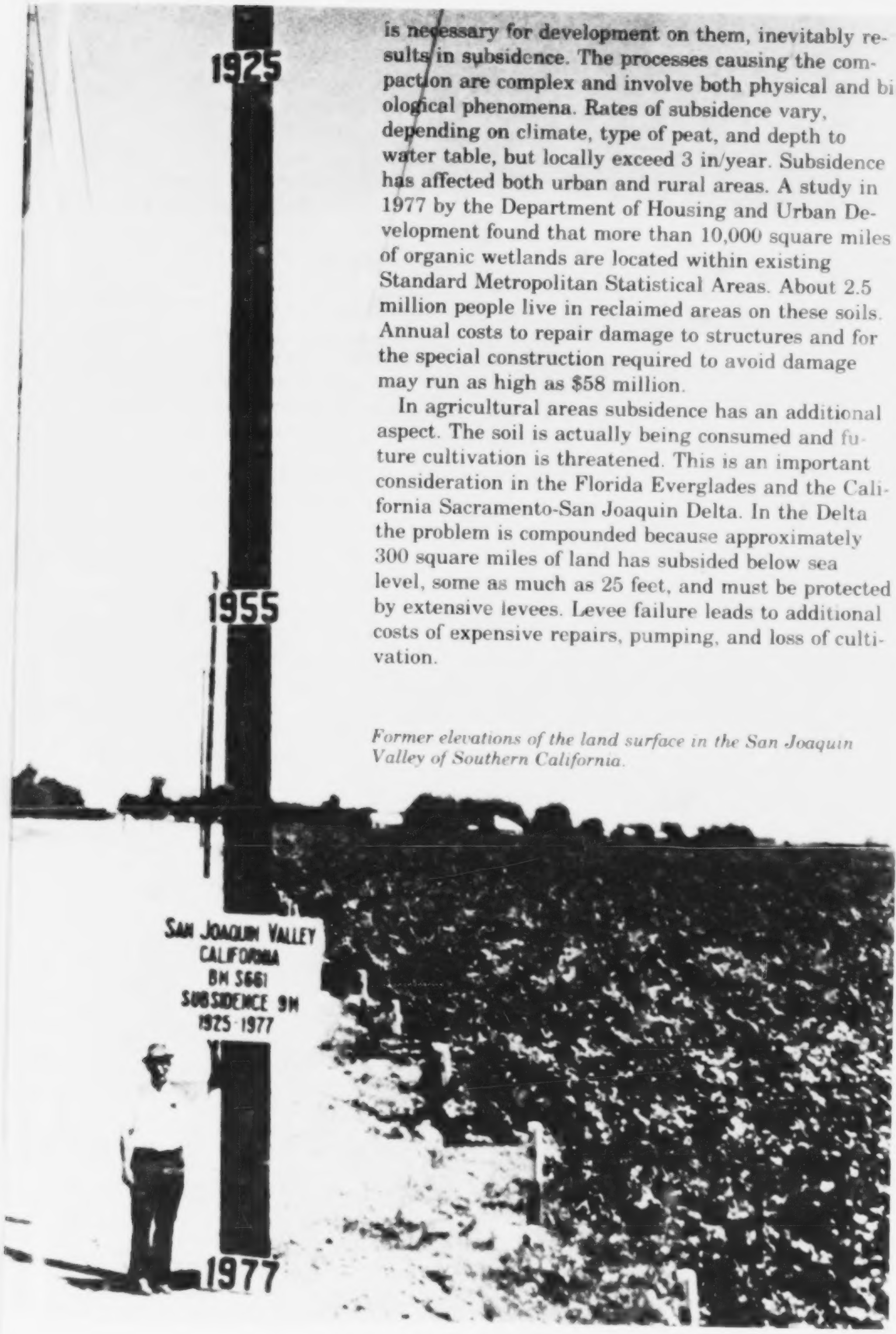

Former elevations of the land surface in the San Joaquin Valley of Southern California.

Sinkholes—catastrophic failures

Probably most individuals think of sinkholes in limestone terrain when they think of subsidence. These sinkholes are one of the most spectacular forms of subsidence because of their dimensions and frequently catastrophic formation. Holes larger than football fields may form within hours. Nationwide statistics on sinkhole formation are meager, but costs are probably less than the other types of subsidence. HUD estimates annual costs may be only a few million dollars. The problem affects a large total area, however. In Standard Metropolitan Statistical Areas, limestone with sinkhole potential underlies 78,000 square miles containing 33 million people. All locations within this area are not at equal risk, because most collapses appear to be associated with ravelling of overburden into preexisting voids and caverns.

Other kinds of mining and hydrocompaction—More causes of subsidence which matter to individuals

Although the preceding four causes of subsidence are nationally the most significant, this is of small consolation to individuals impacted by other types of man-induced subsidence. Locally, underground mining of lead, zinc, and copper ores, solution mining of evaporites and application of water to undercompacted sediment or hydrocompaction have all caused surface collapse. Damage and engineering costs to avoid damage have amounted to millions of dollars.

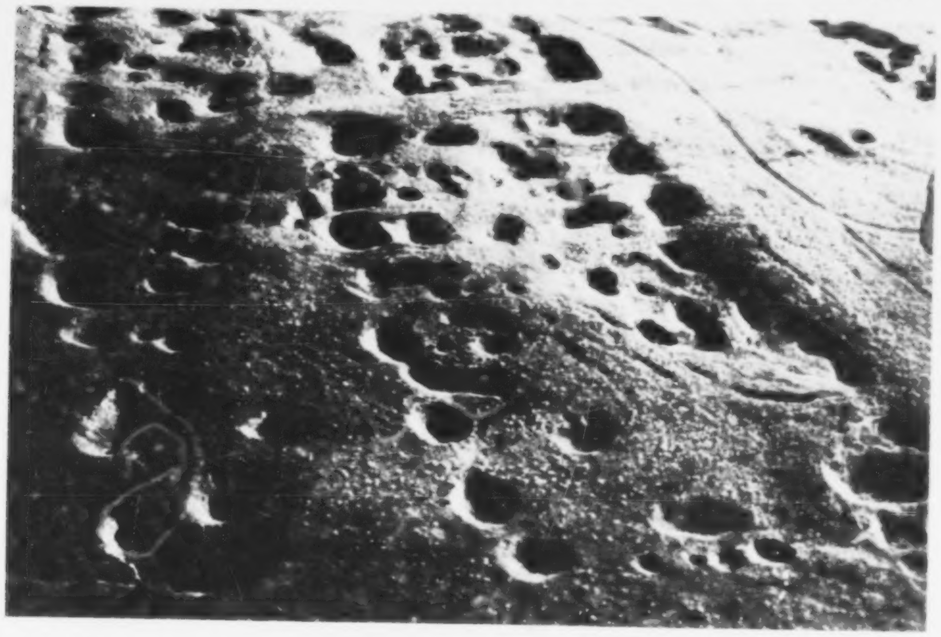

Subsidence pits, troughs, and cracks above an abandoned underground coal mine in the western Powder River Basin, Wyoming. (Photograph by C.R. Dunrud).

What can be done?

The complex variety of causes of land subsidence precludes a single solution or approach for dealing with the Nation's subsidence problem. The association of much subsidence with extraction of natural resources further compounds the problem. The extraction may be either for private or public benefit. To comprehensively address the Nation's subsidence problem four aspects must be considered: prediction, control, hazard avoidance, and a more equitable system of cost distribution.

The level of understanding of the basic processes causing each type of subsidence varies. Improvements in our understanding of these processes enhance our ability to predict subsidence both qualitatively and quantitatively. Moving from theory and the laboratory to field conditions is challenging, however. Characterization of geological conditions has proven particularly difficult. Even if the mechanics of sinkhole subsidence were completely understood, prediction would still be hampered by the difficulty of locating subsurface voids.

In subsidence areas where structures already are at risk, cost-effective methods for controlling subsidence need development and refinement. This requires not only technical advances, but in some cases changes in our institutions. Often legal and institutional obstacles prevent those impacted by subsidence from taking action.

Unregulated resource development or urban growth lie at the heart of some subsidence problems. If geographic areas with subsidence problems can be narrowly identified, land-use controls may provide a method for reducing the net costs to society. Alternatively, if the problem areas cannot be sufficiently delineated, insurance may provide a fairer method of distributing costs within society.

There is a final problem that should be addressed and resolved. It is that private and public entities often benefit from the activity that results in subsidence damage, yet the damage costs are not distributed equally. For example, in the Houston, Texas, area, the whole region benefitted from lower-cost ground water, but only those in the coastal area and located on faults incurred the costs resulting from subsidence. Institutional and legal changes are required to redress this kind of situation.

Subsidence crack or earth fissure in south-central Arizona caused by groundwater withdrawal.

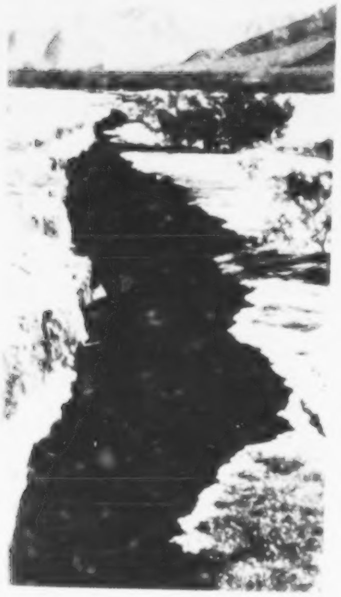

Cooperative Earthquake Research Between the United States and the People's Republic of China

David P. Russ
U.S. Geological Survey
Reston, VA

Leonard E. Johnson
National Science Foundation
Washington, DC

Cooperative research by scientists of the United States and the People's Republic of China (PRC) has resulted in important new findings concerning the fundamental characteristics of earthquakes and new insight into mitigating earthquake hazards. Much of the research is being conducted under the U.S. State Department Protocol for Scientific and Technical Cooperation in Earthquake Studies between the PRC State Seismological Bureau (SSB) and the U.S. Geological Survey and the National Science Foundation. Activities and progress accomplished under the protocol were the subject of two special sessions at the 1985 American Geophysical Union Fall Meeting in San Francisco, Calif.

Several advantages exist in pursuing earthquake studies with the People's Republic of China. China has a high incidence of damaging earthquakes; its government therefore supports an extensive and successful earthquake studies program. The program is accumulating a modern data base to add to its unequalled 2000-year historic earthquake catalog. Joint programs with China provide access to seismically active regions such as Yunnan Province and northeast China, where scientists from the SSB and the United States are establishing operational earthquake prediction networks. United States participation gives

Chinese scientists access to modern equipment and experimental techniques developed in the West. The results of cooperative efforts are of mutual benefit to the earthquake programs and friendship of both countries. At the Fourth Annual U.S.-PRC Science and Technology Commission meeting held in Washington, D.C., on April 15, 1985, George Keyworth, Presidential Science Advisor, cited the Earthquake Studies Protocol for improving U.S.-China relations and for providing progress in the understanding of earthquake occurrence.

There have been over 35 projects cooperatively sponsored by the Earthquake Studies Protocol in the past 5 years. The projects are organized into seven annexes, including investigations in earthquake prediction, intraplate faults and earthquakes, earthquake engineering and hazards investigation, deep crustal structure, rock mechanics, seismology, and data exchange. The SSB is currently developing operational earthquake prediction experiments at two primary sites: western Yunnan Province near the town of Xiaguan, where there are several active faults, and the northeast China plain, where the devastating 1976 Tangshan earthquake occurred. Monitoring and research in western Yunnan centers around a system of strategically located tunnels that contain a variety of seismometers, accelerometers, tiltmeters, strainmeters, and gravimeters. The tunnel monitoring is complemented by surface magnetic and deformation arrays, creepmeters, gas and in situ stress measurement sites, and fault mapping. The United States has provided some of the equipment for the tunnels and surface arrays and is participating in mapping and in the analysis and interpretation of data collected in the region. Earthquake prediction monitoring networks have also been installed in northeast China, although not in a system of tunnels. Many pieces of equipment, including magnetometers, an electronic distance measuring instrument, strainmeters, water well monitors, seismic network supplies, and a real-time seismic detection and processing system have been provided by the United States, and data are being exchanged and analyzed. Both China and the United States are investigating a wide range of phenomena in the search for earthquake precursors. Although similar in many aspects, the earthquake prediction programs of the two countries have some major differences. Emphasis in the U.S. program is placed on strain and deformation monitoring and on the analysis of seismic patterns and parameters. Substantial progress has been made in the determination of long-term earthquake potential through geologic studies and an analysis of the historic seismic record. In China, emphasis is placed on geochemical techniques, water well monitoring, and the analysis of seismic patterns. The approach is heavily weighted toward monitoring and empirical analysis, with a lesser emphasis on those theoretical aspects of the problem that are a large part of the earthquake prediction program in the United States. Participation by American scientists in the Chinese program allows them to test and evaluate hypotheses and equipment in areas where damaging earthquakes are frequent and also permits them to keep abreast of progress made within the Chinese program, particularly in areas not strongly supported by the U.S. domestic program.

Comparisons have been drawn between the tectonic setting and the fault geometry and behavior of major faults in China and in the United States. Although all of China's earthquakes are fundamentally intraplate and may not be directly analogous to those occurring along the Pacific-North American plate boundary in the United States, similarities have been noted between major faults in China and the San Andreas fault, Basin and Range faults, and midcontinent faults in the United States. Field studies to model fault scarps and to calculate slip rates have been carried out in central and eastern China as well as in Yunnan province. Exchange field visits have been made to California, Idaho, New Mexico, Utah, and the Mississippi Valley.

Strong government support and continuing interest by scientists in both countries should ensure a healthy cooperative research program in the next 5 years. New projects are beginning in geodesy and fault mapping, and most existing projects are continuing. Substantial progress is being made in the development of the China Digital Seismic Network, a nine-station state-of-the-art seismographic network designed and built by scientists and engineers from both countries. Installation of the prototype station in Beijing is scheduled to be completed before the end of the year. Data collected by the network will be incorporated into the publicly distributed World Day Tape and will provide an outstanding opportunity to increase our knowledge of the causes and nature of east Asian earthquakes.

About the Authors

Details on **Thomas L. Holzer** appeared in Volume 15, Number 6, p. 236.

Albert Rogers received a Ph.D. in Geophysics at Saint Louis University in 1970. Since then he has conducted research in seismology, first in industry and since 1974 for the USGS. His research interests are related principally to the assessment of the seismic ground-shaking hazard in urban areas and to critical facilities. These interests are reflected in his research on the effects of geologic conditions on the ground-shaking level, reservoir-induced seismicity studies, seismic scale modeling, seismic monitoring, and probabilistic ground-shaking evaluation. Dr. Rogers is currently the Chief of the USGS Branch of Geologic Risk Assessment in Golden, Colo. His outside interests are photography, hiking and fishing.

George Pararas-Carayannis received his doctorate in Marine Sciences from the University of Delaware. Presently he is the Director of the International Tsunami Information Center (TIC), a post he has held since 1974. As Director, he is responsible for monitoring the International Tsunami Warning System and seeking improvements in communications, data networks, data acquisition, information dissemination, and so on among the twenty-four countries participating. Prior to that he served as Director of the World Data Center A-Tsunami, as oceanographer for the National Ocean Survey, and as geophysicist for the Hawaii Institute of Geophysics. His interest in marine archeology has allowed him to study the effects of natural disasters on ancient civilizations as well as underwater exploration and mining. He also finds time to serve as Tsunami Advisor to the Hawaii State Civil Defense Agency, as an officer of the Hawaii Chapter of the National Society of Arts and Letters, to write poetry, and to sail his boat.

David P. Russ coordinates the Earthquake Studies protocol between the United States and the People's Republic of China for the USGS, assists in the management of the National Earthquake Hazards Reduction Program, and coordinates the new USGS Deep Continental Studies Program. He received his Ph.D. in geology from the Pennsylvania State University in 1975. He also directed the multidisciplinary research program that investigated the cause and characters of earthquakes and Quaternary tectonic deformation in the New Madrid seismic zone of the Mississippi River valley.

Leonard E. Johnson received his Ph.D in geophysics from the University of California, San Diego, in 1971. After completing 2 years as a visiting fellow at the Cooperative Institute for Research in Environmental Sciences (CIRES) in Boulder, Colorado, he went to the Department of Geology and Geophysics at the University of California, Berkeley, for the 1973-1974 academic year. In 1974, he joined the National Science Foundation (NSF) as Associate Program Director for Geophysics in the Earth Sciences Division (EAR). While at NSF he has been the Geophysics Program Director, and is currently the Program Director for EAR's new Continental Lithosphere Program.

Cover:

Replica of an early seismoscope developed by the Chinese to determine the direction from which an earthquake originated. Of ingenious design, this first seismoscope was developed by Chang Heng, the Royal Astronomer of the Bureau of Astronomy and Calendar in the year 132 A.D. during the Han Dynasty period. Initially made of bronze, with a diameter of about 6 ft., the seismoscope (literally called the "earthquake weathercock" by its inventor) would vibrate during an earthquake, causing a ball to drop out of a dragon's mouth and be caught by a toad below. The noise produced by the dropping ball served notice of the earthquake, and the particular ball which fell gave the azimuthal direction of the earthquake. The internal mechanism of the seismoscope is unknown but probably employed either a pendulum or inverted pendulum connected to levers that ejected the balls when the instrument was moved. Interestingly, the principle of the seismoscope apparently was lost between 600 and 1200 A.D. Not until 1703 was the first modern seismograph developed, based upon the spilling of an overfilled dish of mercury. (Photograph used by permission of the State Seismological Bureau of the People's Republic of China.)

Back cover:

Ancient Japanese legend held that earthquakes were caused by a monster catfish called Namazu-e that lived beneath the earth. (Photograph courtesy of Teledyne Geotech.)

*U.S. G.P.O. 1986-181-459:40005

U.S. GOVERNMENT PRINTING OFFICE
PUBLIC DOCUMENTS DEPARTMENT
WASHINGTON, D.C. 20402

OFFICIAL BUSINESS
PENALTY FOR PRIVATE USE $300

BULK RATE MAIL
POSTAGE & FEES PAID
USGS
PERMIT No. G23

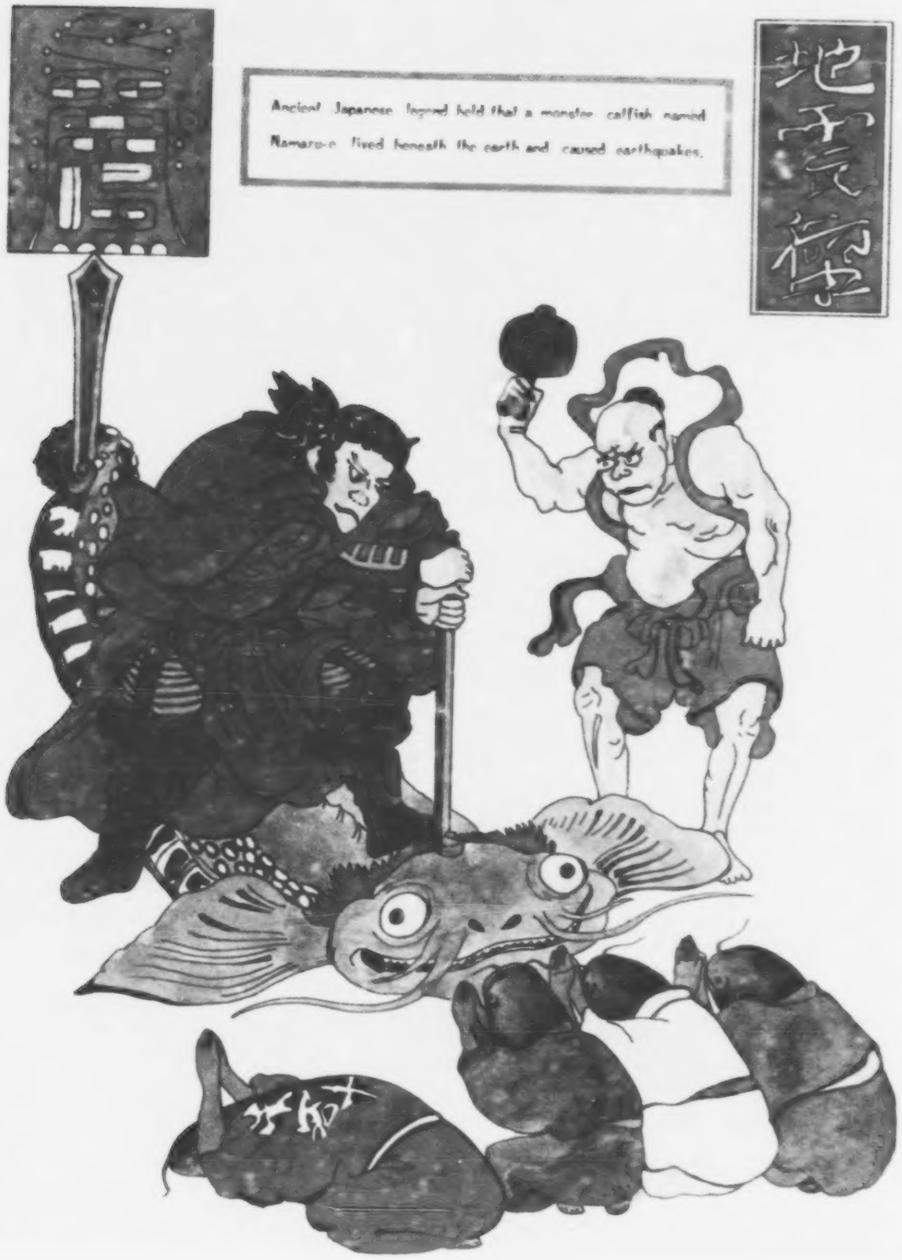

Ancient Japanese legend held that a monster catfish named Namazu-e lived beneath the earth and caused earthquakes.

18/4

Earthquakes & Volcanoes

Volume 18, Number 4, 1986

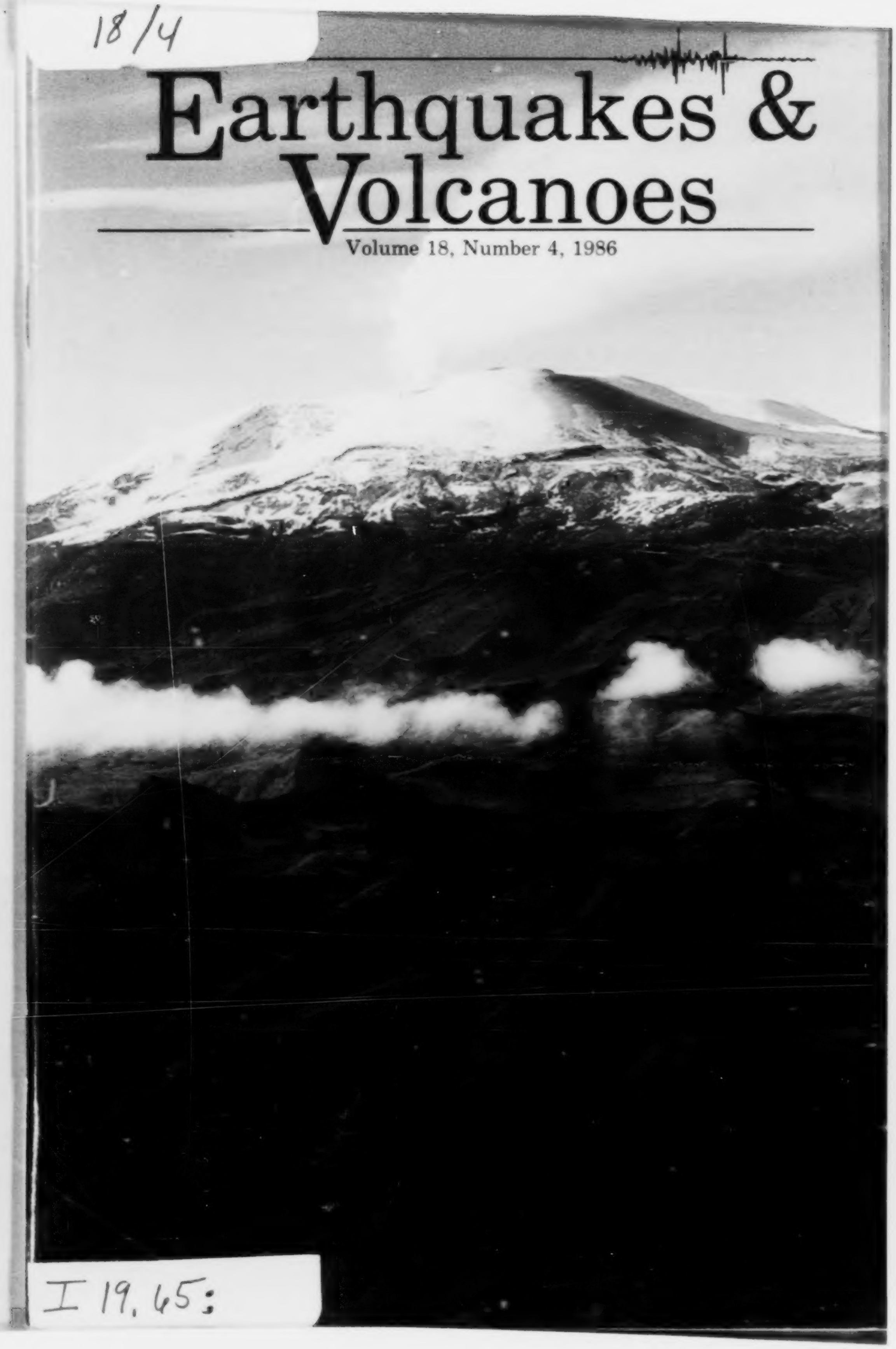

I 19.65:

UNITED STATES DEPARTMENT OF THE INTERIOR
Donald Paul Hodel, Secretary

U.S. GEOLOGICAL SURVEY
Dallas L. Peck, Director

Earthquakes and Volcanoes is published bimonthly by the U.S. Geological Survey to provide current information on earthquakes and seismology, volcanoes, and related natural hazards of interest to both general and specialized readers.

The Secretary of the Interior has determined that the publication of this periodical is necessary in the transaction of the public business required by law of this Department. Use of funds for printing this periodical has been approved by the Office of Management and Budget through June 30, 1989.

Henry Spall—Editor

Earthquakes and Volcanoes
U.S. Geological Survey
904 National Center
Reston, Virginia 22092
Telephone (703) 648-6078

Jill K. Moebus–Graphics Design

Subscription orders should be sent to:

Superintendent of Documents
U.S. Government Printing Office
Washington, DC 20402
Telephone (202) 783-3238

For sale by the Superintendent of Documents. Annual subscription rate—$15.00 (domestic) and $18.75 (foreign). Make check or money order payable to the Superintendent of Documents.

Single copy rate—$3.00 (domestic) and $3.75 (foreign). Single copy rate for issues prior to Volume 15, Number 1—$2.25 (domestic) and $2.85 (foreign). Can be purchased from the Book and Open-File Reports Section, U.S. Geological Survey, Federal Center, Building 41, Box 25425, Denver, CO 80225 (make check or money order payable to the Superintendent of Documents).

Front:
Nevado del Ruiz, Colombia, is the northernmost active volcano in the Andes of South America. This photo was taken shortly after intermittent phreatic explosions began in the summit crater on September 11, 1985. On November 13, 1985, the volcano erupted in a succession of pyroclastic flows and surges that scoured and melted part of the extensive ice cap on the volcano's summit. The meltwater and secondary avalanches of slush and glacier ice generated lahars that swept down river valleys on the flanks of the volcano. The lahars invaded the towns of Armero, Tolima, and Chinchina, Caldas. At least 22,000 people were killed; more than $212 million (US) in property was destroyed. The eruption, although the deadliest since the 1902 eruption of Mount Pelee, Martinique, that killed 28,000, was not unexpected. Colombian and international scientists, concerned by persistent earthquake, fumarolic, and phreatic activity, had warned for nearly a year that Ruiz might erupt. Photograph by Darrell G. Herd, U.S. Geological Survey

Earthquakes & Volcanoes

(formerly *Earthquake Information Bulletin*)
Volume 18, Number 4, 1986

148 Bulletin Board

157 General Publications

161 USGS Publications

168 Earthquakes
  July-August 1985
  September-October 1985
  November-December 1985

Back:
A succession of lahars (volcanic mudflows) initiated by the November 13, 1985, eruption of Nevado del Ruiz volcano, raced down five winding river valleys through the Cordillera Central of Colombia. Moving at velocities locally exceeding 50 km/hr, the lahars swept up slope and valley deposits in their path and scoured valley bottoms to a height of more than 40 m. The largest flows, formed by the merging of lahars initiated in the headwaters of the Rio Lagunillas and Rio Azufrado, moved through the Rio Lagunillas valley between 9:30 and 11:30 p.m. The flows discharged from the mouth of the canyon, 15 km east of this photograph, flooding the town of Armero, Tolima. At least 21,000 people—nearly 90 percent of the population of Armero—were killed. Photograph by Darrell G. Herd, U.S. Geological Survey.

Bulletin Board

Research in Earthquake Prediction—The Parkfield Prediction Experiment

The 15-mile-long Parkfield, California, section of the San Andreas fault is the best understood earthquake source region in the world. Moderate-sized earthquakes of local magnitude (M_L) 5¾ occurred at Parkfield in 1881, 1901, 1922, 1934, and 1966. The only exception to an approximate 21-to 22-year recurrence time is the 1934 shock. The 44 years between 1922 and 1966 is just twice the usual time between the shocks. Thus, the 1966 Parkfield earthquake reestablished the regular timing pattern of the Parkfield earthquakes. If the next Parkfield earthquake conforms to the pattern, it will occur in the next few years, most likely in 1987 or 1988.

In addition to the predictable 22 years between shocks, Parkfield earthquakes share remarkably similar, or characteristic, features. These similar features—magnitude, length, location of rupture along the San Andreas fault (rupture zone), and epicenter—define the characteristic Parkfield earthquake. The concept of a characteristic earthquake with predictable features means that the design of an earthquake-prediction experiment can be tailored to these specific characteristic features. Because the expected recurrence of the next Parkfield earthquake is near and the historic Parkfield earthquakes have been so similar, Parkfield provides a unique opportunity to prepare an experiment to observe the final stages of the process leading up to the earthquake.

The observations and accounts available for the last characteristic Parkfield earthquake, on June 28, 1966, serve as a template for anticipating the features of the next Parkfield earthquake. In the 6 months before June 28, all earthquakes near Parkfield occurred on the San Andreas fault northwest of the rupture zone. The foreshocks, smaller earthquakes occurring near the rupture zone shortly before the main shock, occurred within a mile or so of the main shock epicenter, which was located at the northwest end of the rupture zone; this area has been named the "preparation zone." A similar foreshock and characteristic earthquake pattern occurred in 1934 within this preparation zone. Although many small earthquakes occur on the San Andreas fault northwest of the rupture zone, earthquakes within the critical preparation zone are infrequent. The U.S. Geological Survey has established a very dense network of seismograph stations near Parkfield to monitor the seismicity within and near the preparation zone; any increase in seismic activity will be scrutinized closely.

Some geologists think that earthquakes are preceded by fault creep (movement on a fault without detectable earthquakes). An irrigation pipeline that crosses the San Andreas fault near Parkfield broke without detectable earthquakes about 9 hours before the 1966 earthquake. Unfortunately, the history of the movement that resulted in the broken pipe is unknown; although geologists infer 1 to 2 feet of displacement from the broken pipe, perhaps only a very small part of the displacement occurred in the days and weeks just before the 1966 earthquake. Also, fresh cracks of uncertain origin were observed along the San Andreas fault 12 days before the 1966 earthquake. The broken pipeline and the fresh cracks are consistent with fault creep near Parkfield just before the characteristic earthquake in 1966.

If significant and unusual fault creep precedes the next characteristic Parkfield earthquake, the sophisticated, sensitive devices deployed near Parkfield should record it. Surface fault movement is monitored continuously by several creepmeters, 30-foot-long devices that cross the fault trace. Also, approximately 2- to 5-mile-long lines of sight which cross the fault will be measured each night on a two-color laser distance-measuring geodimeter that can resolve changes of less than one-half of an inch over a distance of 6 miles. Volumetric strainmeters, balloon-like instruments installed in boreholes, will measure minute changes in strain. The two-color laser geodimeter and the borehole strainmeter observations should corroborate changes in seismicity and fault creep. On a more fundamental basis, they will define the deformation process leading up to the next characteristic Parkfield earthquake.

The Parkfield, California, earthquake prediction experiment is an important element of the Geological Survey's earthquake prediction strategy for the United States. The Parkfield experiment is providing important experience in the design and operation of strain-monitoring instruments that ultimately may be adapted for use in a prototype earthquake-prediction network. An understanding of the earthquake process at Parkfield may yield data fundamental to the successful design of earthquake prediction strategies for southern California and other earthquake-prone areas of the United States.

Magnitude

Earthquake magnitude is a measure of the strength of an earthquake, or the strain energy released by it, as calculated from the instrumental record made by the event on a calibrated seismograph. In 1935, seismologist Charles F. Richter first defined local magnitude (M_L), or Richter magnitude, as the logarithm (to the base 10) of the amplitude in micrometers of the maximum amplitude of seismic waves that would be observed on a standard torsion seismograph at a distance of about 60 miles from the epicenter. The seismic waves used for local magnitude have periods ranging from approximately 0.1 to 2 seconds, equivalent to a wavelength of 1,000 feet to 3.8 miles.

NEWARK PU

Parkfield Earthquake Looks to Be on Schedule

The only formally endorsed prediction of an earthquake in the United States appears to be holding up well. The magnitude 5.6 Parkfield earthquake, expected to strike a section of the San Andreas in sparsely populated central California in January 1988, give or take 5 years, would appear to be on schedule despite a jolt to the Parkfield area from the nearby Coalinga earthquake.

Catherine Poley and Allan Lindh of the U.S. Geological Survey in Menlo Park reported at the American Geophysical Union (AGU) annual fall meeting in December that activity at Parkfield has resumed after a quiescence apparently induced by the May 1983 Coalinga earthquake. Shortly after the shock at Coalinga, seismic activity deeper than 6.5 kilometers ceased beneath Middle Mountain, the spot on the San Andreas where the most recent Parkfield earthquake in 1966 began its rupture. At the same time, the creeping of opposite sides of the fault past each other stopped at Middle Mountain and elsewhere. Then both the deep seismicity and the creep at Middle Mountain resumed in August 1984. Within recent weeks, creep elsewhere along the Parkfield section of the San Andreas has apparently resumed, accompanied by a small flurry of seismic activity.

Another, more warily regarded, sign that stress continues to be added to the Parkfield fault section, leading toward its eventual failure, was a small, magnitude 3 earthquake that struck in May of this year close

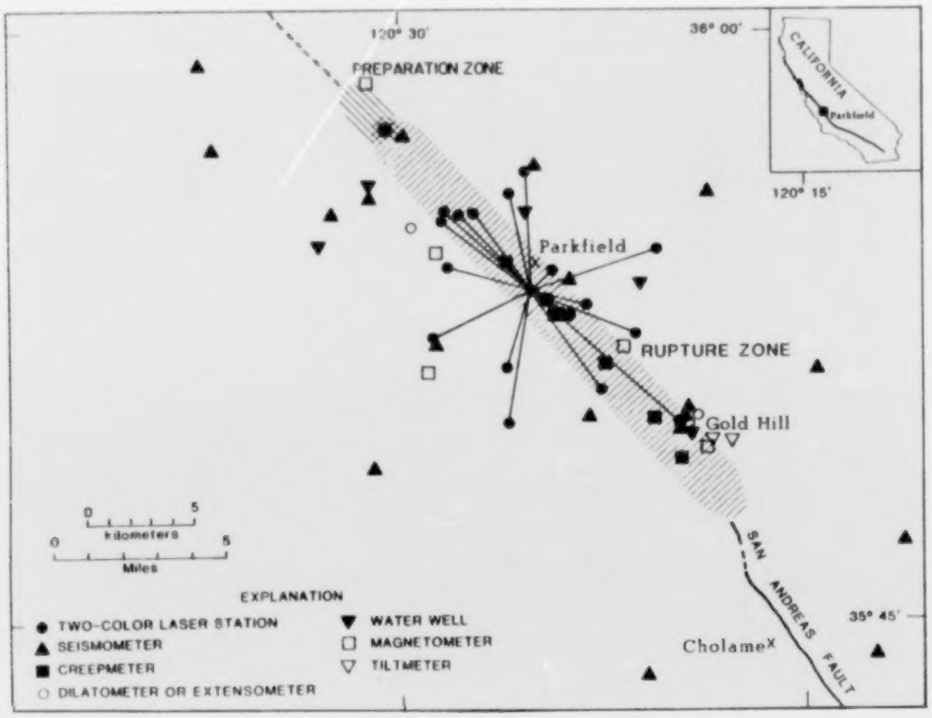
120° 30'
36° 00'
CALIFORNIA
Parkfield
120° 15'
PREPARATION ZONE
Parkfield
RUPTURE ZONE
Gold Hill
SAN ANDREAS FAULT
Cholame
35° 45'
0 5
Kilometers
0 5
Miles
EXPLANATION
● TWO-COLOR LASER STATION
▲ SEISMOMETER
■ CREEPMETER
○ DILATOMETER OR EXTENSOMETER
▼ WATER WELL
□ MAGNETOMETER
▽ TILTMETER

Location of (1) the "preparation zone," (2) the epicenter of the 1966 Parkfield earthquake, (3) the rupture zone, and (4) the location of some of the monitoring devices along the San Andreas fault (a number of other experimental monitoring devices also are being maintained in the Parkfield area).

by the point on the fault where the 1966 rupture began. Lindh had noticed that similar small events had clustered at the same spot, striking every 39 to 41 months since 1971. The April 1984 event "predicted" by this clocklike sequence never appeared, but this May's earthquake, the largest beneath Middle Mountain since 1982, fell at the right place. If one is willing to believe that the Coalinga earthquake simply slowed stress accumulation at Parkfield by about 14 months, as indicated by the quiescence, then this magnitude 3 earthquake could be the expected one. The next event in the sequence would come in August 1988, says Lindh. Conceivably, it could then trigger the main shock awaited by seismologists.

A far more substantial indicator of the imminence of the next Parkfield earthquake comes from geodetic surveys. Ruth Harris and Paul Segall of the USGS in Menlo Park reported that the strain that will be stored by 1988 on the fault will at least equal the strain released during the 1966 rupture. Because the three most recent Parkfield earthquakes were nearly identical in size, the next one will presumably occur when the same amount of strain has been stored. The coincidence of this prediction, based on changes in precisely measured distances across the fault, and the original prediction, based on the regular recurrence of similar earthquakes, points strongly toward 1988 as the most likely time for the next Parkfield earthquake.

—Richard A. Kerr

Reprinted by permission of the American Association for the Advancement of Science.

Not-so-inactive fault in Oklahoma

In connection with a search for geologically quiet areas for siting large engineering ventures such as dams and nuclear power plants, geologists have recently started looking at the Meers fault in southwestern Oklahoma with an intense interest.

The fault is one of many between the Wichita Mountains, a block of 500 million-year-old igneous rocks, and the Anadarko Basin, a deep trough filled with younger sediments. In terms of plate tectonics these structures are part of a "failed rift." The earth's crust tried to spread apart along this southern margin of the North American continent but the process was aborted; the rift however continued to fill up with sediments and the crust had to yield along a series of faults such as the Meers fault. Because, the Anardarko Basin is 300 million years old, there was no reason to suppose that the faults could still be active. Until recently.

Geologists at the Oklahoma Geological Survey, the U.S. Geological Survey (USGS), Texas A&M University and the University of Nevada now know that the last movement on the Meers fault took place about 1000 years ago. The evidence for this has come from a variety of geologic measurements. The original clue that the Meers fault was not an inactive fault was that the fault scarp was more or less evenly eroded along its 15 mile length. If the fault were inactive, then hard rocks would stand out as resistant spurs while soft rocks would have been eroded away.

Further observations showed that there must have been recent movements on the fault. Where streams crossed the fault they had eroded new, deeply-incised channels in order to compensate for vertical displacement of the rocks on either side of the fault. Evidence was also found for horizontal displacement along the fault that produced offsets in ridges crossing the fault. The most critical evidence was that recent movements on the fault have affected sediments that are no older than 2 million years.

Having established that the Meers fault has been recently active, the question is how recently. Answers to this question have been provided by Richard Madole of the USGS using the Carbon 14 dating technique on plant material. He examined two sites where the fault crosses alluvium (valley-floor deposits) and other sediments that were formed in the last 10,000 years. The alluvial deposits were the most important; two of these formed *before* the most recent faulting, one was of the same age, and the fourth was formed after the recent break.

The Carbon-14 ages measured on charcoal in the sediments show that movement on the Meers fault occurred between 600 and 1280 years ago. An age for the actual faulting is suggested at 1100 years ago. Since charcoal can be recycled from older to younger sediments, soil humus was used to provide an independent check on these ages.

Trenches dug across the San Andreas fault in California have been of great help in unravelling the historic record of major earthquakes on this fault; trenches were therefore excavated across the Meers fault by Anthony Crone of the USGS and Kenneth Luza of the Oklahoma Geological Survey. They found that most of the fault deformation was taken up by plastic warping of the sediments; no prominent scarps were produced which, as a result of erosion, normally give rise to distinctive deposits that are used to identify multiple faulting episodes. In fact the trenching evidence suggests only one recent fault event.

Paradoxically, seismic monitoring of the fault over a 12-month period has revealed only two felt events, both of which could be quarry blasts. No earthquake exceeding magnitude 3 has occurred in the area since station TUL at Tulsa, Oklahoma was established 23 years ago; there is a high probability that no felt-earthquake has occurred along the Meers fault since nearby Fort Sill was established in 1869.

Given the fact that earthquakes have occurred on the Meers fault during the geologically recent past, there is an important need to estimate their magnitude and in particular the maximum magnitude that is likely to occur in the future. At present it is impossible to answer these questions. Providing such answers is linked to the cause of the activity on the fault. In turn this is linked to trying to understand why there is seismic activity in what ought to be a stable, interior region of the North American crustal plate.

Reactivation of an otherwise stable part of the North American plate was responsible for three great earthquakes in the New Madrid, Missouri area in 1811-1812. What role faults like the Meers fault in Oklahoma play in predicting the sites of future damaging earthquakes in the central United States will be determined by continued geological studies and seismic monitoring in Oklahoma.

Prototype Operational Earthquake Prediction System

An objective of the U.S. Earthquake Hazards Reduction Act of 1977 is to introduce into all regions of the country that are subject to large and moderate earthquakes, systems for predicting earthquakes and assessing earthquake risk. In 1985, the USGS developed for the Secretary of the Interior a program for implementation of a prototype operational earthquake prediction system in southern California.

The geologic record gives unambiguous evidence that the great southern San Andreas earthquake of 1857 can be regarded as simply the most recent event in a continuously-repeating earthquake cycle. The cycle consists of slow straining of the crust to a critical state followed by sudden strain release when a fault slips during an earthquake. Several independent lines of evidence indicate that much of the 280-mile-long southern San Andreas fault is now capable of generating one or more major earthquakes in the near future. Detailed studies of the fault suggest that several regions along the fault may mark sites where the next large or great earthquakes may nucleate. Continuous direct measurement of strain (changes in volume or shape) and seismicity in these sections of the fault may permit short-term prediction of the earthquakes by detecting accelerated deformation near the fault in the hours or days before the event.

The need to closely monitor localized regions of the San Andreas fault argues for the deployment of clusters of geophysical monitoring devices in concentrated groups to measure crustal deformation continuously, or nearly so, at points within a small region of approximately 13- to 19-miles in extent. The USGS proposes to build clusters of state-of-the-art earthquake prediction instruments like those now under development near Parkfield, at specific locations along the San Andreas fault estimated to have high potential for moderate to large earthquakes. Each earthquake prediction instrument cluster ideally would consist of a pair of 2-color laser strain measurement geodimeters, 10 to 15 borehole strainmeters and tiltmeters emplaced at a 1,000-foot depth or greater, 5 fault slip detectors (creepmeters), 5 displacement meters to measure the earthquake slippage itself, and a meterological station to allow for correction of atmospheric effects. These instruments would be supplemented with a) annual surveys of surrounding, regional 50-line geodolite network; b) annual leveling surveys and precise gravity measurements to monitor vertical movements; and c) resurveys of short-scale (700 foot) fault-crossing alinement arrays to detect possible aseismic fault slippage.

The data collection points at each cluster would serve as nodes in a network of modern digital seismographs with wide sensitivity and recording response. This network would be capable of detecting and providing data for analysis of all earthquakes of magnitude 1.5 or greater within 30 miles of the fault segment being monitored by the strain measurement cluster. A dense 20-station, 3-component network of seismometers would monitor detailed source characteristics of small earthquakes occurring within the cluster. A 40-station network of 3-component strong-motion accelerographs would obtain on-scale recordings of larger events and the main earthquake shock itself.

A central data monitoring and analysis center would analyze seismic and strain data from the clusters continuously and in real time to track any event of geophysical significance. Continuous surveillance of each region would be achieved primarily by automated analysis of each strain-time series and seismic channel by dedicated computer systems programmed to trigger alarms when threshold values are exceeded. An organized team of scientists with intimate knowledge of the region, and a long-term commitment to research on it, would review changes in the geophysical data and develop recommendations for governmental response to the evolving earthquake hazard.

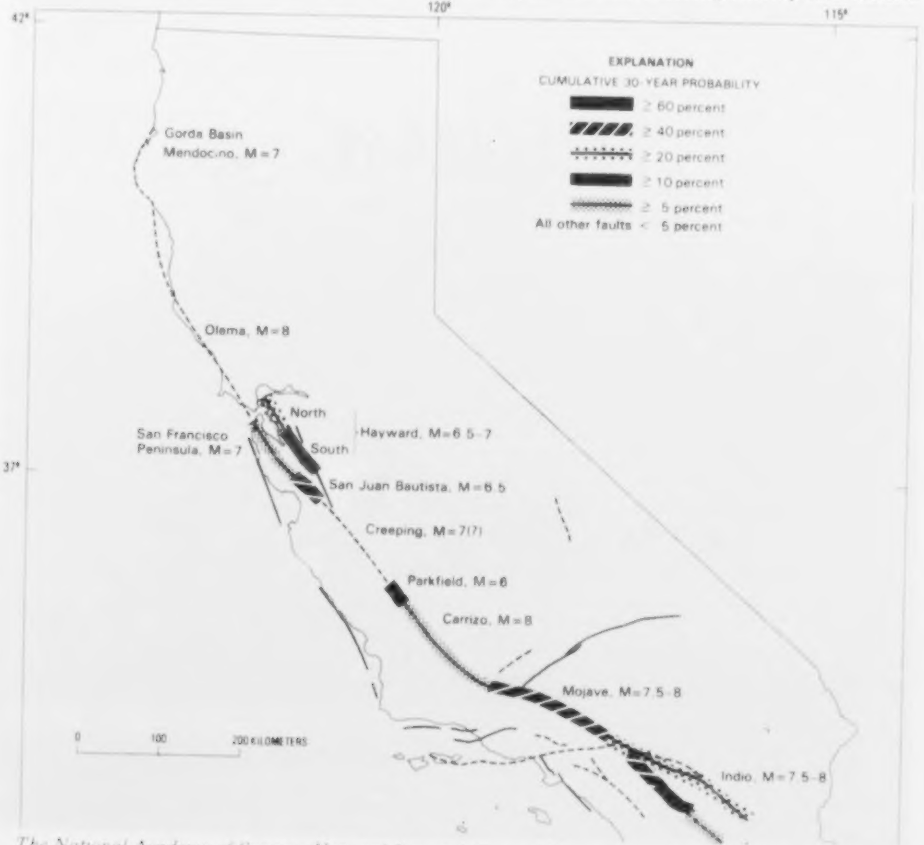
42°
120°
115°
37°
EXPLANATION
CUMULATIVE 30-YEAR PROBABILITY
≥ 60 percent
≥ 40 percent
≥ 20 percent
≥ 10 percent
≥ 5 percent
All other faults < 5 percent
Gorda Basin
Mendocino, M = 7
Olema, M = 8
North
South
Hayward, M = 6.5–7
San Francisco Peninsula, M = 7
San Juan Bautista, M = 6.5
Creeping, M = 7(?)
Parkfield, M = 6
Carrizo, M = 8
Mojave, M = 7.5–8
Indio, M = 7.5–8
0
100
200 KILOMETERS

The National Academy of Sciences/National Research Council Committee on Seismology has recommended a USGS prototype operational earthquake prediction strategy to deploy one to five clusters of earthquake prediction instruments in regions of the San Andreas fault where there is a high potential for moderate to large earthquakes. The first of these clusters would be near Parkfield, California, where initial steps to install a cluster have begun. Other possible cluster sites include: (1) the 25-mile long segment of the San Andreas south of Cholame where slip in 1857 was only 10 to 13 feet and the long-term slip rate is about 1.4 inches/year; (2) the Tejon Pass region near the complex junction of the Garlock and San Andreas faults where future great San Andreas earthquakes may nucleate; (3) the Cajon Pass region near the junction of the San Andreas and San Jacinto faults; (4) the San Gorgonio Pass in a complex structural area between the San Andreas and San Jacinto faults; (5) along the southern terminus of the San Andreas fault east of the Salton Sea and near the boundary between it and the Brawley seismic zone in the Imperial Valley to the south; and (6) the Anza region on the northern half of the San Jacinto fault. Adjacent regions have experienced a series of M > 6.7 earthquakes early in this century while the Anza segment has not sustained significant seismic slip since at least 1890.

Seismic Computerized Alert Network

In 1985 the USGS devised a model for a Seismic Computerized Alert Network (SCAN) that would use continous monitoring of seismic data from existing types of instruments to provide automatic, highly-reliable early warnings of earthquake shaking. In a large earthquake, substantial damaging ground motions may occur at great distances from the earthquake's epicenter. Because of the relatively slow speed of seismic waves, it is possible to construct a system to provide short-term warning (as much as several seconds) of imminent strong ground motion, once an earthquake has begun.

Damaging seismic waves propagate outward from a fault rupture at about 2.2 miles/second. Strong shaking from great earthquakes occurring hundreds of miles away may arrive more than a minute after the initiation of earthquake rupture. Strong shaking from the great (magnitude 8) earthquake of 1857 that ruptured a 190-mile-long segment of the San Andreas fault in southern California, probably occurred in the Los Angeles region at least 1 to 2 minutes after the initial earthquake rupture of the fault. The fault rupture probably started in the vicinity of Parkfield, 170 miles northwest of metropolitan Los Angeles. Assuming a southward-directed unilateral fault rupture at a velocity of about 1.6 miles/second, the strongest shaking in the Los Angeles region probably occurred at least 100 seconds after the ground began to shake at Parkfield.

A Seismic Computerized Alert Network would detect the initial shaking of an earthquake event and send forward electronic warning of the impending shaking. Ground motions recorded by a dense array of broadband, high-dynamic-range seismometers would be digitally telemetered to a central processing site where the occurrence of a large earthquake would be detected. The location, time of origin, amplitude of ground shaking, and reliability estimates would be transmitted instantly to microcomputers in the threatened area. The computers would combine this information with local site data to estimate the time of arrival and the nature of ground motions expected at the site. Decisions already programmed into the computers would then trigger automated safety responses. For example, a SCAN could initiate (a) electrical isolation and protection of delicate computer systems, (b) isolation of electric power grids to avoid widespread blackouts, (c) protection of hazardous chemical systems and offshore oil facilities, (d) closing of natural gas valves to minimize fire hazards, (e) warning for nuclear power plants and national defense facilities, (f) protection of emergency facilities such as hospital and fire stations, and (g) protection of fixed-rail transportation systems.

Although warning times are likely to be short for areas that are damaged by numerous earthquakes of moderate size, areas that experience very strong shaking during great earthquakes would receive longer warning times.

Conceptual design of a Seismic Computerized Alert Network (SCAN)

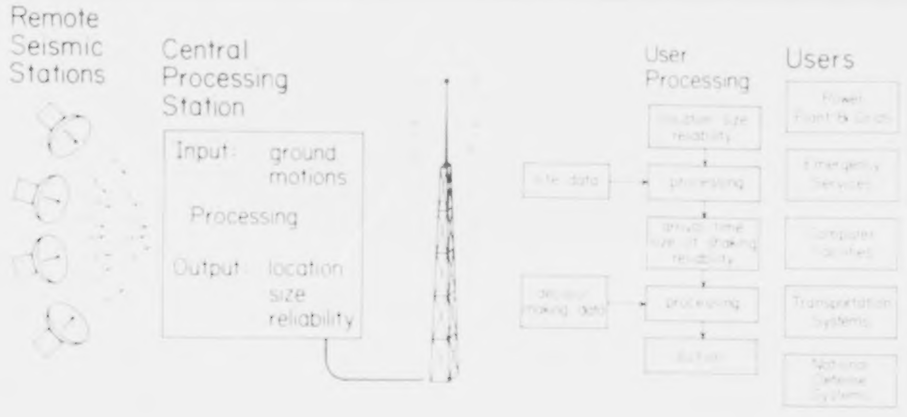
Remote Seismic Stations
Central Processing Station
Input: ground motions
Processing
Output: location size reliability
User Processing
location size reliability
site data
processing
arrival time size of shaking reliability
decision making data
processing
action
Users
Power Plant & Grids
Emergency Services
Computer Facilities
Transportation Systems
National Defense Systems

Long Valley Is Quiet but Still Bulging

Long Valley caldera, the huge volcanic scar just to the east of Yosemite National Park, has been quieting down ever since four magnitude 6 earthquakes rocked the caldera during 3 days in May 1980. The ominous bulging of the valley floor has not gone away, however, suggesting that the vigil at Long Valley could be a long one.

David Hill and Robert Cockerham of the U.S. Geological Survey in Menlo Park reported at the American Geophysical Union (AGU) annual fall meeting in December, 1985, that the quieting down of Long Valley continues. Thirteen earthquakes larger than magnitude 5 have struck the area since October 1978, but the most recent occurred over a year ago in November 1984. Within the caldera, the level of seismicity has dropped from two to three events per day greater than magnitude 1 in most of 1984 to less than 0.5 per day in 1985. John Langbein and his colleagues at the USGS in Menlo Park reported that the growing quiescence extends to the deformation of the southern caldera edge, where a swarm of microearthquakes had marked a possible finger of upward-moving magma. Whatever caused this near-surface disturbance, it seems to have died out for the time being.

Deeper beneath the caldera, things are not so quiet, according to surveys conducted by James Savage of the USGS in Menlo Park. Judging by the bulging of the valley floor detected in surveys of height and distance changes, magma has continued to fill the chamber 10 to 12 kilometers below at a roughly steady rate from 1982 to 1985. The maximum uplift during that time was about 35 millimeters each year while seismic activity tapered off from year to year. If there has been any change in the bulging, it has been a shift of the uplift center toward the western edge of the caldera and the Mono and Inyo crater chains, where volcanic eruptions occurred as recently as 600 years ago.

The steady inflow of deep magma, which is either the direct cause of the seismicity or a product of the crustal stresses that drive all the activity, would imply that more earthquakes or even an eruption could strike Long Valley despite the current quiescence. The timing of any such activity remains problematic. Yellowstone caldera has risen an average of 15 to 20 millimeters per year since 1923 with only the occasional moderate earthquake or seismic swarm.

—Richard A. Kerr

Reprinted by permission of the American Association for the Advancement of Science.

Earthquake-Related Sounds

Karl V. Steinbrugge has updated his catalogue of ***Earthquake-Related Sounds*** published by the Seismological Society of America. The updated tape cassette contains 21 earthquake related sounds. The events include 1954 Eureka (California), 1957 San Francisco, 1963 Sikeston (Missouri), 1964 Anchorage, 1965 Puget Sound, 1967 Caracas, 1969 Santa Rosa (California), 1975 Oroville (California), 1976 Friuli (Italy), 1977 Willits (California), 1979 El Centro, 1983 Coalinga, and 1983 Japan.

The recordings contain the sounds of persons reacting to the event: individuals, small groups of persons, as well as an audience in a large auditorium. Some were schoolchildren in school, two are fire department tapes, and one person had the presence of mind to describe what he was experiencing. The noises also include the creaking of buildings and in some cases, the sounds emanating from the ground.

Detailed notes prepared by Steinbrugge accompany the cassette. The cassette and the supplemental notes will be available for $10 from:

Seismological Society of America
6431 Fairmount Ave., Suite 7
El Cerrito, CA 94530

For addresses outside North America add $2.00 for airmail postage.

BAREPP: Earthquake Preparedness for the San Francisco Bay Area

The threat of major and damaging earthquakes in California is a fact.

How people respond to that threat is a concern shared by many local, state, federal, volunteer and private sector organizations. The Bay Area Regional Earthquake Preparedness Project (**BAREPP**) promotes comprehensive earthquake preparedness actions by these organizations and provides technical and planning assistance for a variety of programs. It is a project of the California Seismic Safety Commission.

BAREPP has sponsored a number of workshops and seminars including a regional conference "IT'S YOUR FAULT: Taking responsibility for earthquake preparedness in the San Francisco Bay Region" on April 9 of this year. This was a prelude to "Serious Faults, Simple Solutions"—the California Earthquake Preparedness Week from April 14-19, 1986. **BAREPP** publishes NETWORKS, a quarterly publication which describes community preparedness and resources in the Bay area.

For further information contact:

BAREPP
Metrocenter
101 8th Street, Suite 152
Oakland, CA 94607
(415) 540-2713

SCEPP: Southern California Earthquake Preparedness Project

Governor George Deukmejian proclaimed April 14-19, 1986, to be "Earthquake Preparedness Week" in the State of California. This was the second annual observation of what will be an ongoing public safety campaign. The focus of the week was to educate the public on the importance of earthquake preparedness and to encourage individuals, communities, and organizations to initiate efforts that would ultimately prepare them for the effects resulting from a major damaging earthquake.

The theme of this year's campaign, Serious Faults—Simple Solutions, emphasized the many preventive measures that could be taken to improve earthquake safety and reduce unnecessary risks at a minimum cost and effort. Getting people to take the earthquake problem seriously is not simple. This was the goal of Earthquake Preparedness Week 1986.

This year's campaign targeted three constituent groups: public and private schools, small businesses, and neighborhoods, including mobile home parks and apartment complexes. Earthquake drill exercises and urban search and rescue demonstrations were scheduled to be conducted during the week.

In southern California, the week's planned activities included a variety of events, from the inauguration of a new earthquake-shaking table and display at the California Museum of Science and Industry in Los Angeles to a joint National Guard/U.S. 6th Army validation test incorporating emergency medical response and communications. Many local jurisdictions were planning to hold exercises of their own to test various aspects of their preparedness plans and programs. Elementary and secondary schools throughout southern California were to initiate earthquake education programs, "drop and cover" and evacuation drills.

For more information on **SCEPP** activities, write to:

SCEPP
600 So. Commonwealth Ave.
Suite 1100,
Los Angeles, CA 90005

Resource Center for School Earthquake Preparedness

The Resource Center for School Earthquake Preparedness provides a complete planning facility for public and private school administrators, teachers and parents. Visitors to the Center will find many written materials and hands-on learning devices. In addition, the Center will coordinate outreach programs to provide staff and students with earthquake safety and survival skills. The Center is a project of QUAKE SAFE, a non-profit corporation dedicated to public earthquake education.

The Center is administered by Ferne Halgren, Executive Director of QUAKE SAFE. As a member of the Los Angeles City and County Earthquake Preparedness Committee, the education committee of the Seismic Safety Commission, and the Governor's Task Force for Earthquake Preparedness, Ferne is well suited to communicate disaster preparedness problems and solutions to the school community. A steering committee comprised of representatives from the Los Angeles area public and private schools contributed ideas and provides guidance to the center.

The Center's library is located in the California Federal Building in West Los Angeles, within a half mile of both the Santa Monica and San Diego freeways. Ample street parking is available. The library is open by appointment to any public or private school administrator, staff member, teacher or parent interested in earthquake preparedness planning. The staff is also available by telephone to answer questions, locate resources, and help solve common problems.

The Resource Center sponsors programs that will help school-disaster planners, whether they are parent volunteers, plant supervisors, physical education and science teachers, nurses or principals. Workshops are held throughout the school yer. A newsletter is published four times a year, and a speakers' bureau is available.

The primary goal of each school's earthquake preparedness planning is to make children as safe as possible when disaster strikes. Trained volunteers from the Center—many of them former teachers—will introduce children to earthquake safety through classroom presentations using creative, hands-on activities. These programs will be offered free of charge to schools throughout the Los Angeles area as Center funding permits.

Resource Center for School Earthquake Preparedness
10680 West Pico Boulevard, Suite 410
Los Angeles, California 90064
(213) 559-5176

Losing by a Landslide

Early in this century, geologic maps of a substantial part of the San Francisco Bay region published by the U.S. Geological Survey did not show a single landslide. By 1970, however, approximately 1,200 landslides had been mapped for the region. As of 1980, after special landslide mapping programs had been carried out by the U.S. Geological Survey, the California Division of Mines and Geology, and geologists under contract to local communities, 70,000 landslides had been identified in the Bay Area.

In January of 1982, a very heavy rainfall saturated the unstable soils in the region and triggered more than 13,000 landslides. Thirty-three people were killed, and property damages exceeded $60 million. Approximately 80% of the landslides were in areas not previously mapped as landslide deposits. The record shows clearly, then, that as recently as 15 years ago only a small percentage of the landslides in the San Francisco Bay region had been identified, and not even special studies had determined the real extent of the problem.

Across the United States, recognition of the landslide problem is comparable to the situation in the Bay Area prior to 1970. Although there are landslides in every state, only a few states, counties, or cities have begun systematic assessments of either the damages or the risks. Individual state departments keep some records of landslides, but no comprehensive records are kept for the nation as a whole. Therefore, it is impossible to assay the costs of landsliding to city and county roads. In addition, there is extensive damage to roads in National Parks, National Forests, and on other federal lands, but the total cost has never been fixed.

In 1981, I undertook an assessment of all state highway departments and geological surveys in order to begin to determine the extent of, and expenses incurred by, the nation's landslide hazard. The figures I had compiled by 1983 showed damages of at least $200 million annually to state roads during the period 1973-83. Damage to private property was set at a minimum of $40 million annually. The difficulties of estimating landslide damage to private property are exacerbated by the fact that individual property owners sometimes fail to report losses to public agencies because they fear that such a disclosure will cause their property values to decline.

The 1983 landslides in Utah are a good example of the complexities involved in compiling loss figures, estimating a reasonable annual damage amount, and then using any of those figures as the basis for a hazard mitigation plan. The total damages to state roads in Utah for the ten years between 1973 and 1983 were about $2 million. However, direct costs for just one landslide at Thistle, Utah, in 1983 will no doubt exceed $200 million. This demonstrates not only that reliable loss estimates are hard to get, but also that states may have landslide catastrophes in the future the likes of which they have never seen.

We must begin at every governmental level to grapple with a severe problem that can only get worse. The stakes are enormous: at least $2.5 billion in direct cumulative landslide damages for the past decade have been documented in the United States, most of them paid for by tax dollars. Yet, in the opinion of informed geologists and engineers, 90% of those losses could have been avoided through proper engineering solutions and/or land-use management practices.

—Earl E. Brabb
U.S. Geological Survey
Menlo Park, CA

Reprinted by permission from ***Natural Hazards Observer,*** *(University of Colorado, Boulder)*

Reference

Minimum Landslide Damage in the United States 1973-1983, by Earl E. Brabb USGS Open-File Report #84-486. Available from the Open-File Services Section, U.S. Geological Survey, Box 25425, Federal Center, Denver, CO 80225.

General Publications

*(Items from **Natural Hazards Observer**, University of Colorado, Boulder)*

When the Snakes Awake: Animals and Earthquake Prediction. *Helmut Tributsch. Cambridge, MA: The MIT Press. 1984. 248 pp. Hardback $20.00; paperback $8.95.*

The possibility of abnormal animal behavior acting as a harbinger of earthquakes was mentioned as early as the first century, B.C. by the Greek historian Diodorus. This book relates numerous anecdotal accounts of such behavior from several parts of the world and examines recent scientific attempts to verify the phenomenon. Topics discussed include receptor characteristics in various life forms, the validity of historical reports and documents, the physical phenomena of an incipient earthquake that could excite animal sensitivity, and the reluctance of some scientific circles to accept popular folklore as a useful starting point in earthquake prediction studies. Written in a nontechnical style, the book attempts to explain anecdotal literature in light of current seismological theories and modern techniques of observing animal behavior. Extensive references (231 citations) and chronological tables of historical precursor accounts aid the reader who wishes to pursue the subject further.

Terra Non Firma: Understanding and Preparing for Earthquakes. *James M. Gere and Haresh C. Shah. New York: W. H. Freeman & Company. 1984. 203 pp. Clothbound $19.95, paperback $11.95.*

Written by two professors at Stanford University's John A. Blume Earthquake Engineering Center, this is an excellent introduction to earthquakes and related phenomena. Technical subjects explained included plate techtonics, types of fault movements, liquifaction, the measurement of energy released by earthquakes, tsunamis, and the efficacy of various predictive methods. Mitigative measures also covered by the authors include structural design and construction practices, building codes, structural retrofitting, lifeline protection, zoning and land use planning, earthquake insurance, securing building contents, educational programs, individual earthquake preparedness, and conduct before, during, and after an earthquake.

An Action Plan for Reducing Earthquake Hazards of Existing Buildings. *ABE Joint Venture. 1985. 75 pp. Copies of the plan may be obtained from the Federal Emergency Management Agency, Earthquake Programs, 500 C Street, S.W.; Washington, DC 20472.*

One of the tasks identified in the National Earthquake Hazards Reduction Program (NEHRP) Five-Year Plan for Fiscal Years 1985-89 is the resolution of problems related to hazardous buildings in active seismic zones. A workshop held in Tempe, Arizona, during March of 1985, attracted 50 seismic safety experts who proposed a five-part plan including: technical and engineering requirements; public policy, legal, and financial strategies; special requirements of historic buildings; multihazard assessment; and information transfer and dissemination. Five-year objectives, various necessary tasks, a recommended schedule for completion, and issues concerning costs and funding sources are presented for each element. The plan suggests several actions to be initiated as soon as possible; identification of local jurisdictions that are likely candidates for early implementation of hazard reduction programs; preparation of standard building inventory and building evaluation methods; development of historic building importance classification systems; and determination of the characteristics and extent of public and private, institutional and individual legal liability.

Proceedings of the U.S.-Japan Workshop on Urban Earthquake Hazards Reduction. *Charles Scawthorn, Chistropher Arnold, and Roger E. School, Editors. Earthquake Engineering Research Institute Publication #85-03. 1985. 278 pp. $9.00. Available from the EERI, 2620 Telegraph Avenue, Berkeley, CA 94704.*

Held July 29 to August 1, 1984, in Palo Alto, California, the workshop examined major seismic hazards facing two of the most highly industrialized and technologically advanced nations on earth. Participants examined several issues that had not previously received adequate attention or that were fundamental to urban seismic hazard reduction. These issues included post-earthquake fire hazard, lifeline vulnerability, the economic analysis of mitigation strategies, and the utilization of damage estimates for urban seismic safety planning and policy making. The proceedings contain 17 papers and five working group reports. Sixty-four specialists in earthquake hazard mitigration and urban planning attended the workshop, which was organized by the

EERI, and was supported by the National Science Foundation and the Federal Emergency Management Agency.

How to Prepare for an Earthquake: A Guide for Business. *Insurance Information Institute. 1985. 123 pp. $20.00 for a single copy; $10.00 each when ordering three copies or more. Contact the Insurance Information Institute, Publications Service Center, 110 William Street, New York, NY 10038, (212) 669-9200.*

This manual presents guidelines to be followed by businesses in preparing for earthquakes. (Actually, it offers suggestions which can help in preparing for any disaster.) In particular, the book discusses in great detail what to expect when an earthquake destroys infrastructures and limits emergency aid and assistance. After identifying the many areas of the United States vulnerable to earthquake losses, it outlines what can be done by businesses in high seismic risk zones to protect employees at the office and at home, to secure office and computer facilities, and to guard against long-term operation stoppages and lost assets.

Corporate Disaster Planning Guide, *2nd Edition. 1985. 118 pp. $20.00. Order from the Red Cross Disaster Resource Center, Golden Gate Chapter, American Red Cross, 1550 Sutter Street, San Francisco, CA 94109, (415) 776-1500, x211. Make checks payable to the Red Cross Disaster Resource Center.*

This comprehensive, expanded edition of the ***Guide*** will be helpful to businesses of all sizes in the development of plans and programs to decrease disaster-related injuries and property damage. Tabbed for easy reference and contained in a 3-ring binder, the document is the product of information gathered from San Francisco business people, city government officials, and Red Cross Emergency Services staff and volunteers. Sections on emergency equipment and supply sources, reference sources for emergency planners, and disaster training materials have been updated. New sections have been prepared on disaster planning for computer systems, vital record protection, and the development of a corporate information system. Special features of the ***Guide*** include a comprehensive outline of the planning process; a flow chart for emergency preparedness activity; selected presentations from Red Cross disaster planning conferences; a prototype plan; sections on equipment, supplies, services, and service vendors; and a list of suggested readings.

Volcanic Emergency Management. *Office of the United Nations Disaster Relief Coordinator (UNDRO). 1985. 86 pp. A limited number of single copies are available free of charge upon request to UNDRO, Room S-2935, United Nations, New York, NY 10017.*

This handbook reviews the experience acquired in recent years in dealing with volcanic emergencies in various parts of the world. It does not discuss the details of local planning and activities, but rather distills from that experience some conclusions and general principles of organization and practice that the contributors hope will prove universal. The first two chapters review the nature of volcanic hazards and describe some recent emergencies caused by eruptions. The third chapter examines the problems involved in assessing volcanic hazards and predicting the onset and development of eruptions. The volume then outlines mitigation and protection measures for volcanic hazards, and describes pre-emergency planning—particularly that necessary for evacuation. The final chapters discuss the perception of and response to risk; decision making in volcanic emergencies; and the problems inherent in communication among scientists, civil authorities, the news media, and the general public. The book concludes with descriptions of organizations which have been established in various countries (Japan, the United States, the Philippines, Iceland, and Papau New Guinea) for volcanic emergency planning and management.

Liquefaction of Soils During Earthquakes. *National Academy of Sciences, National Research Council, Commission on Engineering and Technical Systems, Committee on Earthquake Engineering. Washington: National Academy Press. 1985. 240 pp. A limited number of single copies are available at no cost from the Committee on Earthquake Engineering, National Academy of Sciences, 2101 Constitution Avenue, N.W., Washington, DC 20418. Also available from NTIS, 5285 Port Royal Road, Springfield, VA 22161, as Report #CETS-EE-001. Paper copy $22.95; microfiche $5.95.*

This report describes the causes and effects of liquefaction of soils during earthquakes, documents the state-of-the-art of analyzing liquefaction potential, and recommends future directions for research on the phenomenon. While much of the document deals with technical matters associated with liquefaction, mitigation measures and research needs are also reviewed. Four general classes of mitigation are identified: 1) nonstructural solutions, such as relocation or abandonment of a structure; 2) site solutions, such as chemical stabilization of the soil, or the removal and replacement of unsatisfactory material; 3) structural solutions that enhance the stability of a given project; and 4) drainage solutions, such as dewatering systems, groundwater controls, and the construction of drains. Future research deemed useful includes in-situ studies on stress in various types of soil, continued investigation of earthquake sites where liquefaction has occurred, and instrumentation of selected locations with a high probability for soil liquefaction during an earthquake. Eighteen pages of references are included.

Earthquake Mitigation Management for Harbors and Seaports. *Gilbert B. Siegel and Dorothy M. Bjur. University of Southern California, Institute for Marine and Coastal Studies. 1985. 261 pp. A limited number of free copies are available from Gilbert Siegel, School of Public Administration, University of Southern California, VKC 368, University Park-MC 0041, Los Angeles, CA 90089-0041, (213) 743-2241. After the supply is exhausted, additional copies can be obtained from the same source for $10.00—the cost of xeroxing and postage.*

The objective of the research presented in this report is to provide information to seaport and harbor managers on what is known about earthquake mitigation, the extent to which it has been implemented in seaports and harbors, and its general efficacy. The research includes: 1) case studies of the 1964 Alaska and 1960 Chile earthquakes and subsequent recovery/reconstruction; 2) a collection of expert opinion on U.S. Pacific Basin seaport earthquake mitigation measurings; and 3) a questionnaire survey of their mitigation practices. Findings and recommendations from the research indicated that Alaskan seaports benefitted considerably from the infusion of federal funds during the rebuilding of port facilities following the 1964 earthquake, whereas in Chile, a lack of resources and bad governmental decisions have resulted in negative economic impacts. In addition, the researchers found a genuine need for seismic risk analysis and modern seismic engineering in vulnerable seaports. Few state-of-the-art mitigation measures have been applied to Pacific Basin seaports, and seaports currently rely mostly on building codes and construction permit enforcement to mitigate the effects of future earthquakes.

Seismic Damage to Unrefinforced Masonry Buildings. *Robert Reitherman. 1964. 28 pp. $34.50. Available from scientific Services, Inc., 517 East Bayshore, Redwood City, CA 94063, (415) 368-2931.*

Although damage to unreinforced masonry buildings is one of the major risks in earthquakes, there is relatively little information of a statistical nature on such damage. Research presented in this report utilizes the Wailes and Horner Damage Intensity Scale, a scale the author deems superior to existing scales for estimating damage to unreinforced masonry buildings. The report concludes that: 1) there is great danger to people who flee these buildings or find themselves outside of, but near such buildings during an earthquake; 2) there is also a great danger that unreinforced masonry buildings will collapse in a major earthquake; 3) there is no orderly system in place to ensure that comparable earthquake damage data are gathered and saved after major earthquakes; and 4) studies attempting to predict damage from future earthquakes can benefit from data derived from the Wailes and Horner Scale because the scale makes it possible to estimate a distribution of damage, rather than only a mean value. The report is one of the products of the research project, "Case Studies of the Earthquake Performance of Unreinforced Masonry Buildings," funded by the National Science Foundation.

Report on the Coalinga Earthquake of May 2, 1983. *Kathleen J. Tierney. Report #SSC 85-01. 1985. 101 pp. Single copies available free from the California Seismic Safety Commission, 1900 K Street, Suite 100, Sacramento, CA 95814, (916) 322-4917.*

At 4:42 p.m. on May 2, 1983, Caolinga was struck by an R6.7 earthquake that virtually destroyed the town's central area. To be found amidst the debris in the days following the disaster were a large number of researchers who collected and frequently published pieces of information on the earthquake and its effects. Despite this unprecedented volume of research, however, no one did a comprehensive study of the event, summarized all the findings, or pointed out the lessons to be learned from the disaster. With a mandate from the California State Legislature, the California Seismic Safety Commission utlimately did undertake such a study (which will be followed by a guidebook on policies and procedures for cities and counties to adopt in preparing for and dealing with future earthquakes). Included in this volume are chapters on community awareness and preparedness in Coalinga before the quake, the earthquake itself and its implications for other California communities, injuries and damage in the quake, emergency response, disaster assistance, recovery and reconstruction assistance, and community recovery. Recommendations include developing policies and programs to deal with the hazard posed by unreinforced masonry buildings (see the model ordinance cited below); improving organizational linkages and disaster planning; increasing awareness, education, and training efforts; changing disaster assistance programs to focus more on providing technical and financial assistance during community recovery; and conducting basic and applied research to provide the technical data needed to address important policy questions. Together with the forthcoming ***Guidelines,*** this volume will be essential reading for civic leaders and emergency personnel in all communities threatened by earthquakes.

Social Responses to Volcanism in Japan and the United States. *Ronald W. Perry and Hirotada Hirose. 1985. 139 pp. While supply lasts, single copies are available free of charge from Ronald Perry, Office of Disaster Studies, School of Public Affairs, Arizona State University, Tempe, AZ 85287. Also available from NTIS, 5285 Port Royal Road, Springfield, VA 22161, as Report #PB85-223782. Paper copy $22.95, microfiche $5.95.*

The authors present a comparative analysis of the responses of citizens from two different cultures to volcanic eruptions. Data were gathered from both the Mt. Usu (1977) and the Mount St. Helens (1980) eruptions; effects were compared in broad areas of citizen response, including warning receipt, evacuation behavior, and shelter utilization; and longer-range impacts including changes in interpersonal relationships, community organization, and citizen perceptions of the efficacy of preparedness planning. Although some differences were observed, the researchers found striking similarities between the responses of the two cultures to the eruptions. 1) The general response to the imposition of access controls was the same. Local businesspeople allied to fight access controls, while emergency managers and public safety personnel opposed lifting restrictions. 2) Both communities had a high level of citizen compliance with evacuation warnings. 3) The nature of problems in emergency sheltering were much the same regardless of whether the shelter facilities were public or private. 4) Most of those surveyed felt that their personal standard of living had not deteriorated due to the eruptions.

Earthquake Damage Mitigation for Computer Systems. *Robert A. Olson and Charles C. Thiel, Jr., Editors. 1983. 128 pp. $12.00. Available from the Earthquake Engineering Research Institute, 6431 Fairmount Avenue, Suite 7, El Cerrito, CA 94530, (415) 525-3668.*

Electronic data processing lies at the heart of modern banking procedures. The many losses that would be incurred if these services were interrupted by an earthquake would far exceed those associated with physical damage. Concern about the vulnerability of data processing facilities prompted several California banks and the Federal reserve Bank of San Francisco to form the Committee on Finance, Insurance, and Monetary Services, and to convene a workshop on computer damage mitigation. The proceedings of that meeting, held July 12, 1983, provide valuable guidelines for organizations that maintain sensitive data management equipment in earthquake-prone areas. The contributors review the possible impacts of a quake on such facilities; discuss the many engineering, design, and construction practices that can mitigate damage to those facilities, their contents, and the utility and communication systems that allow them to function; and describe possible improvements in these practices.

Rehabilitating Hazardous Masonry Buildings: A Draft Model Ordinance. *Report #SSC 85-06. 1985. 55 pp. Single copies available free from the California Seismic Safety Commission, 1900 K Street, Suite 100, Sacramento, CA 95814, (916) 322-4917.*

It is well established that unreinforced masonry buildings constitute one of the greatest threats to life and safety in earthquakes (see, for example, the report above by Tierney). However, only a few cities have initiated programs to identify and reinforce hazardous buildings. The California Seismic Safety Commission has issued this draft ordinance (modeled on one adopted by Los Angeles in 1981) with a set of recommendations to aid and encourage local governments in developing such programs. The provisions of the ordinance are not intended to protect structures completely from damage due to earthquakes, but rather to maximize safety and protection of life. The recommendations of the Seismic Safety Commission describe implementation of the ordinance and other mitigation measures. Also included is a sample brochure that answers common questions about the ordinance.

Natural Hazards Slide Sets

Six unique sets of 35-mm slides that depict natural hazards throughout the world are available from the NOAA National Geophysical Data Center. Each slide set includes 20 illustrations covering the following subjects:

- Earthquake Damage in Mexico City, Mexico, September 1985 (Color)
- Earthquake Damage—General (Color)
- Earthquake Damage to Schools (B&W, Color)
- Volcanoes in Eruption (B&W, Color)
- Volcanic Rocks (Color)
- Tsunami—General (B&W, Color)

The slides are available for $31.00 per set. **Prepayment is required:** orders may be paid by check or credit card. For more information contact:

National Geophysical Data Center
NOAA, Code E/GC4, Dept. MM1
325 Broadway
Boulder, CO 80303
(303) 497-6541

Geodynamic Maps of the Circum Pacific Region: Pacific Basin Sheet, *published by the Circum-Pacific Council for Energy and Mineral Resources.*

The map depicts geodynamic information crustal stress, Holocene and active volcanoes, seismicity, earthquake first motions and active lithospheric plates. The map Pacific Basin sheet, is at a scale of 1:17,000,000 and extends from the eastern part of the Indian Ocean across the Pacific, including most of North and South America as well as the entire Caribbean. It was published in mid-1985 and it includes a separate explanatory text.

The cost of this map is $15 to destinations in North America and $16.50 to destinations outside of North America. Post and the explanatory text is included free of charge with any order.

The entire set of Geodynamic Maps (including the four quadrants of the Pacific and Antarctica at a scale of 1:10,000,000 and the Pacific Basin sheet described above) is available at a cost of $46 to North Americans or $49 to destinations outside of North America (surface mail).

Maps can be purchased from the AAPG Bookstore, P.O. Box 979, Tulsa, Oklahoma 74101.

U.S. Geological Survey Publications

Books and Maps by Mail

When ordering books, give the series designation and number, such as Geological Survey Bulletin 738, and the full title. When ordering maps, give name or series designation and number, such as I-1243. Include your full address and zip code, plainly printed. Prepayment is required and should be made by check or money order payable to U.S. Geological Survey. Postage stamps are not accepted. Do not send cash. Remittances must be in United States funds.

Prices listed include cost of domestic surface transportation. For transmittal outside the United States (except to Canada and Mexico), a surcharge of 25 percent of the net bill should be included to cover surface transportation.

Books

Professional papers, bulletins, circulars, and single copies of *Earthquakes and Volcanoes* are obtainable by mail from:

U.S. Geological Survey
Books and Open-File Reports
Federal Center, Bldg. 41
Box 25425
Denver, CO 80225

Maps

Maps are obtainable from:

U.S. Geological Survey
Map Distribution
Federal Center, Bldg. 41
Box 25286
Denver, CO 80225

Books and Maps Over the Counter

Books

Book reports of the Geological Survey are available *over the counter* at the following Geological Survey offices:

Washington, D.C.–General Services Bldg., Rm. 1028, 19th and F Sts., NW (20244)
Denver, Colorado–Federal Bldg., Rm. 169, 1961 Stout St. (80294)
Dallas, Texas–Federal Bldg., Rm. 1C45, 1100 Commerce St. (75242)
Los Angeles, California–Federal Bldg., Rm. 7638, 300 N. Los Angeles St. (90012)
Menlo Park, California–Bldg. 3 (Stop 33), Rm. 122, 345 Middlefield Road (94025)

Reston, Virginia – 503 National Center, Rm. 1C402, 12201 Sunrise Valley Dr. (22092)
Salt Lake City, Utah – Federal Bldg., Rm. 8105, 125 South State St. (84138)
San Francisco, California – Customhouse, Rm. 504, 555 Battery St. (94111)
Spokane, Washington – U.S. Courthouse, Rm. 678, West 920 Riverside Ave. (99201)
Anchorage, Alaska – 4230 University Drive, Rm. 101, (99508-4664)
Anchorage, Alaska – 701 C Street, Box 53, (99513)

Maps

Maps may be purchased *over the counter* at the U.S. Geological Survey offices where books are sold and at the following Geological Survey offices:

Rolla, Missouri – 1400 Independence Road
Denver, Colorado – Bldg. 41, Federal Center
Fairbanks, Alaska – New Federal Bldg., 101 Twelfth Avenue

BOOKS

PROFESSIONAL PAPERS

P 1276. HAWAII. Ground deformation associated with the 1975 magnitude-7.2 earthquake and resulting changes in activity of Kilauea Volcano, Hawaii, by P. W. Lipman, J. P. Lockwood, R. T. Okamura, D. A. Swanson, and K. M. Yamashita. 1985. 45 p. $2.50.

The 1975 earthquake, the largest on Hawaii Island in more than 100 years, was associated with major gravitational slumping of the seaward flank of Kilauea Volcano; maximum displacements were as much as 3.5 m vertically and 8 m horizontally. After the earthquake, deformation patterns at Kilauea changed notably and were accompanied by the longest period of eruptive inactivity in 10 years.

P 1335. WASHINGTON. Observations of the eruptions of July 22 and August 7, 1980, at Mount St. Helens, Washington, by R. P. Hoblitt. 1986. 44 p. $2.50.

The explosive eruptions of July 22 and August 7, 1980, at Mount St. Helens, Wash., were both composed of multiple eruptive pulses. Three of the pulses – two on July 22 and one on August 7 – were witnessed and photographed. The observations and photographs document in detail: (1) the generation and movement of pyroclastic density flows; (2) the shift with time from column collapse to convective rise; and (3) phenomena associated with the displacement of air by an advancing pyroclastic density flow. Mechanisms are proposed to account for the various observations.

P 1342. CALIFORNIA. The evolution of the Southern California Uplift, 1955 through 1976, by R. O. Castle, M. R. Elliott, J. P. Church, and S. H. Wood. 1984. 136 p.; 16 plates in pocket. $10.

At its zenith, the Southern California Uplift formed a 150-km-wide crustal swell that extended about 600 km eastward and east-southeastward from Point Arguello to the Colorado River and the Salton Sea, respectively; its amplitude exceeded 0.30 m over at least half its extent. Although the growth of the uplift consisted of two well-defined spasms of positive movement, the second of which was closely followed by partial collapse, there exists no evident correlation between the growth of this feature and the regional seismicity. Recognition of an early 20th century episode of uplift and partial collapse within the same general area suggests that the recent uplift represents but a single cycle in an ongoing process, conceivably associated with decoupling and with viscous flow at the base of the seismogenic zone.

P 1360. Evaluating earthquake hazards in the Los Angeles region; an earth-science perspective, edited by J. I. Ziony. 1985. 505 p. $24.

Potentially destructive earthquakes are inevitable in the Los Angeles region of California. This multiauthored volume presents an integrated set of studies that identify the principal geologically controlled earthquake hazards (surface faulting, strong ground shaking, ground failure, and tsunamis), summarizes methods for evaluating their areal extent and severity, and suggests opportunities for their reduction. To demonstrate some of the techniques, many of which are newly developed, the geologic and seismologic effects of a magnitude 6.5 earthquake along the northern part of the Newport-Inglewood fault zone are predicted. The methods described can be used for evaluating and mapping earthquake hazards in other urban regions threatened by earthquakes.

BULLETINS

B 1659. The National Earthquake Hazards Reduction Program; scientific status, by T. C. Hanks. 1985. 40 p. $1.75.

This report sets forth the significant scientific accomplishments of the National Earthquake Hazards Reduction Program, on the basis of letters and discussions by numerous scientists from Government, academia, and industry. Stimulated by several major earthquakes in the early 1970's, the Earthquake Hazards Reduction

Act of 1977 (Public Law 95-124) established the program with funding to four Federal agencies, including the U.S. Geological Survey. The objectives of this program are not only the advancement of scientific knowledge but also the application of this knowledge in effective implementation of hazard-reduction policies and emergency-preparedness plans.

B 1655. United States earthquakes, 1982, edited by C. W. Stover. 1985. 141 p. $7.50.

B 1630. Earthquake hazards in the offshore environment, by R. A. Page, U.S. Geological Survey and P. W. Basham, Canadian Department of Energy, Mines and Resources. 1985. 69 p. $6.50.

Much of the current petroleum exploration on the continental shelves is in areas of moderate to high earthquake potential that may be subject to surface faulting, uplift or subsidence, seismic shaking, seafloor failure, and tsunamis. If the resources in these areas are to be developed economically and safely, potential earthquakes hazards must be identified and mitigated both in planning and in regulating activities and in designing, constructing, and operating facilities. Mitigation strategies include avoidance, accommodation, and emergency response planning.

MISCELLANEOUS INVESTIGATIONS SERIES MAPS

I-1613. WASHINGTON. Seismotectonic map of the Puget Sound region, Washington, by H. D. Gower, J. C. Yount, and R. S. Crosson. 1985. Lat 46°37'30" to 49°, long 121° to 123°30'. Scale 1:250,000 (1 inch = about 4 miles). Sheet 42 by 58 inches. (Accompanied by 15-page text.) $2.40.

MISCELLANEOUS FIELD STUDIES MAPS

MF-0585. CALIFORNIA. Preliminary map showing recency of faulting in coastal Southern California, by J. I. Ziony, C. M. Wentworth, J. M. Buchanan-Banks, and H. C. Wagner. 1974. Three sheets. Sheet 1, lat 33° to 34°45', long about 118°45' to 120°45'; sheet 2, lat about 32°30' to about 34°15', long 116°45' to 118°30'; sheet 3, lat about 33° to about 35°, long about 117° to about 120°. Scale 1:250,000 (1 inch = about 4 miles). Sheet 1, 30 by 33 inches; sheet 2, 31 by 41 inches; sheet 3, 35 by 36 inches. (Reprint.) $4.50.

MF-0709. CALIFORNIA. Maps showing maximum earth-quake intensity predicted in the southern San Francisco Bay region, California, for large earthquakes on the San Andreas and Hayward faults, by R. D. Borcherdt, J. F. Gibbs, and K. R. Lajoie. 1975. Three sheets. Sheet 1, lat about 37°15' to 37°52'30", long about 121°45' to about 122°30'; sheet 2, lat about 37° to 37°52'30", long about 121°30' to 122°30'. Scale 1:125,000 (1 inch = about 2 miles). Sheet 1, 26 by 33 inches; sheet 2, 38 by 40 inches; sheet 3, 37 by 38 inches. (Accompanied by 11-page text.) (Reprint.) $4.50.

MF-1781. NEW JERSEY. Attitude, movement history, and structure of cataclastic rocks of the Flemington Fault; results of core drilling near Oldwick, New Jersey, by W. C. Burton, and N. M. Ratcliffe. 1985. Sheet 35 by 42 inches. $1.50.

MF-1819. MONTANA. Seismicity map of the State of Montana, by B. G. Reagor, C. W. Stover, and S. T. Algermissen. 1985. Two sheets. Sheet 1, lat about 45° to about 49°, long about 104° to about 116°. Scale 1:1,000,000 (1 inch = about 16 miles). Sheet 1, 25 by 38 inches; sheet 2, 37 by 53 inches. $3.

MF-1845-A. HAWAII. Aeromagnetic map of the rift systems of Kilauea and Mauna Loa volcanoes, Island of Hawaii, Hawaii, by V. J. Flanigan, C. L. Long, Donald Rohret, and Pamela Mohr. 1986. Lat about 19° to about 19°40', long about 154°50' to about 155°45'. Scale 1:100,000 (1 inch = about 1.6 miles). Sheet 37 by 44 inches. $1.50.

MF-1845-B. HAWAII. Apparent-resistivity map of the rift systems of Kilauea and Mauna Loa volcanoes, Island of Hawaii, Hawaii, by V. J. Flanigan, C. L. Long, Donald Rohret, and Pamela Mohr. 1986. Lat about 19° to about 19°40', long about 154°50' to about 155°45'. Scale 1:100,000 (1 inch = about 1.6 miles). Sheet 37 by 44 inches. $1.50.

MF-1852. ARIZONA. Seismicity map of the State of Arizona, by C. W. Stover, B. G. Reagor, and S. T. Algermissen. 1986. Lat about 31° to about 37°, long about 109° to about 115°. Scale 1:1,000,000 (1 inch = about 16 miles). Sheet 35 by 47 inches. $1.50.

MF-1856. UTAH. Seismicity map of the State of Utah, by C. W. Stover, B. G. Reagor, and S. T. Algermissen. 1986. Lat about 37° to about 42°, long about 109° to about 114°. Scale 1:1,000,000 (1 inch = about 16 miles). Sheet 39 by 57 inches. $1.50.

MF-1857. IDAHO. Seismicity map of the State of Idaho, by C. W. Stover, B. G. Reagor, and S. T. Algermissen. 1986. Lat about 42° to about 49°, long about 111° to about 117°. Scale 1:1,000,000 (1 inch = about 16 miles). Sheet 43 by 56 inches. $1.50.

MF-1863. MISSOURI. Seismic-reflection profiles of the New Madrid seismic zone; data along the Mississippi River near Caruthersville, Missouri, by A. J. Crone, S. T. Harding, D. P. Russ, and K. M. Shedlock. 1986. Four sheets. Sheet 1, 39 by 56 inches; sheet 2, 38 by 40 inches; sheet 3, 38 by 39 inches; sheet 4, 39 by 40 inches. $6.

PRELIMINARY DETERMINATION OF EPICENTERS

For sale by the Superintendent of Documents, U.S. Government Printing Office, Washington, DC 20402. Annual subscription $21 domestic, $26.25 foreign.

Single copies of monthly issues may be purchased only from U.S. Geological Survey, Books and Open-File Reports, Federal Center, Bldg. 41, Box 25425, Denver, CO 80225, for $2 domestic, $2.50 foreign. Make check or money order payable to Department of the Interior–USGS.

Preliminary determination of epicenters. Monthly listing for October 1985. 25 p.

Open-File Reports

"Open-file report" is applied by the Geological Survey to results of investigations that are made available to the public outside the formal USGS publication series. These informal reports include manuscript or map copy, basic data, field notes, or other data that are not reproduced and distributed in quantity but are available for public inspection at the indicated depositories.

Most open-file reports are available at cost from the Open-File Services Section (OFSS), U.S. Geological Survey, Federal Center, Bldg. 41, Box 25425, Denver, CO 80225 [telephone: (303) 236-7476].

Check or money order, in exact amount for open-file reports ordered, should be payable to U.S. Geological Survey. Prepayment is required. For transmittal outside the United States (except Canada and Mexico), a surcharge of 25 percent of the bill should be included to cover surface transportation. Specific instructions for ordering are given under listing.

In the open-file report listings that follow, offices where reports may be inspected are identified by the symbols listed below.

A	Public Inquiries Office, 4230 University Drive, Rm. 101, Anchorage, AK 99508-4664
Da	Library, 1526 Cole Blvd. at West Colfax Ave., Golden, Colo. (Mail address: Stop 914, Box 25046, Federal Center, Denver, CO 80225.)
Db	Public Inquiries Office, Federal Bldg., Rm. 169, 1961 Stout St., Denver, CO 80294.
F	Library, 2255 North Gemini Dr., Flagstaff, AZ 86001.
LA	Public Inquiries Office, Rm. 7638, Federal Bldg., 300 North Los Angeles St., Los Angeles, CA 90012.
M	Library, 345 Middlefield Rd., Menlo Park, CA 94025.
NC	Library, Rm. 4A100, National Center, 12201 Sunrise Valley Dr., Reston, VA 22092.
S	Public Inquiries Office, Rm. 678, U.S. Courthouse, West 920 Riverside Ave., Spokane, WA 99201.
SF	Public Inquiries Office, Rm. 504, Customhouse, 555 Battery St., San Francisco, CA 94111.
T	Public Inquiries Office, Rm. 1C45, Federal Bldg., 1100 Commerce St., Dallas, TX 75242.
U	Public Inquiries Office, Rm. 8105, Federal Bldg., 125 South State St., Salt Lake City, UT 84138.
Wa	Public Inquiries Office, Rm. 1028, General Services Bldg., 19th and F Sts., NW., Washington, DC 20244.
Wb	U.S. Department of Interior, Natural Resources Library, Gifts and Exchange Section, 18th and C Sts., NW., Washington, DC 20240.

OF 85-0041. CALIFORNIA. Deformation of Long Valley Caldera, eastern California, 1983-1984, by J. C. Savage, M. Lisowski, J. E. Estrem, and R. O. Castle. 16 p. (NC, Da, M, SF, LA; California Dep. of Conservation, Div. of Mines and Geol., 2815 O St., Sacramento, CA 95816; 367 Civic Dr., Pleasant Hill, CA 94523; and State Office Bldg., 107 South Broadway, Los Angeles, CA 90012.) Microfiche $4; paper copy $4.25.

OF 85-0150. WASHINGTON, OREGON, CALIFORNIA. Analysis of linear features mapped from Landsat images of the Cascade Range, Washington, Oregon, and California, by D. H. Knepper, Jr. 31 p. (NC, Da, M, SF, LA, S; California Dep. of Conservation, Div. of Mines and Geol., 2815 O St., Sacramento, CA 95816; 367 Civic Dr., Pleasant Hill, CA 94523; and

State Office Bldg., 107 South Broadway, Los Angeles, CA 90012; Div. of Geol. and Earth Resources, Dep. of Natural Resources, Olympia, WA 98504; Oregon Dep. of Geol. and Mineral Industries, 1005 State Office Bldg., Portland, OR 97201.) Microfiche $4; paper copy $4.75.

OF 85-0201. Minutes of the National Earthquake Prediction Evaluation Council, by C. F. Shearer. 84 p. (NC, Da, M, SF, LA; California Dep. of Conservation, Div. of Mines and Geol., 2815 O St., Sacramento, CA 95816; 367 Civic Dr., Pleasant Hill, CA 94523; and State Office Bldg., 107 South Broadway, Los Angeles, CA 90012.) Microfiche $4; paper copy $12.75.

OF 85-0211. CALIFORNIA. Quaternary faults of California, by J. J. Lienkaemper. 12 p. (NC, Da, M, SF, LA; California Dep. of Conservation, Div. of Mines and Geol., 2815 O St., Sacramento, CA 95816; 367 Civic Dr., Pleasant Hill, CA 94523; and State Office Bldg., 107 South Broadway, Los Angeles, CA 90012.) Microfiche $4; paper copy $2.

OF 85-0276-A. Feasibility of a nationwide program for the identification and delineation of hazards from mud flows and other landslides; Chapter A, Landslide classification for identification of mud flows and other landslides, by R. H. Campbell, D. J. Varnes, R. W. Fleming, M. A. Hampton, D. B. Prior, D. A. Sangrey, D. R. Nichols, and E. E. Brabb. 32 p., 2 over-size sheets. (NC, Da, M.) Microfiche $5.50; paper copy $8.50.

OF 85-0276-B. Feasibility of a nationwide program for the identification and delineation of hazards from mud flows and other landslides; Chapter B, Methods and costs for the delineation of susceptibility to mud flows and other landslides, compiled by R. H. Campbell. 19 p. (NC, Da, M.) Microfiche $4; paper copy $3.

OF 85-0276-C. Feasibility of a nationwide program for the identification and delineation of hazards from mud flows and other landslides; Chapter C, Methods and costs for the delineation of susceptibility to mud flows and other landslides, compiled by R. H. Campbell. 6 p. (NC, Da, M.) Microfiche $4; paper copy $1.50.

OF 85-0276-D. OHIO, Feasibility of a nationwide program for the identification and delineation of hazards from mud flows and other landslides; Chapter D, The economics of landslide mitigation strategies in Cincinnati, Ohio; a methodology for benefit cost-analysis, by R. L. Bernknopf, D. S. Brookshire, R. H. Campbell, C. D. Shapiro and R. W. Fleming. 35 p. (NC, Da, M.) Microfiche $4; paper copy $5.25.

OF 85-0286. Earthquake catalog of Peru, by A. F. Espinosa, L. A. Casaverde, J. A. Michael, J. Alva-Hurtado, and J. Vargas-Neumann. 618 p. (NC, Da, M.) Microfiche $4; paper copy $94.50.

OF 85-0290-A. IDAHO. Proceedings of Workshop XXVIII on the Borah Peak, Idaho earthquake; Volume A, edited and convened by R. S. Stein and R. C. Bucknam. 686 p. (NC, Da, M, U, SF, S, Idaho Bur. of Mines and Geol., Univ. of Idaho Campus, Moscow, ID 83843.) Microfiche $4.50; paper copy $106.

OF 85-0290-B. IDAHO. Proceedings of Workshop XXVIII on the Borah Peak, Idaho earthquake, edited and convened by R. S. Stein and R. C. Bucknam; Volume B, Fault scarps, landslides and other features associated with the Borah Peak earthquake of October 28, 1983, central Idaho; a field trip guide, by A. J. Crone, *with a section on the* Doublespring Pass road trench, by M. H. Hait, Jr. 23 p., 3 over-size sheets, scale 1:24,000 (1 inch = 2,000 feet). (NC, Da, M, U, SF, S, Idaho Bur. of Mines and Geol., Univ. of Idaho Campus, Moscow, ID 83843.) Microfiche $6.25; paper copy $10.25.

OF 85-0365. CALIFORNIA. Distribution and geologic relations of fault systems in the vicinity of the central Transverse Ranges, Southern California, by J. C. Matti, D. M. Morton, and B. F. Cox. 27 p., 2 over-size sheets, scale 1:250,000 (1 inch = about 4 miles). (NC, Da, M, SF, LA; California Dep. of Conservation, Div. of Mines and Geol., Room 1341, Resources Bldg., 1416 9th St., Sacramento, CA 95814; 367 Civic Dr., Pleasant hill, CA 94523-1997, and State Office Bldg., 107 South Broadway, Room 1065, Los Angeles, CA 90012.) Microfiche $5.50; paper copy $10.75.

OF 85-0371. An introduction to technical issues in the evaluation of seismic hazards for earthquake-resistant design, by W. W. Hays. 112 p. (NC, Da, M.) Microfiche $4; paper copy $17.

OF 85-0375. Processed strong-motion records from Monasavu Dam, Fiji: earthquakes of February 13, 14, and 23, 1983, by Barry Silverstein. 59 p. (NC, Da, M.) Microfiche $4; paper copy $9.

OF 85-0378. SOUTH CAROLINA. Detailed sections from auger holes and outcrops in the Cainhoy, Charleston, and Fort Moultrie quadrangles, South Carolina, by R. E. Weems, and E. M. Lemon, Jr. 72 p. (NC; South Carolina Geol. Surv., Harbison Forest Rd., Columbia, SC 29210.) Microfiche $4; paper copy $11.

OF 85-0382. UTAH. Landslides and debris flows east of Mount Pleasant, Utah, 1983 and 1984, by E. W. Lips. 14 p., 1 over-size sheet, scale 1:24,000 (1 inch = 2,000 feet). (NC, Da, M, U, Db; Utah Geol. and Mineral Surv., 606 Black Hawk Way, Salt Lake City, UT 84108.) Microfiche $4.75; paper copy $13.75.

OF 85-0397. Earthquake Data Archiving and Retrieval System; archived data sets in the standardized library, SL000001 to SL000100, by D. M. Tottingham, J. T. Newberry, and W. H. Lee. 291 p. (NC, Da, M.) Microfiche $4; paper copy $43.75.

OF 85-0436. Earthquake Data Archiving and Retrieval System; archived data sets in the general library, GL000001 to GL000200, by T. M. Messier, M. E. O'Neill, and W. H. Lee. 317 p. (NC, Da, M.) Microfiche $4; paper copy $47.75.

OF 85-0457. Estimation of earthquake effects associated with large earthquakes in the New Madrid seismic zone, edited by M. G. Hopper. 140 p., 7 over-size sheets, scale 1:1,000,000 (1 inch = about 16 miles). (NC, Da, M.) Microfiche $9.25; paper copy $34.75.

OF 85-0464. National Earthquake Hazards Reduction Program; summaries of technical reports, Volume XX, prepared by participants in the National Earthquake Hazards Reduction Program, July 1985, compiled by M. L. Jacobson and T. R. Rodriguez. 558 p. (NC, Da, M.) Microfiche $4; paper copy $86.

OF 85-0507. Minutes of the National Earthquake Prediction Evaluation Council, March 29-30, 1985, Pasadena, California, by C. F. Shearer. 193 p. (NC, Da, M.) Microfiche $4; paper copy $3.

OF 85-0521. Proceedings of the Workshop on geothermal resources of the Cascade Range, May 22-23, 1985, Menlo Park, California, edited by Marianne Guffanti, and L. J. Muffler. 85 p. (NC, Da, M, SF, LA, S; California Dep. of Conservation, Div. of Mines and Geol., 2815 O St., Sacramento, CA 95816; 367 Civic Dr., Pleasant Hill, CA 94523; and State Office Bldg., 107 South Broadway, Los Angeles, CA 90012; Dep. of Geol. and Mineral Industries, 910 State Office Bldg., Portland, OR 97201-5528; Div. of Geol. and Earth Resources, Dep. of Natural Resources, 4224 SE 6th Ave., Rowsix, Bldg. 1, Lacey, WA 98503.) Microfiche $4; paper copy $13.25.

OF 85-0529. New Mexico. Seismic and vibration hazard investigations of Chaco Culture National Historical Park, by K. W. King, S. T. Algermissen, and P. J. McDermott. 59 p. (NC, Da, M, Db, U, T; New Mexico Bur. of Mines and Mineral Resources, Campus Station, Socorro, NM 87801.) Microfiche $4; paper copy $9.50.

OF 85-0533. Tsunamis; hazard definition and effects on facilities. 138 p. (NC, Da, M.) Microfiche $4; paper copy $21.75.

OF 85-0542. Preliminary report of investigations of the central Chile earthquake of March 3, 1985, edited by S. T. Algermissen. 180 p. (NC, Da, M.) Microfiche $4; paper copy $27.50.

OF 85-0560. Floods from dam failures, by J. E. Costa. 54 p. (NC, Da, M, Wb.) Microfiche $4; paper copy $9.

OF 85-0583. CALIFORNIA. Report on recommended list of structures for seismic instrumentation in San Bernardino County, California, by G. Brady, M. Celebi, C. Rojahn, W. Iwan, G. Hart, G. Pardoen, L. Schoelkopf, R. Haskell, K. Topping, E. Safak, and R. Maley. 18 p. (NC, Da, M, SF, LA; California Dep. of Conservation, Div. of Mines and Geol., Room 1341, Resources Bldg., 1416 9th St., Sacramento, CA 95814; 367 Civic Dr., Pleasant Hill, CA 94523-1997; and State Office Bldg., 107 South Broadway, Room 12065, Los Angeles, CA 90012.) Microfiche $4; paper copy $2.75.

OF 85-0613. WASHINGTON. Three component long-period data for the 1949 South Puget Sound, Washington earthquake, by G. E. Baker. 8 p. (NC, Da, M, S, SF, LA; Div. of Geol. and Earth Resources, Dep. of Natural Resources, 4224 SE 6th Ave., Rowsix, Bldg. 1, Lacey, WA 98503.) Microfiche $4; paper copy $1.50.

OF 85-0660-H. National Earthquake Information Center wave-form catalog, August 1985, by M. D. Zirbes, J. M. Lishner, and R. J. Moon. 199 p. (NC, Da, M.) Microfiche $4; paper copy $30.

OF 85-0584. CALIFORNIA. Processed strong-motion records from the Coalinga, California, aftershock on July 9, 1983 0740 UTC, by Barry Silverstein. 169 p. (NC, Da, M, SF, LA; California Dep. of Conservation, Div. of Mines and Geol., 2815 O St., Sacramento, CA 95816; 367 Civic Dr., Pleasant Hill, CA 94523; and State Office

Bldg., 107 South Broadway, Los Angeles, CA 90012.) Microfiche $4; paper copy $26.

OF 85-0615. Auxiliary programs for support of seismic hazard analysis, by S. L. Hanson, and D. M. Perkins. 115 p. (NC, Da, M.) Microfiche $4; paper copy $17.75.

OF 85-0661. CALIFORNIA. Map of faulting accompanying the 1966 Parkfield, California, earthquake, by J. J. Lienkaemper, and R. D. Brown. 8 p., 3 over-size sheets, scale 1:12,000 (1 inch = 1,000 feet). (NC, Da, M, SF, LA; California Dep. of Conservation, Div. of Mines and Geol., Room 1341, Resources Bldg., 1416 9th St., Sacramento, CA 95814; 367 Civic Dr., Pleasant Hill, CA 94523-1997; and State Office Bldg., 107 South Broadway, Room 1065, Los Angeles, CA 90012.) Microfiche $6.25; paper copy $14.

OF 85-0714. Seismograph station codes and coordinates, 1985 edition, by B. W. Presgrave, R. E. Needham, and J. H. Minsch. 391 p. (NC, Da, M.) Microfiche $4; paper copy $59.

OF 85-0719. Preliminary response activities and recommendations of the USGS Landslide Hazard Research Team to the Puerto Rico landslide disaster of October 7, 1985, by R. H. Campbell, D. G. Herd, and R. M. Alonso. 13 p. (NC.) Microfiche $4; paper copy $2.25.

OF 85-0731. A workshop on Reducing potential losses from earthquake hazards in Puerto Rico, edited by W. W. Hays and P. L. Gori. 326 p. (NC, Da, M.) Microfiche $4; paper copy $49.

OF 85-0754. CALIFORNIA. Minutes of the National Earthquake Prediction Evaluation Council, July 26-27, 1985, Menlo Park, California, by C. F. Shearer. 445 p. (NC, Da, M.) Microfiche $4; paper copy $68.

Ground breakage from the 1966 Varto, Turkey, earthquake. Photograph by Robert E. Wallace.

EARTHQUAKES

Waverly J. Person
National Earthquake Information Center
U.S. Geological Survey
Denver, Colorado

July - August 1985

Two major earthquakes (7.0-7.9) occurred during this reporting period; one was in the New Britain region and the other in China. A destructive earthquake also hit the Hindu Kush region causing casualties in Pakistan.

In the United States a magnitude 5.9 earthquake on August 4 caused slight damage in central California.

Idaho

A light earthquake occurred in eastern Idaho on July 1 at 9:04 p.m. MDT. The magitude 4.0 earthquake was located about 80 km southeast of Idaho Falls; intensity MM IV effects were noted at Palisades and MM III at Irwin. The quake was also felt at Alpine, Wyoming.

New Britain

A major earthquake struck the eastern part of this island on July 3. The magnitude 7.2 earthquake was centered about 75 km east of Rabaul. The earthquake caused damage, landslides and ground cracks on New Ireland and in the Rabaul area, New Britain. Intensity MM VII effects were experienced at Rabaul. A 1.3 m tsunami was observed in Rabaul's harbor followed by a seiche that lasted 15 hours. The quake was also felt at Panguna, Solomon Islands.

Hawaii

The southern part of the island of Hawaii was shaken by a magnitude 4.4 earthquake on July 7 at 2:01 p.m. HST. It was located about 30 km south of Mauna Loa and was felt over the southern half of the island. There were no reports of damage.

On August 22 at 6:28 a.m. HST, a magnitude 4.3 earthquake occurred near the west coast of the island of Hawaii about 20 km southwest of Kauluoa Point. This earthquake was felt widely in the western part of the island. There were no reports of damage.

California

A light earthquake occurred in the southern part of this state on July 18 at 7:05 a.m. PDT. This magnitude 4.3 earthquake was located about 80 km northeast of San Bernardino. Intensity MM III effects were noted at Fawnskin and Yucca Valley and it was also felt at San Bernardino.

A magnitude 4.7 earthquake was located off the coast of northern California about 250 km southwest of Eureka on July 30 at 3:57 a.m. PDT. The quake was felt at Bayside, Fortuna and Eureka, maximum intensity MM III.

On August 4 at 5:02 a.m. PDT, the central part of the state was shaken by a sharp earthquake. The magnitude 5.9 earthquake was located about 20 km east-northeast of Coalinga. Slight damage was experienced at Avenal, Hanford, Kettleman City and Lemoore, intensity MM VI. Intensity MM V effects were noted in many areas of Kern, Kings, Fresno, Tulare and San Luis Obispo Counties and the quake was felt throughout much of central California. This earthquake was preceded by a magnitude 4.7 quake on August 4 at 4:29 a.m. PDT. A number of aftershocks followed including three with magnitudes of 4.0 or greater: a 4.5 on August 4 at 8:16 a.m. PDT, a 4.4 on August 5 at 7:46 a.m. PDT and a 4.1 on August 6 at 5:16 p.m. PDT. All three were felt in the Coalinga area.

On August 15 at 6:51 p.m. a magnitude 4.5 earthquake occurred about 55 km north of China Lake in the Haiwee Reservoir area. Intensity MM III effects were noted at Olancha, Ridgecrest and Woodville.

The Bishop area was shaken mildly by a magnitude 4.3 earthquake on August 26 at 8:04 p.m. PDT. Intensity MM III effects were experienced at Bishop, Dunlap, Badger and Bass Lake and the quake was also felt at North Fork and Lake Sabrina.

Afghanistan

The Hindu Kush region of this country was rocked by a destructive earthquake on July 29. The magnitude 6.7 quake was centered about 250 km northeast of Kabul near the Pakistan and USSR borders. At least five people were killed, about 38 were injured, considerable damage occurred and landslides were reported in the Chitral and Swat districts of Pakistan. Damage (MM VIII) occurred and many people were reported homeless in the Khorog-Ishkashim area of the USSR. Also in the USSR, extensive damage was reported in the Kurgan-Tyube area and damage (MM VII) in the Dushanbe area. The quake was also felt in other parts of the USSR. Avalanches were reported in northern India and avalanches and landslides were reported in southern Tajikistan, USSR. The quake was felt strongly in northeastern Afghanistan, northern Pakistan and much of northern India including New Delhi.

British Columbia

A minor, but widely felt earthquake occurred in British Columbia on August 6 at 6:54 p.m. PDT. The magnitude 3.6 quake was located about 450 km northeast of Seattle, Washington. The earthquake was felt at Trail and Creston, British Columbia. Intensity MM IV effects were noted at Cusick, Washington and at Nordman, Idaho. The quake was felt at Lane, Newport, Metaline and Usk, Washington and also at Priest River and Porthill, Idaho.

Wyoming

This state experienced a series of earthquakes during this reporting period. The first, a magnitude 3.5 on August 13 at 2:57 p.m. (MDT) was located about 55 km northeast of Rock Springs. Intensity MM IV effects were noted at Point of Rocks.

On August 16 at 5 minutes after midnight, a magnitude 4.3 earthquake occurred about 30 km southeast of Riverton. Intensity MM IV effects were experienced at Lander, Jeffrey City, Midwest, South Pass City and Point of Rocks. It was also felt at Casper, Rock Springs, Ethete, Hanna, Superior, Basin, Edgerton and Hyattville.

The Jackson, Wyoming area experienced two sharp earthquakes on August 21 at 12:06 a.m. MDT and August 30 at 3:08 p.m. MDT. These earthquakes were located about 35 km south of Jackson. The first had a magnitude of 4.8 and was felt strongly in the Jackson area. Intensity MM V effects were noted at Alpine and MM IV at Lander and Wilson. The quake was also felt at Palisades, Victor and Swan Valley, Idaho. The second quake, a magnitude 4.3, also produced intensity MM V effects at Alpine and was felt in the Jackson area and parts of eastern Idaho. A number of smaller earthquakes followed but they were not large enough to be felt.

Hungary

A moderate but damaging earthquake hit the western part of this country on August 15. The magnitude 5.0 earthquake was centered about 80 km southwest of Budapest near Lake Balaton. The quake occurred at 6:39 a.m. local time and awakened and frightened many people. Considerable damage was experienced in the Berhida-Peremarton area (maximum intensity MM VIII). Slight damage was also noted at Budapest and the earthquake was felt strongly throughout western Hungary. It was also felt at Zagreb, Yugoslavia and in Burgenland and at Vienna, Austria. A number of aftershocks followed but none caused additional damage.

New Mexico

Parts of this state experienced a sharp earthquake on August 16 at 8:57 a.m. MDT. The magnitude 4.3 earthquake was located about 10 km northeast of Socorro. Slight damage (intensity MM VI) occurred at Socorro and Lemitar. Intensity MM IV effects were noted at Bingham and the quake was also felt at Magdalena and San Antonio.

Montana

A minor earthquake occurred in the Hebgen Lake area on August 17 at 6:43 p.m. MDT. This earthquake had a magnitude of 3.5 and was felt at West Yellowstone, Montana and at the West Entrance area of Yellowstone National Park.

Peru

A strong earthquake struck near the northern coast of this country on August 21. The magnitude 6.1 shock was centered near Chimbote. At least 100 people were injured, 60 homes were destroyed and there was damage to other buildings in the Chimbote area. The quake was felt strongly along the coast from Chiclayo in the north to Chincha in the south.

China

A major earthquake hit western China on August 23. The magnitude 7.6 earthquake was centered in southern Xinjiang about 75 km northeast of Kashi in the vicinity of Wuqia. At least 67 people were killed, many were injured and extensive damage was reported in the Wuqia-Shufu area. The quake was felt in the Andizhan-Fergana-Namangan and Tashkent areas, USSR and also in northern Pakistan. A number of aftershocks have followed; some caused additional deaths and damage.

Greece

The western part of this country experienced a damaging earthquake on August 31. The magnitude 4.4 earthquake was centered about 40 km northwest of Preveza. The quake caused some minor injuries and damaged houses, churches and a ceramics factory in the port city of Preveza. A landslide blocked a highway connecting Preveza and northwestern Greece.

PRELIMINARY LOCATIONS
July - August 1985

Date	Origin time	Region	Coordinates Lat	 Long	Depth km	Magnitudes
Jul 2	03 03 56.6	Eastern Idaho	43.2 N	111.2 W	5	4.0ML
Jul 3	04 36 52.4	New Britain region	4.5 S	152.8 E	41	7.2MS
Jul 7	12 00 37.5	Hawaii	19.2 N	155.6 W	9	4.4ML
Jul 18	14 05 25.5	Southern California	34.4 N	116.5 W	6	4.3ML
Jul 29	07 54 44.3	Hindu Kush	36.2 N	70.9 E	101	6.7mb
Jul 30	10 57 04.2	Off coast of northern California	40.8 N	125.3 W	5	4.7ML
Aug 4	11 29 14.7	Central California	36.1 N	120.1 W	10	4.7mb
Aug 4	12 01 57.3	Central California	36.2 N	120.2 W	5	5.9MS
Aug 4	15 15 37.7	Central California	36.0 N	120.0 W	10	4.5mb
Aug 5	14 45 37.0	Central California	36.1 N	120.1 W	10	4.4mb
Aug 6	13 27 58.9	British Columbia	49.4 N	116.7 E	5	3.6ML
Aug 7	00 16 04.5	Central California	36.0 N	120.1 W	11	4.1mb
Aug 13	20 57 00.8	Wyoming	41.8 N	108.6 W	5	3.5ML
Aug 15	04 28 47.1	Hungary	47.1 N	18.1 E	10	5.0MS
Aug 16	01 51 20.8	California-Nevada border region	36.2 N	117.8 W	10	4.5mb
Aug 16	06 05 22.4	Wyoming	42.9 N	108.1 W	10	4.3ML
Aug 16	14 56 52.9	New Mexico	34.1 N	106.8 W	7	4.1ML
Aug 18	00 42 45.3	Hebgen Lake	44.6 N	111.0 W	5	3.5ML
Aug 21	11 26 28.8	Near coast of northern Peru	9.2 S	78.9 W	61	6.1mb
Aug 21	18 05 38.5	Wyoming	43.2 N	110.8 W	5	4.8mb
Aug 22	16 28 00.0	Hawaii	19.3 N	156.1 W	44	4.3ML
Aug 23	12 41 59.7	Southern Xinjiang	39.4 N	75.3 E	33	7.6MS
Aug 27	03 04 06.8	California-Nevada border region	37.4 N	118.6 W	6	4.3ML
Aug 30	21 08 06.7	Wyoming	43.2 N	110.9 W	5	4.3ML
Aug 31	06 03 47.3	Greece-Albania border region	39.2 N	20.6 E	23	4.4mb

U.S. ACTIVITY*
July - August 1985

Alaska	9	New Mexico	1
California	19	Tennessee	1
Hawaii	13	Washington	1
Idaho	3	Wyoming	6
Montana	1		—
		Total	54

*Felt earthquakes as reported from many sources.

September - October 1985

There was one great earthquake (8.0 and above) and two major earthquakes (7.0-7.9) during this reporting period. The devastating great earthquake occurred in Mexico on September 19 and was followed by a 7.5 aftershock the next day. The other major quake was in the Kermadec Islands.

The largest earthquake to affect the United States was a magnitude 6.5 south of Alaska on October 9.

New Mexico

A very minor earthquake occurred in the southwestern part of this state on September 5 at 11:23 p.m. MDT. The magnitude 2.6 tremor was located in the Radium Springs area; it was felt there and also at Leasburg.

Arkansas

A sharp earthquake was experienced in the northwestern part of this state on September 6 at 5:17 p.m. CDT. This magnitude 3.6 earthquake was located about 140 km northwest of Little Rock near Lurton. Intensity MM V effects were noted at Green Forest, Kingston and Nail and the quake was felt throughout much of the northwestern part of the state.

Wyoming

The western part of this state continued to experience earthquakes as a sharp earthquake shook the area on September 6 at 9:47 p.m. MDT. The magnitude 4.6 earthquake was located about 25 km south of Jackson. Intensity MM V effects were noted at Alpine and MM IV effects at Wilson, Wyoming and at Palisades and Victor, Idaho. The quake was also felt at Bondurant, Moose and Jackson, Wyoming. Rockslides were also triggered in the Snake River Canyon south of Jackson, temporarily closing U.S. highway 89.

Illinois

A minor earthquake shook the western suburbs of Chicago on September 9 at 5:07 p.m. CDT. The quake, a magnitude 3.0, was located in the LaGrange-Elmhurst area and was felt with an intensity of MM V at Clarendon Hills, Edgebrook and LaGrange and an intensity of MM IV at Brookfied and Western Springs. The quake was felt with lesser intensity at Country Side, Lindenwood and Villa Park.

China

The western part of this country was struck by another damaging earthquake on September 11 (previous shock August 23, 1985 — see page 169). This magnitude 6.6 aftershock killed 4 people, injured 61 and caused considerable damage in the Wuqia-Kashi-Shufu area. It was reported that all the buildings of the Kashi Hydropower Station were flattened and the station's dam was seriously damaged. Hundreds of aftershocks have followed since August 23 but most were not large enough to cause additional damage.

Alaska

A moderate earthquake occurred in the southeastern part of this state on September 14 at 4:28 p.m. YST. This earthquake had a magnitude of 5.3 and was centered about 125 km northwest of Juneau. Intensity MM V effects were noted at Haines and Gustavus and MM IV effects at Skagway, Pelican and Juneau. It was also felt at Auke Bay, Elfin Cave, Kake and Yakutat. In the

Yukon Territory, the quake was felt at Whitehorse, Carcross and Haines Junction.

On October 9 at 34 minutes after midnight YST, a magnitude 6.5 earthquake occurred about 100 km southeast of Sand Point. Slight damage, intensity MM VI, was experienced at Sand Point and MM V effects were experienced at Cold Bay, Chignik Lake and Chignik Lagoon. The quake was also felt at False Pass, King Cove and Port Heiden.

In the Aleutian Islands, the Fox Islands were hit by three moderate earthquakes; the first, on October 1 at 5:55 a.m. AST, was located about 200 km southwest of Dutch Harbor. The second, a magnitude 5.6, occurred on October 24 at 4:09 p.m. AST and was located about 325 km southwest of Dutch Harbor. These two quakes were both felt at Nikolski. The third, a magnitude 5.8 on October 31 at 9:33 a.m. AST, was located about 100 km south of Dutch Harbor. It was felt with an intensity of MM IV at Unalaska and was felt mildly at Sand Point.

In the Rat Islands, Aleutian Islands a magnitude 5.6 earthquake occurred on October 30 at 9:06 a.m. AST. This quake was located about 130 km southwest of Vega Point, Kiska Island and was felt on Shemya.

Indonesia

A strong earthquake struck the sparsely populated area of western Irian Jaya on September 15. The magnitude 6.3 earthquake was centered about 550 km southwest of Jayapura in the vicinity of Enarotali. At least nine people were killed, seven were injured and damage occurred in the Enarotali area. Slumping was also observed in the epicentral area.

Texas

A minor earthquake occurred in the central part of this state on September 18 at 10:54 a.m. CDT. This quake had a magnitude of 3.3 and was located about 80 km north of Dallas. Intensity MM V effects were noted at Sanger and MM IV effects at Valley View and Era. The quake was also felt at Muenster and Saint Jo.

Mexico

This country was hit by one of the most devastating earthquakes in its history on September 19 at 7:18 a.m. local time. The magnitude 8.1 earthquake was centered about 380 km west-southwest of Mexico City. At least 9,500 people were killed, about 30,000 were injured, 100,000 were left homeless and extensive damage was caused in parts of Mexico City and several states of central Mexico. According to some reports the death toll from this earthquake may be as high as 35,000. It is estimated that the earthquake seriously affected an area of approximately 825,000 square kilometers, caused between 3 and 4 billion dollars in damage and was felt by almost 20 million people. Four hundred twelve buildings collapsed and another 3,124 were badly damaged in Mexico City, and about 60 percent of the buildings were destroyed at Ciudad Guzman, Jalisco. Damage also occurred in the states of Colima, Guerrero, Mexico, Michoacan, Morelos, parts of Veracruz and in other areas of Jalisco. The maximum intensity was MM IX at Mexico City, Ciudad Guzman and the Pacific coast towns of Lazaro Cardenas, Ixtapa and La Union. The quake was felt in other areas of Mexico and as far away as Guatamela City, Guatemala and Houston, Texas. It was also felt at Brownsville, McAllen, Corpus Christi, Ingram and El Paso, Texas. A tsunami was generated which caused some damage at Lazaro Cardenas, Zihuatenejo and Manzanillo. Estimated wave heights were 3 meters at Zihuatenejo and 2.8 meters at Lazaro Cardenas. Tide stations recorded maximum wave heights (peak-to-trough) of 1.4 meters at Acapulco, Mexico, 60 cm. at La Libertad, Ecuador, 58 cm. at Acajutla, El Salvador and lesser wave heights in other areas around the Pacific. Seiches were observed in East Galveston Bay, Texas and in swimming pools in Texas, New Mexico, Colorado and Idaho. Water well fluctuations were recorded at Ingleside, Texas; Santa Fe, New Mexico; Rolla, Missouri; Hillsborough County, Florida and Smithsburg, Maryland.

About 36 hours after the main shock, on October 20 at 7:37 p.m. local time, a magnitude 7.5 earthquake occurred in the same area. This earthquake caused additional casualties and damage in the Mexico City area and was felt in many parts of central Mexico. This quake also generated a local tsunami which caused no additional damage. Again on October 29 at 9:02 a.m. local time, a magnitude 5.6 earthquake in the same area caused a great deal of panic and 13 people were injured in the Mexico City area. Many more aftershocks occurred but caused very little additional damage.

Kermadec Islands

A major earthquake centered about 600 km south of Raoul struck this remote area on September 26. This earthquake had a magnitude of 7.0 and was felt on Raoul and on the eastern and southern parts of North Island and at Christchurch and Dunedin.

South Island, New Zealand. There were no reports of damage.

Solomon Islands

A strong earthquake struck Guadalcanal Island on September 27. The magnitude 6.9 earthquake was centered about 50 km southeast of Honiara. Several houses were destroyed on the island. Maximum intensity MM VII was experienced at Viso and the quake was felt throughout Guadalcanal.

Yugoslavia

The southeastern part of this country was struck by a damaging earthquake on September 28. The magnitude 4.8 earthquake was centered about 60 km southeast of Skopje. Sixteen people were reported injured and about 500 buildings were damaged in the Negotino-Demir Kapija area, maximum intensity MM VII. Intensity MM V effects were noted at Skopje and the quake was felt strongly throughout Yugoslavian Macedonia.

New York

A very minor earthquake occurred in the upper part of this state on September 30 at 9 minutes after midnight EDT. The magnitude 2.7 tremor was located about 100 km north of Albany. Intensity MM IV effects were noted at Cleverdale and Fort Ann and the earthquake was also felt at Lake Luzerne.

On October 19 at 6:08 a.m. EDT, the southern part of the state was shaken by a sharp earthquake. The magnitude 4.0 quake was felt over a wide area and intensity MM V effects were observed in Westchester and Rockland Counties, New York and in parts of Bergen County, New Jersey. The quake was also felt from Philadelphia and southern New Jersey to southern Canada and into the Boston area. The main shock was preceded by a magnitude 2.0 earthquake at 6:06 a.m.

On October 21 at 6:37 a.m. EDT, a magnitude 2.8 aftershock occurred and again was felt with a maximum intensity of MM V in parts of Westchester County, New York. It was felt in northern New Jersey and southern Connecticut.

Nevada

A minor earthquake occurred about 110 km south of Eureka on October 2 at 12:45 p.m. PDT. The earthquake had a magnitude of 3.5 and was felt at Tonopah and Warm Springs.

California

The southern part of this state experienced a moderate earthquake on October 2 at 4:44 p.m. PDT. The magnitude 5.0 earthquake was located about 15 km northeast of Riverside. Intensity MM V effects were experienced in the areas of Banning, Bryn Mawr, Colton, Hesperia, Riverside and San Bernardino. The quake was also felt in many areas of Riverside, San Bernardino, Los Angeles and Orange Counties.

Japan

A magnitude 5.8 earthquake, the largest in many years, struck the Tokyo area on October 4. Eighteen people were injured, mostly from falling objects, and transportation was disrupted in the Tokyo area. The quake was felt strongly in much of Tokyo and the surrounding areas. It was felt to the north as far as Akita and south to Hachijo-jima and west to Toyooka.

Canada

The Northwest Territories experienced a strong earthquake on October 5 at 9:24 a.m. MDT. The magnitude 6.6 earthquake was centered about 400 km west of Yellowknife. Slight damage occurred at Wrigley and Fort Liard. The quake was felt strongly at Fort Simpson and was felt in parts of the Yukon Territory, British Columbia and Alberta. The quake was also felt at Juneau and Sitka, Alaska. Many aftershocks have followed, some large enough to be felt.

Guatemala

A damaging earthquake hit this country on October 10 at 9:39 p.m. local time. The magnitude 4.6 earthquake was located about 75 km north of Guatemala City. Two people were injured and about 500 houses were destroyed at San Miguel Uspantan. About 80 percent of the buildings in San Miguel Uspantan sustained some damage. The quake was felt strongly in western Guatemala and at Guatemala City.

Tajik SSR

The Republic of Tajikistan, in the Soviet Union, was hit by a destructive earthquake on October 13. The magnitude 5.9 earthquake was centered about 100 km south of Tashkent in the vicinity of Kayrakkum. At least 29 people were killed, 80 were injured and about 8,000 were homeless in the Kayrakkum-Gafurov area. About 90 percent of the multi-story brick buildings were destroyed at Kayrakkum and about 900 buildings were destroyed at Gafurov. Leninabad also had considerable damage. Landslides were reported in the epicentral area. Maximum intensity MM IX was noted at Kayrakkum, intensity MM VIII at Gafurov and MM VII at Leninabad. Intensity MM V effects were experienced at Tashkent and in the Fergana Basin and the quake was also felt at Samarkand, Dushanbe, Nurek and Kulyab.

Massachusetts

The northeastern part of this state experienced a minor earthquake on October 15 at 4:01 p.m. EDT. The magnitude 3.0 quake was located about 40 km northwest of Boston. It was felt over a wide area of the northeastern part of the state. The highest intensity, MM IV, was at Carlisle, Chelmsford, Harwood, Littleton, North Chelmsford, North Billerica and Westford.

Montana

A swarm of earthquakes occurred along the border between Montana and Wyoming, beginning in early October. Some of the larger ones occurred on October 19: a magnitude 4.1 at 9:35 a.m. MDT, a magnitude 4.0 at 10:33 a.m. MDT and a magnitude 3.8 at 10:45 a.m. MDT. These earthquakes are located about 8 km east of West Yellowstone, Montana. They were felt at Gardiner and West Yellowstone, Montana and also at Old Faithful and Madison Junction, Yellowstone National Park, Wyoming.

Algeria

The eastern part of this country was struck by a damaging earthquake on October 27. The magnitude 5.9 earthquake was centered about 350 km east of Algiers near Constantine. Six people were killed and damage occurred in the Annaba-Setif-Souk Ahras area. The earthquake was felt strongly in much of eastern Algeria.

Idaho

A light earthquake occurred in the western part of this state on October 29 at 2:31 p.m. MST. The magnitude 4.1 earthquake was located about 15 km southeast of Challis and was felt at Challis.

PRELIMINARY LOCATIONS
September - October 1985

Date	Origin time	Region	Coordinates Lat	Coordinates Long	Depth km	Magnitudes
Sep 6	05 22 46.2	New Mexico	32.5 N	106.9 W	5	2.6DUR
Sep 6	22 17 02.0	Arkansas	35.8 N	93.1 W	10	3.6mbLg
Sep 7	03 47 28.3	Wyoming	43.2 N	110.8 W	5	4.6ML
Sep 9	22 06 31.8	Illinois	41.9 N	88.0 W	5	3.0mbLg
Sep 11	20 45 51.7	Southern Xinjiang, China	39.3 N	75.4 W	33	6.6MS
Sep 15	01 28 17.8	Southeastern Alaska	59.2 N	136.5 W	14	5.3mb
Sep 15	02 42 54.4	West Irian region	4.2 S	136.1 E	10	6.3MS
Sep 18	15 54 04.5	Central Texas	33.5 N	97.0 W	5	3.3mbLg
Sep 19	13 17 47.8	Michoacan, Mexico	18.2 N	102.6 W	33	8.1MS
Sep 21	01 37 13.8	Near coast of Guerrero, Mexico	17.8 N	101.7 W	33	7.5MS
Sep 26	07 27 48.9	South of Kermadec Islands	34.6 S	178.7 W	33	7.0MS
Sep 27	03 39 08.2	Solomon Islands	9.8 S	159.8 E	30	6.9MS
Sep 28	14 50 16.6	Yugoslavia	41.6 N	22.2 E	20	4.8mb

PRELIMINARY LOCATIONS
September - October 1985 (cont.)

Date	Origin time	Region	Coordinates		Depth km	Magnitudes
			Lat	Long		
Sep 30	04 08 56.3	New York	43.4 N	73.5 W	5	2.7CL
Oct 1	15 54 51.3	Fox Islands, Aleutian Islands	52.3 N	168.8 W	33	5.7mb
Oct 2	19 44 38.7	Nevada	38.5 N	115.7 W	5	3.5ML
Oct 2	23 44 12.0	Southern California	34.0 N	117.2 W	16	5.0ML
Oct 4	12 25 51.1	Near coast of Honshu, Japan	35.8 N	140.0 E	90	5.8mb
Oct 5	15 24 02.2	Northwest Territories, Canada	62.3 N	124.3 W	10	6.6MS
Oct 9	09 33 32.8	South of Alaska	54.8 N	159.6 W	31	6.5MS
Oct 11	03 39 11.0	Guatemala	15.3 N	90.8 W	5	4.6mb
Oct 13	15 59 53.5	Tajik SSR	40.3 N	69.8 E	33	5.9MS
Oct 15	20 00 39.3	Massachusetts	42.5 N	71.5 W	2	3.0CL
Oct 19	10 07 40.3	New York	41.0 N	73.8 W	6	4.0ML
Oct 19	15 34 59.5	Hebgen Lake region	44.7 N	111.0 W	5	4.1ML
Oct 19	16 32 35.2	Hebgen Lake region	44.7 N	111.0 W	5	4.0ML
Oct 19	16 45 05.7	Hebgen Lake region	44.7 N	111.0 W	5	3.8ML
Oct 21	10 37 15.0	New York	41.0 N	73.8 W	5	2.8ML
Oct 25	02 09 04.4	Fox Islands, Aleutian Islands	52.1 N	171.3 W	33	5.6MS
Oct 27	19 34 57.0	Algeria	36.4 N	6.7 E	10	5.9MS
Oct 29	15 02 27.1	Michoacan, Mexico	18.2 N	102.5 W	33	5.6mb
Oct 29	21 30 34.7	Western Idaho	44.4 N	114.1 W	5	4.1ML
Oct 30	19 05 37.4	Rat Islands, Aleutian Islands	51.8 N	175.6 W	33	5.6mb
Oct 31	19 33 07.1	Fox Islands, Aleutian Islands	53.3 N	166.9 W	33	5.8mb

U.S. ACTIVITY*
September - October 1985

Alaska	19	Montana	3
Arkansas	1	Nevada	1
California	12	New Mexico	1
Hawaii	9	New York	4
Idaho	2	Texas	1
Illinois	1	Wyoming	3
Maine	1		—
Massachusetts	1	Total	59

*Felt earthquakes as reported from many sources.

November-December 1985

There were four major earthquakes (7.0-7.9) during the last two months of the year. One was in the remote area of West Irian (formerly West New Guinea) and the other three were in the sparsely populated Vanuatu Islands of the South Pacific.

There were no damaging earthquakes in the United States during this reporting period.

Alaska

A moderate earthquake shook the central part of this state on November 4 at 3:28 p.m. YST. The magnitude 5.1 earthquake was located about 180 km northwest of Anchorage. Intensity MM IV effects were experienced at Talkeetna and MM III effects at Denali National Park, Chugiak, Sutton, Kasilof, Cooper Landing and Willow. The quake was also felt at Anchorage, Fairbanks and Palmer.

On November 14 at 11:17 p.m. YST, a magnitude 5.7 earthquake occurred about 70 km south of Sand Point and produced intensity MM V effects at Cold Bay and MM IV effects at Sand Point, King Cove and False Pass.

The southern part of the state was shaken by a sharp earthquake on December 30 at 3:41 a.m. YST. This quake had a magnitude of 5.5 and was located about 25 km northwest of Anchorage. Intensity MM V effects were noted at Anchorage and Eagle River and MM IV at Palmer, Peters Creek, Girdwood, Kenai, Sutton, Wasilla and Elmendorf Air Force Base. The quake was also felt at Seward.

Again on December 30 at 11:13 a.m. YST, a magnitude 5.1 earthquake occurred about 200 km southwest of Fairbanks. This quake was felt in Denali Park.

Turkey

A moderate but damaging earthquake struck the eastern part of this country on November 7. This earthquake had a magnitude of 5.1 and was located about 135 km northeast of Erzurum. Fourteen people were injured and at least 113 houses were damaged in the Erzurum area.

Montana

Earthquakes continued to occur in the Hebgen Lake region. On November 9 at 4:38 a.m. MST, a magnitude 4.8 was experienced, the largest in the area to date. Intensity MM V effects were noted at West Yellowstone, Montana and MM IV effects at Pony and Twin Bridges, Montana. The quake was also felt at Springdale, Montana and Alpine, Wyoming. This quake was followed by a magnitude 4.1 at 4:40 a.m. MST, a 4.0 at 4:59 a.m. followed by a 4.4 twenty-four seconds later, a 4.2 at 6:09 a.m., a 4.4 on November 26 at 2:35 a.m. MST and a 4.2 on December 3 at 11:38 p.m. MST. The last two earthquakes were felt at West Yellowstone, Montana. Many smaller earthquakes have occurred in the area; some were reported felt.

Indonesia

A major earthquake occurred in an unpopulated area of West Irian on November 17. The magnitude 7.1 earthquake was centered about 100 km southwest of Biak. There were no reports of damage.

California

The central part of this state was shaken by earthquakes on November 24 at 11:22 a.m. PST and on November 28 at 7:14 a.m. PST. The first quake was located about 115 km southeast of Monterey near San Ardo and had a magnitude of 4.4. Intensity MM V effects were noted at San Ardo and MM IV effects at Bradley, King City and Lockwood. The quake was also felt at Coalinga, Creston, Templeton and Pacific Grove. The second quake, a magnitude 4.5, was located about 40 km southeast of Hollister and produced MM IV effects in the areas of Hollister, Tres Pinos, Aptos, Carmel, Big Sur, Salinas and Santa Cruz.

Vanuatua Islands

The Vanuatua Islands (formerly New Hebrides Islands) were hit by three major earthquakes during this reporting period. The first two were on November 28 and had magnitudes of 7.0 and 7.1; the third, on December 21, had a magnitude of 7.3. These earthquakes were centered about 200 km northeast of Brisbane, Australia in an unpopulated part of the islands so there were no reports of casualties or damage.

Arkansas

A sharp earthquake occurred in the northeastern part of this state near the Tennessee border on December 5 at 5:00 p.m. (CST). The magnitude 3.9 earthquake was located about 10 km west of Blytheville. The quake was felt over a wide area of northeastern

Arkansas. Intensity MM V effects were noted at Blytheville Air Force Base and MM IV effects at Blytheville, Osceola, Burdette, Keiser, Joiner and Tomato, Arkansas. The quake was felt with lesser intensities in other parts of Arkansas and with intensity MM IV at Henning, Tennessee.

Hawaii

There were three earthquakes in Hawaii during this reporting period which had magnitudes of 4.0 or greater. A magnitude 4.3 earthquake on December 12 at 9:01 a.m. HST was located about 5 km north of Maui. It was felt on Maui and on the big island in the areas of Honokau, Hilo, Kamuela and Volcano.

Again on December 12 at 11:19 a.m. HST, a magnitude 4.0 occurred about 30 km west of Mauna Loa and was felt along the west coast of the island of Hawaii in the Captain Cook, Kailua and Kealakekua areas. On December 13 at 1:21 p.m. HST, a magnitude 4.0 occurred about 20 km southeast of Volcano. It was felt on the southeastern part of the island of Hawaii.

Nicaragua

The southwestern part of this country was struck by two damaging earthquakes on December 14 at 6:39 a.m. local time and on December 15 at 8:45 p.m. local time. The first was centered about 80 km south of Managua and had a magnitude of 5.0. The first quake caused some damage and was felt strongly in the Managua-Rivas area. It was also felt at Cartago, Costa Rica. The second quake, a magnitude 6.0, was centered about 50 km southeast of Managua. This shock caused landslides which injured six people and damaged about 100 buildings in the Rivas area; the quake was felt strongly along the Pacific Coast of Nicaragua. It was also felt at Atenas and San Jose, Costa Rica and at San Salvador, El Salvador.

New Mexico

A minor earthquake occurred about 20 km northwest of Santa Rosa on December 15 at 12:15 a.m. The tremor had a magnitude of 3.4 and was felt at Variodero, Trujillo and Trementina.

Canada

The Northwest Territories were struck on December 23 by the strongest earthquake ever known to have occurred in that area. The magnitude 6.9 earthquake was centered about 580 km northeast of Whitehorse near Fort Simpson. It was felt strongly at Fort Liard, Fort Simpson and Wrigley. Some people fled from buildings in Edmonton, Alberta, about 1100 km from the earthquake. The quake was felt in parts of the Yukon Territory, British Columbia, Alberta, Saskatchewan and Manitoba. It was also felt at Camas and Spokane, Washington; Grand Forks, North Dakota; Juneau, Alaska and Helena, Montana. This area was struck by a magnitude 6.6 earthquake on October 5, 1985, causing some minor damage at Wrigley and Fort Liard. Hundreds of earthquakes have occurred since the beginning of this series, some large enough to be felt.

Sicily

On December 25 an earthquake associated with the eruption of Mount Etna caused a resort hotel to collapse, killing one person and injuring 14. The magnitude 4.3 earthquake was centered in the Mount Etna area about 30 km north of Catania.

Illinois

A minor earthquake occurred in the southern part of this state on December 29 at 2:57 a.m. CST. This quake had a magnitude of 3.5 and was located about 25 km northwest of Mt. Vernon near Centralia. It was felt in the Centralia, Iuka, Salem areas.

PRELIMINARY LOCATIONS
November-December 1985

Date	Origin time UTC	Region	Coordinates		Depth km	Magnitudes
			Lat	Long		
Nov 5	01 28 00.4	Central Alaska	62.5 N	151.5 W	88	5.1mb
Nov 7	08 26 18.1	Turkey	40.4 N	42.4 E	10	5.1mb
Nov 9	11 38 18.5	Hebgen Lake region	44.7 N	111.1 W	51	4.8mb
Nov 9	11 40 22.5	Hebgen Lake region	44.8 N	111.1 W	5	4.1mb
Nov 9	11 58 49.5	Hebgen Lake region	44.7 N	111.1 W	5	4.0ML
Nov 9	13 09 15.2	Hebgen Lake region	44.7 N	111.1 W	5	4.2ML
Nov 14	22 17 44.6	South of Alaska	54.8 N	159.8 W	33	5.7MS
Nov 17	09 40 21.7	West Irian	1.6 S	135.0 E	13	7.1MS
Nov 24	19 21 39.7	Central California	36.0 N	120.9 W	8	4.4ML
Nov 26	09 34 40.5	Hebgen Lake region	44.6 N	111.0 W	5	4.4ML
Nov 28	02 25 42.3	Vanuatu Islands	14.1 S	166.2 E	33	7.0MS
Nov 28	03 49 53.9	Vanuatu Islands	14.0 S	166.2 E	33	7.1MS
Nov 28	15 13 57.2	Central California	36.6 N	121.1 W	10	4.5ML
Dec 4	06 37 51.3	Hebgen Lake region	44.7 N	111.0 W	5	4.2ML
Dec 5	22 59 40.1	Arkansas	35.9 N	90.0 W	5	3.9mbLg
Dec 12	19 01 22.0	Hawaii	21.0 N	155.8 W	33	4.3mb
Dec 12	21 18 39.3	Hawaii	19.5 N	155.9 W	12	4.0ML
Dec 13	23 20 57.4	Hawaii	19.3 N	155.1 W	9	4.0ML
Dec 14	12 39 18.0	Nicaragua	11.4 N	86.0 W	33	5.0mb
Dec 15	07 14 54.7	New Mexico	35.1 N	104.8 W	5	3.4mbLg
Dec 16	02 44 35.6	Nicaragua	11.7 N	85.9 W	21	6.0MS
Dec 21	01 13 21.0	Vanuatu Islands	14.0 S	166.5 E	33	7.3MS
Dec 23	05 16 03.9	Northwest Territories, Canada	62.2 N	124.3 W	10	6.9MS
Dec 25	02 38 57.0	Sicily	37.8 N	15.0 E	10	4.3mb
Dec 29	08 56 56.7	Southern Illinois	38.5 N	89.0 W	5	3.5mbLg
Dec 30	12 41 03.0	Southern Alaska	61.6 N	150.3 W	62	5.5mb
Dec 30	20 13 20.3	Central Alaska	63.6 N	151.3 W	33	5.1mb

U.S. ACTIVITY*
November-December 1985

Alaska	22	Nevada	1
Arkansas	1	New Mexico	1
California	10	Tennessee	1
Hawaii	11	Wyoming	1
Illinois	1	Total	54
Montana	5		

*Felt earthquakes as reported from many sources.

LIST OF EARTHQUAKES
Magnitude 7.0 or Greater, 1985

Date	Origin time UTC	Region	Coordinates		Depth km	Magnitudes
			Lat	Long		
Mar 3	22 47 06.9	Near coast of central Chile	33.16 S	71.98 W	33	7.8MS
Mar 3	23 38 31.4	Near coast of central Chile	32.74 S	71.22 W	33	7.1MS
Apr 9	01 56 59.4	Near coast of central Chile	34.13 S	71.62 W	38	7.5MS
May 10	15 35 50.5	New Britain region	5.60 S	151.05 E	27	7.1MS
Jun 3	12 06 21.1	Samoa Islands region	15.29 S	173.52 W	33	7.0MS
Jul 3	04 36 51.7	New Britain region	4.44 S	152.83 E	33	7.2MS
Aug 23	12 41 56.1	Southern Xinjiang, China	39.43 N	75.22 E	7	7.3MS
Sep 19	13 17 47.3	Michoacan, Mexico	18.19 N	102.53 W	28	8.1MS
Sep 21	01 37 13.4	Near coast of Guerrero, Mexico	17.80 N	101.65 W	33	7.6MS
Sep 26	07 27 51.1	South of Kermadec Islands	34.69 S	178.66 W	33	7.5MS
Nov 17	09 40 21.7	West Irian region	1.59 S	135.01 E	13	7.1MS
Nov 28	02 25 42.3	Vanuatu Islands	14.01 S	166.24 E	33	7.0MS
Nov 28	03 49 53.9	Vanuatu Islands	13.95 S	166.17 E	33	7.1MS
Dec 21	01 13 21.0	Vanuatu Islands	14.04 S	166.51 E	33	7.3MS

U.S. GOVERNMENT PRINTING OFFICE
PUBLIC DOCUMENTS DEPARTMENT
WASHINGTON, D.C. 20402

OFFICIAL BUSINESS
PENALTY FOR PRIVATE USE $300

BULK RATE MAIL
POSTAGE & FEES PAID
USGS
PERMIT No. G23

Earthquakes & Volcanoes

Volume 18, Number 5, 1986

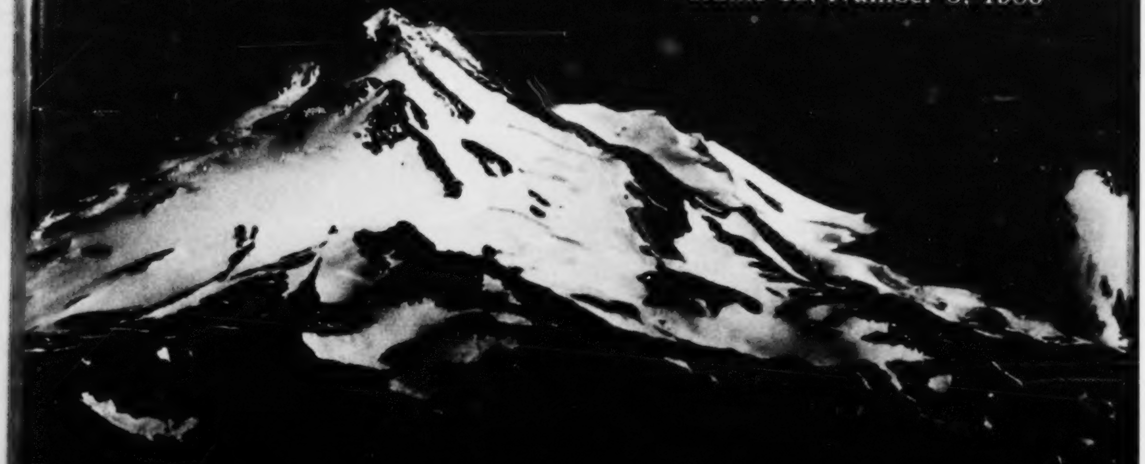

I 19.65:

UNITED STATES DEPARTMENT OF THE INTERIOR
Donald Paul Hodel, Secretary

U.S. GEOLOGICAL SURVEY
Dallas, L. Peck, Director

Earthquakes and Volcanoes is published bimonthly by the U.S. Geological Survey to provide current information on earthquakes and seismology, volcanoes, and related natural hazards of interest to both generalized and specialized readers.

The Secretary of the Interior has determined that the publication of this periodical is necessary in the transaction of the public business required by law of this Department. Use of funds for printing this periodical has been approved by the Office of Management and Budget through June 30, 1989.

Henry Spall—Editor

Earthquakes and Volcanoes
U.S. Geological Survey
904 Nationa Center
Reston, Virginia 22092
Telephone (703) 648-6078

Jill K. Moebus—Graphics Design

Subscription orders should be sent to:

Superintendent of Documents
U.S. Government Printing Office
Washington, DC 20402
Telephone (202) 783-3238

For sale by the Superintendent of Documents. Annual subscription rates—$15.00 (domestic) and $18.75 (foreign). Make check or money order payable to the Superintendent of Documents.

Single copy rate—$3.00 (domestic) and $3.75 (foreign). Single copy rate for issues prior to Volume 15, Number 1—$2.25 (domestic) and $2.85 (foreign). Can be purchased from the Book and Open-File Reports Section, U.S. Geological Survey, Federal Center, Building 41, Box 25425, Denver, CO 80225 (make check or money order payable to the Superintendent of Documents).

Earthquakes & Volcanoes

(formerly *Earthquake Information Bulletin*)
Volume 18, Number 5, 1986

NEWARK PUBLIC LIBRARY
JUN 23 1987
U.S. GOVT. PUBS
DEPOSITORY 376

Reports from the U.S. Geological Survey's Cascades Volcano Observatory at Vancouver, Washington

184 **Tree-ring dating of volcanic deposits**
by Steven Brantley, David Yamaguchi, Kenneth Cameron and Patrick Pringle

195 **Volcanic debris avalanches**
by Steven Brantley and Harry Glicken

207 **Two dome-building episodes at Mount St. Helens in 1984 and 1985 and the accompanying seismicity**
by Steven Brantley

218 **About the authors**

Tree-Ring Dating of Volcanic Deposits

*Steven Brantley, David Yamaguchi,
Kenneth Cameron, and Patrick Pringle*

Introduction

The best guide available to geologists for identifying volcanic hazards and for forecasting future eruptions is the eruptive history of a volcano. By applying a fundamental concept of geology in reverse—the past is a key to the present and future—geologists estimate the types and magnitudes of potential eruptions from a volcano based on the rocks and deposits preserved in its geologic record. The areal extents of different types of deposits around a volcano—deposits of debris avalanches, pyroclastic flows, lava flows, lahars ("mudflows"), and tephra ("ash") falls—delineate areas likely to be affected by future volcanic activity. The frequency of past activity can also be inferred by determining when various deposits were emplaced. Ages of deposits may reveal a pattern of recurrence useful for forecasting future activity. Not all deposits are preserved or recognized in the geologic record, however, so the apparent frequency of past eruptions is a minimum frequency.

The ages of recent but prehistoric deposits are commonly determined by radiocarbon dating. The uncertainty of individual radiocarbon dates may be large, however, especially relative to the ages of young deposits. For example, a radiocarbon date of 10,000 years may have an error range of 150 to 300 years; a radiocarbon date of 300 years commonly has the same uncertainty. Additional ambiguity arises in calibrating carbon-14 ages with calendar years. Therefore, it is impossible, using radiocarbon dating, to determine the specific year or years of recent activity.

A more precise method of dating volcanic deposits of recent age is to identify anomalous growth patterns among the annual rings of trees growing at the time the deposits were emplaced. Trees that were injured but not killed by tephra or lahars may show a sequence of narrow rings beginning at the time of impact. "Cross-dating," the matching of ring-width variation patterns in one tree with corresponding ring patterns in another, should be used to ensure that dating errors are not introduced by missing rings (see section on cross-dating below). A minimum age can also be determined for deposits from the ages of new trees growing on them. Such minimum ages are approximate because they do not account for the period of time required for trees to colonize newly emplaced deposits. Depending on the tree species, climate, and type of deposit, tree establishment might take 1 to 20 years. In some cases, the ring patterns of buried dead trees can be cross-dated with those of living trees. In this manner, deposits responsible for killing the trees can be dated exactly. Tree-ring dating is helping to determine the ages of deposits and eruptive frequencies of several volcanoes in the Cascade Range.

Cross-dating

Among the effects on pine trees of the 1943-52 eruptions of Paricutin Volcano, Mexico, was the absence of some annual growth rings. Willis Eggler, a geologist at Dartmouth College, cut cross sections from several pines near Paricutin and found that one to three rings were missing along selected radii in several disks. This showed that although annual rings are formed every growing season, rings may not form completely along all radii in years of limited growth. If a core is collected from a tree where one or more rings are missing, the age of the tree or the dates of volcanically induced narrow ring sequences will be inaccurate. Missing rings can be detected by "cross-dating," or matching, the ring-width variation patterns of sampled trees with the ring patterns of other trees growing nearby (Stokes and Smiley, 1968; Fritts, 1976). Cross-dating is possible in most of North America for several reasons:

(1) Total seasonal growth of a tree is the result of many interacting factors—tree species and site conditions such as slope, aspect, soil, and climate—but climatic factors typically dominate in limiting growth.
(2) Rainfall and daily temperatures vary from year to year.
(3) Climatic fluctuations limit tree growth similarly over large geographical areas.

Throughout much of North America, annual tree growth is limited by low precipitation; in Alaska it is limited by cold temperatures. Though ring-width variation patterns will be similar from tree to tree, the actual widths of rings in different trees will vary.

The ring-width variation patterns of different trees will match year for year up to the point where rings are missing in some trees because of volcanic activity or drought. Beyond this point, ring counts will be one or more years off unless corrections are made by "inserting hypothetical rings" at the proper places until ring-width patterns again match those of control trees. Because of the possible occurrence of missing rings, tree samples should be cross-dated rather than dated by ring counting.

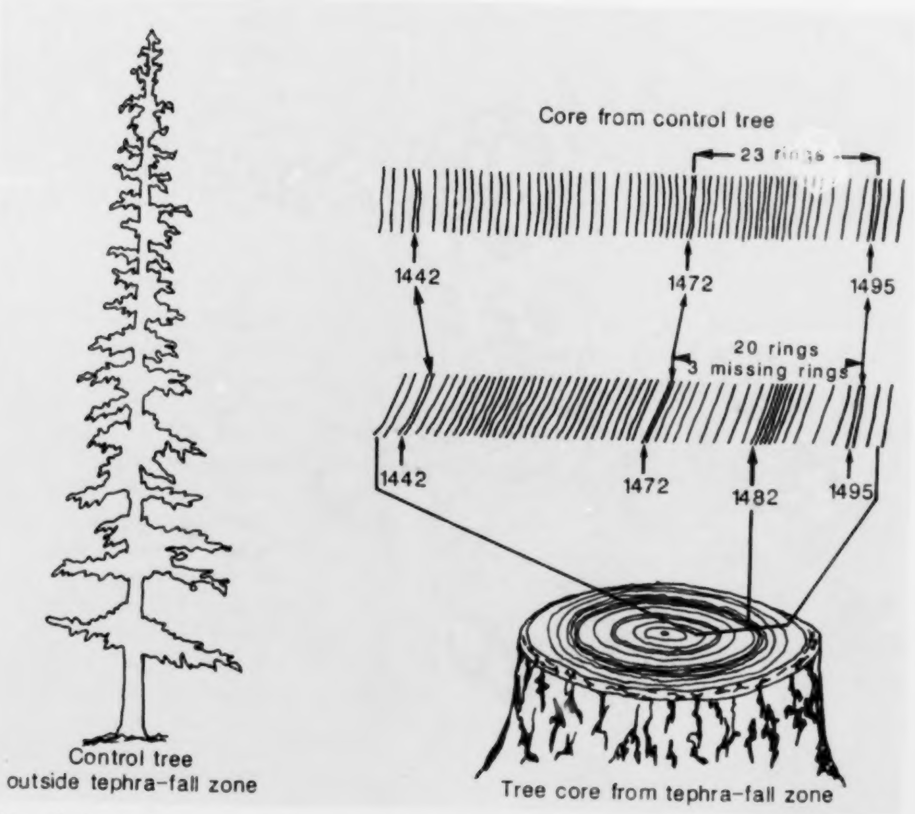
Core from control tree
23 rings
1442
1472
1495
20 rings
3 missing rings
1442
1472
1482
1495
Control tree
outside tephra-fall zone
Tree core from tephra-fall zone

Cross-dating with narrow rings can often identify missing rings. Control tree shows 23 annual rings between the 1472 and 1495 narrow rings, while the tree in the We tephra-fall zone shows only 20 rings. The series of missing and narrow rings starting with the 1482 ring were caused by tree injury during fallout of layer We. Because of possible missing rings, dates of past volcanic events cannot be determined unequivocably by counting back to a series of narrow rings.

Mount St. Helens

Stratigraphic studies at Mount St. Helens, Washington, have identified many sets of tephra layers erupted from this volcano (Mullineaux, 1986). The layers range widely in thickness, age, and distribution. Tephras emplaced during the past 700 years are well suited for tree-ring dating because they fall within the life spans of Douglas-fir trees growing near the volcano. Douglas-fir are ideal for dating tephra fallout because the widths of their annual rings reflect environmental changes, and are also sensitive to year-to-year climatic variation, a feature central to cross-dating.

Cross-dating was recently used to precisely date three thick pumiceous tephra layers erupted from Mount St. Helens within the life spans of living trees (Yamaguchi, 1983, 1985). These layers are named layers Wn, We, and T. The approximate ages of these tephras were previously known from tree-ring counting and radiocarbon dating, but age estimates ranged widely. In the late 1930s botanist Donald Lawrence recognized that trees on the south shore of Spirit Lake were rooted beneath the thick blanket of pumice now known as layer T. His cores from these trees revealed anomalous narrow growth rings. By counting the number of annual rings back to the narrow rings, Lawrence identified 1802 as a tentative date for fallout of the pumice. In the 1970s, U.S. Geological Survey geologist Dwight Crandell recognized that layer Wn

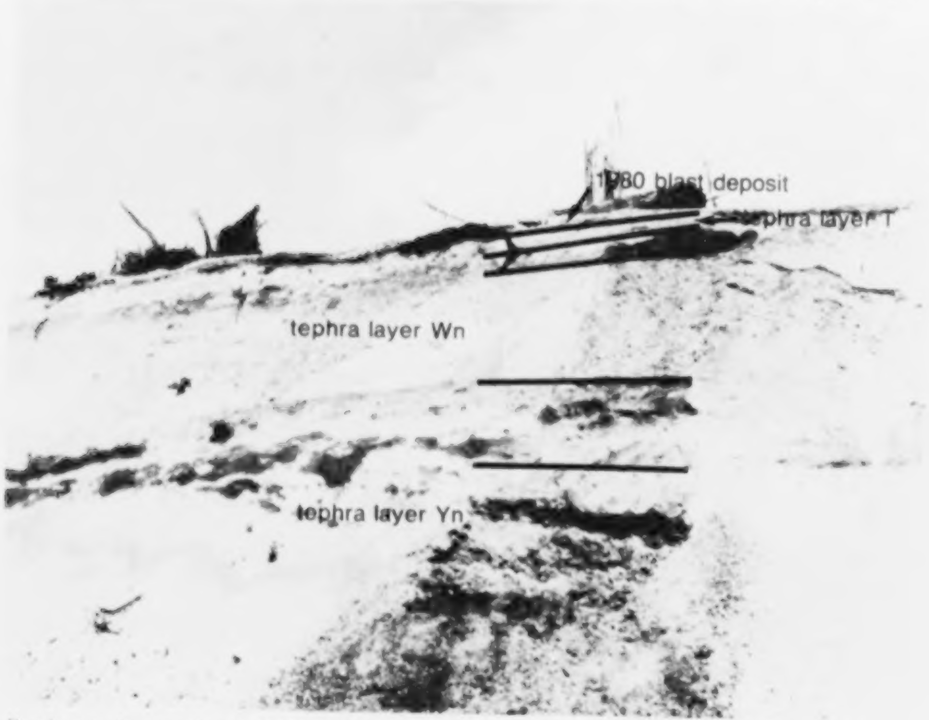

Roadcut 10 km northeast of Mount St. Helens showing some of the tephra layers erupted by this volcano during the past 4,000 years. Layers Wn and T are shown; layer We occurs south of this site. Note how thin the 1980 deposit is relative to older tephra layers. Layer Yn is about 3,800 years old; tephras between layers Wn and Yn are 1,100-3,700 years old.

Map showing the distributions of tephra layers Wn, We, and T near Mount St. Helens. Sampling locations of tree cores shown in a later figure are marked. (Modified from an illustration by David Yamaguchi in Geology, vol. 13, p. 554.)

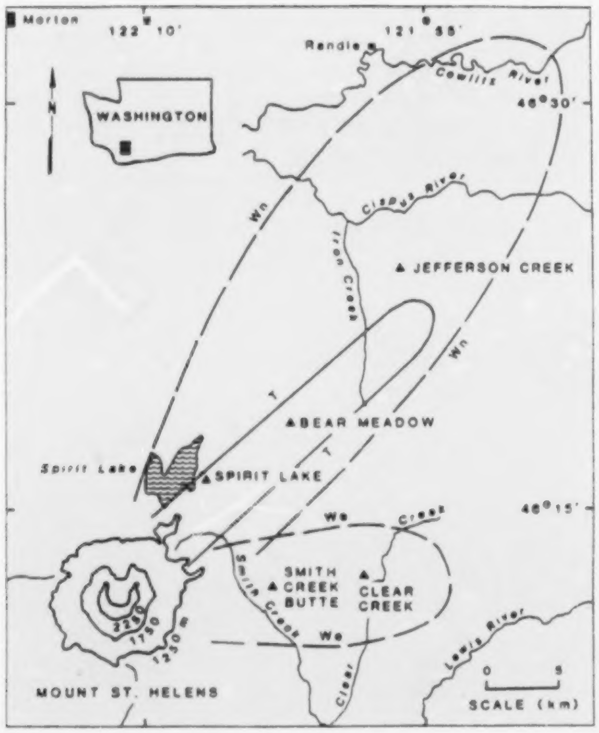
Morton
122°10'
121°55'
Randle
Cowlitz River
46°30'
WASHINGTON
N
Wn
Cispus River
Iron Creek
JEFFERSON CREEK
Wn
T
BEAR MEADOW
T
Spirit Lake
SPIRIT LAKE
We
Creek
46°15'
SMITH CREEK BUTTE
CLEAR CREEK
Smith Creek
2250
1750
1250 m
We
Clear
Lewis River
MOUNT ST. HELENS
0
5
SCALE (km)

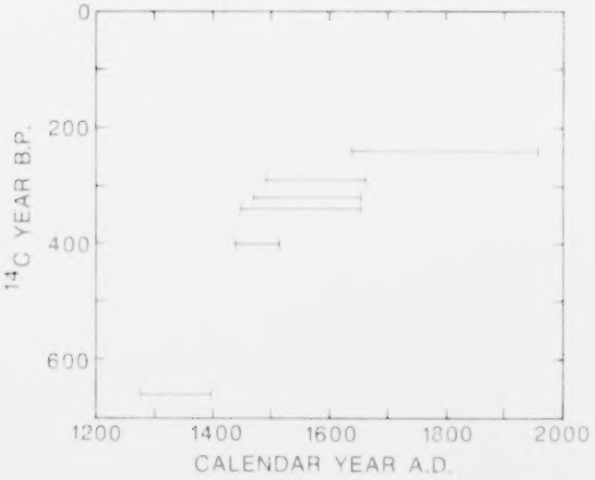

Graph showing the wide range in ages in tephra layers Wn and We suggested by radiocarbon dating.

was at least 435 years old because trees of that age were growing on top of deposits laid down after the Wn pumice at Mount Rainier, 80 km downwind of Mount St. Helens. Crandell and his colleague, Donal Mullineaux, also determined that layer We was slightly younger than layer Wn on the basis of field evidence.

Collecting a core from a tree in the fallout zone of the layer T tephra. Trees at this site were blown down by Mount St. Helens' May 18, 1980, eruption. Photograph by David Yamaguchi, 1981.

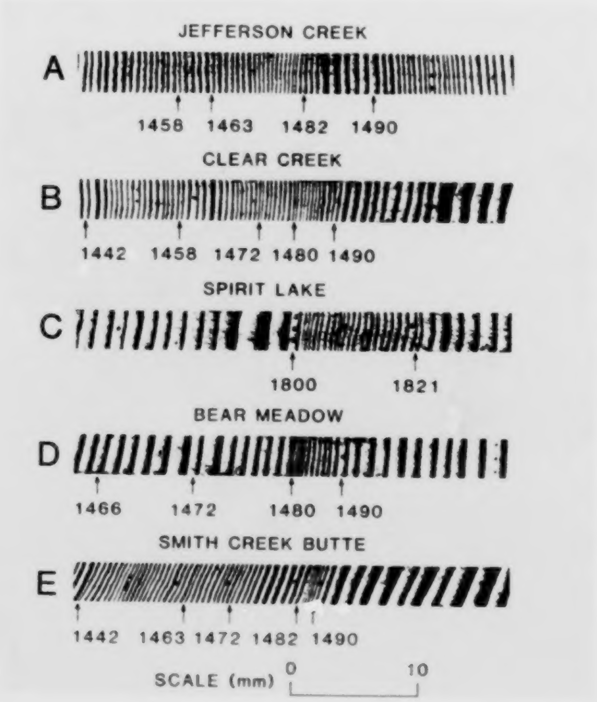
JEFFERSON CREEK
A
1458 1463 1482 1490
CLEAR CREEK
B
1442 1458 1472 1480 1490
SPIRIT LAKE
C
1800 1821
BEAR MEADOW
D
1466 1472 1480 1490
SMITH CREEK BUTTE
E
1442 1463 1472 1482 1490
SCALE (mm) 0 10

Cores from Douglas-fir near Mount St. Helens; sampling locations are shown in an earlier figure. Bark lies toward the right in all cores. Single dots on cores denote decades; triple dots denote centuries. A & B: ring patterns at indicated sites. Note narrow 1442, 1458, 1472 and 1480 cross-dating rings. C: Narrow-ring pattern beginning with the 1800 ring from a tree in the area affected by tephra T. D: Narrow-ring pattern beginning with the 1480 ring from a tree affected by tephra Wn. E: Narrow- and missing-ring pattern starting with the 1482 ring from a tree affected by tephra We. (Modified from a figure by David Yamaguchi in Geology, vol. 13, p. 555.)

No precise estimates of the dates of eruption of these W pumice layers or the length of time separating them were known, however.

Cores were then collected from old Douglas-fir along the axes of the layer Wn, layer We, and layer T tephra deposits and at control sites beyond the limit of the tephra falls. Marker rings, narrow rings or rings with light-colored wood present in all cores, were used in cross-dating. Such studies clearly identified the 1800 annual ring as the first ring of the narrow-ring pattern among trees affected by the T tephra; this date is two years earlier than initially estimated by Lawrence. The same method also identified narrow- and missing-ring sequences that started forming in 1480 and 1482 in response to the fallout of tephra layers Wn and We, respectively. The intensity and duration of these three anomalous ring patterns decrease rapidly with distance from the volcano. Such strong gradients in tree-ring patterns cannot be attributed to factors such as climate or an insect outbreak.

The 1480 and 1482 tree-ring dates are important because they provide evidence that two large prehistoric explosive eruptions of Mount St. Helens occurred about 2 years apart. This finding provides evidence from the geologic record that Mount St. Helens is capable of producing several large explosive eruptions closely spaced in time.

Mount Hood, Oregon

Old Maid Flat, a broad flat area along the Sandy River 10 to 15 km downstream from the summit of Mount Hood, Oregon, is covered by a thick carpet of mosses and lichens, rhododendron, huckleberry, and sparse stands of lodgepole pine and Douglas-fir. This forest "carpet" overlies a lahar deposit 1 to 6 m thick. Correlative deposits can be traced 90 km downstream to the Columbia River. Radiocarbon dates from wood and charcoal in the deposit show it is less than about 300 years old. A recent study using the journal of Lt. Broughton of the Vancouver Expedition, the journals of Lewis and Clark, and tree-ring dating suggests this lahar was emplaced in the early 1790s (Cameron and Pringle, 1986).

Historical Accounts

The earliest written account of the exploration of the area, the journal of Lt. Broughton, describes a journey up the Columbia River in October 1792 at least as far as the mouth of the Sandy ("Baring") River. Broughton observed logs stranded 4 m above the water level at the mouth of the Sandy, and an unusual submerged bar

Aerial view of Mount Hood, Oregon, and Old Maid Flat; view is looking east. Note standing snags in Muddy Fork drainage that were drowned by an ephemeral lake that formed behind the Old Maid lahar deposit. The lahar originated on the volcano and flowed down the Sandy River at least 30 km. Correlative deposits occur 90 km downstream near the Columbia River. Photograph by Austin Post, 1980.

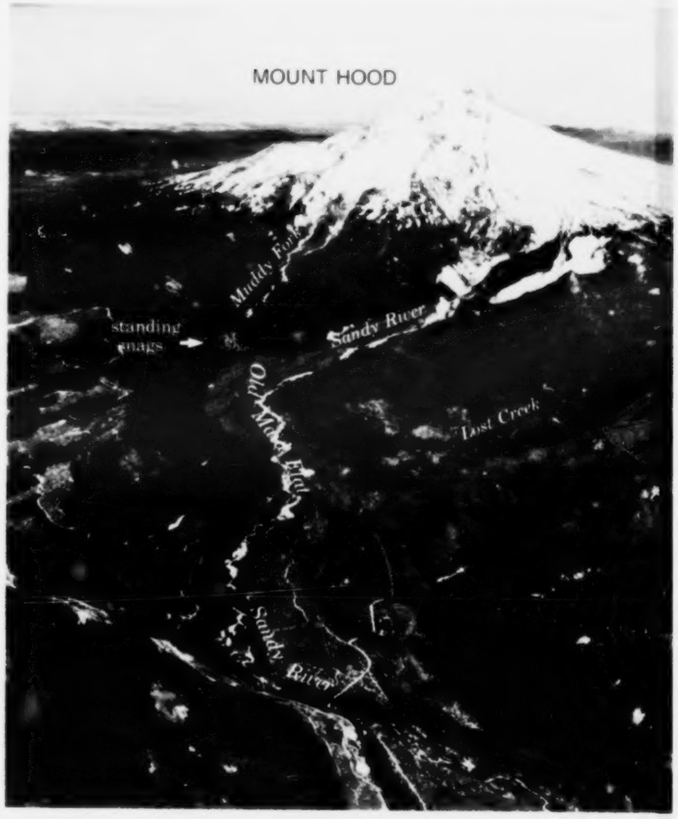
MOUNT HOOD
Muddy Fork
standing snags
Sandy River
Old Maid Flat
Lost Creek
Sandy River

Map of Mount Hood and the Sandy River showing Old Maid Flat and the path of the lahar down the Sandy to the Columbia River. In 1805 and 1806, Lewis and Clark described the Sandy as a sediment-laden stream, and thus named it "Quicksand River."

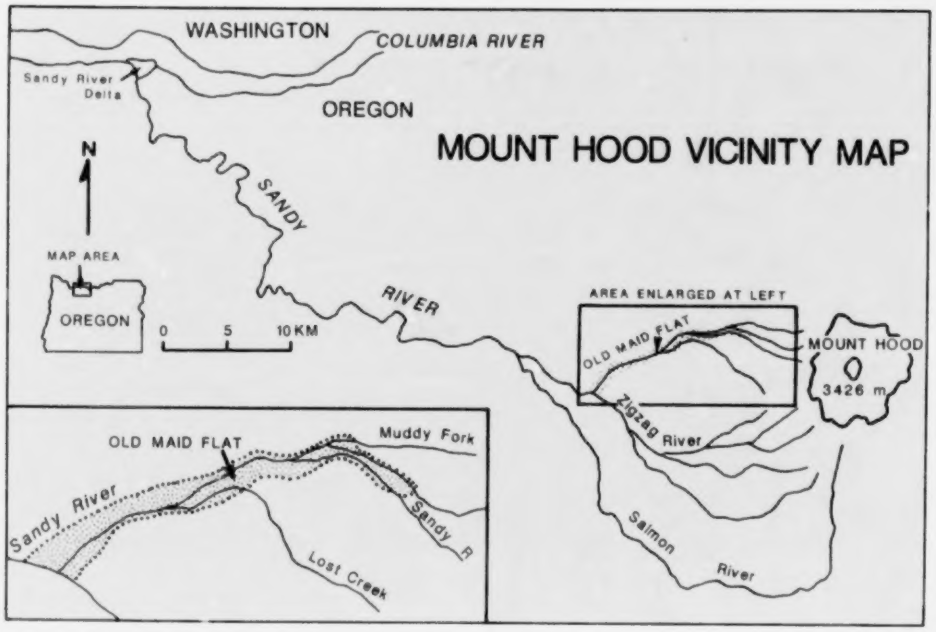
WASHINGTON
COLUMBIA RIVER
Sandy River Delta
OREGON
MOUNT HOOD VICINITY MAP
N
SANDY
RIVER
MAP AREA
OREGON
0
5
10 KM
AREA ENLARGED AT LEFT
OLD MAID FLAT
MOUNT HOOD
3426 m
Zigzag River
Salmon River
OLD MAID FLAT
Muddy Fork
Sandy River
Sandy R
Lost Creek

Core from a surviving western redcedar along the margin of Old Maid Flat; bark is toward the right. Note narrow sequence of rings starting near the 1794 ring. Core has not been cross-dated so this date is provisional.

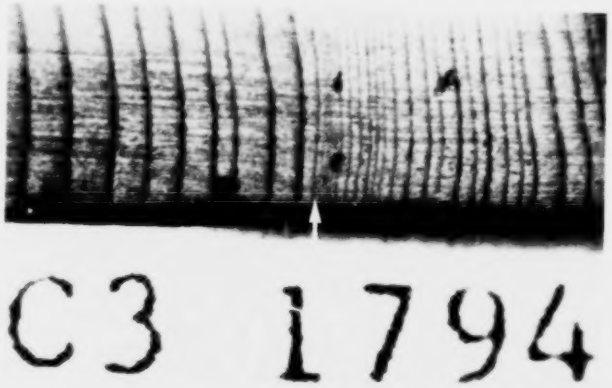

that extended from the Sandy across the Columbia River.

In 1805 and 1806, Lewis and Clark explored a tributary of the Columbia River that they named Quicksand River, but was later renamed the Sandy River. Clark described the mouth of the river in his journal, reproduced here with its original spelling:

"November 3rd Sunday 1805
... I arrived at the enterance of a river which appeared to scatter over a Sand bar, the bottom of which I could See quit across and did not appear to be 4 Inches deep in any part; I attempted to wade this Stream and to my astonishment found the bottom a quick Sand, and impassable. I called to the Canoes to put to Shore.... & Capt. Lewis and my Self walked up this river about 1-1/2 mile to examine this river which we found to be verry considerable Stream Dischargeing its waters through 2 chanels which forms an Island of about 3 miles in length on the river and 1-1/2 miles wide, composed of corse sand which is thrown out of this quick sand river compressing the waters of the Columbia and throwing the whole current of its waters against its Northern banks... This Stream has much the appearance of the River Platt. roleing its quick sands into the bottoms with great velocity after which it is divided into 2 chanels by a large sand bar before mentioned, the narrowest part of this River is 120 yards...

"Tuesday April 1st 1806
This morning early we dispatched Sergt. Pryor, with two men in a small canoe up quick sand river with orders to proceed as far as he could and return this evening.... Sergt. Pryor returned in the evening and reported that he had assendd. the river six miles; that above the point which it divides itself into two chanels, it is about 300 yards wide tho' the chanel is not more than 50 yards, and only 6 feet deep. the other part of

the river from 2 to 4 inches water. the bead of this river is formed entirely of quick sand; its banks are low and at present overflown. the water is turbed and current rapid...."

These descriptions of the Sandy River are strikingly similar to the present appearance of the sediment-laden Toutle River, Washington, which was impacted by lahars from the May 18, 1980, eruption of Mount St. Helens. The Sandy now has a deep, narrow, boulder-strewn channel devoid of quicksand and rarely overflows its banks. The island Clark described was the Sandy River delta; it is still present but is now covered by vegetation.

Tree-ring Dating

Remnants of trees buried by the lahar at Old Maid Flat show that a mature forest of western redcedar and Douglas-fir once stood on the floor of the Sandy River valley. Cedar snags, highly resistant to decay, still stand today as tall as 30 m above the lahar surface. Abrasion marks from the lahar are still visible on their upstream sides. Douglas-fir buried upright by the lahar have largely rotted away leaving vertical tree wells as much as 6 m deep and 2 m wide. A few cedar and Douglas-fir along the margins of the deposit, however, were not killed by the lahar and are living today. Cores from these trees reveal the abrupt onset of narrow rings in the early 1790s. The extreme uniformity and thinness of the rings and the possibility of missing rings prevented a precise date from being determined.

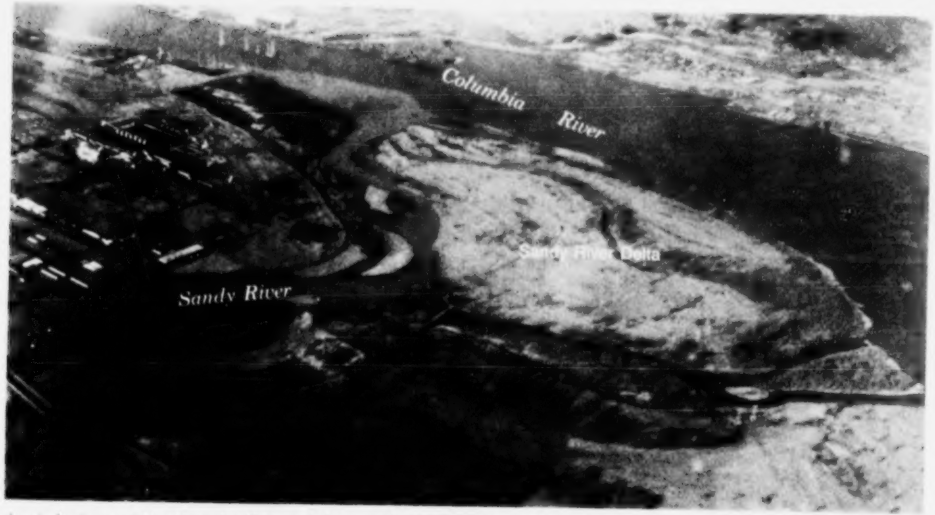

Aerial view of the Sandy River delta at the Columbia River. Photograph by Kenneth Cameron, 1984.

However, the oldest known tree growing on the flats, determined by ring counting, was at least 173 years old in 1984. Assuming one to two decades elapsed before this tree colonized the Old Maid lahar deposit, the lahar probably occurred between 1791 and 1801. This age for the Old Maid lahar inferred from tree-ring data suggests that if Lewis and Clark or possibly Broughton had journeyed west a few years earlier, they might have witnessed Mount Hood in eruption.

Conclusion

These examples illustrate how tree rings can be used to date young volcanic deposits. Tree-ring methods have similarly been employed to estimate the frequency of debris flows on the flanks of Mount Shasta, California (Hupp, 1984), and determine minimum ages for tephras erupted from volcanic vents in central eastern California (Miller, 1985). By faithfully recording the passage of time and yearly fluctuations in climate, tree rings record years in which tree growth was temporarily slowed or stopped by volcanic activity.

References cited

Cameron, K. A. and Pringle, P., 1986, Post-glacial lahars of the Sandy River basin, Mount Hood, Oregon: Northwest Science, v. 60, p. 225-237.

Eggler, W. A., 1967, Influence of volcanic eruptions on xylem growth patterns: Ecology, v. 48, p. 644-647.

Fritts, H. C., 1976, Tree rings and climate: Academic Press, New York, 567 p.

Hupp, C. R., 1984, Dendrogeomorphic evidence of debris flow frequency and magnitude at Mount Shasta, California: Environmental Geology and Water Sciences, v. 6, p. 121-128.

Lawrence, D. B., 1939, Continuing research on the flora of Mount St. Helens: Mazama, v. 21, no. 12, p. 49-54.

Miller, C. D., 1985, Holocene eruptions at the Inyo volcanic chain, California: implications for possible eruptions in Long Valley caldera: Geology, v. 13, p. 14-17.

Mullineaux, D. R., 1986, Summary of pre-1980 tephra-fall deposits erupted from Mount St. Helens, Washington State, U.S.A.: Bulletin of Volcanology, v. 48, p. 17-26.

Stokes, M. A., and Smiley, T.L., 1968, An introduction to tree-ring dating: University of Chicago Press, Chicago, 73 p.

Yamaguchi, D. K., 1983, New tree-ring dates for recent eruptions of Mount St. Helens: Quaternary Research, v. 20, p. 246-250.

Yamaguchi, D.K., 1985, Tree-ring evidence for a two-year interval between recent prehistoric explosive eruptions of Mount St. Helens: Geology, v. 13, p. 554-557.

Volcanic Debris Avalanches

Steven Brantley and Harry Glicken

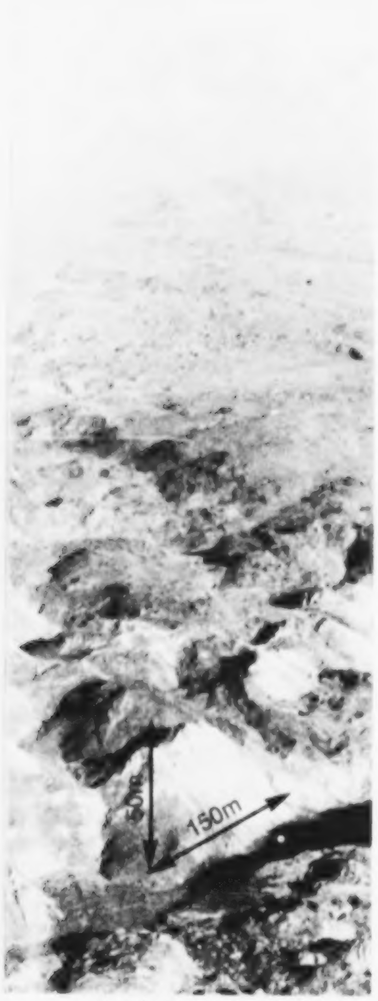

Aerial view of hummocky debris-avalanche deposit filling North Fork Toutle River valley; Mount St. Helens in distance. The avalanche deposit covers the valley floor to an average depth of 45 m for 25 km; it is as thick as 180 m in some places. Note size of hummock in foreground. Photo by Harry Glicken, 1980.

As Mount St. Helens illustrated so dramatically on May 18, 1980, debris avalanches from volcanoes pose significant hazards to people and property. Debris avalanches may occur without warning, move great distances at high speed, cover large areas, initiate lateral blasts, and, if they enter the sea, cause tsunamis. The May 18 eruption was the first time eyewitness accounts and photographs documented the emplacement of a large volcanic debris avalanche. The debris-avalanche deposit at Mount St. Helens has provided a basis for interpretation of similar deposits elsewhere and has led to the realization that large-scale gravitational slope failures of volcanoes are more common than previously thought. Since 1980, volcanic hazard assessments have included consideration of hazards posed by debris avalanches in addition to other, more common products of eruptions, such as pyroclastic flows, lahars, lava flows, and tephra.

More than 150 Quaternary debris-avalanche deposits have been identified in recent studies by Lee Siebert of the Smithsonian Institution in Washington, D.C., on the basis of geologic literature, topographic maps, and aerial photographs. Siebert's compilation shows that 17 volcanic debris avalanches are known or inferred to have formed in the last 400 years, about 4 per century. This rate is several times the historic rate for eruptions producing Krakatau-type calderas, one of the most hazardous types of explosive eruptions. Siebert also notes that debris avalanches occurring on volcanoes near the ocean may produce tsunamis by entering the sea; in historic times three debris avalanches and associated tsunamis have claimed about 17,000 lives. These observations underscore the importance of including debris avalanches in volcanic hazard studies.

Mount St. Helens rockslide-debris avalanche deposit

The debris-avalanche deposit at Mount St. Helens covers about 60 square km of the North Fork Toutle River valley with about 2.5 cubic km of unconsolidated rock debris. For a distance of 25 km the deposit fills the valley to an average depth of 45 m but is locally as deep as 180 m. The most conspicuous feature of the deposit is its hummocky chaotic surface morphology. Levees as high as 30 m occur along the margins of the deposit against valley walls. Individual hummocks and ridges as high as 70 m are separated by low-lying areas and closed depressions, many of which form ponds.

The deposit contains a wide range of debris reflecting the variation in volcanic material of the cone from which it was derived. The debris includes pieces of lava flows and domes and the deposits of lahars and pyroclastic flows. Individual rock fragments range from clay-sized particles to boulders several meters in diameter. The deposit is divided into block facies (unmixed) and matrix facies (mixed). The block facies, which make up most of the deposit, consist of pieces of the old Mount St. Helens that were shattered during the initial rockslide and blast, but were not disaggregated. Some of these debris- avalanche blocks are several thousand cubic meters in volume. They were transported gently in the debris avalanche and deposited relatively intact. Some of the original stratigraphy of lava flows and volcanic dikes in the old mountain is preserved in debris-avalanche blocks, yet most of the large clasts in the lava flows and dikes were thoroughly shattered. The matrix facies consist of all rock types from the old Mount St. Helens, as well as juvenile material from the May 18, 1980, eruption, blended together. Then matrix facies was produced by mixing

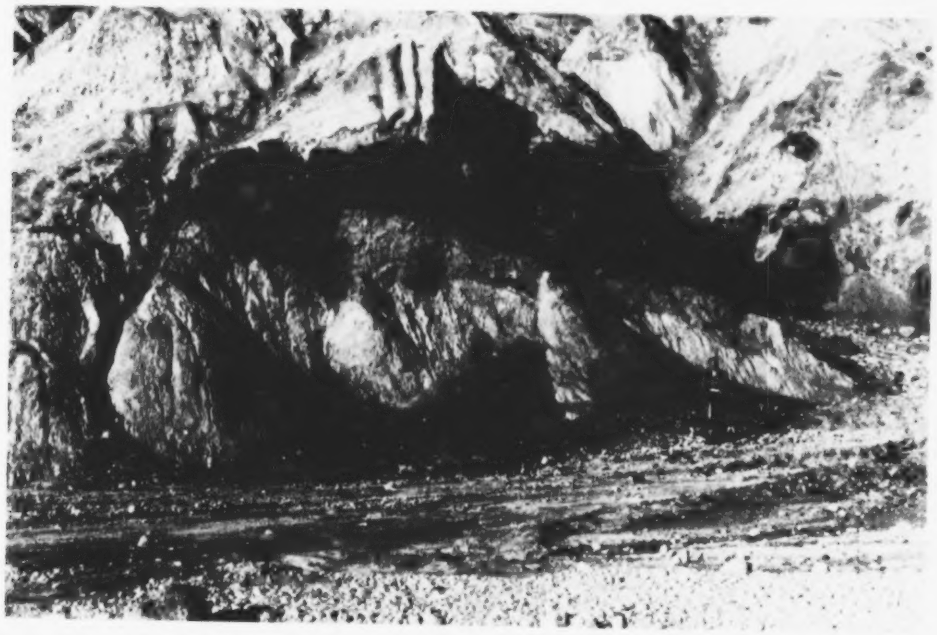

Exposure of Mount St. Helens debris-avalanche hummock showing layers of lava flows and pyroclastic debris that were transported nearly undisturbed about 6 km. Note person for scale. Photo by Harry Glicken, 1982.

Geologists discuss characteristics of debris avalanche deposit during field trip at Mount St. Helens. Field trip was organized by Cascades Volcano Observatory and International Association of Volcanology and Chemistry of the Earth's Interior (IAVCEI) to discuss mechanisms of catastrophic eruptions like the May 18, 1980, event. Photo by Steven Brantley, 1984.

of material during the explosions of the blast as well as from disaggregation and mining of debris-avalanche blocks during transport.

Other volcanic avalanche deposits

The 1980 debris avalanche deposit at Mount St. Helens has enabled geologists to reinterpret the origin of similar deposits around other steep-sided stratovolcanoes of the Pacific Rim. Previously, these deposits were generally referred to as erosional remnants of ancient volcanic terrains, lahars, pyroclastic flow deposits, or manmade. A few of these are presented here.

Mount Shasta

For more than a century, hundreds of mounds, hills, and ridges of volcanic rocks in Shasta valley, north-central California, had puzzled geologists. In a guidebook of the Western United States, geologist John Diller wrote in 1915 that the hummocks were "in part at least, the products of minor and local eruptions that broke through the Cretaceous beds, each vent contributing its little pile of material." Subsequent interpretations suggested that the hillocks were moraine deposits left by a glacier, or small bodies of magma that had risen from a sill intruded beneath Shasta valley, or erosional remnants of old volcanic rocks of the Western Cascades. Comparison with the Mount St. Helens debris-avalanche deposit, however, clearly establishes that the hills are part of a giant debris-avalanche deposit derived from a volcano ancestral to Mount Shasta, according to a recent report by U.S. Geological Survey geologists Rocky Crandell, C. Dan Miller, Harry Glicken, Christopher Newhall, and Robert Christiansen.

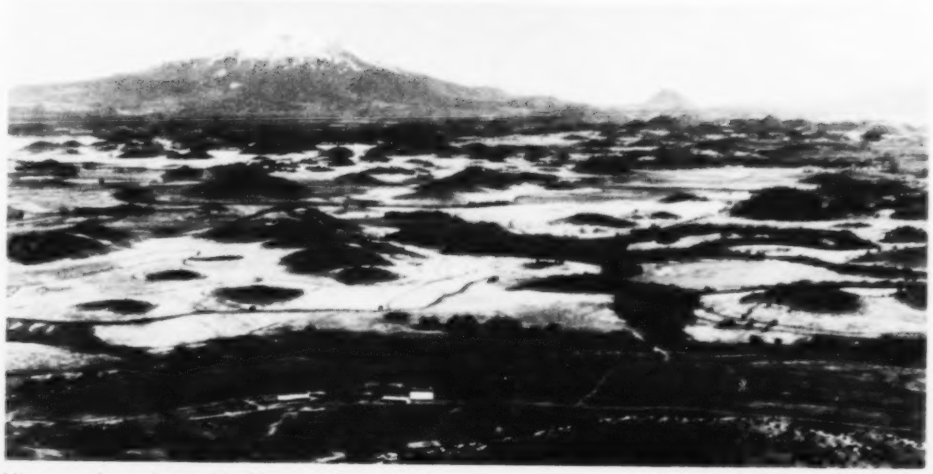

View southward towards Mount Shasta Volcano across hummocky topography. Early geologists interpreted the hummocks as small, eroded remnants of an ancient volcanic terrain, as moraine deposits left by a glacier or as small bodies of magma that had risen to just beneath the valley floor. Comparison with the debris avalanche deposit at Mount St. Helens, however, reveals that the hummocks are fragmented pieces of a former Mount Shasta that form a gigantic debris-avalanche deposit. The deposit is estimated to be about 10 times larger than the deposit at Mount St. Helens. Photo by C. Dan Miller, 1982.

In addition to similarities in surface morphology, the internal structure of both deposits is similar—the Mount Shasta deposit also consists of block facies and matrix facies. The block facies form hummocks and include individual debris-avalanche blocks ranging in size from tens to hundreds of meters in maximum dimension. Such blocks consist of a single rock type or layers of airfall tephra, pyroclastic flows, lahars, and pieces of soil. These blocks formed part of the former volcanic cone. The debris-avalanche blocks are generally not as shattered as in the Mount St. Helens deposit. Surrounding these debris-avalanche blocks, sometimes forming dikes that penetrate narrow cracks and joints in the blocks, is a mixture of clasts that range in size from microns to meters in diameter—the matrix facies. Most of the largest clasts in the matrix facies are andesitic rocks, similar to rocks that make up the present Mount Shasta volcano. Other clasts include sedimentary and metamorphic rocks, and rocks derived from alluvial and lake sediments incorporated by the avalanche as it traversed the floor of Shasta Valley. Fossils of lacustrine organisms are also found in the matrix facies at several localities.

The Mount Shasta debris-avalanche deposit covers an area of at least 450 square km with about 26 cubic km of debris—roughly 10 times the volume of the 1980 Mount St. Helens avalanche deposit. Radiometric ages of rocks in the deposit and of a post-avalanche basalt flow indicate that the avalanche occurred between about 300,000 and 360,000 years ago.

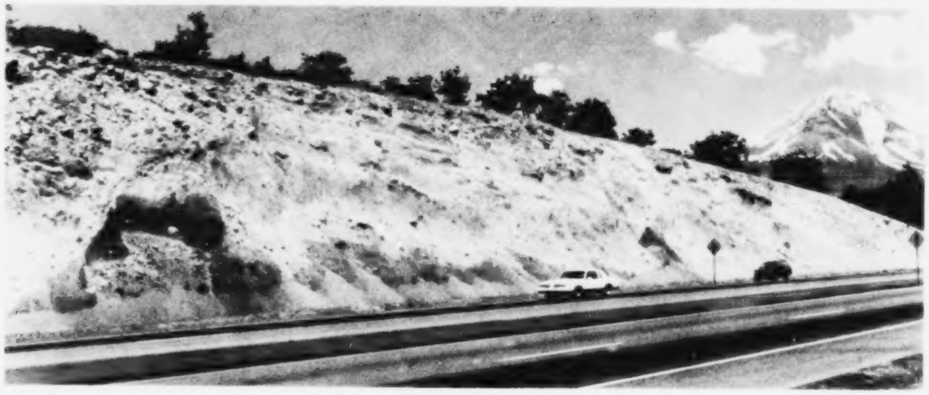

Road-cut through hummock of debris avalanche along Interstate 5 highway, Mount Shasta about 12 km distant. These layered pyroclastic flow deposits were moved intact from the volcano; individual layers are discontinuous and are offset by many small faults that probably formed during rapid transport as well as settling of the fragmented material after deposition. Photo by Steven Brantley, 1986.

Galunggung Volcano, Indonesia

On the southeast slope of Galunggung Volcano on the densely populated island of Java, a hummocky deposit called the "Ten Thousand Hills of Tasik Malaja" drew the attention of European geologists in the early part of the 20th century. Dutch geologist B.G. Escher hypothesized that a breakout of a crater lake resulted in a watery landslide that formed the deposit. The hummocks were likely material left behind as the more watery parts of the slide flowed away. Austrian geologist F.X. Schaffer suggested that the hummocks might be manmade; as the local people cleared the land to make ricefields, they made dumps of the boulders and cobbles that they found. The dumps became hummocks, and were used as sites for homes and fruit trees, as they offered protections from hostile people as well as from the mosquitoes and rats of the rice fields. Schaffer noted that the volume of material might seem large for "occidentals but it is not beyond the powers of the numerous and industrious Malays."

The horseshoe shape of Galunggung's crater and the nature of the hummocks, however, suggest a different cause for the formation of the Ten Thousand Hills. Since 1980, geologists from the Volcanological Survey of Indonesia and the U.S. Geological Survey have reinterpreted the deposit as a debris-avalanche deposit. Quarry exposures show pieces of the old volcano—the block facies—shattered but intact, that are similar to the deposits at Mount St. Helens and Mount Shasta. Radiocarbon dates of a lava flow within the deposit show that the debris avalanche is less than 23,000 years old.

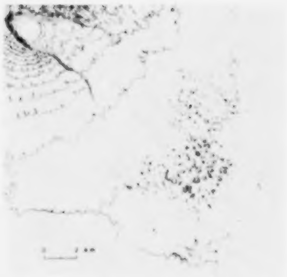

Map of the southeast flank of Galunggung volcano showing hummocks of a debris-avalanche deposit forming the "Ten Thousand Hills of Tasikmalaja." The deposit is less than 23,000 years old. Map from B.G. Escher, 1925.

Bandai Volcano, Japan

Nearly a century ago, the north flank of Bandai Volcano in Japan collapsed during an eruption quite similar to the May 18, 1980, eruption of Mount St. Helens. After a week of seismic activity, a large earthquake on July 15, 1888, was followed by a tremendous noise and a large explosion. Eyewitnesses heard about 15 to 20 additional explosions and observed that the last one was projected almost horizontally to the north.

S. Sekiya and Y. Kikuchi from the Imperial University of Tokyo visited Bandai Volcano within days of the eruption. After spending several months studying the new crater and area of devastation, they published a report (in English) that is a classic of volcanology. They described a "deluge of rock and earth" (debris

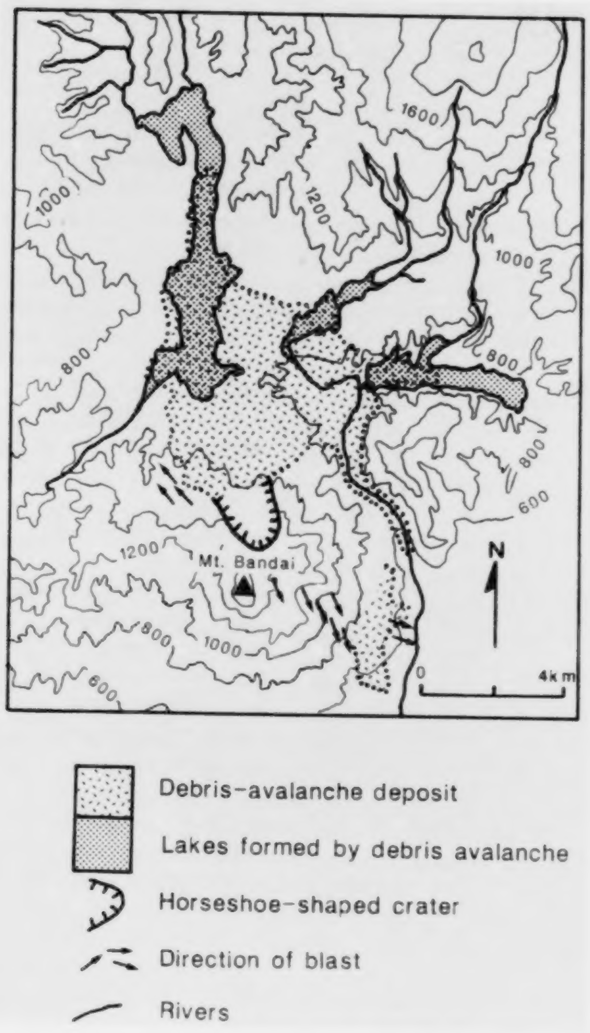
1600
1200
1000
1000
800
800
800
600
1200
Mt. Bandai
800
1000
600
N
0
4km
Debris–avalanche deposit
Lakes formed by debris avalanche
Horseshoe–shaped crater
Direction of blast
Rivers

Map of Bandai volcano, Japan, showing effects of the 1888 eruption. The debris-avalanche deposit is about 1.5 cubic km in volume, smaller than the one at Mount St. Helens. The avalanche and associated lateral blast killed 461 people, blew down thousands of trees, and dammed 3 lakes.

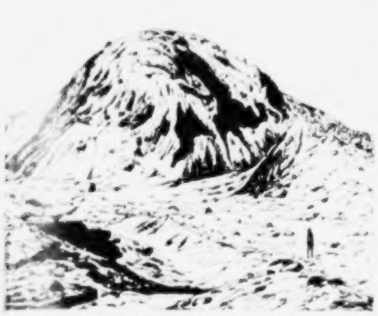

Sketch made from photograph of individual hummock of the Mount Bandai debris-avalanche deposit. Sketch reproduced from report by S. Sekiya and Y. Kikuchi, The Eruption of Bandai-san, 1890.

avalanche) that descended the north side of the mountain and covered several villages and killed 461 people. They described conical hills and small cones up to 15 m in height "standing out from the debris like so many miniature Fujiyamas." They also described "heated blasts of steam and air (lateral blasts) thickly mixed with dust and rock fragments fierce enough to crush the trees and strip them of not only of the branches but even of their bark." In a drainage basin on the east side of the mountain these blasts had felled a forest so that "trees with a diameter of more than a meter had been laid prostrate on the ground in thousands."

Although the Bandai eruption was similar in many ways to the recent eruption of Mount St. Helens, there were some significant differences. Seikiya and Kikuchi noted that the destructive agency was merely the "sudden expansion of imprisoned steam, unaccompanied by lava flows or pumice ejection." A study of the eruption by Yoichi Nakamura of Utsonomiya University in Japan in the 1970's confirmed the absence of juvenile material (new magma). The lateral blast and debris avalanche deposits at Mount St. Helens, however, contain about 100 million cubic m. of juvenile material. The debris-avalanche and blast-affected areas at Bandai are both considerably smaller than those areas at

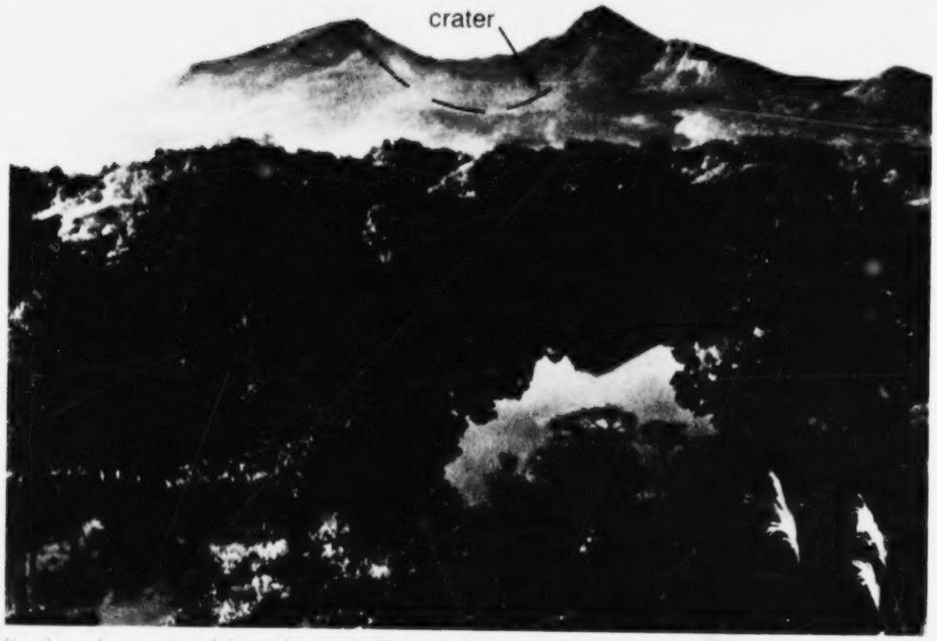

Bandai volcano viewed from the north. The once-barren, hummocky debris-avalanche deposit is now covered with vegetation. Shallow depressions surrounding hummocks have filled with water, forming hundreds of ponds.

Mount St. Helens. Blast deposits were not documented on the north side of the volcano by Seikiya and Kikuchi, even though the lateral blast was observed to be directed primarily to the north; likely most of the blast deposits were lost amid the hummocks of the debris-avalanche deposit. They were found only where the blast explosions spilled over the south flank of the volcano.

Today Bandai Volcano and the area around it is a ski and vacation resort. The area is heavily vegetated, and the only signs of the catastrophic eruption are the horseshoe-shaped crater and the debris-avalanche hummocks. The trees "laid prostate on the ground in thousands" are nowhere to be found, and the blast deposit is not easily recognized.

Molokai Island, Hawaiian Chain

That large landslides may have played a major role in the history of the Hawaiian Islands is suggested by Molokai Island, one of the small islands in the Hawaiian chain. The island of Molokai is composed of three shield volcanoes, East Molokai, the Kalaupapa Peninsula, and West Molokai. The windward north shore of East Molokai Volcano is characterized by huge cliffs ascending 1100 m from the sea at an angle of more than 55 degrees. The southern flank slopes gently to the sea, typical of shield volcanoes. Early researchers hypothesized that the unusually high sea cliffs might be a fault scarp or the result of marine erosion.

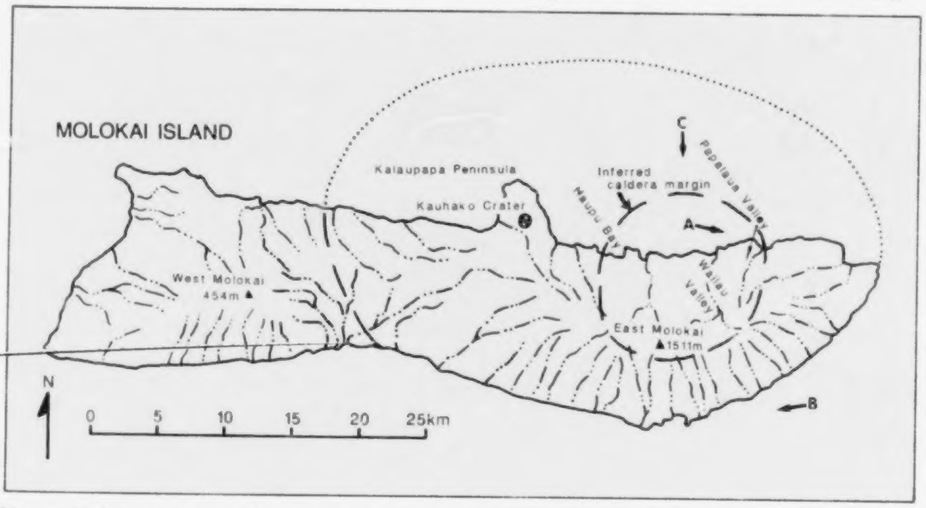

Map of Molokai Island of the Hawaiian chain. Based on the inferred presence of a caldera in the summit area of East Molokai Volcano, the northern part of the island is missing (indicated by the dotted shoreline). Holcomb and his colleagues discovered the caldera by mapping the magnetic polarity of lavas exposed in the steep cliffs near Haupu Bay and Papalaua Valley. Letters mark locations and perspective of photographs and sketch in the figures following.

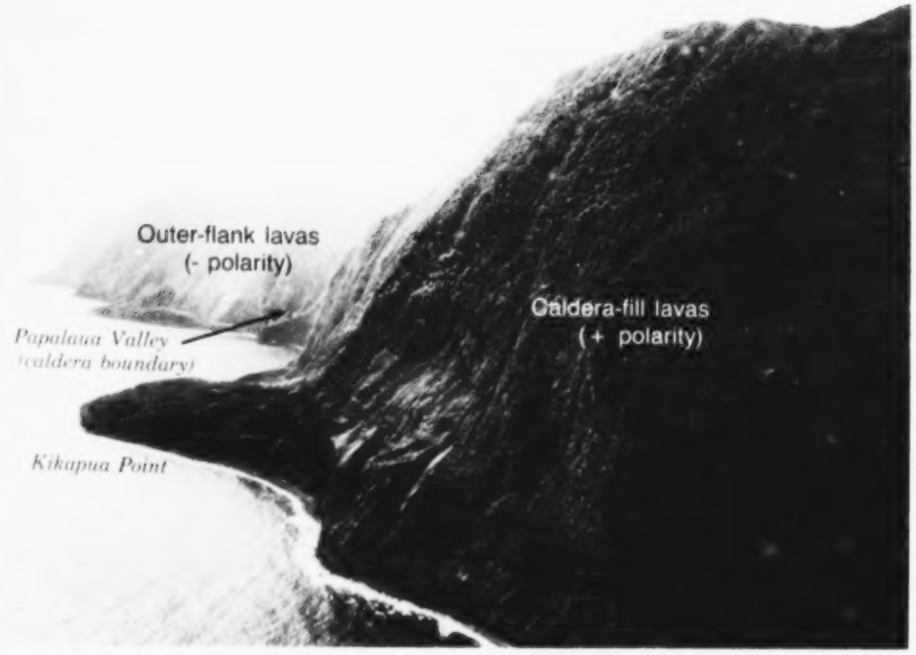

Aerial view of the great sea cliffs along north coast of East Molokai Volcano. View is looking east (letter A in the map of Molokai Island). The cliffs are between 650 and 800 meters high here but reach 1100 meters further west. East of Papalaua Valley, the cliffs consist of lavas with a reversed magnetic polarity, representing lavas of the outer flank; cliffs in the foreground have a normal polarity, representing younger lavas that filled a caldera. Photograph by Robin Holcomb, 1981.

but these interpretations were made with only a sketchy view of the volcano's structure and without any knowledge of the seafloor topography north of the cliffs. Recent studies by James Moore and Robin Holcomb of the U.S. Geological Survey suggest that a tremendous landslide bisected East Molokai Volcano, forming the sea cliffs and a lumpy seafloor deposit adjacent to the cliffs.

The geologic and magnetic-polarity stratigraphy of rocks in the north sea cliffs, recently mapped by Holcomb and his colleagues, shows that East Molokai's summit contains a caldera much larger than was previously estimated—the caldera is bisected and the northern half is removed. Holcomb's field party identified vertical polarity boundaries in rocks exposed at Haupu Bay and Papaluaua Valley. This type of boundary, which separates lava flows of normal polarity in the central section and lava flows of reversed polarity on the flanks, indicates an age difference between the two lava-flow sequences. Vertical polarity boundaries can occur where younger caldera-filling flows abut against older outward-sloping lava flows along near-vertical caldera walls.

At Haupu Bay, a vertical contact separates thin-bedded lavas to the west and lavas ponded atop lithified talus breccia of the caldera to the east. This exposure was previously interpreted to be a small pit crater on the flank of East Molokai Volcano. The age difference between the lavas on either side of the exposure, revealed by their magnetic polarities, however, indicates that they were erupted at different times. Based on this new interpretation of the structure of East Molokai Volcano, Holcomb estimates that about 500 cubic km is missing from the northern half of the volcano.

Holcomb contends that marine erosion would be too slow to account for the removal. The shield volcano comprising the Kalaupapa Peninsula is almost unaffected by marine erosion, yet recent K-Ar dates show that it is nearly 0.5 million years old. East Molokai Volcano stopped growing only about 1.5 million years ago, so unless the rates of erosion were much greater before Kalaupapa grew, half of East Molokai could not have been eroded in only 1 million years. Instead, the northern half of East Molokai must have sunk beneath the sea, probably in a giant landslide that James Moore proposed in 1964.

An irregular, "lumpy" seafloor extending at least 80 km north of Molokai and 160 km northeast of Oahu was reported by Moore when techniques of seafloor mapping were new. Bathymetric maps of the area revealed massive structures commonly from 8 to 25 km long and

Aerial view of the gently sloping south coast of East Molokai Volcano (letter B in the map of Molokai Island). Note partially enclosed areas that were once used as fish ponds by native Hawaiians. Photograph by Robin Holcomb, 1981.

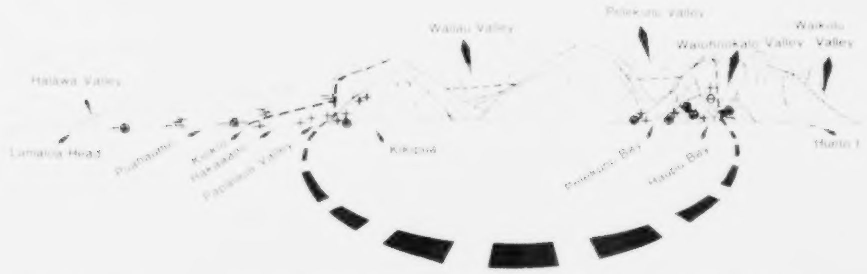
Halawa Valley
Lamaloa Head
Puahaunui
Kukaiwaa
Hakaaano
Papalaua Valley
Wailau Valley
Kikipua
Pelekunu Valley
Pelekunu Bay
Haupu Bay
Waiohookalo Valley
Waikolu Valley
Huelo I

*Sketch of the north coast of **East Molokai** volcano (letter C in the map of **Molokai Island**). Magnetic polarites of lava flows (uncircled) and dikes (circled) are indicated; magnetic-polarity boundaries are shown by heavy dashed lines. The boundary at **Haupu Bay** coincides with the caldera margin which is shown extending out to sea and back in a closed loop.*

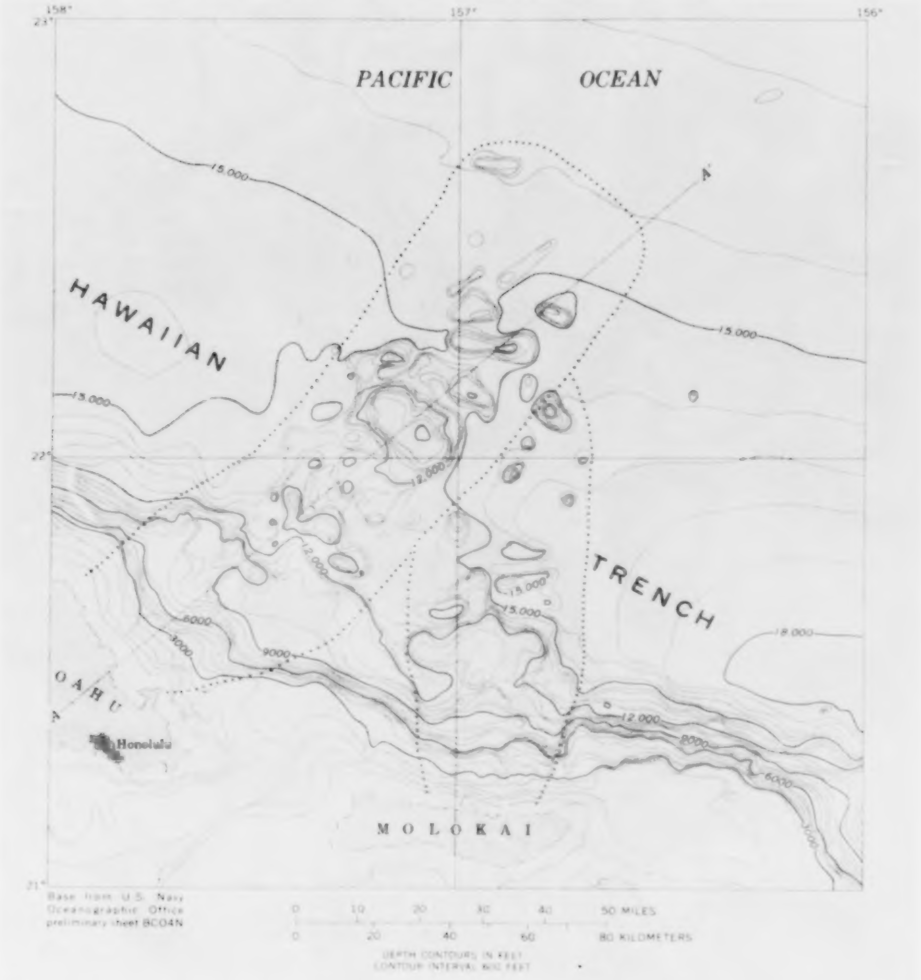
158°
157°
156°
23°
22°
21°
PACIFIC
OCEAN
HAWAIIAN
TRENCH
A′
A
15,000
12,000
9000
6000
3000
18,000
OAHU
Honolulu
MOLOKAI
Base from U.S. Navy Oceanographic Office preliminary sheet BC04N
0
10
20
30
40
50 MILES
0
20
40
60
80 KILOMETERS
DEPTH CONTOURS IN FEET
CONTOUR INTERVAL 600 FEET

*Map of submarine topography next to the islands of **Oahu** and **Molokai**. The irregular surface of the seafloor was interpreted in 1964 by **James Moore** of the **U.S. Geological Survey** to consist of large submarine landslide deposits. Inferred boundaries of landslides are shown by dotted lines. **Holcomb**'s contention that the summit caldera of **East Molokai Volcano** is bisected and northern half removed agrees well with **Moore**'s interpretation of the seafloor.*

5 to 15 km wide. They are commonly bounded by steep slopes as high as 2,000 m and may have relatively flat tops of which most are tilted toward the Hawaiian Ridge, a volcanic ridge which extends 2,600 km west-northwest from the island of Hawaii. The upper end of these features is marked by a concave escarpment. Moore interpreted these features as deposits from submarine landslides originating on the Hawaiian Ridge, one of the Earth's steepest and youngest major topographic features. The lumpy terrain is likely analogous to the hummocky subaerial debris-avalanche deposits.

Bibliography

Crandell, D. R., Miller, C. D., Glicken, H. X., Christiansen, R. L., and Newhall, C. G., 1984, Catastrophic debris avalanche from ancestral Mount Shasta volcano, California: Geology, v. 12, p. 143-146.

Holcomb, R. T., 1985, The caldera of East Molokai Volcano, Hawaiian Islands: National Geographic Society Research Reports, v. 21, p. 81-87.

Moore, J. G., 1964, Giant submarine landslides on the Hawaiian Ridge: U.S. Geol. Survey Prof. Paper 501-D, p. 95-98.

Siebert, Lee, 1984, Large volcanic debris avalanches: characteristics of source areas, deposits, and associated eruptions: Journal of Volcanology and Geothermal Research, v. 22, no. 3-4, p. 163-197.

Voight, B., Glicken, H., Janda, R. J., and Douglass, P. M., 1981, Catastrophic rockslide avalanche of May 18: *In* P. W. Lipman and D. R. Mullineaux (eds.), The 1980 eruptions of Mount St. Helens, Washington: U.S. Geol. Survey Prof. Paper 1250, p. 347-377.

Two Dome-Building Episodes at Mount St. Helens in 1984 and 1985 and Their Accompanying Seismicity

Steven Brantley

(Observations and data reported in this article were gathered from preliminary reports and published abstracts from the combined staffs of the Cascades Volcano Observatory and the Geophysics Program at the University of Washington.)

Introduction

The lava dome in the crater of Mount St. Helens has grown 250 meters high and 1000 meters in diameter during 15 eruptive episodes in the past 6 years (Fig. 1). Each episode, generally lasting between 1 and 3 weeks, enlarged the dome both by the intrusion of magma into the dome and by extrusion of lava onto its surface. These dome-building events each added between 1 and 7 million cubic m. of new material. During one episode in 1983, magma continuously rose into the dome for 12 months. Although similarities exist between the dome-growth episodes, the dome's history has been complex. Observations of the dome- building activity at Mount St. Helens are more comprehensive than for any other lava dome and have yielded useful insights into how lava domes grow.

Figure 1. Mount St. Helens crater and lava dome. Measuring 1000 m in diameter and 250 m. high, the dome has grown by 15 eruptive episodes. Each episode added between 1 and 7 million cubic m. of magma to the dome. Photograph by Lyn Topinka, July 25, 1985.

Two recent dome-building episodes considerably modified the lava dome and generated unusual seismicity. The September 1984 and May-June 1985 episodes consisted of extremely high rates of endogenous dome growth and intense disruption of the dome as magma intruded its molten core. Some of the magma leaked onto the surface of the dome, forming stubby lava flows called lobes. During the September 1984 episode, discrete earthquakes were replaced by a continuous tremor-like ground shaking at the height of activity, and during the May-June 1985 episode, seismicity was more energetic than at any time since the eruption on May 18, 1980. Poor weather during the most active periods of both episodes frustrated attempts to observe the important details of dome growth and accompanying seismicity.

Dome-Building Episodes

September 1984

Deformation

In a typical precusory manner, spreading rates of the north and west flanks of the dome began to increase in mid-August, more than 3 weeks before lava was extruded on the dome. The northeast, southeast, and south flanks, however, showed no precursory spreading. In contrast, the east and south sectors of the dome were the most mobile flanks during the 12-month-long continuous dome-building episode in 1983. The changing location of activity underscores the importance of monitoring all flanks of the dome.

Spreading rates of the north flank of the dome accelerated until the extrusion occurred and recorded the most rapid endogenous growth yet observed for the 1980-86 dome. One target on the north flank was displaced at steadily increasing rates between mid-August and early September, and reached nearly 4 m per day on September 8 (Fig. 2). This rate increased dramatically on September 9 and, between the afternoon of September 9 and the morning of September 10, peaked at slightly more than 50 m per day before abruptly slowing. These rates were measured over a few minutes or hours and then extrapolated to calculate a daily rate. The north flank of the dome was shoved as a block 56 m northwestward before the targets were destroyed by rockfalls on September 10 (Fig 3). This displacement was associated with wedging apart of the dome as magma entered its interior.

The top of the dome was severely disrupted during the peak of endogenous growth. Observations on September 8 revealed several major east-northeast trending cracks a few meters wide and tens of meters long

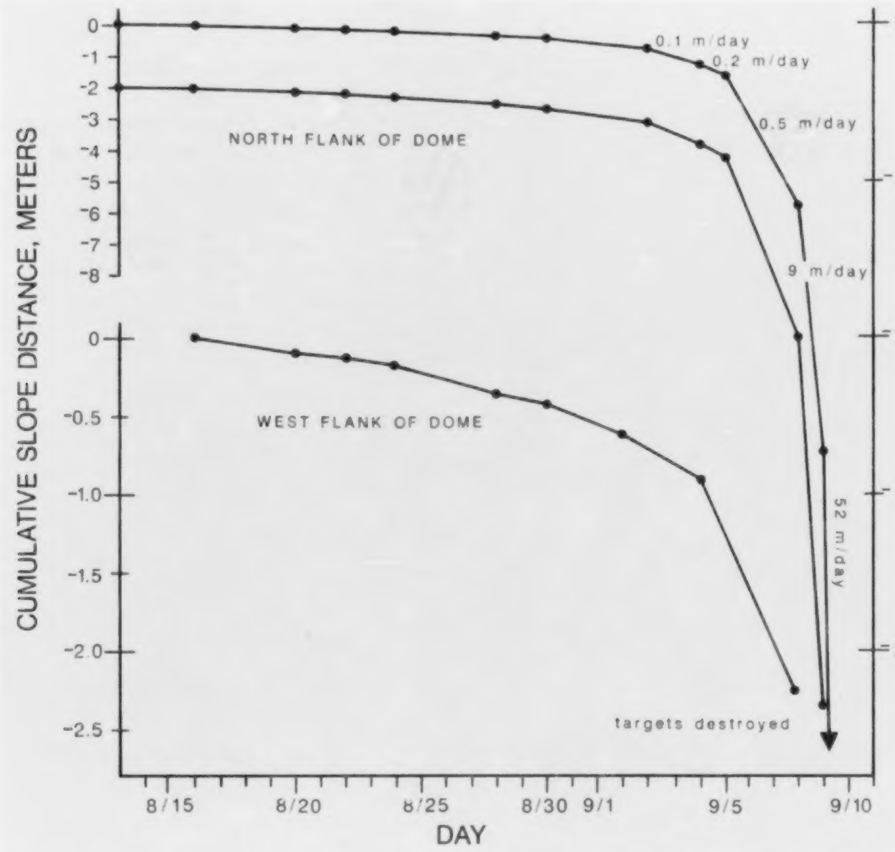

Figure 2. Graph showing cumulative displacement of targets on north and west sides of dome. Targets are surveyed from crater floor using theodolite and electronic distance meter. Rate of displacement or spreading of the dome increases as magma nears the surface.

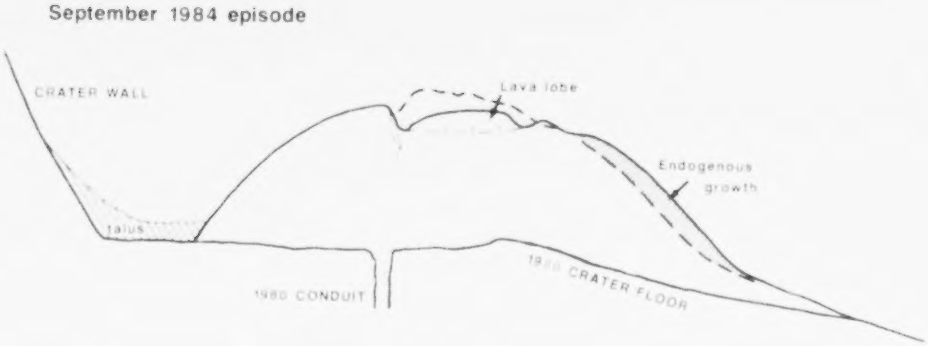
September 1984 episode
CRATER WALL
Lava lobe
Endogenous growth
talus
1980 CONDUIT
1980 CRATER FLOOR

Figure 3. Cross section of dome showing results of September 1984 episode of rapid growth; shaded portion represents endogenous growth. Note area of subsidence on top of dome that was partly filled by a new lava tube. View is to the west.

and also a graben several meters deep cutting across the summit of the dome. These structures were evidence that part of the dome was widening and subsiding. Clouds obscured the top of the dome on September 9. By September 10 much of the summit area had dropped down at least 34 m, forming a major collapse feature bounded on its eastern and southern sides by steep cliffs (Fig. 4). Photographs taken the same day showed that a new lava lobe occupied part of the collapsed area and was already 1/3 to 1/2 its final volume. An estimated 4 to 5 million cubic m. of magma was added to the dome during this episode by intrusion of magma and by extrusion on top of the dome.

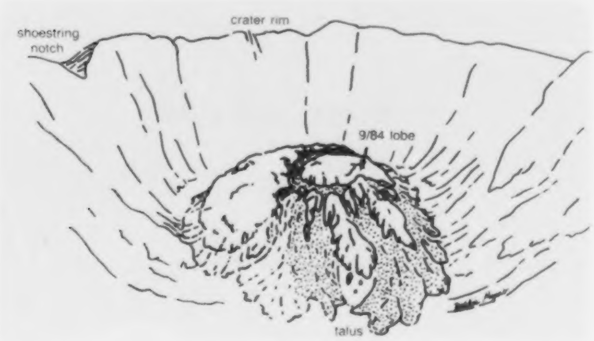

Figure 4. Sketch of dome showing area of subsidence and location of lava lobe extruded during September 1984 episode. View is south.

Seismicity

Unlike previous precursory patterns, the seismicity changed character several times during this episode. After a typical precursory increase in the number of shallow earthquakes, a sudden hiatus occurred about 0200 UTC (Universal Time Code) on September 10 (Fig. 5). A very weak volcanic tremor-like signal began about this time and increased in strength until 1000 UTC, when it was strong enough to be observed on seismographs 100 km away from the volcano. This tremor then became pulsating, with individual pulses spaced farther and farther apart with time. By about 1230 UTC isolated pulses could be recognized as individual earthquakes on some seismograms; all earthquakes were nearly the same size. The length of time between earthquakes gradually increased until by 1000 UTC on September 11 they were 5 minutes apart. Seismicity returned to a background level on September 13.

It was almost impossible to distinguish between volcanic tremor and back-to-back earthquakes at about 1100 on September 10. The length of time between

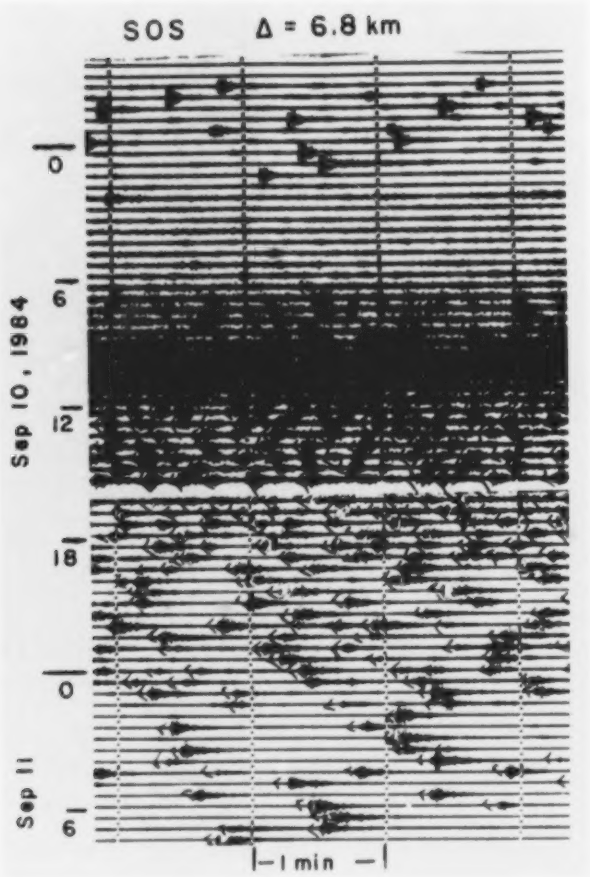

Figure 5. Seismogram on September 10-11, 1984, from seismometer located 6.5 km from crater. Tic marks are 1-minute intervals; hours are marked along left margin (Universal Time Code). Note volcanic tremor-like signal that is replaced by individual earthquakes closely spaced in time between about 1000 and 1200 UTC.

recognizable earthquakes, plotted on a logarithmic scale in Figure 6, increased from about 6 seconds to 200 seconds between 1300 UTC on September 10 and 1000 UTC on September 11. If this relation is extrapolated back to 0200 UTC on September 10, the time between earthquakes would only be about 2 seconds—too closely spaced in time for seismologists to identify them as separate events. This is evidence that at least some volcanic tremor consists of many volcanic earthquakes of about the same size occurring one after another, such that their coda merge into a continuous signal.

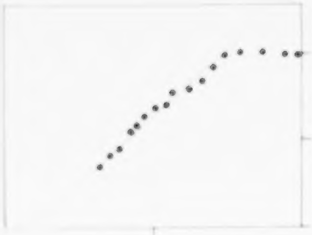

Figure 6. Graph of time interval between individual earthquakes versus day (plotted on logarithmic scale). By extrapolating linear curve back to about 0200 UTC on September 10, length of time between earthquakes would be about 2 seconds—too short for individual earthquakes to be distinguished.

May-June 1985

Deformation

The largest dome-building episode since 1980 literally tore apart the south third of the dome in late May and early June 1985. The south part of the dome was shoved southward 100 m by intruding magma, leaving in its wake a huge graben slicing across the top of the

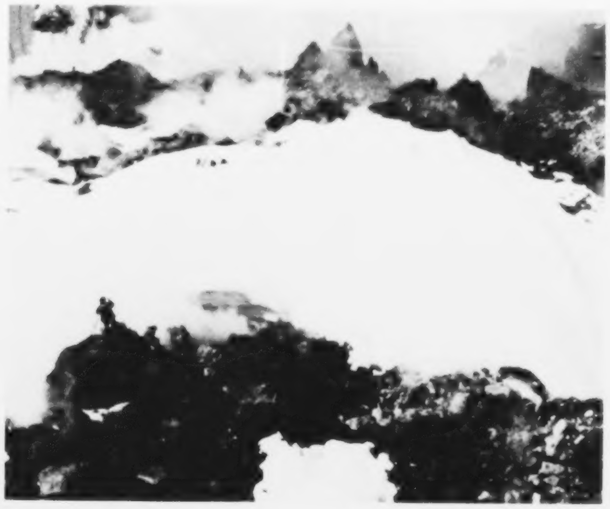

Figure 7. Geologists surveying on top of dome before the May-June 1985 episode. Surveying instruments are set over Lonesome benchmark, located on top of warm fumarole. Photograph by Lyn Topinka, April 1, 1985. See figure 8.

dome. One or more large thrust faults are inferred beneath the snow cover on the south crater floor—the faults produced the largest displacement of the crater floor thus far measured. Unlike the previous eruptive episode, the north flank of the dome was notably quiet.

The May-June epsiode was the first for which a geodetic network atop the dome was surveyed during a precursory period, and it proved extremely useful in determining how the disruption of the dome took place (Fig. 7). Stations on the south and east sides of the summit area first began showing increased movement on May 13. A principal instrument station (Lonesome) on the dome was itself moving southward, and distances from it to targets were increasing at accelerating rates until the last measurements on May 23 (Fig. 8). Poor weather and heavy fume prevented detailed observations or additional measurements until June 10.

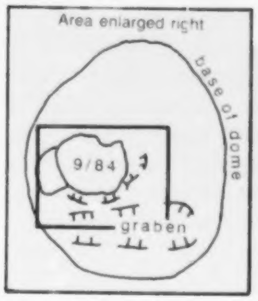

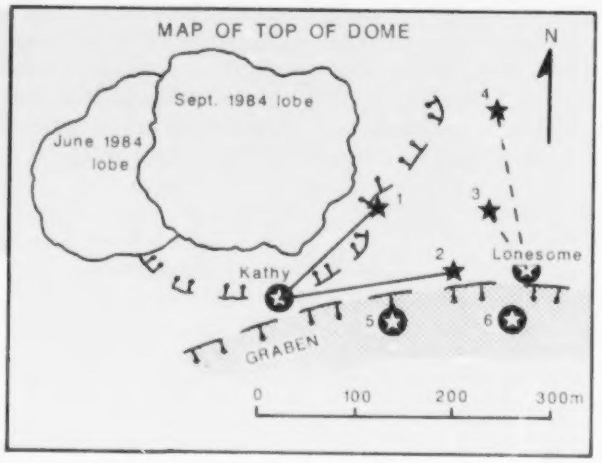

Figure 8. Map of top of dome and displacement of targets across dome. Numbered targets were surveyed from two instrument sites, Kathy and Lonesome. Note location of graben that formed during the May-June 1986 episode.

The south summit area of the dome began subsiding between May 21 and May 23, as indicated by several targets that dropped between 80 and 130 cm (Fig. 9). Field observers on May 23 saw no geologic evidence that a graben was forming; instead new cracks radiated outward from the center of the dome, cross-cutting the east-west trend of the subsequent graben. Aerial observations of the dome on May 27, however, revealed an arcuate trough cutting across the southern summit of the dome. The graben was about 500 m long, 50 m wide, and bounded on the north by a 10 m high scarp and on the south by a 5 m high scarp. Observers early on May 30 (0830 PDT) found a new lobe that had oozed from the southeast end of the graben and nearly reached the crater floor. The volume of the lobe was 0.9 million cubic m., small by comparison with previous lobes. In the afternoon the same observers who sighted the graben on May 27 saw that vast changes had occurred on top of the dome—the graben was now 250 m wide and 58 m deep, and the south flank of the dome had been shoved about 100 m outward (Fig 10).

Targets and instrument stations on top of the dome were resurveyed on June 10, when hazards were

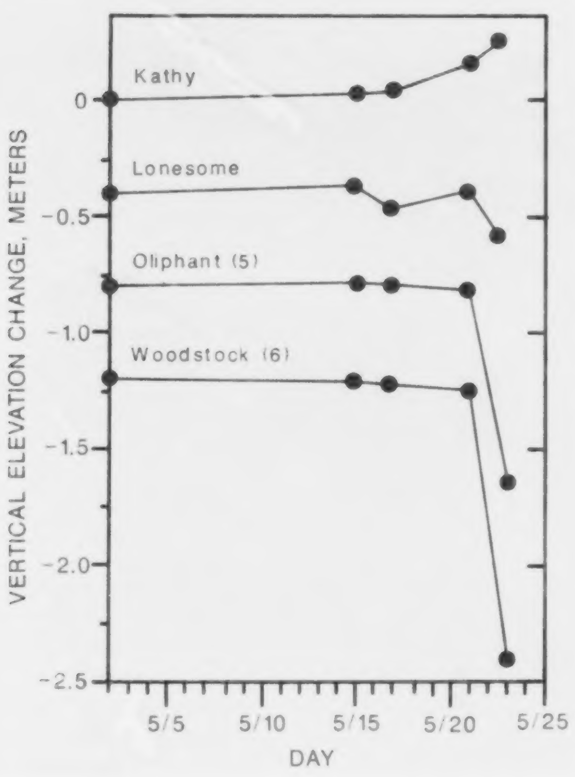

Figure 9: Graph showing vertical displacements of targets atop dome. Target locations shown in Figure 8. Note initial subsidence of targets located in area where graben formed. Some targets dropped 51 meters during episode and remained upright.

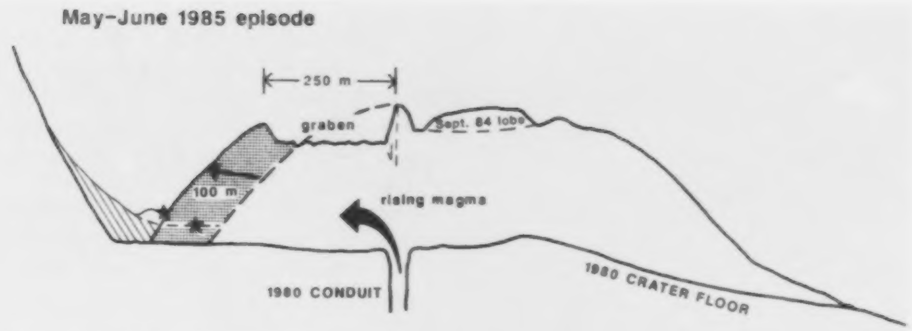
May–June 1985 episode
250 m
graben
Sept. 84 lobe
100 m
rising magma
1980 CONDUIT
1980 CRATER FLOOR

Figure 10. Sketch and cross-section of dome showing graben and May 1985 lava lobe. Cross section illustrates displacement of south side of dome and warping of crater floor caused by magma rising into dome's molten interior. Sketch by Bobbie Myers.

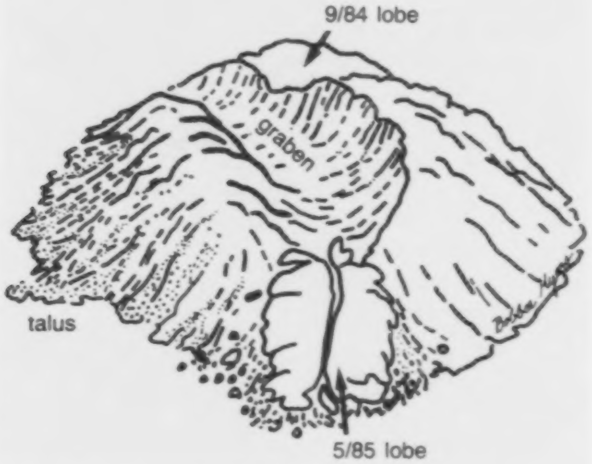
9/84 lobe
graben
talus
Bobbie Myers
5/85 lobe

deemed low. Incredibly, three targets survived being downdropped into the graben; they remained upright and barely tilted despite a lateral displacement of 30 m and subsidence of 51 m measured at one of them. A target on the south crater floor near the dome moved southward 45 m and upward 17 m between May 17 and June 8. This target presumably rode the upper plate of a thrust fault, whose movement warped the surface of snow covering the crater floor. An estimated 7 million cubic meters of magma entered the dome, more than during any episode at Mount St. Helens since June 12, 1980.

Seismicity

The most energetic earthquake sequence since the May 18, 1980, eruption accompanied the dominantly endogenous dome-growth episode of May-June 1985. Earthquake activity increased in a normal precursory pattern between May 15 and May 25. Most of the earthquakes were relatively small until May 27. The magnitude of individual events then increased until they were significantly larger than any of the typical earthquakes associated with dome-building episodes. Between May 27 and June 2, earthquakes between magnitude 2.5 and 2.8 occurred every 5 to 10 minutes and smaller earthquakes occurred every few minutes (Fig. 11). These larger earthquakes stopped on June 4 and seismicity returned to pre-eruption levels by June 17.

Many of the larger earthquakes generated medium-frequency signals that are near duplicates of one another—the waveforms are almost the same. Close inspection of the seismograms reveals several different types of duplicate waveforms or earthquake "families." An estimated 25 percent or more of the large earthquakes fall into one family or another. Seismograms of five earthquakes from two different "families" are shown in Figure 12. One family was also recognized on seismograms from the precursory sequence to the September 1984 episode.

Duplicate waveforms suggest the source of the earthquakes was within a small volume (within a few tens of meters) and was caused by the same mechanism. Alternatively, the high level of seismicity during the May-June episode may be a natural consequence of the large displacement of the south side of the dome (see Fig. 10) and the large volume of magma that ascended the conduit and entered the dome.

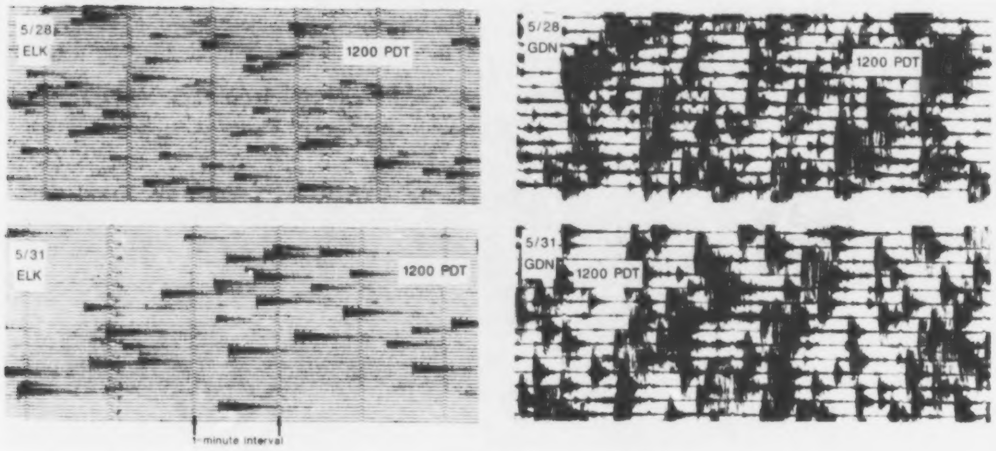

Figure 11. Seismograms from two seismometers during May-June 1985 dome-building episode. ELK station located about 15 km west-northwest of crater; GDN station in crater. Earthquakes between magnitude 2.5 and 2.8 were occurring every 5 to 10 minutes between May 27 and June 2. Tic marks represent 1-minute intervals; horizontal lines represent 15-minute intervals.

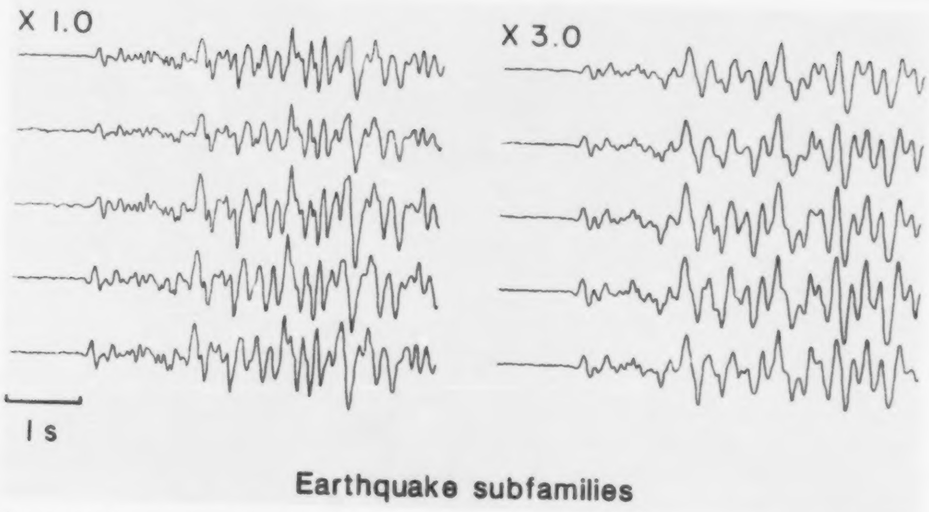

Figure 12. Seismogram from DIG seismic station located in crater illustrating single "family" of earthquakes that consists of two subfamilies. On left are examples from subfamily during 12 hour period on May 28. On right are examples from subfamily during 38 hour period between May 31 and June 1. Scale factor indicated.

Long-Term Growth of the 1980-1985 Dome

The lava dome has grown episodically since its formation in 1980, but the long-term rate of magma supply to the dome has been uniform during two distinct periods. Fifteen episodes of growth each added between 1.2 and 7 million cubic meters of magma to the dome during 1980-1985, both by the intrusion of magma into its core and by extrusion of stubby lava flows. Most of the growth during a typical episode occurs in only a few days, but, beginning in February 1983, it was continuous for 12 months. Quiet intervals which separate the growth episodes last less than 2 months to more than 9 months. Despite these irregularities, a graph of the volume of the dome versus time reveals that its growth was surprisingly regular in 1980-85. The cumulative volume of magma in the dome after each eruptive episode is plotted against time in Figure 13, and best-fit curves are applied to the data. The graph shows:

1. **The long-term rate of growth (average monthly rate) slowed during the winter of 1981-82.**
2. **The long-term growth rates of the dome before and after the winter of 1981-82 are linear. In 1980-1981 about 1.8 million cubic m. of magma were added to the dome each month, and in 1982-85 about 0.9 million cubic m. were added.**

3. **The growth of the dome is volume-predictable—the volume of magma added to the dome is proportional to the length of time between eruptive episodes. The longer the interval of quiet, the larger the volume of magma that will be added to the dome during the next episode. For example, the largest volume added to the dome followed the longest interval of quiet—the dome grew about 7 million cubic m. in May-June 1985 following an 8-month quiet interval.**

The volume-predictable relation, if it holds in the future, will enable geologists to predict the size of future eruptive episodes based on the length precursory signs of unrest indicate that new growth is imminent. No clear relation exists, however, between the length of quiet between eruptive episodes and the type of activity to occur during the next event, and no pattern is evident in the length of quiet intervals. The long-term rate of magma supply to the dome is important in understanding the processes and dynamics operating on the magma reservoir beneath the volcano.

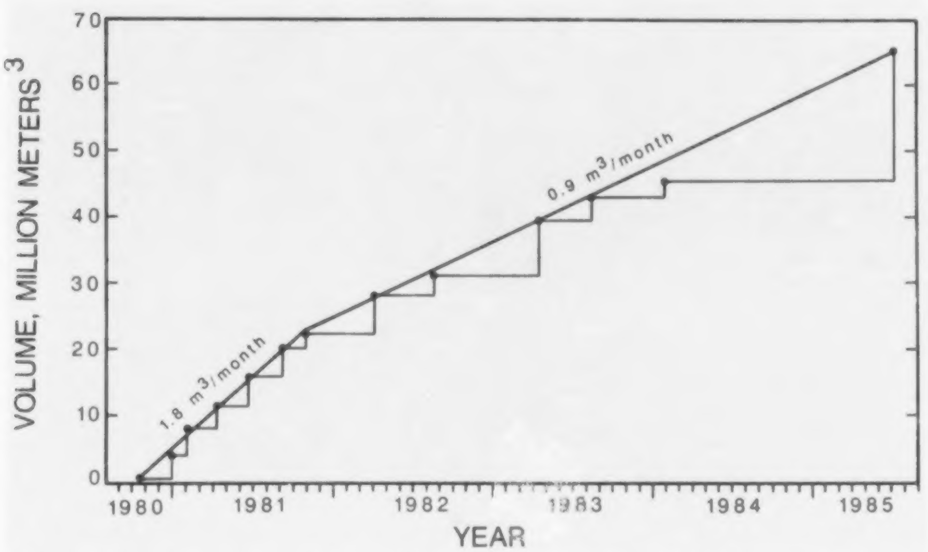

Figure 13. Graph showing cumulative growth of dome. Note change in long-term growth rate in 1982. Although short-term volume change of the dome increases episodically, long-term volume change of dome is linear.

About the Authors

A biography for Steven Brantley appeared in Volume 16, p. 123.

Kenneth Cameron completed his graduate studies on volcanic stratigraphy in the Oregon Coast Range in 1980. Since then he has worked on various projects including sediment transport along bay floors and biostratigraphy in the northern Oregon Coast Range. At the Cascades Volcano Observatory, he studies volcanic hazards, especially those associated with hydrologic processes, lahar stratigraphy, and the post-glacial eruptive histories of the major Cascade volcanoes.

Patrick Pringle received his M.S. in geology from the University of Akron, Ohio. Since 1982 he has been at the Cascades Volcano Observatory where he has studied deposits and geomorphic changes that have resulted from recent eruptions of Mount St. Helens, the post-glacial eruptive histories of other Cascade volcanoes, and debris flows in tributaries of the Grand Canyon, Arizona. He is currently the public information scientist at the observatory.

David Yamaguchi received a bachelor's degree in biology from Yale in 1979, and a Ph.D. in forest ecology/tree-ring analysis from the University of Washington in 1986. He is presently continuing his Mount St. Helens studies as a National Research Council-USGS Research Associate at the Cascades Volcano Observatory.

Harry Glicken received his undergraduate degree in geology from Stanford in 1980. He has been working with the USGS at Mount St. Helens since April 1980. In 1986, he completed his Ph.D. in geology at the University of California, Santa Barbara, studying the debris avalanche of Mount St. Helens' May 18, 1980, eruption. His current research involves the study of other large volcanic debris avalanches; he has worked on such deposits in the Cascade Range, in Alaska, and in Indonesia. He is presently a postdoctoral fellow at the University of Tokyo, Japan.

U.S. GOVERNMENT PRINTING OFFICE
PUBLIC DOCUMENTS DEPARTMENT
WASHINGTON, D.C. 20402

OFFICIAL BUSINESS
PENALTY FOR PRIVATE USE $300

BULK RATE MAIL
POSTAGE & FEES PAID
USGS
PERMIT No. G23

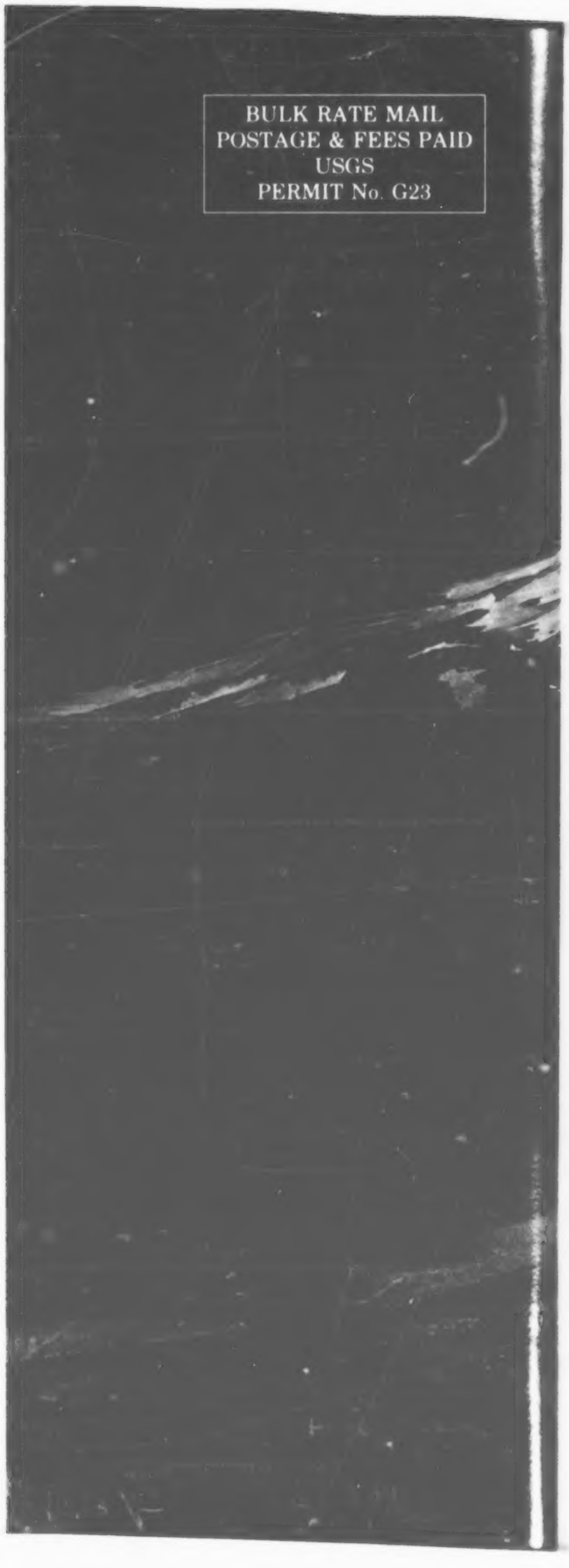

Mount Shasta volcano, California, and Shastina cone, 4,305 meters. View is to the southeast. Interstate 5 is in lower foreground. The largest known volcanic debris avalanch from Mount Shasta occurred between about 300,000 and 360,000 years ago. See page 195. Photograph by Lyn Topinka, July 1984.